

**BIOREACTIVITY OF METAL COMPONENTS FOUND
IN AIR POLLUTION PARTICLES**

LUCIANO L P MEROLLA



**A thesis presented for the degree of Doctor of Philosophy
at
Cardiff University
October 2005**

**Cardiff School of Biosciences
Cardiff University
Museum Avenue
Cardiff
CF10 3US**

UMI Number: U208252

All rights reserved

INFORMATION TO ALL USERS

The quality of this reproduction is dependent upon the quality of the copy submitted.

In the unlikely event that the author did not send a complete manuscript and there are missing pages, these will be noted. Also, if material had to be removed, a note will indicate the deletion.



UMI U208252

Published by ProQuest LLC 2013. Copyright in the Dissertation held by the Author.
Microform Edition © ProQuest LLC.

All rights reserved. This work is protected against
unauthorized copying under Title 17, United States Code.



ProQuest LLC
789 East Eisenhower Parkway
P.O. Box 1346
Ann Arbor, MI 48106-1346

To Mum and Dad

Contents

Title	i
Dedication	ii
Contents	iii
Acknowledgements	ix
Declaration	x
Publications	xi
Abbreviations	xii
Abstract	xiv

1.0 General Introduction

1.1	Overview	1
1.2	Introduction – Gross Anatomy of the Human Lung	1
1.2.1	Complex Anatomy of the Lung – The Alveolar Unit	2
1.2.2	Functions of the Lung	3
1.2.3	Xenobiotic Deposition in the Lung	4
1.3	Defence Mechanisms of the Lung	7
1.3.1	Cellular Defences	7
1.3.1.1	Mucociliary Transport	7
1.3.1.2	Macrophages	8
1.3.1.3	Polymorphonuclear Leukocytes (PMNs)	8
1.3.1.4	Immunological Response	9
1.3.2	Non-cellular Defences	9
1.3.2.1	Respiratory Tract Lining Fluid (RTLFL)	11
1.4	Ambient Environmental Pollution	13
1.4.1	Historical Perspectives	13
1.4.1.1	Meuse Valley	15
1.4.1.2	Donora	15
1.4.1.3	London	16
1.4.1.4	Utah Valley	16
1.4.2	Particulate Pollution	17
1.4.2.1	UK Particulate Pollution	18
1.4.2.2	Residual Oil Fly Ash	18
1.4.2.3	EHC-93	20

1.4.3	Health Effects	21
1.5	PM-Induced Oxidation	24
1.5.1	Reactive Oxygen Species	25
1.5.1.1	DNA Oxidation	26
1.5.1.2	Lipid Peroxidation	27
1.5.1.3	Oxidation of Proteins	27
1.5.1.4	Metal-Induced Oxidative Effects	28
1.5.2	Metals	28
1.5.2.1	Copper	31
1.5.2.2	Iron	32
1.5.2.3	Manganese	33
1.5.2.4	Vanadium	34
1.5.2.5	Zinc	35
1.5.2.6	Arsenic	35
1.5.2.7	Lead	36
1.6	Use of ‘Omic Technologies in Toxicology	36
1.6.1	Toxicogenomics	37
1.6.1.1	Applications of Toxicogenomics	37
1.6.1.2	Negative Aspects of Toxicogenomics	38
1.7	Aims	39
2.0	<i>In Vitro</i> Toxicology of Ambient Particulate Matter	
2.1	Introduction	41
2.2	Equipment and Materials	43
2.2.1	PM ₁₀ Collection	44
2.2.2	PM ₁₀ and ROFA Preparation	45
2.2.3	The Plasmid Scission Assay	45
2.2.4	pX174-RF Plasmid Selection and Preparation	46
2.2.5	PM Test Sample Preparation and Incubation	47
2.2.6	Agarose Gel Preparation and Sample Loading	47
2.2.7	Quantification of Results	48
2.2.8	Statistical Analysis	49
2.3	Results	49
2.3.1	Optimising the Quantitation Protocol	49
2.3.2	Port Talbot Study – Bioreactivity	49

2.3.3	Port Talbot Study – ICP-MS	55
2.3.4	Comparative Analysis of Bioreactivity and Metal Content	58
2.3.5	Effects of Local Environment (Five Site Study) – Bioreactivity	59
2.3.6	Effects of Local Environment (Five Site Study) – ICP-MS	63
2.3.7	ROFA	66
2.4	Discussion	67
3.0	<i>In Vitro</i> Interactions of Water-Soluble Metals	
3.1	Introduction	72
3.2	Materials and Methods	74
3.2.1	Equipment and Materials	74
3.2.2	Preparation of Metal Mixtures	75
3.2.3	Generation of Concentrated BALF Solution	76
3.2.4	BALF Fractionation (Microcon)	77
3.2.5	Preparation of Glutathione	77
3.2.6	Statistical Analysis	77
3.3	Results	78
3.3.1	Assessment of PM Surrogate Mixtures	78
3.3.2	Analysis of Metals and Oxidation States	81
3.3.3	Effects of Secondary Components	83
3.3.4	Analysis of Metal Combinations	84
3.3.5	Effects of BALF on Metal Bioreactivity	85
3.4	Discussion	88
4.0	<i>In Vivo</i> Toxicology of PM Surrogates	
4.1	Introduction	92
4.2	Materials and Methods	94
4.2.1	Equipment and Materials	94
4.2.2	Dose Justification	95
4.2.3	Sample Preparation	95
4.2.4	Instillation	96
4.2.5	Body Mass Monitoring	97

4.2.6	Sacrifice and Dissection	97
4.2.7	Pulmonary Lavage	99
4.2.8	Free Cell Counts	99
4.2.9	Cytospins	99
	4.2.9.1 Staining	99
	4.2.9.2 Differential Cell Counts	100
4.2.10	Total Lavage Protein	100
4.2.11	Inductively-Coupled Plasma Mass Spectrometry	100
	4.2.11.1 Operational Process of ICP-MS	101
	4.2.11.2 Sample Preparation:	
	Microwave Digestion of Tissues	102
	4.2.11.3 Analysis	103
4.2.12	Statistical Analysis	103
4.3	Results	104
	4.3.1 Instillation	104
	4.3.2 Body Mass Analysis	104
	4.3.3 Lung:Body Mass Ratio	106
	4.3.4 Free Cell Counts	106
	4.3.5 Differential Cell Counts	108
	4.3.6 Lavage Protein Concentration	112
	4.3.7 Effects of Oxidation States and Metal Synergies	112
	4.3.8 Organ-Specific ICP-MS Analysis	115
	4.3.8.1 Lung	115
	4.3.8.2 Heart	117
	4.3.8.3 Liver	117
	4.3.8.4 Kidney	118
4.4	Discussion	118

5.0 Histopathology of Metal-Induced Pulmonary Effects

5.1	Introduction	124
5.2	Materials and Methods	125
	5.2.1 Equipment and Materials	125
	5.2.2 Gross Morphology of Lungs and Lymph Nodes	125
	5.2.3 Lung Tissue Fixation	126
	5.2.4 Processing Tissue for Light Microscopy	126

5.2.4.1	Tissue Processing	126
5.2.4.2	Paraffin Embedding	127
5.2.4.3	Sectioning	127
5.2.4.4	Haematoxylin and Eosin Staining	128
5.2.4.5	Massons's Trichrome Staining	128
5.2.4.6	Slide Production	129
5.2.5	Light Microscopy	129
5.2.6	Statistical Analysis	129
5.3	Results	130
5.3.1	Recovery of Lavage Fluid	130
5.3.2	Gross Morphology	130
5.3.3	Morphology of the Lymph Nodes	133
5.3.4	Histopathology	136
5.3.4.1	Four Hours Post-Instillation	136
5.3.4.2	Twenty-Four Hours Post Instillation	137
5.3.4.3	Three Days Post Instillation	138
5.3.4.4	Seven Days Post Instillation	138
5.4	Discussion	143
6.0	Systemic Toxicogenomics	
6.1	Introduction	148
6.2	Materials and Methods	150
6.2.1	Equipment and Materials	150
6.2.2	Sample Preparation	151
6.2.2.1	RNA Isolation	151
6.2.2.2	RNA Quantitation	152
6.2.2.3	RNA Quality Assessment	153
6.2.3	Macroarray Procedure	153
6.2.3.1	Prehybridisation of Array Membranes	153
6.2.3.2	Preparation of Targets	153
6.2.3.3	Column Chromatography (Purification of Target)	153
6.2.3.4	Processing the Phosphorimager Screen	154
6.2.3.5	Stripping the Membranes	154
6.2.4	Quality Control	155
6.2.5	Data Handling, Filtering and Analysis	156

6.2.5.1	Fold Change	156
6.2.5.2	Coefficient of Variation	157
6.2.5.3	Statistical Analysis	157
6.2.5.4	Functional Grouping	158
6.2.6	Methodological Summary	158
6.3	Results	160
6.3.1	RNA Purity and Integrity	160
6.3.2	Macroarray Analysis	161
6.3.2.1	Lung	161
6.3.2.2	Heart	164
6.3.2.3	Comparative Functional Classification	164
6.4	Discussion	168
6.4.1	Functional Groups	168
6.4.1.1	Metabolism	169
6.4.1.2	Cell Cycle	169
6.4.1.3	Stress Response	170
6.4.1.4	Intracellular Transducers, Effectors, Modulators	171
6.4.1.5	DNA Synthesis, Recombination and Repair	171
6.4.1.6	Post Translational Modification Protein Folding	171
6.4.1.7	Translation	172
6.4.1.8	DNA Binding and Chromatin Repair	172
6.4.2	Technical Critique	172
6.4.3	General Summary	173
7.0	General Discussion	175

Acknowledgements

I feel very privileged to have been given the chance to study for a PhD as I believe the opportunity was not well deserved. There are many people who have helped me along the way, none more so than Roy and Leona. I would like to thank Leona very much for convincing me to give science another go and for giving me the courage to face a hard day's work for once in my life. Your support knows no bounds and I must concede you are the formatting queen and you have a scary amount of scientific knowledge tucked away in that tiny head of yours. Seriously though, you have inspired me in many ways to approach the PhD with enthusiasm, enjoyment, and a sense of commitment which I have to say was very novel for me. And to Roy, whose faith in me has been going since as long as I can remember, which is a little difficult to do, due to the number of beers he bought me throughout my undergraduate days. You have stuck up for me on many fronts, when most people would have washed their hands of me. Your guidance, feedback and passion for science will stand me in good stead for the future. For all of that I am eternally grateful.

I would like to thank Kelly BeruBe for agreeing to be my supervisor after Roy retired and for all the late nights she has spent in the company of her red pen and my many, many chapters. New duvet cover is in the post.

I was very lucky to get the opportunity to visit China, which was absolutely breathtaking and probably one of the most hospitable places I have ever been. For this I would like to thank Tim Jones. I must also thank him for the good deal he got me on the ICP machine.

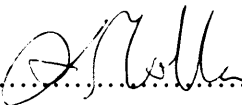
When I have been a little lost in the lab I have always been able to rely on Keith for technical support and a keen willingness to help. Also Martina and Dom for their help with my *in vivo* pracs. Too many long days me thinks. I would like to thank Dr. Teresa Moreno for supplying me with a great deal of help and a great deal of PM samples to get this project rolling.

Thanks must be paid to the rest of W 201 especially to Yant, Saira, Liz, Sanj and Kojee (when he was here) for making the social side of the PhD most enjoyable.

Finally I must give a huge thanks to my mum and dad who have helped me through the highs and lows of my life and have always been there, no matter what.

Declaration

This work has not previously been accepted for any degree and is not concurrently submitted in candidature for any degree.

Signed  (candidate)

Date 11/10/05

Statement 1

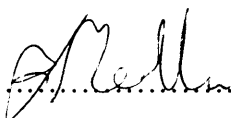
This thesis is the result of my own investigations, except where otherwise stated. Other sources are acknowledged by footnotes giving explicit references. A bibliography is appended.

Signed  (candidate)

Date 11/10/05

Statement 2

I hereby give consent for my thesis, if accepted, to be made available for photocopying and for inter-library loan, and for the title and summary to be made available to outside organisations.

Signed  (candidate)

Date 11/10/05

Publications

BéruBé KA, Jones TP, Moreno T, Sexton K, Balharry D, Hicks M, **Merolla L** and Mossman BT. (2006) Characterisation of Airborne Particulate Matter and Related Mechanisms of Toxicity. In: Air Pollution Reviews, Vol. 3. Eds. J. Ayres, R. Maynard & R. Richards. Imperial College Press, London, *in press*.

Merolla L and Richards RJ. (2005) *In Vitro* Effects of Bioavailable Metals Present in UK PM₁₀. *Experimental Lung Research* 31(7):671-683

BéruBé KA, Whittaker A, Jones TP, Moreno T and **Merolla L**. (2005) London's Smogs: How did They Kill? *Proceedings of the Royal Microscopy Society*, *in press*.

Merolla L and Richards RJ. (2005) *Oxidative Capacity of Soluble Metals in UK PM₁₀*. <http://www.le.ac.uk/ieh/publications/publications.html>: 61-63.

Moreno T, **Merolla L**, Gibbons W, Greenwell L, Jones T, Richards RJ (2004) Variations in the Source Metal Content and Bioreactivity of Technogenic Aerosols: A Case Study from Port Talbot, Wales, UK. *Science of the Total Environment* 333:59-73.

Merolla L, Moreno T, Richards RJ (2004) Oxidative Capacity of PM₁₀ from Different Sources in the Same Location. *Experimental Lung Research*, 30(6):625-649

Merolla L and Richards RJ. (2003). A Study into the Effects of Bioavailable Metals Present in UK PM₁₀ both *in Vitro* and *in Vivo*. *Experimental Lung Research*, 29(2):174.

Communications

Merolla L, Richards RJ and BéruBé, K. (2005) *An in Vitro Assessment of the Bioreactivity of Metals Endogenous to UK PM₁₀*. The Mineralogical Society Meeting, Bath.

Merolla L and Richards RJ. Invited Speaker (2004) *In Vitro and In Vivo Toxicology of Inhaled Pollutant Metals*. University of Beijing, China.

Merolla L and Richards RJ. (2004) *Oxidative Capacity of Soluble Metals in UK PM₁₀*. 8th Annual Review Meeting of the Joint Research Programmes on Outdoor and Indoor Air Pollution, Institute of Environment and Health, Leicester.

Merolla L, Moreno T, Richards RJ.(2003) *Oxidative Capacity of PM₁₀ from Different Sources in the Same Location*. British Association of Lung Research, Brighton.

Merolla L and Richards RJ. (2002) *A Study into the Effects of Bioavailable Metals Present in UK PM₁₀ Both in Vitro and in Vivo*. British Association of Lung Research, Leicester.

Abbreviations

AP	Air Pollution
ATP	Adenosine Triphosphate
BALF	Broncho-Alveolar Lavage Fluid
CDS	Complimentary DNA Sequence
cpm	Counts per Minute
CV	Coefficient of Variance
dc	Direct Current
DEP	Diesel Exhaust Particles
dNTP	deoxynucleotide Triphosphate
DNA	Deoxyribobucleic Acid
EDTA	Ethylenediaminetetracetic Acid
ELF	Epithelial Lining Fluid
ESD	Equivalent Spherical Diameter
GSH	Glutathione
H&E	Haematoxylin and Eosin
HPLC	High Pressure Liquid Chromatography
IA	Image Analysis
ICPMS	Inductively-Coupled Plasma Mass Spectrometry
IL	Interleukin
LFC	Lavage Free Cells
LM	Light Microscopy
MMAD	Mean Mass Aerodynamic Diameter
MT	Masson's Trichrome
NE	North East
NEx	Nucleospin Extraction
NW	North West
PAH	Polyaromatic Hydrocarbon
PM	Particulate Matter
PM ₁₀	Particulate Matter with an Aerodynamic Diameter less than 10 µm
PMN	Polymorphonuclear Leukocyte
qPCR	Quantitative Polymerase Chain Reaction
rf	Radio Frequency
RNA	Ribonucleic Acid

RNS	Reactive Nitrogen Species
ROFA	Residual Oil Fly Ash
ROS	Reactive Oxygen Species
RTLF	Respiratory Tract Lining Fluid
SC	Saline Control
SD	Surrogate Dose
SDS	Sodium Dodecyl Sulphate
SE	South East
SSC	Saline-Sodium Citrate Buffer
SW	South West
TBE	Tris Borate EDTA
TD ₅₀	Toxic Dose necessary to cause 50% damage
TGF	Transforming Growth Factor
TNF	Tumour Necrosis Factor
TSP	Total Suspended Particulate
3SD	3x Surrogate Dose
3SD(Fe ³⁺)	3x Surrogate Dose containing Fe ³⁺
3SD(-Zn ²⁺)	3x Surrogate Dose without Zn ²⁺
3Zn ²⁺	3x Zn ²⁺ Surrogate Dose alone

Abstract

The water-soluble fraction of 1950s London smogs and modern particulate matter (PM) is commonly associated with adverse cardio-pulmonary health effects. The cause of this may be due to metal ion content within the water-soluble fraction. This study was designed to further explore the possible correlation between PM bioreactivity and metal ion content whilst considering external factors such as local environment and seasonal variation. In order to gain a more comprehensive understanding of which metals could be implicated and their mechanisms of action, their bioreactivity (individually and in mixtures) was assessed *in vitro*. The principle metal ions deemed bioreactive *in vitro* were then used to generate surrogate metal mixtures in the exact proportions found in an original London 1958 PM sample. These mixtures were used to evaluate possible adverse effects both *in vitro* and *in vivo*, specifically investigating target organs (including lung and heart), using conventional toxicological analysis, histopathology and toxicogenomic macroarray technology.

A correlation was found between individual metal content and *in vitro* bioreactivity of particulate samples (in both ambient PM samples from Port Talbot and ROFA samples). Global factors such as particulate origin and seasonal variation were also identified as playing a role. A bioreactivity hierarchy of metals was then established: $\text{Fe}^{2+} > \text{Cu}^{2+} > \text{Fe}^{3+} > \text{VO}^{2+} > \text{Zn}^{2+} > \text{As}^{3+} = \text{Pb}^{2+} = \text{VO}_3^-$ indicating the importance of oxidation state and suggesting a role for redox mechanisms. Strong synergistic effects were observed between Zn^{2+} and various bioreactive metal ions (Cu^{2+} , Fe^{3+} , VO^{2+}) *in vitro*. However, this effect was limited to ions which could be readily reduced to a more active form (no synergy with Fe^{2+}). *In vivo*, the surrogate water-soluble metal mixtures gave rise to a transient (7-14 day) metal ion concentration and valence dependent increase in lung:body weight ratio, protein levels (pulmonary oedema) and differential cell counts (inflammation) in a dose and time dependent manner. Light microscopy of the lung tissue revealed an acute phase response to the instillation of the metal mixture with peripheral damage and inflammation followed by bronchiolisation, hyperplasia and increased collagen deposition in repair. There was evidence of organ-specific changes in RNA production in both the heart and lung. In both organs, the primary responses revolved around up regulating redox-specific, stress mechanisms and metabolism pathways, suggesting activation of xenobiotic biotransformation systems.

The conclusions drawn from this study indicate that although a bioreactive hierarchy of metals from ambient PM exists, the toxic potential of PM is liable to be determined by the synergistic, redox potential of combinations of components with zinc playing a pivotal role. Varying metal mixture surrogates caused damage *in vivo* and findings from genomic analysis pointed to oxidative response mechanisms being affected at the molecular level both locally and systemically.

CHAPTER 1

GENERAL

INTRODUCTION

1.1 Overview

The process of inhalation is a fundamental requirement for mammalian survival as the body requires a constant gaseous exchange to the bloodstream. This is the primary function of the lung, which has an extensive surface area (usually assumed to be 140 m² for a typical adult) as well as a rich blood supply to facilitate gas exchange. For these reasons, the lung is highly susceptible to damage from airborne toxicants, as the resting tidal volume for an average human is approximately 1 m³ per hour (Staub, 1993; Vincent, 1995).

The ambient air we breathe has become progressively more polluted and the process of breathing is becoming a more hazardous activity, as the respiratory tract is the first point of contact for airborne pollutants. Advances have been made in identifying and characterising the toxicological relationships between inhaled substances and the increased risk in disease. Research has highlighted particulate pollution as being very damaging to the lungs possibly due to its ability to produce reactive oxygen species (ROS) (Li *et al.*, 2003; Cho *et al.*, 2005) from many sources such as transition metals (Wilson *et al.*, 2002; Knappen *et al.*, 2002; Sorensen *et al.*, 2005). Due to the heterogeneity of different pollutants present in the air, the mechanisms of action of lung damage is poorly understood, hence the need for further research in this area of respiratory toxicology is significant.

1.2 Introduction - Gross Anatomy of the Human Lung

The respiratory system is a specialized and unique region of the body, which can be categorised into the upper and lower respiratory tract. The upper respiratory tract (extrathoracic region) comprises nasal and oral cavities, pharynx, larynx, and trachea. The lower respiratory tract (tracheo-bronchial and parenchymal regions of the lung) consists of the lower trachea, the two primary bronchi and the alveoli (Figure 1.2)

The lungs lie on either side of the mediastinum, which is situated in the thoracic cavity. They consist of a diverse network of airways, vessels, lymphatics, lymph nodes, nerves and supportive connective tissue. The lungs consist of five lobes in total, the right lung having three and the left lung two. The main bronchus branches into the bronchioles and then the terminal bronchioles. This region forms the conducting zone. The terminal bronchioles then branch into the respiratory

bronchioles and from this the alveolar ducts, alveolar sacs and finally the alveoli. Collectively, this region is referred to as the respiratory zone.

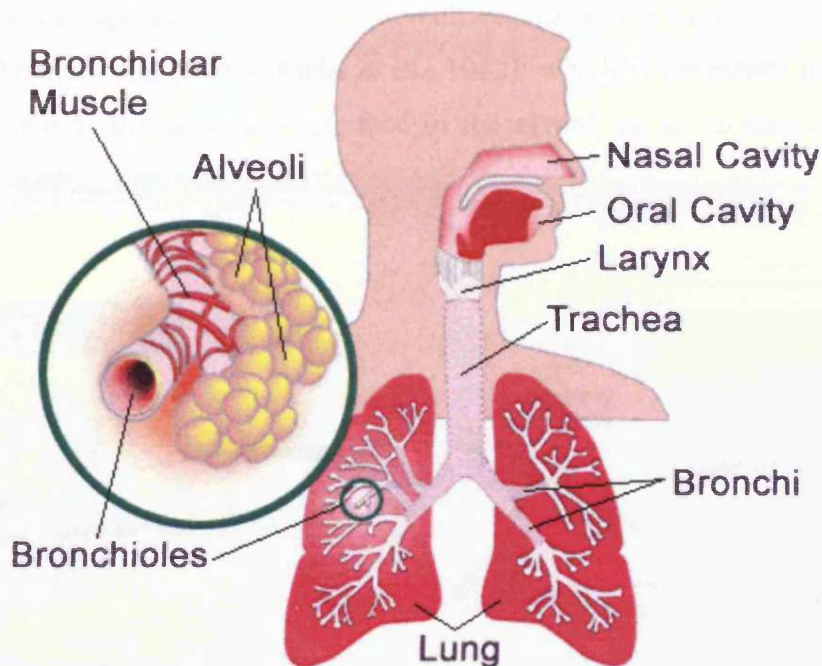


Figure 1.2 Diagram representing the different regions of the respiratory system (Ali, 2004)

1.2.1 Complex Anatomy of the Lung: the Alveolar Unit

The alveoli are blind ending terminal sacs which are tiny in size and there are thought to be approximately 300 million of these structures present in an adult lung. Due to their large number they account for the majority of lung volume and surface area. The components of the alveolar unit are depicted in Figure 1.2.1. The walls comprise two types of epithelial cells known as type I and type II pneumocytes. Type I cells are flat (squamous) epithelial cells exhibiting an attenuated cytoplasm containing flattened nuclei and few mitochondria. These cells represent approximately 40% of the alveolar cell population but within the alveolar unit, represent 93% of the alveolar surface (Mason *et al.*, 1977). Their flat attenuated cytoplasm provides for close proximity of the alveolar lumen and the bloodstream (pulmonary capillaries) thus forming the air: blood barrier for gaseous exchange of O_2 (from inhaled air) and CO_2 (from red blood cells). Type II pneumocytes (which are the progenitors of Type I cells)

comprise the remaining 7% of alveolar wall surface lining and account for 60% of the alveolar cell population. They are thick, cuboidal, epithelial cells, which are round in shape and highly specialised. Type II cells have a rounded nuclei, cytoplasm rich in mitochondria and microvilli on their surface. The microvilli aid in the distribution of antioxidants and specialised secretions. With regard to the latter, these secretions include pulmonary surfactant (Dobbs *et al.*, 1982), which is necessary to reduce the surface tension at the air-liquid interface in the alveoli so as to maintain alveolar stability.

Respiratory Bronchiole

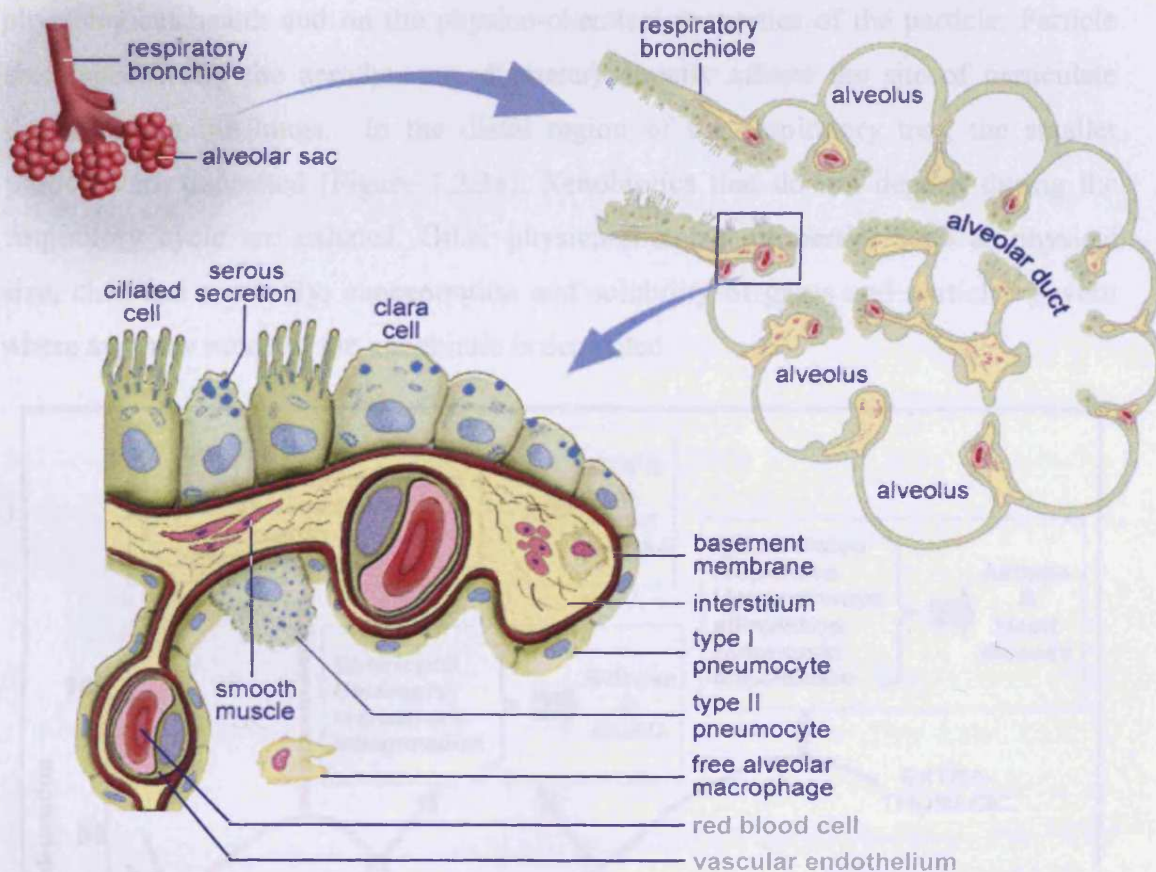


Figure 1.2.1. Architectural schematic of the respiratory bronchiole and alveolar unit (approximate alveolar diameter = 100 μ m) (adapted from McKee, 2002)

1.2.2 Functions of the Lung

The respiratory tract is functionally complex. Its primary function is to facilitate the flow of air from the mouth and nose via the airways to the alveoli. In the alveoli, gas

exchange can occur, thereby allowing the net movement of oxygen into the body via the bloodstream and the expulsion of carbon dioxide. It is also a site for metabolism via the cytochrome P450 system and potential biotransformation of xenobiotic compounds. Moreover, the respiratory tract plays a key role in acid-base balance, serves as a blood reservoir and has immunological capabilities (e.g. influx of macrophages and neutrophils).

1.2.3 Xenobiotic Deposition in the Lung

The respiratory tract is a portal of entry to many different xenobiotics. These foreign bodies undergo different processes of deposition depending on the inhalation technique of an individual (i.e. nasal or oro-nasal), the frequency and depth of breath, physiological health and on the physico-chemical properties of the particle. Particle size (specifically the aerodynamic diameter) directly affects the site of particulate deposition in the lungs. In the distal region of the respiratory tree, the smaller particles are deposited (Figure 1.2.3a). Xenobiotics that do not deposit during the respiratory cycle are exhaled. Other physico-chemical properties such as physical size, chemical reactivity, concentration and solubility of gases and particles govern where and how much of the xenobiotic is deposited.

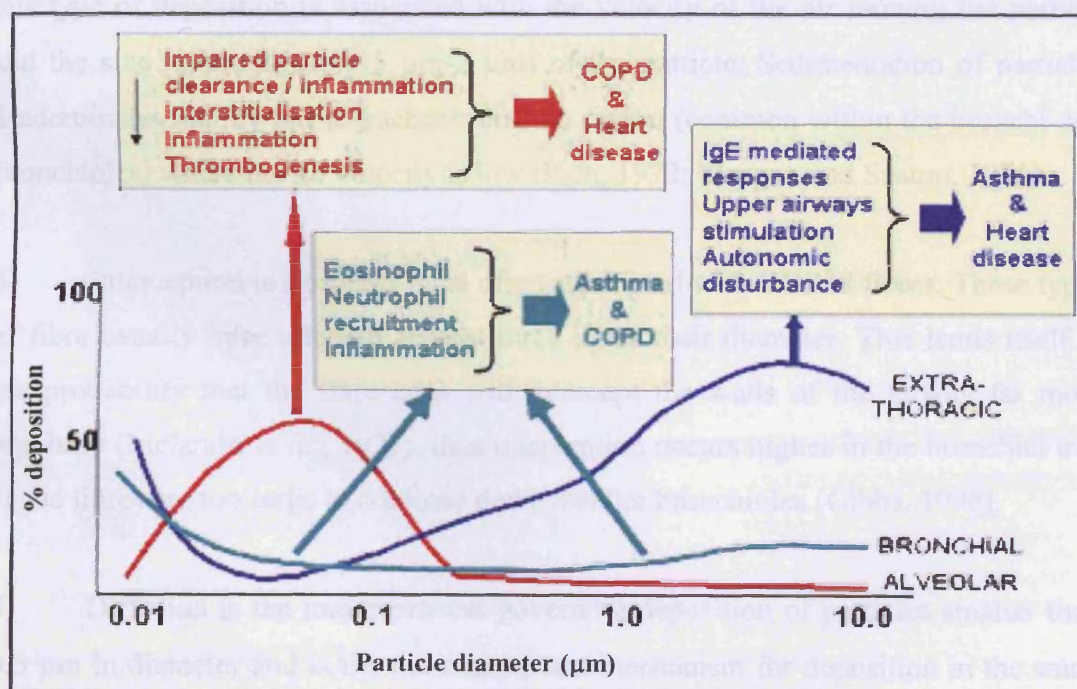


Figure 1.2.3a Fractional deposition of inhaled particles related to aerodynamic diameter (BeruBe *et al.*, 2005). COPD= chronic obstructive pulmonary disorder

There are four main processes associated with deposition of neutral xenobiotics in the lung: (1) impaction, (2) sedimentation, (3) interception and (4) diffusion (Chen and Yu, 1993; Sarangapani and Wexler, 1999). Aerodynamic characteristics of the particles have a large influence on the first three parts of this process:

1) Inertial impaction is the principle mechanism of large particle deposition within the upper airways and is dependent on the velocity and size of the particle. The prominence of this type of mechanism is due to the high air speed and the many turns in the nasopharyngeal airway as well as the branching of airways within the tracheobronchial region. This type of deposition occurs due to changes in direction of air-current within which the particles are suspended. Rather than following the airflow around a bend, suspended particles in the air travel along their original path due to their momentum and thereby impact and deposit frequently at bifurcation points within the respiratory tract (Brain and Valberg, 1979).

2) The process of sedimentation occurs when gravitational forces and air resistance overcomes the buoyancy of the particle in air (i.e. the tendency for the particle to stay airborne). The particles will thus settle on a surface of the lung and this type of deposition is associated with the velocity of the air moving the particle and the size (approximately 5 μm -2 μm) of the particle. Sedimentation of particles predominates mainly in the tracheobronchial region (common within the bronchi and bronchioles) where the air velocity is low (Pich, 1972; Morgan and Seaton, 1975).

3) Interception is a process most often associated with inhaled fibres. These types of fibre usually have a length at least three times their diameter. This lends itself to the probability that the fibre ends will intercept the walls of the airway far more regularly (Melandri *et al.*, 1977), thus interception occurs higher in the bronchial tree as the fibres are too large to continue down smaller bronchioles (Gibbs, 1996).

4) Diffusion is the major process governing deposition of particles smaller than 0.5 μm in diameter and is the most important mechanism for deposition in the small airways and alveoli (Ingham, 1975). The air within the alveolar region (the lower lung area) is essentially calm and the particles tend to move in a random motion until they deposit on the lung wall by chance.

The factors influencing deposition within the respiratory tract range from lung morphometry and breathing patterns to particle properties. Deposition of particles vary both intra- and inter-species. Intra-species difference affects deposition patterns due to the genetic biovariability of individual animals. Inter-species difference is an important point as understanding of the variances between species is crucial when extrapolating animal toxicology results to humans (Jarabek *et al.*, 1989), for example toxicological assessment of inhaled xenobiotics based upon animal studies may show effects that would not occur in humans. Moving down the respiratory system, the dominant deposition mechanisms change (Figure 1.2.3b). This is due to the velocity of the airflow changing. The velocity decreases in the lower regions of the respiratory tree because the cross-sectional area increases and thus the residence time of the airborne xenobiotic also increases, facilitating more passive deposition mechanisms.

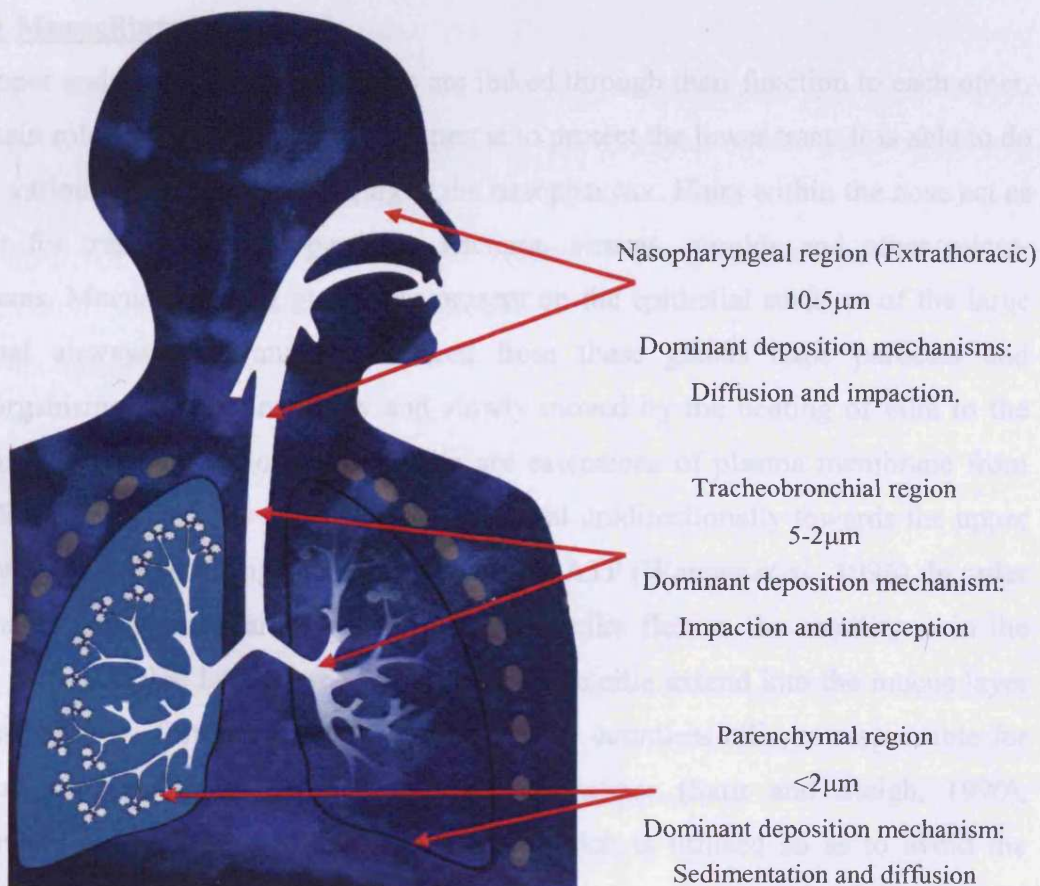


Figure 1.2.3b Sites and types of particle deposition in the respiratory system as related to particle size

1.3 Defence Mechanisms of the Lung

The lungs possess the largest surface area of the body in contact with the environment and thus provide an excellent pathway for infection or damage by inhaled foreign material (Halliwell and Gutteridge, 1989). Consequently, defence mechanisms are vital so as to reduce the risk of damage and to prevent infection. Defence mechanisms can be categorised as cellular, immunological or non-cellular defences.

1.3.1 Cellular Defences

Cellular protective mechanisms in the lung are composed of both chemical and physical entities. They include a mucociliary transport system, macrophage and polymorpho-nuclear leukocyte (PMN) recruitment and immunologic responses.

1.3.1.1 Mucociliary Transport

The upper and lower respiratory tracts are linked through their function to each other. The main role of the upper respiratory tract is to protect the lower tract. It is able to do this in various ways, such as filtering at the nasopharynx. Hairs within the nose act as a filter for trapping coarse particles, bacteria, viruses, moulds and other microorganisms. Mucus-secreting glands are present on the epithelial surfaces of the large proximal airways. The mucus produced from these glands traps particles and microorganisms and is continually and slowly moved by the beating of cilia to the pharynx where it is swallowed. The cilia are extensions of plasma membrane from specialised epithelial cells (ciliated cells) and beat unidirectionally towards the upper respiratory tract by utilising energy in the form of ATP (Wanner *et al.*, 1996). In order to minimise energy use and increase efficiency, cilia flex so the motility is in the serous peri-epithelial layer. Once fully re-coiled the cilia extend into the mucus layer thus propelling it forward. This cycle, repeated by countless cilia, is responsible for transport of xenobiotics up the mucociliary escalator (Satir and Sleight, 1990). Swallowing is another protection mechanism, which is utilised so as to avoid the aspiration of food. Chemicals, particles or infective materials can stimulate receptors located within the bronchi known as irritant C fibres. Upon stimulus a reflex contraction of bronchial smooth muscle occurs, which reduces airway diameter and increases mucus secretion. This process limits the penetration of the foreign body (Samet, 1994).

1.3.1.2 Macrophages

There are three types of lung macrophage; airway, interstitial and alveolar (Lohmann-Matthes *et al.*, 1994). The most prominent are alveolar macrophages which are found throughout the respiratory tract but predominantly reside on the alveolar surface lining or septal tissue and are derived from blood monocytes. They are the first line of cellular defence in the lower respiratory tract (Berg, 1993). Macrophages provide a double-edged sword with regards to being an important line of defence against xenobiotic particles. They engulf the foreign material in a process known as phagocytosis and are then transported up the respiratory tract by mucociliary clearance or transported to the lymphatic system. In the process of phagocytosis of particles, macrophages become activated and release a wide range of mediators such as ROS/reactive nitrogen species (RNS) including hydrogen peroxide and superoxide anions which induce PMN activation (van Eeden *et al.*, 2001). Also they release tumour necrosis factor alpha (TNF- α) which is a pro-inflammatory cytokine that can generate responses within the airway epithelium depending on the concentration of ROS and RNS present (Long *et al.*, 2004). A complex cascade of events may then commence via the initiation of signal transduction pathways, which lead to inflammation and contribute to airway pathology and tissue injury. The topic of ROS is discussed in greater detail in Section 1.5.1.

1.3.1.3 Polymorphonuclear Leukocytes

It has been postulated that PMN-induced apoptosis leads to the resolution of lung inflammation after bacterial infection (Meduri *et al.*, 1995) via phagocytosis (Monton and Torres, 1998). PMNs are inflammatory cells and are usually recruited as injury occurs. They circulate in the blood and as inflammation develops they accumulate in the capillaries and then migrate into the interstitium and epithelial cell barriers to gain access to the alveoli. Stimulated PMNs can have a detrimental effect on lung tissue due to the fact they have the ability to release proteolytic enzymes (Gadek, 1992), produce prostanoids (Grimminger *et al.*, 1988) and generate ROS (Knaapen *et al.*, 1999). They are usually associated with a more persistent inflammation forming a secondary line of defence following alveolar macrophage influx and are important in the modulation of the inflammatory response in the lung (Lam *et al.*, 2002).

1.3.1.4 Immunological Response

Another type of cellular response involves protective immune responses. These responses are usually in relation to inflammation and its regulation. A pro-inflammatory response is regulated by a group of small molecular weight proteins known as cytokines which accelerate inflammation. These inflammatory mediators include interleukin (IL)-1, -6, TNF- α (all responsible for acute phase effects), IL-8 and interferon- γ (phagocyte activation). The net effect of an inflammatory response is determined by the balance between pro-inflammatory cytokine and anti-inflammatory cytokines. Cytokines such as IL-4, IL-10 (inhibit pro-inflammatory cytokine release) and transforming growth factor (TGF)- β (growth inhibitor) play a role in anti-inflammatory responses (Fiorentino *et al.*, 1991; Schuerwegh *et al.*, 2003) (Figure 1.3.1.4). Attenuation of inflammation is necessary as prolonged inflammation can result in tissue damage and possibly the onset or exacerbation of certain types of lung disease. It is therefore necessary for lung inflammation to be regulated. Increasing evidence reveals persistent imbalances between pro-inflammatory and anti-inflammatory mechanisms as causative in diffuse lung disease as a result of increased pro-inflammatory mediators, as reviewed in Keane and Strieter (2001). It is clear that protective responses are necessary in combating damage caused by xenobiotics. As a result, in many *in vivo* studies, it is often indeterminate whether cellular injury is due to either initial toxicologic insult or the subsequent immunologic responses.

1.3.2 Non-Cellular Defences

Triggering of sensory nerves by a wide range of xenobiotics can induce a cough or a sneeze reflex to clear the extrathoracic region. These reflexes exert a physical force on the irritants, resulting in their propulsion up the tracheo-bronchial region from which they are expelled from the body by sneezing/coughing or swallowed down the gastrointestinal tract (Berger and Keller, 1983). Other non-cellular defences encompass the array of airway secretions found in respiratory tract lining fluid (RTLFL).

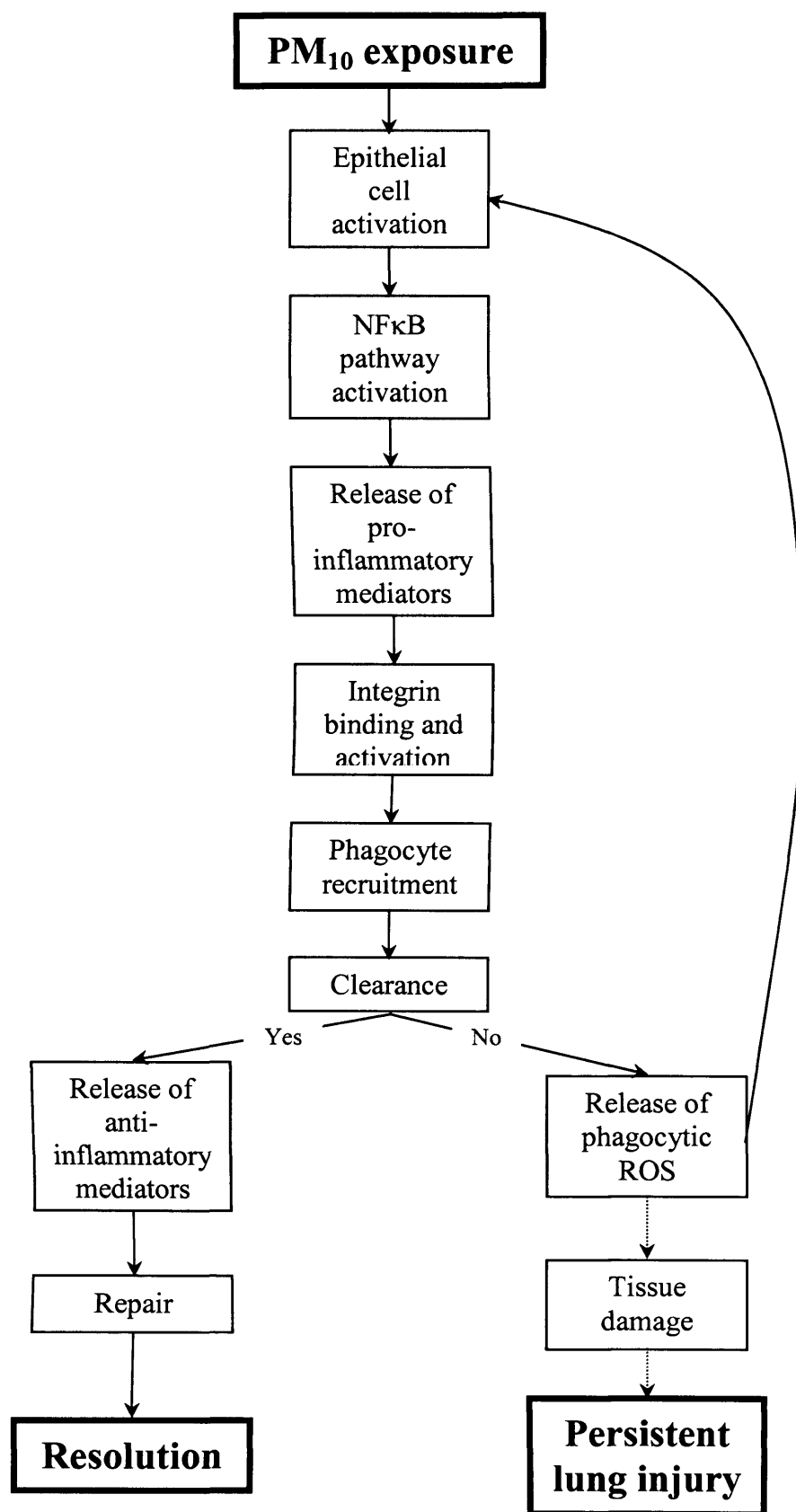


Figure 1.3.1.4 The putative immunological inflammatory response of the lung following xenobiotic inhalation

1.3.2.1 Respiratory Tract Lining Fluid

RTLF comprises a heterogeneous group of substances including phospholipids, apolipoproteins such as surfactant and small amounts of carbohydrate along with cellular debris. It is located within the nasal cavity and extends down to the alveoli and its composition and quantity alter throughout the pulmonary system. RTLTF exists as a bilayer comprising an upper mucosal gel phase and a lower aqueous phase (Quinton, 1979). Within this lower aqueous phase is epithelial lining fluid (ELF), which is located extracellularly and covers lung epithelial surfaces. The many components that are found within ELF hinder the progress of many toxicants and subsequently reduce the xenobiotic products that reach the epithelium. The components of ELF include metal binding proteins such as transferrin (which combat the oxidant effects of metal ions such as copper and iron), as well as antioxidant enzymes that are synthesised and secreted from epithelial cells (e.g. superoxide dismutase and glutathione peroxidase (Cantin *et al.*, 1987; Peden *et al.*, 1990). Also present are high-molecular weight sacrificial antioxidants like albumin, as well as various water soluble (e.g. ascorbate) and lipid soluble (e.g. α -tocopherol) non-enzymatic antioxidants. Their modes of action are summarised in Table 1.3.2.1a-d.

Table 1.3.2.1a Major pulmonary oxidant scavengers

Enzyme	Action
Catalase	Catalyses dismutation of H ₂ O ₂ , reduces methyl and ethyl hydroperoxides (Chance <i>et al.</i> , 1979; Heffner and Repine, 1990)
Superoxide dismutases	Catalyse dismutation of \bullet O ₂ to H ₂ O ₂ (McCay <i>et al.</i> , 1985)
GSH redox cycle GSH peroxidase	Catalyses reduction of H ₂ O ₂ and other hydroperoxides (lipid peroxides, lipoxygenase products) (Denke, 2000)
GSH reductase	Catalyses reduction of low-molecular weight disulfides (Denke, 2000; Winkler, 1992)
Glucose-6-phosphate dehydrogenase	Supply NADPH to the GSH redox cycle. Vital in protecting against oxidative stress (especially in red blood cells)

Table 1.3.2.1b High-molecular weight sacrificial antioxidants

Enzyme	Action
Tracheo-bronchial mucus	Scavenges inhaled oxidants (Cross <i>et al.</i> , 1994)
Albumin	Binds transition metals. Reacts with oxidants as a "sacrificial" antioxidant (Halliwell, 1988)

Table 1.3.2.1c Lipid-soluble compounds

Enzyme	Action
α -Tocopherol	Converts $\bullet\text{O}_2$, $\bullet\text{OH}$ and lipid peroxy radicals to less reactive forms. Breaks lipid peroxidation chain reactions (Bodner <i>et al.</i> , 1999)
β -Carotene	Scavenges $\bullet\text{O}_2$, reacts directly with peroxy radicals ($\text{ROO}\bullet$) (Comhair and Erzurum, 2001)
Bilirubin	Chain-breaking antioxidant. Reacts with $\text{ROO}\bullet$ (Comhair and Erzurum, 2001)

Table 1.3.2.1d Water-soluble compounds

Enzyme	Action
Ascorbate	Directly scavenges $\bullet\text{O}_2$ and $\bullet\text{OH}$ (Anbar and Neta, 1967). Neutralizes oxidants from stimulated PMNs. Contributes to regeneration of vitamin E (Packer, 1979)
Urate	Scavenges $\bullet\text{OH}$, $\bullet\text{O}_2$, oxoheme oxidants and peroxy radicals (Becker, 1993)
Glucose	Prevents oxidation of vitamin C. Binds transition metals Scavenges $\bullet\text{OH}$ (Pacht and Davis, 1988)
Cysteine	Reduces various organic compounds by donating electron from sulfhydryl groups
Cysteamine	Same as cysteine
GSH	In addition to role as substrate in GSH redox cycle, reacts directly with $\bullet\text{O}_2$, $\bullet\text{OH}$ and organic free radicals (Winkler, 1992)
Taurine	Conjugates xenobiotics, reacts with HOCl (Comhair and Erzurum, 2001)

For a more detailed review of these antioxidants, including a comparison between human and animal species the reader is referred to Kelly and Richards (1999).

1.4 Ambient Environmental Pollution

Air pollution (AP) is composed of a plethora of entities that can cause harm to many biological systems. Pollution can be defined as “the adverse effect on the natural environment, including human, animal or plant life, of a harmful substance that does not occur naturally, e.g. industrial and radioactive waste, or the concentration to harmful levels of a naturally occurring substance”. There are two main types of AP generated from a vast array of sources. The first is anthropogenic (man-made) pollution which is generated mostly from combustion sources. The second is naturally occurring AP, that is produced from volcanoes, forest fires, soil erosion and biological processes. Such pollution creates a wide variety of environmental problems that include damage to crops and vegetation, weather and climate change and acid deposition via acid rain. It can also be involved in metal corrosion and reduce the useful life span of materials such as leather, rubber and various fabrics.

Anthropogenic pollution arises from a number of identifiable sources such as coal burning plants, metal smelters or various motor vehicles such as planes, trains and automobiles (primary pollutants). It may also arise from chemical reactions within the environment (secondary pollutants). Primary pollutants are commonly found close to the emission source, whereas secondary pollutants are found to have a much wider area of distribution. The major pollutant classes are summarised in Table 1.4.

1.4.1 Historical Perspectives

AP has been seen as a potential source of adverse health effects from as early as Roman times (Brimblecombe, 1977, 1978). It was around the 13th century that two major events caused pollution to be more problematic. The first event was in the form of timber shortages, which caused people to revert to coal burning. This type of fuel combustion source created more carbonaceous particles when compared to wood burning and was severe enough by the 1280s to need regulation.

Table 1.4 Components of UK air pollution

Pollutant	Properties	Major sources	Damage caused
Sulphur Oxides (SO_x)	Acidic sulfate gases	Fossil fuel combustion and smelting	Reactive sulphate species modulate RTLF redox status (Giles <i>et al.</i> , 2001), cause upper airway irritation and allergenicity (Munoz <i>et al.</i> , 2004)
Carbon Oxides (CO_x)	Odourless, colourless gas	Burning of fossil fuels, transportation	Poisonous (CO) by oxygen abstraction from haemoglobin (Haldane and Priestley, 1935)
Nitrogen Oxides (NO_x)	Collective name for nitrogen oxides	High temperature combustion	Can form RNS – exert similar oxidative effects as ROS, and cause reduction in lung function (Ackermann-Liebrich and Rapp, 1999)
Ozone (O₃)	Odourless, colourless gas	Formed within the atmosphere	Cellular proliferation and alteration (Paige <i>et al.</i> , 2000) and lagged reduction in lung function (Thurston and Ito, 1999)
Volatile Organic Compounds (VOC)	Organic gases such as benzene	Incomplete combustion or evaporation of organic liquids	Initiate oxidative stress, can be allergenic (Diaz-Sanchez, 1997)
PM	Airborne, solid particles	Anthropogenic or natural	Transient inflammation, mild pulmonary oedema. (Murphy <i>et al.</i> , 1998)

The second major event was the emergence of cities, which caused a greater pollution density and thus, caused people to be exposed to a greater pollutant concentration.

Subsequently, the industrial revolution led to a significant increase in chimneys and the advent of the steam engine. Since the industrial revolution, the burning of coal and more recently the combustion of oil as a source of energy have figured largely in the western world. The impact of the resultant AP on urban mortality was observed during extreme fog episodes. These episodes in the early part of the 20th century were the main source of information on a link between poor health and AP and allowed detailed studies to be made on various populations. These studies include the Meuse Valley, Belgium (1930), Donora, USA (1948), London, UK (1952) and the Utah Valley, USA (1986-1988).

1.4.1.1 Meuse Valley

Located between the towns of Liege and Huy is the Meuse valley. Between the days of the 1st –5th of December 1930, a concentrated amount of metal rich pollutants sourced from the highly industrialised town of Liege had mixed with a thick fog (Roholm, 1937). This stagnant smog was attributed to adverse health effects such as laryngeal irritation, coughing fits and pulmonary oedema (Nemery *et al.*, 2001). More than 60 deaths occurred (Haldane, 1931), but a rapid resolution from these effects occurred after the fog had passed (Firket, 1936). This provided evidence that air pollution could lead to fatality (Nemery *et al.*, 2001).

1.4.1.2 Donora

A smog episode lasted 5 days between October 26th –31st, 1948 in a town called Donora in Pennsylvania, USA. This arose as a result of limited airflow in conjunction with fog and an accumulation of pollutants. The smog was rich in industrial contaminants, thought partly to be from the Donora Steel works and a zinc plant (Snyder, 1994). Up to half the residents of the 14000 populated town were adversely affected, with 400 hospitalisations and 20 fatalities (Bryson, 1998). Due to the scale of the disaster it paved the way for research to be carried out into the causes and control of AP and resulted in the enactment of the Air Pollution Control Act in 1955. Further acts in the latter half of the 20th century led to tighter controls and improvement in US air quality (Helfand *et al.*, 2001).

1.4.1.3 London

In December 1952 a stagnant air mass and a high-pressure system contributed to a smog episode which would be noted as one of the most dramatic pollution episodes in history. From an epidemiological perspective, it was a land-mark period as it was associated with 4000 deaths and thousands of hospitalisations (Ministry of Health, 1954). It is now accepted that this pollution episode is linked to 12000 deaths (Bell *et al.*, 2004). The deaths were derived from susceptible populations, such as the elderly, the very young and those with pre-existing cardio-respiratory disease. The particulate pollution of that era was very metal-rich (Whittaker, 2003) and this is hypothesised to have been causative in the onset of symptoms.

1.4.1.4 Utah Valley

Epidemiological studies in the late eighties by C. Arden Pope III were conducted looking at the association between fine particulates and health effects in Provo, situated in the Utah Valley. Due to the geographical morphology, communities situated in the valley were commonly subjected to temperature inversions during the winter, which trapped pollutants in stagnant air for days at a time. Various endpoints were studied such as hospital admissions, asthmatics' peak flows and death rates for pulmonary and cardiac diseases (Pope *et al.*, 1989, 1991, 1992). A chance closure of a steel mill for a year in 1987, while Pope was conducting his work, caused particle levels to drop and the subsequent fall in adverse health effects. This improvement diminished in 1988 when the steel mill reopened.

Ghio *et al.* (2000) saw this as a unique opportunity to evaluate whether ambient particulate matter (PM) toxicity varied before, during and after closure of the plant and whether this correlated well with epidemiological findings. Several *in vitro*, *in vivo* and human volunteer studies were conducted on the PM filters collected of the ambient air between 1986-1988. Bioavailable transition metal content (including zinc, iron and copper) was greater during the years the steel mill was open and this correlated to increased oxidant generation, cytokine expression and cytotoxicity *in vitro* (Frampton *et al.*, 1999). Increased metal levels in 1986 and 1988 correlated with pulmonary injury, inflammation and airway hyper-responsiveness *in vivo* even though the metal content comprised only 1% of the total mass of PM (Dye *et al.*, 2001). Human exposures to aqueous PM extracts before and after the steel mill closure

showed that experimental inflammation could be initiated. This was not seen with the 1987 sample because the mill was closed during that year (Ghio and Devlin, 2001). Chelex-treated (chelex is an inert polymer that can remove certain positively charged metal ions from aqueous solutions) aqueous samples of metal-rich PM displayed an attenuated toxicological profile compared to non-treated samples both *in vitro* and *in vivo* (Molinelli *et al.*, 2002). This particular piece of work has greatly supported the hypothesis that damage caused by PM is dependent on bioavailable metal content. The health effects in animal models and humans and the *in vitro* effects observed also correlated well with the epidemiological findings by Pope *et al.* (1995).

1.4.2 Particulate Pollution

Airborne PM is a heterogeneous mixture consisting of both natural and man-made particles. The particles are very diverse in origin, composition and aerodynamic behaviour. Those particles which are inhalable and thus, a risk to human health, fall into three general size fractions (which are source dependent):

- The coarse fraction is defined as all particles with an aerodynamic diameter of between 10 and 2.5 microns. The coarse fraction is made up of particles that are usually generated from mechanical processes, soil and other crustal material.
- PM_{2.5}, which is also known as the fine fraction, is defined as all particles having an aerodynamic diameter between 2.5 and 0.1 microns. The fine fraction contains a mixture of soot in association with metals and organic compounds. It also contains sulphate and nitrate particles.
- Ultrafine particles have an aerodynamic diameter of less than 0.1 microns. These contain the highest number of particles per volume and are derived primarily from diesel type exhausts of automobile engines.

Collectively, these three size ranges are commonly referred to as PM₁₀ (PM less than 10 microns aerodynamic diameter (QUARG, 1996)).

The coarse, fine and ultrafine are the common metric used to distinguish particles by size but the distinction is not clear cut. This is because larger crustal or salt particles often have many fine or ultrafine particles attached to their surface (Greenwell, 2003; Whittaker *et al.*, 2004). In addition, many ultrafine particles will aggregate e.g. diesel

exhaust particles (DEP) (BeruBe, 1998). Thus PM₁₀ particles can act as nucleation sites or co-transporters during transport into the lung.

1.4.2.1 UK Particulate Pollution

UK PM₁₀ is predominantly composed of primary particles from combustion sources, the majority of which, by number, are found in the ultrafine size range (Greenwell *et al.*, 2002) (Figure 1.4.2.1). The solubility of collected PM₁₀ varies according to geographical location and meteorological conditions (Moreno *et al.*, 2004). Metals were found to comprise up to approximately 5% of a typical PM₁₀ sample mass, with iron being the most predominant metal species, followed by zinc and copper (Harrison, 1995). From an epidemiological perspective, PM₁₀ is associated with both acute and chronic adverse health effects (Prescott *et al.*, 1998; Bremner *et al.*, 1999). Greenwell *et al.* (2002, 2003) demonstrated that PM₁₀ bioreactivity was retained in the water-soluble fraction and hypothesised that this toxicity could be due to ROS formation. This supports previous findings that the mechanism behind PM₁₀ toxicity is due to ROS, potentially catalysed by Fenton-type reactions (Donaldson *et al.*, 1997).

1.4.2.2 Residual Oil Fly Ash

Residual Oil Fly Ash (ROFA) is emission source PM that is formed from the anthropogenic combustion of oil. ROFA samples have a mass median aerodynamic diameter (MMAD) of around 2 µm. The MMAD is a statistically derived value. Taking ROFA as an example, it is calculated on the basis that 50% of the total sample mass present having an aerodynamic diameter less than 2 µm. ROFA is a chemically complex type of PM even though it contains few or no organic or biological components. Present in ROFA are many silicates, sulfates, carbon and nitrogen containing compounds along with an abundance of water-soluble metal salts (Costa and Dreher, 1997). There are many transition metal compounds contained in ROFA, in particular iron, vanadium and nickel compounds. Due to the physico-chemical nature of ROFA, it makes it a very useful surrogate for ambient PM in studies of biological effect. Many *in vivo* and *in vitro* studies have been carried out using ROFA so as to identify the health effects it initiates.

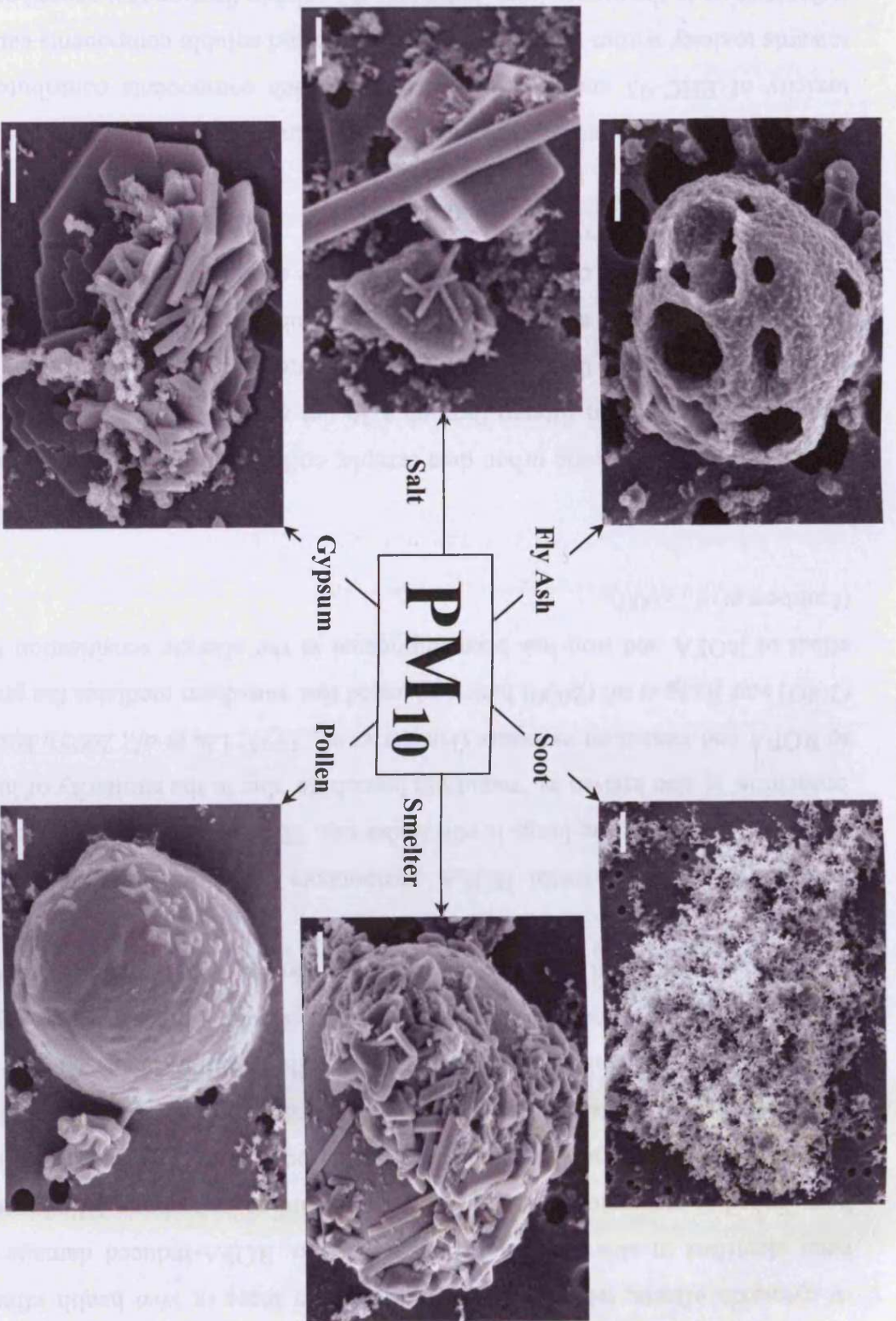


Figure 1.4.2.1 Scanning electron micrographs of typical UK PM₁₀ (adapted from Greenwell, 2003) (scale = 500nm)

In vivo ROFA has been shown to increase airway responsiveness (Dreher *et al.*, 1996), pulmonary fibrosis (Kodavanti *et al.*, 1997), enhance allergic sensitisation (Lambert *et al.*, 2000) and initiate lung inflammation (Dreher *et al.*, 1997). A number of cytotoxic effects, which may be implicated in these *in vivo* health effects, have been identified in airway epithelial cells *in vitro*. ROFA-induced damage has also been linked to systemic health effects such as cardiac arrhythmia (Watkinson *et al.*, 1997). The mechanisms by which these events occur could be due to the oxidative properties of the metals present in ROFA. Cellular damage has been linked to oxidative stress and linked to the depletion of cellular anti-oxidant capacity (Jiang *et al.*, 1999). These observations have been reinforced with work carried out by Ghio *et al.* (2002) who reported that extracellular SOD lowered the toxic effects of ROFA.

Research into which metal ROFA components are most important in initiating oxidative damage to the lungs is still underway. The industrial disease ‘Boilermakers bronchitis’ is also known as ‘vanadium bronchitis’ due to the similarity of lung injury to ROFA and vanadium exposure (Hauser *et al.*, 1995; Liu *et al.*, 2005). Huang *et al.* (2003) and Jiang *et al.* (2000) have suggested that vanadium mediates the pro-oxidant effect of ROFA and iron has been implicated in the allergic sensitisation to ROFA (Lambert *et al.*, 2000).

1.4.2.3 EHC-93

EHC-93 is an atmospheric urban dust sample, collected from ambient air in Ottawa, Canada which has been filtered through a 36 µm mesh. A large proportion (99%) of these particles is less than 3.0 µm in aerodynamic diameter. The sample contains various metals as well as sulfates and is 15% soluble by mass (Vincent *et al.*, 1997). The principle metallic components of the soluble sample are Al, Cu, Fe, Pb, Sn and Zn (Vincent *et al.*, 1997).

As with ROFA, instillation experiments have been carried out to assess the potential toxicity of EHC-93 and to try to ascertain which components contribute greatest towards toxicity within the lung. Both insoluble and soluble components caused mild inflammation in the mouse lung, but it was the soluble fraction that caused cell injury. Further research identified bioavailable zinc (the most abundant metal present in the soluble fraction) as the main toxic component within the soluble fraction of EHC-93.

This outcome supports previous research conducted by Amdur (1982) (guinea pig studies) and Richards *et al.*, (1989) (rat studies), who both identified zinc as a bioreactive component in the lung. An experiment using soluble metal salts identified copper as another potential cause of toxicity when at the same concentration at which zinc was in the dust sample (Preiditis and Adamson, 2002).

Work involving EHC-93 has thus implicated redox inactive Zn and redox active Cu within the soluble fraction of the PM as the main components exerting toxic effects within the lung (Adamson *et al.*, 2000)

1.4.2.4 Health Effects

Whilst assessment of immediate morbidity and mortality linked to PM exposure is easily monitored via epidemiological studies the assessment of lagged effects can be problematic. However, ambient PM is hypothesised to play a role in:

- Chronic respiratory and cardiovascular disease
- Alteration of body functions such as lung ventilation and oxygen transport
- Reduced work and athletic performance
- Sensory irritation of the eyes, nose, and throat
- Aggravation of existing disease such as asthma.

Over the last few years epidemiological studies have reported an association between adverse health effects in both children and adults with an increase in exposure to ambient PM. The association between PM and various human health endpoints range from acute difficulties to chronic disorders and from transient effects to mortality. There are many indicators of respiratory damage such as onset of wheeze and cough, shortness of breath, reduced lung function, chest discomfort, restricted activity, hospitalisation and mortality. There is also increasing evidence that an acute exposure to PM can be associated with cardiovascular mortality along with increased incidence of myocardial infarction and ventricular fibrillation (Table 1.4.4). PM has also been linked to the exacerbation of allergic responses such as rhino-conjunctivitis, eczema and asthma. Many of these issues have been extensively reviewed (Dockery and Pope,

1994; Pope *et al.*, 1995; Richards 1997; Brunekreef and Holgate, 2002). A summary of current epidemiology can be found in Table 1.4.4.

Table 1.4.4 Current epidemiology of ambient PM & total suspended particulate (TSP)

Area of focus	Effect	Reference
All-cases mortality Mortality	Active PM ₁₀ component resides mostly in fine fraction although absolute effects unclear	Anderson <i>et al.</i> , 2001
	Fine PM ₁₀ fraction correlates to mortality	McDonnell <i>et al.</i> , 2000
	Fine PM ₁₀ associated with respiratory, cardiovascular and all causes mortality	Samet <i>et al.</i> , 2000 Dominici <i>et al.</i> , 2005
	True correlation between PM ₁₀ and daily deaths – not affected by seasonal illness	Braga <i>et al.</i> , 2000
	Link between PM ₁₀ and all causes mortality stronger correlation between PM ₁₀ and mortality in pre-existing respiratory and cardiovascular disease sufferers	Schwartz, 1994
	Link between PM ₁₀ and mortality. stronger correlation with respiratory than cardiovascular mortality	Vajanapoom <i>et al.</i> , 2002
	Greater association with respiratory and cardiovascular diseases and air pollution	Bremner <i>et al.</i> , 1999 Johnson and Graham, 2005
	Deaths from respiratory diseases were associated with PM ₁₀ and TSP	Sandstrom <i>et al.</i> , 2005
	Small but significant association between concentrations of black smoke and respiratory mortality in the older age group	Prescott <i>et al.</i> , 1998

Mortality cont.	PM ₁₀ caused a time lag onset of respiratory mortality but immediate cardiovascular mortality	Braga <i>et al.</i> , 2001
	Evidence of a time lag relationship between mortality and air pollution	Campbell and Tobias, 2000
Respiratory system	Prevalence of nonasthmatic respiratory symptoms decreased as concentration of TSP decreased	Heinrich <i>et al.</i> , 2000
	Strong correlation between transient and persistent cough and phlegm and TSP exposure in adults and children	Zhang <i>et al.</i> , 1999 Sinclair and Tolsma, 2004
	Fine particles have much stronger respiratory effects than coarse	Schwartz and Neas, 2000
Cardiovascular system	PM has adverse effects on cardiac function and increases risk of cardiac death	Dockery, 2001 Pope <i>et al.</i> , 2004
	Air pollution causes immediate and temporal adverse cardiovascular effects	Glantz, 2002 Vallejo <i>et al.</i> , 2005
	PM exposure may exacerbate atheromatous plaque formation and destabilisation and reduces systemic antioxidant capacity	Donaldson <i>et al.</i> , 2001
Allergic disease	PM ₁₀ has a non-significant correlation with increased asthma incidence	Shima <i>et al.</i> , 2002
	PM can cause allergic sensitisation in genetically susceptible cases and can exacerbate allergic responses	Polosa, 2001 Gong <i>et al.</i> , 2004
	PM ₁₀ does not induce asthma but may exacerbate existing disease	Donaldson <i>et al.</i> , 2000
	Diesel exhaust particulate can may play an important role in the increased incidence of allergic airway disease by enhancing B cell differentiation and initiating and elevating IgE production	Diaz-Sanchez, 1997 Brunekreef and Forsburg, 2005

Lung cancer	Increased risks of incident lung cancer were associated with elevated long-term ambient concentrations of PM ₁₀	Beeson <i>et al.</i> , 1998 Cohen <i>et al.</i> , 2005
	Increase in PM concentration increases risk of lung cancer, mostly in susceptible groups	Donaldson, 2003

There is a high degree of subjectivity related to epidemiological studies, which needs to be validated by toxicological evidence. Polosa (2001) supported his epidemiological findings with toxicology, whereas Donaldson *et al.*, (2000) had a conflicting account but no toxicological evidence to support the findings. There seems to be a large body of evidence that suggests PM₁₀, and especially the fine fraction of PM₁₀, exerts a causative effect on all-cases mortality. Some findings suggest that there is no relationship between PM and all-cases mortality. However, in many cases time-lag relationships seem to have been overlooked. The findings of Campbell and Tobias (2000) indicate that episodes of increased PM concentrations lead to 'delayed' increases in health effects arising several days after the pollution event.

The effects of PM are not limited to the respiratory system. It also has marked adverse effects on the cardiovascular system. Due to the range of responses initiated by PM exposure (inflammation, sensitisation and carcinogenicity) a variety of toxic mechanisms have been hypothesised, which centre on PM-induced oxidation driven by the metal content of the particles and the subsequent generation of ROS.

1.5 PM-Induced Oxidation

PM is known to generate or induce generation of ROS. The production of ROS can cause an oxidative stress in biological systems. Due to the heterogeneity of PM, ROS production can be catalysed by different sources and the types of ROS differ depending on the source and mechanism of production. Sources of free radical production are transition metals, redox active quinones or polycyclic aromatic hydrocarbons (PAHs), which can be metabolically converted to redox active quinones in the lung (Greife and Warshawsky, 1993). PM also causes macrophages and

neutrophils to release ROS during a respiratory burst (Becker *et al.*, 1996, Goldsmith *et al.*, 1998).

1.5.1 Reactive Oxygen Species

It is hypothesised that the metals present in PM samples give rise to ROS. These ROS can cause a myriad of destructive effects in the lung and elsewhere around the body or are able to play an integral role in the modulation of several physiological functions. ROS, as the name suggests, are derived from molecular oxygen and can be generated at a low level in the lung by the transfer of an electron during aerobic metabolism (Figure 1.5.1). Endogenous derived ROS can be generated enzymatically by cytochromes P450 and NADPH oxidase (Finkel, 1999) within biological systems. They are required in cell signalling in the autocrine and paracrine systems (Suzuki, 1997) and can exert biocidal effects against tumor cells (Babior, 1978a/b). Excess amounts of ROS production can lead to inflammation and tissue damage (Halliwell *et al.*, 1992). The reduction of molecular oxygen by four electrons to form water yields several different ROS, which can be classified as radical species such as superoxide anion radical $\cdot\text{O}_2^-$, hydroxyl radicals ($\cdot\text{OH}$), hydroperoxyl radicals $\text{HO}_2\cdot$ and peroxy radicals ($\text{R-O}_2\cdot$). There are also non-radical species such as hydrogen peroxide (H_2O_2), ozone (O_3), singlet oxygen ($^1\text{O}_2$) and hypochlorous acid (HOCl) (Farber *et al.*, 1990). These species differ in function and reactivity with the hydroxyl radical being the most reactive (Aust and Eveleigh, 1999).

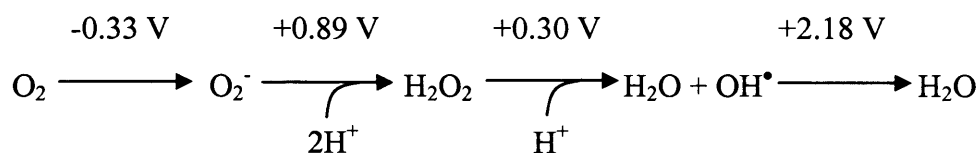


Figure 1.5.1 Redox potentials of ROS at pH 7.0 (Kanner *et al.*, 1987).

Significant amounts of the strong oxidant $\cdot\text{O}_2^-$ can be activated by sub-cellular organelles such as mitochondria, as well as granulocytes, especially PMNs (McDonald and Usachenko, 1999). Superoxide anions are charged particles and have difficulty in passing through the lipid bilayer of membranes, so they exert their effect by oxidizing certain anti-oxidants such as α -tocopherol, thus impairing its protective effects against lipid peroxidation (Bielski *et al.*, 1985). The conversion of $\cdot\text{O}_2^-$ to $\text{HO}_2\cdot$

can occur near the plasma membrane and it is this conversion of a hydrophilic to a hydrophobic molecule, which allows penetration through the membrane. Hydroperoyl radicals are weak acids and are moderately strong oxidants (Bielski *et al.*, 1985).

Hydrogen peroxide is a weak oxidant and is present at low concentrations in aerobic cells. It can be generated by a number of enzymes such as glycolate oxidase or aldehyde oxidase, as well as by sub-cellular organelles. It can be reduced to the far more potent $\cdot\text{OH}$ (Halliwell and Gutteridge 1989). The hydroxyl radical has a very short half-life and due to its solubility and high reactivity there are many target molecules which it can affect (Grisham, 1992).

There are three principal mechanisms where by ROS react to cause cell injury:

- DNA damage - strand breakages and point mutations (Aust and Eveleigh, 1999; Shi *et al.*, 2003).
- Lipid peroxidation - formation of pro-inflammatory molecules such as thromboxane (Minotti and Aust, 1992).
- Oxidation of proteins - alteration of protein activity and inactivation of antioxidant proteins (Fialkow *et al.*, 1994).

It should be noted that when all of these factors are categorised, they still lead to the same end-point and that is cell destruction.

1.5.1.1 DNA Oxidation

The consequences of this type of reaction are modified base and sugar moieties, DNA single strand and double strand breakage (involves two modifications to DNA in close proximity) (Box *et al.*, 2001), as well as DNA-protein cross-links. The oxidative modifications can lead to errors in transcription and conformational changes to the DNA molecule, thereby affecting its ability as a successful template and affecting cell division. These are a few of the changes that can be associated with the modulation of carcinogenesis and mutagenesis (Klaunig *et al.*, 1998).

Measurements of the products from ROS-mediated DNA damage can be used as biomarkers for oxidative stress. Eight hydroxyguanosine is particularly sensitive to

oxidation (Helbock, 1999) and forms 8-hydroxy-deoxyguanosine (8-OH-dG) (Floyd *et al.*, 1986). Its measurement is useful providing the product being measured is a consequence of the oxidative stress within the biological system and not as a result of oxidation during sample preparation (Dizdaroglu *et al.*, 2002).

1.5.1.2 Lipid Peroxidation

Plasma membranes and cellular membranes are primary targets for ROS. Double bonds found in fatty acid side chains of the phospholipids that make up the membrane undergo peroxidation by abstraction of a hydrogen atom. This process can be divided into three separate stages; initiation, propagation and termination (Figure 1.5.1.2). The abstraction yields a new radical species which is free to interact with molecular oxygen. The abstraction of another hydrogen atom by the peroxy radical is initiated and a chain reaction established. This affects the lipid composition and in turn affects membrane fluidity. The barrier function of epithelial membranes can be compromised during ROS attack. This can facilitate PMN recruitment in the lung and subsequent leakage of chemoattractant molecules such as chemokines. Some of the oxidised fatty acids are involved in signalling pathways which can result in apoptosis (Cummings *et al.*, 1997). The mechanistics behind the induction of apoptosis is poorly understood but possible candidates are thought to be lipid peroxides (Sandstrom *et al.*, 1994) or lipid messengers (Maccarrone *et al.*, 1997).

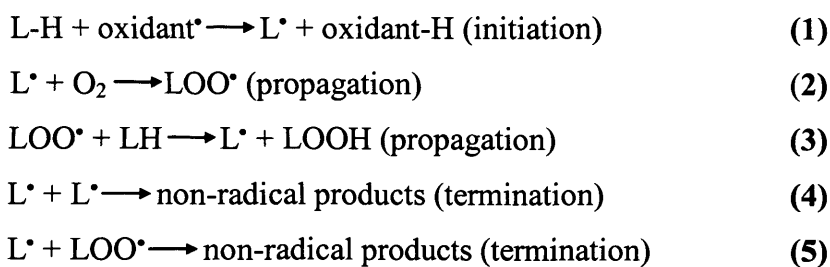


Figure 1.5.1.2 Oxidation of lipids (L = lipid); (Niki *et al.*, 2005).

1.5.1.3 Oxidation of Proteins

The oxidative damage caused to proteins by ROS is determined by a number of factors and different parts of the protein molecule can be affected. The mechanism involves the abstraction of a carbon linked hydrogen atom initiated by a hydroxyl free radical ($^{\bullet}OH$) (Davies, 1987, 1988, 2005). The modifications made to the protein vary

and have been reviewed by Stadtmann and Berlett (1991). They include the oxidation of the polypeptide backbone forming protein fragmentation or intra and inter-protein cross-linkages via formation of disulfide bridges. Amino acid residue side-chains may also be oxidised. Metal catalysed, site-specific modification of proteins (Requena *et al.*, 2001) may occur in the presence of Fe^{2+} or Cu^+ in conjunction with enzymatic and non-enzymatic mixed function oxidation systems (Stadtmann and Oliver, 1991).

The oxidation of proteins can lead to the generation of carbonyl derivatives. Elevation of such protein carbonyl derivatives can be measured and linked to various conditions such as Alzheimer's (Harris *et al.*, 1995), muscular dystrophy (Murphy and Kehrer, 1989) and respiratory distress syndrome (Gladstone and Levine, 1994). The oxidation of proteins usually render them inactive and they are removed from biological systems (Grune *et al.*, 1997), but an accumulation can occur which is related to ageing.

1.5.1.4 Metal-Induced Oxidative Effects

The common targets of metal-induced oxidation are found to be DNA and proteins. These are the subjects most frequently researched, as they have the greatest implications in health effects, possibly linked to carcinogenesis (Kasprzak, 2002). The mechanism by which metals exert oxidative damage is hotly debated. For example, Li *et al.*, (2001) found that DNA damage was differentially induced by Cu^+ and Fe^{2+} through Fenton-type mechanisms in a site-specific manner. This is supported by Toyokami and Sagripanti (1996). In contrast, Barbouti *et al.*, (2001) found that Fe but not Cu participated in DNA damage, and Aust and Eveleigh (1999) found DNA damage to occur in a site non-specific manner. They also found that oxidation of guanosine bases to 8-OH-dG can lead to GC-TA transversions, which could have promutagenic effects. Bal and Kasprzak (2002) also found that metals can have promutagenic effects through binding to histone proteins and causing subsequent DNA damage.

1.5.2 Metals

Analytical techniques, such as inductively-coupled plasma mass spectrometry (ICP-MS), have provided evidence that PM contains a large and diverse range of metallic elements that can be found in both the water-soluble and whole fractions. The metals

are bioavailable in the soluble fraction whereas they seem to be associated with large organic and silica based entities in the insoluble fraction (Whittaker, 2003). The most common metals found in PM are transition metals in addition to lead and arsenic.

The transition metals are characterised by atoms whose outermost electrons (valence electrons) are distributed between two electronic shells of different energy levels. This is in contrast to other metals whose valence electrons are present in one shell. Each atomic electron shell is designated by the numbers 1-7, then subdivided further into subshells. The first principal shell has one subshell designated as the *1s* shell. The second principal shell has two subshells designated as *2s* and *2p*. The third shell has three subshells designated *3s*, *3p*, and *3d*. The fourth shell has four subshells, *4s*, *4p*, *4d*, and *4f* etc.

As the electrons of the outer subshells in transition metals are so close in energy (*3d* and *4s*), all or most of these electrons can be involved in bonding even though they are subshells of different shells, facilitating several different possible oxidation states for which the transition metals are noted. This is attributed to the presence of valence electrons in more than one shell, whereas other types of metals have only one or two oxidation states, since they have valence electrons in only one shell. The ability for transition metals to exist in more than one oxidation state is fundamental to their reactivity and thus their ability to produce ROS.

Transition metals fulfil a variety of roles in biology. Cells rely on several transition metals to regulate a wide range of metabolic and signalling functions. The diversity and efficiency of their physiological functions are derived from atomic properties that are specific to transition metals, most notably an incomplete inner valence subshell. These properties impart upon these elements the ability to fluctuate among a variety of positively charged ionic forms and a chemical flexibility that allows them to impose conformational changes upon the proteins to which they bind. By these means, transition metals can serve as the catalytic centres of enzymes for redox reactions including molecular oxygen and endogenous peroxides

The metal-induced epidemiological effects (putatively induced by oxidative stress exerted by ROS) have been linked with many biological systems. The effects include

damage to both pulmonary and cardiovascular systems and other systemic organs. Negative effects caused by metal inhalation are reviewed in Table 1.5.2.

Table 1.5.2 Epidemiological effects of metals

Effect	Reference
Cu ²⁺ and Fe(^{2+,3+}) oxidative systems alter surfactant lipid and protein but not function	Mark and Ingenito, 1999
In terms of pro-inflammatory effects in the rat <i>in vivo</i> Cu ²⁺ >Mn ²⁺ =Ni ²⁺ >V ⁴⁺ =Fe ²⁺ =Zn ²⁺	Rice <i>et al.</i> , 2001
Concentrations of ascorbic acid, glutathione (GSH) and lipid determine oxidative effect of ROFA in RTLf	Sun <i>et al.</i> , 2001
Ultrafine particles and Cu ²⁺ and Fe ^{2+,3+} together potentiate ROS production <i>in vitro</i> and inflammation <i>in vivo</i>	Wilson <i>et al.</i> , 2002
ROFA's metallic constituents and pulmonary inflammation together mediate enhancement of sensitisation	Lambert <i>et al.</i> , 2000
Iron chelators reduce ROS-mediated damage <i>in vivo</i>	Marx and van Asbeck, 1996
Soluble transition metals induce pro-inflammatory effects of welding fume particulate	McNeilly <i>et al.</i> , 2004
PM metal concentration directly correlates to cardiac autonomic function variation	Magari <i>et al.</i> , 2002
ROFA induced ROS production in rat lung is equivalent to that of vanadium containing mixture or vanadium alone.	Kadiiska <i>et al.</i> , 1997
ROFA derived vanadium and nickel induced toxicity differ mechanistically	Kodavanti <i>et al.</i> , 1998
Different metal ions act by individual mechanisms producing distinct pulmonary effects	Johansson and Camner, 1986
Iron is essential for normal function however increased concentrations cause acute and chronic pulmonary damage	Quinlan <i>et al.</i> , 2002
Metals and pulmonary inflammation act adjuvantly	Costa and Dreher, 1997

PM ₁₀ causes iron dependent oxidation particularly in the macrophage lysosome	Gilmour <i>et al.</i> , 1996
Fe-doped combustion particles cause greater incidence of chromosomal aberration in mice	Park <i>et al.</i> , 2005
Fe ²⁺ not Cu ²⁺ causes intracellular DNA damage through a Ca ²⁺ dependent mechanism	Barbouti <i>et al.</i> , 2001
PM-induced cellular effects (proliferation and cellular metabolism) are linked to soluble metal content	Okeson <i>et al.</i> , 2003
Zinc counteracts iron induced oxidation by competitive inhibition and synergism with existing antioxidants.	Zago and Otieza, 2001
Evidence indicates that vanadate generates hydroxyl radicals via a Fenton-like rather than Haber-Weiss reaction	Shi and Dalal, 1993
Metals play a significant role in the pulmonary toxicity of welding fumes	Antonini <i>et al.</i> , 2004
Copper acts as catalyst in formation of ROS and catalyses peroxidation of membrane lipids	Chan, <i>et al.</i> , 1982
Administration of lead to rats results in production of ethane, an index of lipid peroxidation	Ramstoeck <i>et al.</i> , 1980
Metals from combustion-derived PM exert display different potencies in cellular toxicity (V<Zn<Cu<Ni<Fe)	Riley <i>et al.</i> , 2005
Iron causes hydroxyl radical production and lipid peroxidation by different mechanisms	Halliwell and Gutteridge, 1988

1.5.2.1 Copper

Copper occurs naturally in elemental form and is also a component of many minerals. It exists in two oxidation states, cuprous (Cu⁺) and cupric (Cu²⁺), and has many uses both in industry and physiologically (ACGIH, 1986). Due to its high electrical and thermal conductivity it is widely used in the manufacture of electrical equipment. Common copper salts such as sulfates, carbonates and sulfides are used as components of pyrotechnics and ceramics, electroplating, fungicides and in many other industrial applications. Physiologically, copper is an essential nutrient and is present in a wide variety of tissues. It is essential for the utilisation of iron and is a

component of a number of metalloenzymes such as catalase, peroxidases and cytochrome-c oxidase (Ferguson-Miller and Babcock, 1996). Metals such as copper are transported to the enzyme in which they are required e.g. SOD1 via metallochaperones (O'Halloran and Culotta, 2000)

Maintenance of copper balance within cells is essential as disturbances in copper homeostasis have been linked to cardiovascular disease and osteoporosis. Genetic modifications in certain copper transporting ATPases such as MNK can lead to Menkes disease. The MNK protein is located in the trans-Golgi network and relocates to the plasma membrane of cells with a high concentration of copper and thus is utilised in copper efflux. Modification in the protein thus affects its ability to aid in the maintenance of copper homeostasis within the cell (Petris et al., 2000)

Usually copper toxicity is associated with the cupric form rather than the cuprous. Short-term exposure to copper fumes or dust may cause headaches, vertigo, drowsiness and eye and respiratory tract irritation. A condition known as 'metal fume fever' can occur due to acute inhalation exposure and is characterised by an influenza-like syndrome with dryness in the mouth and throat. Inhalation of dusts of copper salts can result in irritation of the pharynx and the nasal mucous membranes. Also ulceration can occur with perforation of the nasal septum. Pulmonary copper deposition, granulomas and fibrosis have been reported in vineyard workers exposed to a mixture of copper sulfate and lime, with the exhibition of degenerative changes of the lung (U.S. AF, 1990). Systemic effects rising from chronic exposure to copper include renal failure, cardiac arrhythmias and depression of the central nervous system (Barceloux, 1999).

1.5.2.2 Iron

The two most important oxidation states in which iron exists is in the ferrous form (Fe^{2+}) and the ferric form (Fe^{3+}). Iron has considerable industrial and economic importance and more importantly, it plays a vital role in many biological systems. In humans, the majority of iron is bound to haemoglobin and is a constituent of many enzymes, cytochromes and myoglobin. Only a tiny proportion of iron is found in its unbound state because the majority of it is bound to iron-storage proteins.

Iron absorption and storage is tightly regulated, as iron overload is very hazardous and can result in organ and tissue damage due to free radical formation (Evans and Halliwell, 2001). Inhalation of iron has also been implicated in both acute and chronic lung injury (Pritchard *et al.*, 1996), as well as in allergic airway disease (Holgate and Finnerty 1988), commonly through ROS formation. This free radical formation may come about by a Fenton-type reaction and can only occur if iron is in its free state or catalytically active (Minotti and Aust, 1992). Iron can also induce free radical production via the decomposition of peroxides. Possible mechanisms of iron-mediated ROS production in the absence of reducing agents have been postulated (Lund and Aust 1990) (Figure 1.5.2.3). Certain xenobiotics can not only form ROS via redox cycling but also facilitate the release of complexed iron (Ryan and Aust, 1992).

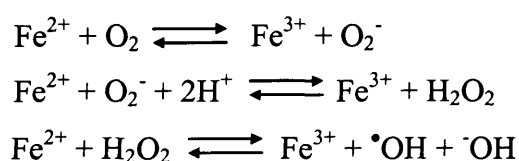


Figure 1.5.2.3 Fe-mediated ROS production in the absence of reducing agents

1.5.2.3 Manganese

Manganese can exist in many oxidation states (-3 to +7), the most common being +4 in the form of manganese dioxide. Manganese is an essential element in living systems and is most abundant in the +2 oxidation state. It is involved as an activator or cofactor with a number of diverse enzymes, in protein and lipid metabolism, energy metabolism and digestion. In industry, the metal is used in the manufacturing of metal alloys as it increases hardness and corrosion resistance.

The inhalation of manganese oxide can cause ‘metal fume fever’ beginning 4-12 h after exposure, which promptly diminishes after 24 h. No permanent damage is caused unless exposure is continuously repeated (Proctor *et al.*, 1988). Many epidemiological studies on human populations have produced findings that show an overlap to exist between the inhalation and oral routes of manganese exposure. This is because manganese present in particles greater than 2.5 microns are deposited in the

tracheo-bronchial and extrathoracic regions, then cleared via the mucociliary transport system and swallowed into the gastro intestinal tract. The respiratory system effects following chronic and subchronic exposures are colds, bronchitis, pneumonia and nasal irritation.

1.5.2.4 Vanadium

Vanadium occurs in many different chemical forms and in six oxidation states. In the body, vanadium can exist in the +4 or +5 oxidation state and can form chemical complexes with blood proteins. It has its uses in industry as an alloying agent in steels and various metals such as copper, titanium and aluminium and also applications as part of a superconductor. Vanadium compounds also have uses in industrial environments such as catalysts or in ceramic or chemical specialities and have minor uses as colour modifiers in mercury-vapour lamps, corrosion inhibitors in flue-gas scrubbers and dryers in paints and varnish.

Atmospheric vanadium is most prevalent in particulate form and in various studies the acute toxic effects of inhaled vanadium have been shown to be limited to the eye and respiratory tract with evidence of a latency period of 1-6 days before symptoms such as coughing, wheezing, sore throat and chest pain occur (Barceloux *et al.*, 1999). Long-term inhalation exposures to vanadium-containing dusts were reported to cause irritation to the respiratory tract with the most common symptoms being bronchospasm, pulmonary congestion and bronchitis (Guidotti *et al.*, 1997). However, chronic lung disease cannot be associated with exposure to vanadium compounds due to the lack of evidence. *In vitro*, vanadium compounds exert cytotoxic effects. They have been shown to reduce enzyme activity (Cortizo *et al.*, 2000), induce genotoxic and mutagenic effects (Stemmler and Burrows 2001), possibly through initiation of ROS, which have lead to DNA strand breaks (Shi *et al.*, 1996).

Research indicates that vanadium does not cause long term systemic toxicity. One reason for this could be that free vanadium which is likely to cause adverse effects, is in very low amounts within cells as it is bound to fat molecules (Nakai *et al.*, 1995).

1.5.2.5 Zinc

Zinc exists only in the +2 oxidation state and is commonly mistaken for a transition metal. Due to its stable *d* and *s* orbital configuration it lacks any redox properties (Williams, 1993). Zinc is an essential element and is present in all tissues. After zinc has been absorbed it binds to many protein complexes including metallothionein which acts as a carry and transport mechanism. Zinc is also a vital component in many enzyme systems including RNA polymerase, superoxide dismutase, alcohol dehydrogenase as well as in the metalloenzyme carbonic anhydrase, which regulates CO₂ exchange.

Zinc is also used in an industrial capacity, primarily in galvanising metals and metal alloys. Zinc salts have various commercial uses - zinc chloride is used in cements for metals, wood preservatives, in the manufacture of artificial silk, parchment paper, and glues. Zinc sulfate is used in agriculture, rayon manufacture and zinc plating. Zinc oxide is used in the rubber industry to slow down oxidation and as a vulcanization activator and accelerator.

Inhalation of zinc compounds has been associated with 'metal fume fever' and some individuals exhibit radiographic lung abnormalities. Inhalation of zinc chloride has been shown to produce oedema in rats (Richards *et al.*, 1989) and has been associated with ulcerative and oedematous changes in mucous membranes, advanced pulmonary fibrosis, respiratory distress syndrome and sub-pleural haemorrhage (Barceloux, 1999).

1.5.2.6 Arsenic

Inorganic arsenic exists in three oxidation states (-3, +3, +5), and these oxidation states along with the physical and chemical properties of the compound in which the arsenic occurs determine its toxicity. Trivalent arsenic is usually more toxic than the pentavalent form. However the toxicity of both these forms may also be dependent on the water solubility of the compound in which they exist. The less soluble compounds tend to cause chronic pulmonary effects if inhaled, whereas the more soluble forms tend to have systemic effects.

As with most particle deposition in the lung, size and water solubility are key determinants. Absorption via the pulmonary system may be difficult to quantify since a proportion of deposited particles may be cleared from the lungs via the mucociliary system, then swallowed and absorbed via the GI tract (Lagerkvist *et al.*, 1986). Various occupational health studies involving human inhalation exposures to inorganic arsenic provide good information on the type of acute and chronic damage caused (Gerhardsson *et al.*, 1988). Acute inhalation exposures can damage the mucous membrane, cause laryngitis and pharyngitis and cause the nasal septum to perforate (Mazumder *et al.*, 2000). Chronic inhalation exposures, as occurring in the workplace can lead to tracheobronchitis, rhino-pharyngo-laryngitis, hyperpigmentation, hyperkeratosis and peripheral vascular disorders amongst others (Morton *et al.*, 1989). Occupational exposure studies have shown a close positive correlation between arsenic exposure and lung cancer mortality.

1.5.2.7 Lead

Lead exists in one main oxidation state – Pb^{2+} . Lead is a soft, malleable metal with a bluish-white, silvery grey colour, which exists naturally as a sulfide in galena. In the presence of oxygen, water or weak organic acids can attack lead. Many of the lead salts are insoluble in water (carbonate, phosphate, sulfide, sulfate and oxides) with chloride being slightly soluble and nitrate and acetate being fully soluble (Budavari *et al.*, 1989).

Human exposure occurs primarily through ingestion and inhalation. Approximately 90% of inhaled lead particles deposited in the respiratory tract are absorbed into the systemic circulation compared with only 15% absorption of ingested lead. Once absorbed, lead is distributed to three main sites: blood, soft tissue and bone. There is evidence that shows that lead is a multitargeted toxicant causing effects in the cardiovascular system, G.I. tract, central and peripheral nervous systems (Triebig, 1984), kidneys (Cooper *et al.*, 1985), reproductive system and more. Lead can cause hypertension (elevated blood pressure) in the cardiovascular system.

1.6 Use of ‘Omic Technologies in Toxicology

The advent of ‘omic technology developed from the use of polymerase chain reaction (PCR) and other molecular biology techniques. Genomics facilitated the identification

of target genes for an extensive range of toxicological endpoints. The development of transcriptomics and proteomics then further identified whether observed gene changes were effectual on a cellular level (Pandey and Mann, 2000). Genomics and proteomics can be useful tools when monitoring interactions between genes, gene products and the environment (Afshari, 2002; Waters *et al.*, 2003). The functionality of these proteins can be studied using metabolomics (Nicholson *et al.*, 2002). Loosely termed the ‘omics’, these research tools are then combined in Systems Biology in order to gain a broader understanding of the mechanistic of the test system. These new technologies are being adapted rapidly throughout industry and academia to investigate a range of endpoints.

1.6.1 Toxicogenomics

Exposures of chemical and xenobiotics to biological systems and the mechanistic involved in the effects these toxins play are the basis of toxicological investigations. As research develops, closer scrutiny of these mechanisms at the molecular level is essential in the understanding of mechanistic behaviour. Toxicogenomics can broadly be defined as “the study of the relationship between the structure and activity of the genome (the cellular complement of genes) and the adverse biological effects of exogenous agents” (Aardema and MacGregor, 2002).

1.6.1.1 Applications of Toxicogenomics

Toxicant exposure, including inhalation of xenobiotics, can alter gene expression either directly or indirectly and the majority of toxicological effects are achieved under molecular control. Gene profiles can be constructed and the toxicological profiles of uncharacterised xenobiotics can be compared to established patterns, minimising testing costs and time compared to conventional toxicological methods. Application of this technology could benefit end-users in many other ways, including making improvements to public health policy (Henry, 2002) and risk analyses (Pennie and Kimber, 2002; Olden, 2004).

Mechanisms of toxicity can be also elucidated by analysing patterns of gene expression initially used as a ‘fishing’ tool. This can lead to identification of molecular targets of toxicants, biomarkers (important for effect and exposure) and improved mechanistic understanding (Pennie, 2000; Pennie *et al.*, 2000). The use of

this technology can also enhance toxicological understanding through identification of dose-response relationships from induction of toxicity. Utilisation of these data can provide the basis for chemical screening tools and predictive toxicology. Toxicogenomics has already been successfully applied to elucidating environmental effects on animal and human health (Reynolds and Richards, 2001; Whittaker, 2003; Schonwalder and Olden, 2003).

Toxicogenomics also has many clinical applications. This has already proved useful in identifying tumour-specific expression patterns (Perou *et al.*, 2000), molecularly-distinct disease sub-types (Alizadeh, 2000) and novel malignancy genes (Bittner, 2000). Possible future applications encompass the identification of novel candidate genes as therapeutic targets and subsequent development of preventative strategies, identification of novel markers for diagnostic and prognostic purposes (Olden and Guthrie, 2001) and prediction of endpoints. Work is currently underway in identifying susceptible populations (Lobenhofer *et al.*, 2001) and to elucidate inter-individual differences in substance metabolism based on genetic polymorphisms (Thomas *et al.*, 2002).

1.6.1.2 Negative Aspects of Toxicogenomics

Although 'omic' technology provides an exciting, novel opportunity in toxicology, it is not without its drawbacks. Primarily, the generation of a profligate amount of data without sufficient technical understanding can lead to misinterpretation and error, for instance the detection of subtle fold-changes in genes and analysis of their relevance. Without concurrent data regarding the relative up- or down-regulation of the functional proteins, significant findings can be overlooked and false positives followed. An example of this is the lack of distinction between causative (primary) transcriptional changes and subsequent 'knock-on' (secondary) changes.

The ultimate objective is to achieve a complete understanding of human toxicology, but as yet there are insufficient human data and human test systems with which to accomplish this goal. The poor inter-species correlation means the current reliance on extrapolation from animal models to human exacerbates inaccuracies (Vanden Heuvel, 1999). Also, as with all novel technologies, use of these systems is expensive, particularly when considering high throughput screening (Thomas, 2002).

1.7 Aims

Previous investigations have revealed that PM₁₀ has oxidative properties. These properties have been related to its ability to generate free radicals, which is commonly associated with bioavailable metals. The aim of the study was to investigate the toxicological properties of endogenous metals found in UK PM₁₀ *in vitro* and *in vivo*.

1. The first hypothesis under investigation in this study is that water-soluble metal ions present in ambient PM are the source of any observed bioreactivity. To assess the oxidative bioreactivity of PM₁₀ samples, collected from different sites around the UK, using a simple, *in vitro*, plasmid scission assay. Different fractions of these samples will be analysed using inductively coupled plasma-mass spectrometry (ICP-MS) to ascertain metal content. The bioreactivity of the predominant metals found in the water-soluble fraction will be assessed individually and in combination. The metals will also be analysed in combination with different size fractions of broncho-alveolar lavage fluid (BALF) to elucidate any attenuation in bioreactivity.
2. To test the hypothesis that the water-soluble metal content of PM can also inflict damage *in vivo*, the effects of appropriate mixtures of metal will be assessed *in vivo* using a non-invasive instillation technique. Various endpoints will be monitored including acute toxicity, inflammatory responses, persistent effects and recovery. Other parameters ranging from whole body pathology and changes in the epithelial lining fluid to the systemic distribution of the metals to various organs (including heart, liver and kidney) will also be studied.
3. To analyse the ultrastructural changes in pulmonary morphology histopathological assessment will be used. End points will include changes to airway thickness, collagen and fibrin deposition, as well as changes to airway microvasculature as well as any evidence of subsequent recovery from any observed damage with time.
4. The final hypothesis to be tested is that pulmonary exposure to water-soluble metals will cause alterations in the gene expression profiles of both the lung and heart and that these changes will be quantifiable shortly after instillation (within a

few hours). To obtain a more comprehensive molecular understanding of the toxicological mechanisms already identified, a toxico-genomic study of acute systemic effects will be carried out using leading edge macro-array technology.

CHAPTER 2

***IN VITRO* TOXICOLOGY**

OF AMBIENT PARTICULATE MATTER

2.1 Introduction

The mechanisms by which PM induces adverse health effects are still unknown. Compounds present in PM such as transition metals may be one of the contributing factors that could impact negatively on human health via their ability to produce reactive oxygen species (ROS).

The water-soluble fraction of PM, which is thought to have the greatest bioreactivity, is commonly rich in bioavailable metals including transition metals (Molinelli *et al.*, 2002). Previous studies have found this fraction to be oxidative (Greenwell *et al.*, 2002) and various links have been made and positive correlations found between the toxicity of the water-soluble fraction of PM₁₀ with the metal content. Studies using EHC93 (an ambient, atmospheric PM) suggested that cell injury and the observed pulmonary response were related to the soluble fraction (Adamson *et al.*, 1999). Incidence of adverse respiratory health effects in Utah Valley residents correlated well with pulmonary effects in rats (Dye *et al.*, 2001) and inflammatory effects *in vitro* (Ghio *et al.*, 1999) following exposure to the water-soluble fraction of PM. Ambient PM effects have also been found to vary in a metal dependent manner (Frampton *et al.*, 1999). Based on previous findings, the hypothesis tested in this study was that water-soluble metal component endogenous to UK PM₁₀ are the key factors determining bioreactivity of PM samples.

Reactivity of a PM sample may be determined by technogenic origins, which include road traffic and industrial sources. These sources may have a bearing on the metal composition of a sample of PM. Prevailing weather conditions such as wind speed and direction as well as rainfall and temperature have a bearing on the chemical content of collected samples (Sharan, 1996). Precipitation can induce a loss of particle mass in the air and high temperatures favour the resuspension of particles (Ragosta *et al.*, 2002).

The primary objective of this study was to assess the oxidative capacity of PM₁₀ samples from different emission sources in an urban-industrial conurbation and deduce which source had the greatest bioreactivity in both whole and water-soluble samples. Port Talbot (S.Wales, U.K.) was selected because its air quality regularly fails to meet government standards. From these results comparisons could be made

between bioreactivity and metal composition determined using inductively coupled plasma-mass spectrometry (ICP-MS). The samples were collected from the same location but from different wind directions (Figure 2.1). The wind directions represented different ambient conditions. The north east (NE) winds blew from the surrounding hills and countryside. The north west (NW) wind blew over the town. The south east wind (SE) was blown over the motorway and the south west/south east (SW/SE) was from the Port Talbot steel works and the motorway (wind direction fluctuated between SE and SW during this collection period).

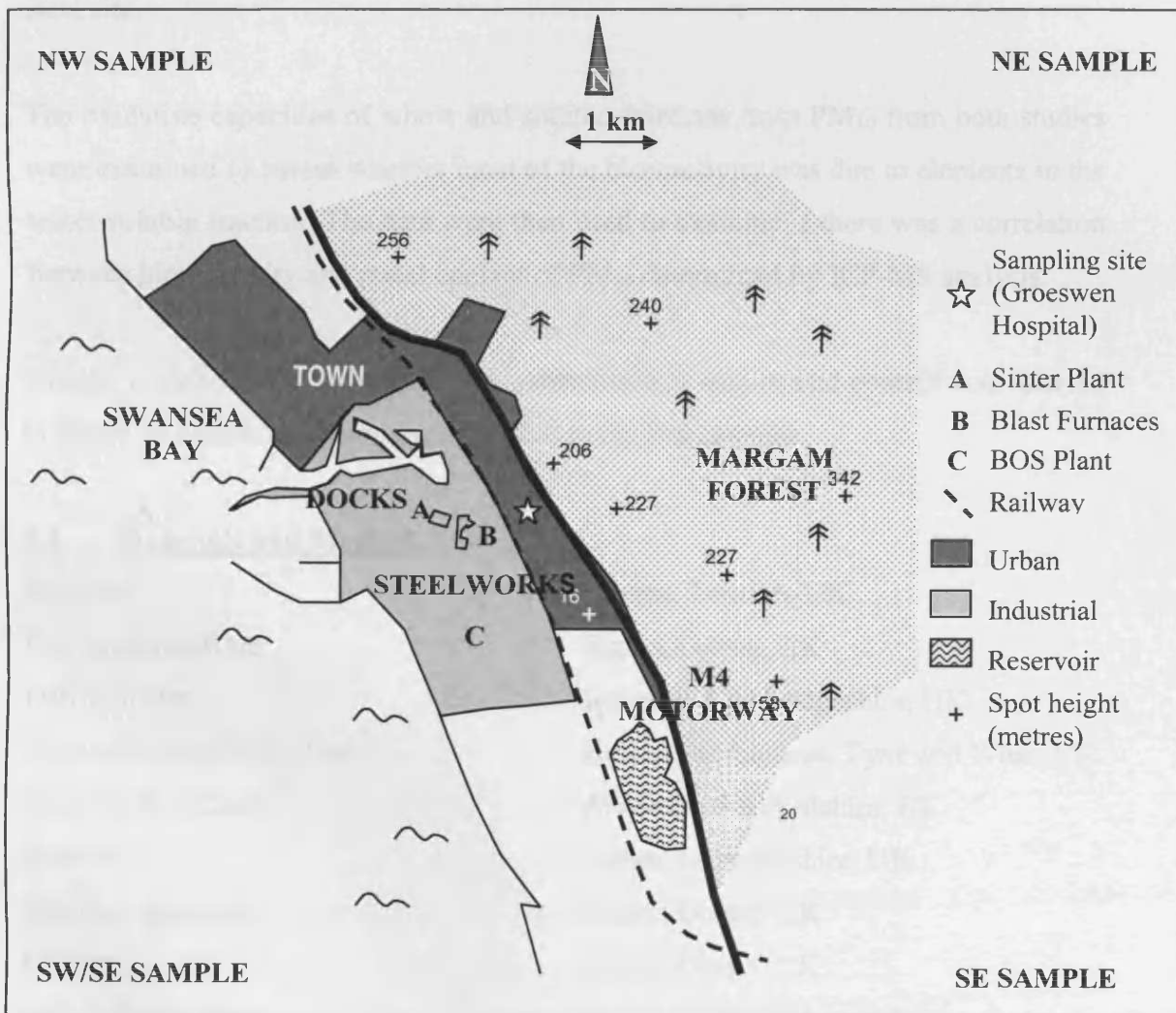


Figure 2.1 Location map of the site at Port Talbot where samples were collected (place marked with a star). (NE = Rural, NW = Urban, SE = Motorway, SW/SE = Industrial/Coastal) (adapted from Moreno *et al.*, 2004)

The secondary aim was to assess the oxidative capacity of PM₁₀ from five different locations in the UK, collected in two different seasons of the year using a high volume collector. The five locations were Birmingham, Cornwall, London, Port Talbot and Sheffield. The collections from each site allowed a broad cross-section of environmental surroundings to be analysed. Cornwall was chosen because it is remote and rural, whereas Birmingham and London are examples of urban inner city areas with high traffic density. Sheffield and Port Talbot were good examples of highly industrialised locations. Such a study should give a good indication of whether the more industrialised sites had UK PM₁₀ of a greater bioreactivity than samples from a rural site.

The oxidative capacities of whole and soluble fractions from PM₁₀ from both studies were examined to assess whether most of the bioreactivity was due to elements in the water-soluble fraction. The data were then used to examine if there was a correlation between bioreactivity and metal content of PM₁₀ determined by ICP-MS analysis.

Finally, a highly water-soluble ROFA sample with a large metal content was assayed to assess its bioreactivity and to compare it to the PM samples.

2.2 Materials and Method

Agarose	Bioline, London, UK
Bromophenol Blue	Sigma, Dorset, UK
Densitometer	Syngene, Cambridgeshire, UK
Electrophoresis Maxi Tank	Helena Biosciences, Tyne and Wear, UK
Eppendorfs (0.2ml)	Anachem, Bedfordshire, UK
Ethanol	Fisher, Leicestershire, UK
Ethidium Bromide	Sigma, Dorset, UK
Glycerol	Sigma, Dorset, UK
HPLC-Grade Water	Fisher, Leicestershire, UK
Microcentrifuge	Jencons, E. Sussex, UK
φX174-RF plasmid	Promega, Hampshire, UK
Tris-Borate-EDTA	Sigma, Dorset, UK
Vortex Genie 2	Jencons, E. Sussex, UK

2.2.1 PM₁₀ collection

The PM samples were collected at each site during two different times of the year in the five location study (Port Talbot wind direction study was carried out within one month), thus monitoring the effects of seasonal variation in emissions. The collection period ran from January 2001 to July 2003 and PM was collected on metal free polyurethane foam filters. All PM collections, sample preparation and ICP-MS analysis were generously conducted by Dr Teresa Moreno according to the protocol in Section 4.2.11.

Table 2.2.1 Airborne sample collection of PM₁₀ from five locations at varying times of the year

Location	Period	Total mass (mg)	Average mass mg/day
Birmingham (winter)	28/09/01- 01/11/01	450.42	13.65
Birmingham (summer)	17/06/02- 22/07/02	126.96	4.70
Cornwall (summer)	01/03/02- 27/05/02	860.61	14.34
Cornwall (winter)	07/01/03- 21/02/03	488.29	10.62
London (summer)	20/08/01- 17/09/01	322.51	11.52
London (winter)	11/01/02- 28/02/02	588.66	14.02
Port Talbot (winter)	01/11/01- 14/12/01	424.73	12.14
Sheffield (winter)	07/11/02- 06/01/03	793.33	13.22
Sheffield (summer)	09/06/03- 11/07/03	416.23	13.01

2.2.2 PM₁₀ and ROFA Preparation

The collected PM filter samples were each placed in pre-weighed 15 ml falcon tubes containing HPLC-grade water and shaken on a vortex genie for one hour followed by a 2 minute sonication. The filters were then taken out of the tubes and the particle solutions were divided in half. One half was centrifuged in a microcentrifuge for 80 minutes at 13000 rpm after which the supernatant was extracted into new pre-weighed tubes. All the tubes with either the whole fraction or the water-soluble fraction were frozen and then freeze-dried. The weights of the dried whole and water-soluble particles were subsequently recorded. Each sample was then reconstituted in sterile HPLC-grade water to a known final concentration.

The ROFA was obtained in dry powder form (kindly donated by Dr Kevin Dreher) and a known quantity was mixed with sterile HPLC-grade water to a specific final concentration. Dry ROFA powder was stored in the dark at room temperature and ROFA solutions were used immediately after generation in order to avoid any loss of bioreactivity seen previously in stored samples (data not shown).

2.2.3 The Plasmid Scission Assay

An *in vitro* assay was employed to assess the bioreactivity of different PM samples as both a whole fraction and a soluble fraction. The assay was designed to quantify oxidative damage to supercoiled bacterial DNA, initiated following incubation with varying concentrations of PM. The working hypothesis of the assay is that ROS produced/catalysed by PM “nick” the outer part of the supercoiled DNA which causes the molecule to unwind and change its conformation into a relaxed coil molecule, which has a far lower electrophoretic mobility. ROS can exert further damage by reacting with the relaxed form of the molecule causing the DNA to become linearised (Figure 2.2.3). The difference in mobility of these three forms of DNA allows them to be separated by gel electrophoresis and thus their relative amounts and proportions quantified by densitometric analysis (Greenwell *et al.*, 2002).

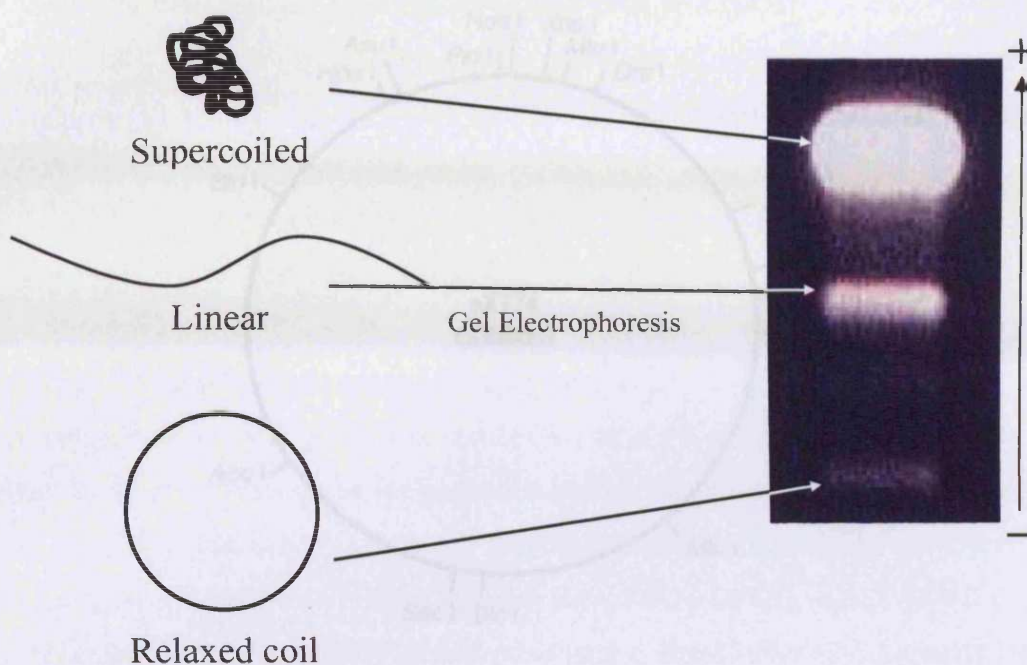


Figure 2.2.3 A schematic diagram of the plasmid scission assay denoting the separation of three categories of DNA by electrophoretic mobility following exposure to PM.

2.2.4 ϕ X174-RF Plasmid Selection and Preparation

The plasmid of choice was an icosahedral bacteriophage ϕ X174-RF with a molecular weight of 5,386bp (Figure 2.2.4). The plasmid was chosen as it had been shown to be optimal for the plasmid scission assay in previous protocols (Greenwell *et al.*, 2002) and because it had no antibiotic resistance genes meant it was quite susceptible to damage.

The ϕ X174-RF plasmid was bought in concentrated stock and stored at -80°C . In order to avoid any damage due to repeat freezing/thawing, the DNA was diluted to a concentration of $200 \mu\text{g ml}^{-1}$ using sterilised HPLC-grade water and then aliquoted into 40, 20, and 10 μl aliquots and stored at -80°C until use. After use, any residual DNA was discarded.

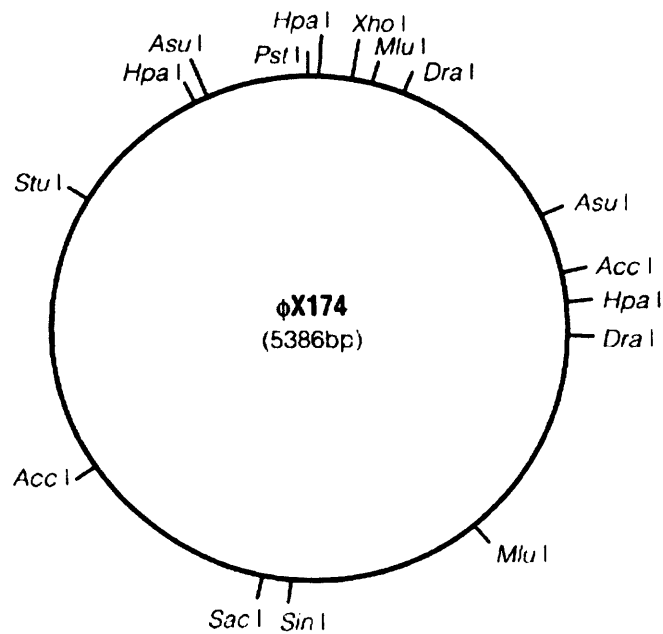


Figure 2.2.4 Plasmid map of ϕ X714-*RF* bacteriophage (taken from the Promega 2004 catalogue)

2.2.5 PM Test Sample Preparation and Incubation

PM samples were removed from the freezer and allowed to thaw at room temperature (approximately 24°C). The stock solutions were vortexed immediately prior to aliquoting in order to ensure full resuspension of any PM sedimentation. Small, concentrated volumes of the stock solutions were added to the test samples with the desired concentration of PM. The incubations were all made up to a final volume of 20 μ l each. This comprised 1 μ l plasmid (20 ng), the stock solution and remaining volume of sterile HPLC-grade water. The negative controls contained simply DNA and water and underwent the same incubation procedure as the test samples. The samples (n=4 per dose) were put on a gentle shake setting on a vortex-agitator for 6 h.

2.2.6 Agarose Gel Preparation and Sample Loading

The gels comprised 0.6% agarose in 450 ml 1xTBE. This was heated at 850 W for 4 minutes in a microwave oven in order to achieve the agarose melting point of 85°C. The agarose mixture was allowed to cool to approximately 40°C before addition of 10 μ l of 10 mg/ml ethidium bromide and was then poured into a sealed gel tray using two 40-tooth combs to create 80 wells each 20 μ l in volume. Gels were allowed to set

at room temperature for a minimum of 2 h. The gels were then placed into tanks containing 1% TBE buffer. After the incubation time had elapsed, 3.5 µl of loading dye (2 ml TBE, 80 µg bromophenol blue, 8 ml sterilised HPLC-grade water, 10 ml 100% glycerol) was added to each sample. The samples were then mixed thoroughly by pipetting and loaded into the wells. The gels were run for 16 h at room temperature in a 30 V electric field.

2.2.7 Quantification of Results

After 16 h the finished gels were photographed using the Genesnap program and densitometric analysis was performed using the Genetools program (both provided by Syngene systems). Densitometry was performed on the relevant areas of each lane and bioreactivity was calculated as the combined amount of DNA in the damaged forms (relaxed coil and linearised) as a proportion of the total amount of DNA in each lane. This yielded semi-quantitative data expressed as a percentage of damaged DNA in each lane. The amount of damaged DNA found in the controls for each gel was subtracted from the percentage damage resulting from each test dose. This subtraction was carried out in order to standardise each gel to ensure accurate comparisons, but the data was also used for quality control - only gels with between 10% and 20% damages in the controls were accepted for analysis. Therefore maximal damage of each test sample would be between 80% and 90% in each gel. Not all test samples achieved maximal DNA damage. However it was not deemed imperative for this maximum to be reached, as it did not affect the subsequent calculations. Four replicates of each test were quantified in this way and the means and standard errors were calculated. Dose response third order regression curves were generated from the resultant data (mean DNA damage plotted against PM concentration) and an arbitrary value was determined to facilitate comparison between PM samples. This arbitrary value was defined as the toxic dose of particles necessary to cause 50% of the DNA to become damaged (TD₅₀).

2.2.8 Statistical Analysis

All data handling and graphical representation of results were performed in Microsoft Excel '97. Statistical analyses included Andersson-Darling normality tests, 2-sample T-test and non-parametric Mann-Whitney tests. A two-sample t test was chosen as an appropriate test due to the data being derived from two independent random samples. This test was used if the data was normal and the variances were equal within each group. If this was not the case, a non-parametric Mann-Whitney test was used. All analyses were performed in Microsoft Minitab 13. Significance was assumed at $p \leq 0.05$. High significance was assumed at $p \leq 0.01$.

2.3 Results

2.3.1 Optimising the Quantitation Protocol

Previous studies using the plasmid assay have used a linear regression as a model to generate TD_{50} values. However in this particular study a linear regression was not suitable as the plots did not form a straight line (Figure 2.3.1a). A second order regression was also deemed unsuitable (Figure 2.3.1b). The graphs that were generated seemingly represented two parts of the reaction. Initially, the first part of the plot represented a Michaelis-Menten type reaction followed by a sigmoidal type plot as the second part. It was decided for the purpose of the exercise (which was to generate arbitrary TD_{50} values) to ignore the first part of the graph and model the second part using a third order regression plot (Figure 2.3.1c). All TD_{50} values using PM_{10} were generated in this way. The graphs were not strictly third order plots even though a third order regression gave the most accurate fit to the data points. TD_{50} values were determined graphically using gridlines.

2.3.2 Port Talbot Study - Bioreactivity

The samples collected in Port Talbot from the four wind directions were analysed using the plasmid scission assay. Both the whole and soluble fractions were analysed to assess the oxidative capacity and to evaluate whether there was a difference in bioreactivity between the soluble and insoluble fractions of the same samples. A dose response was observed for both fractions from each wind direction (Figure 2.3.2a-h).

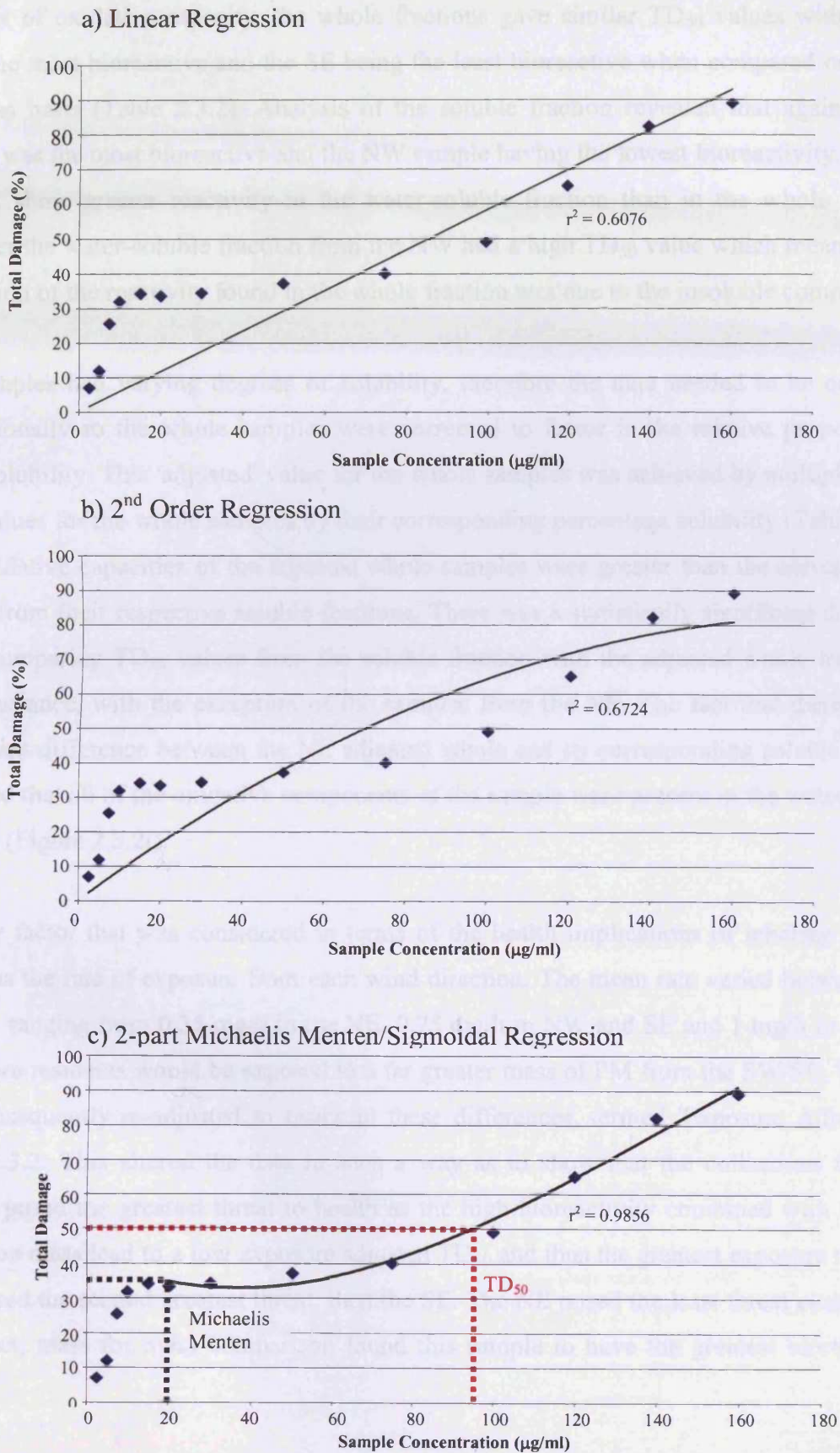
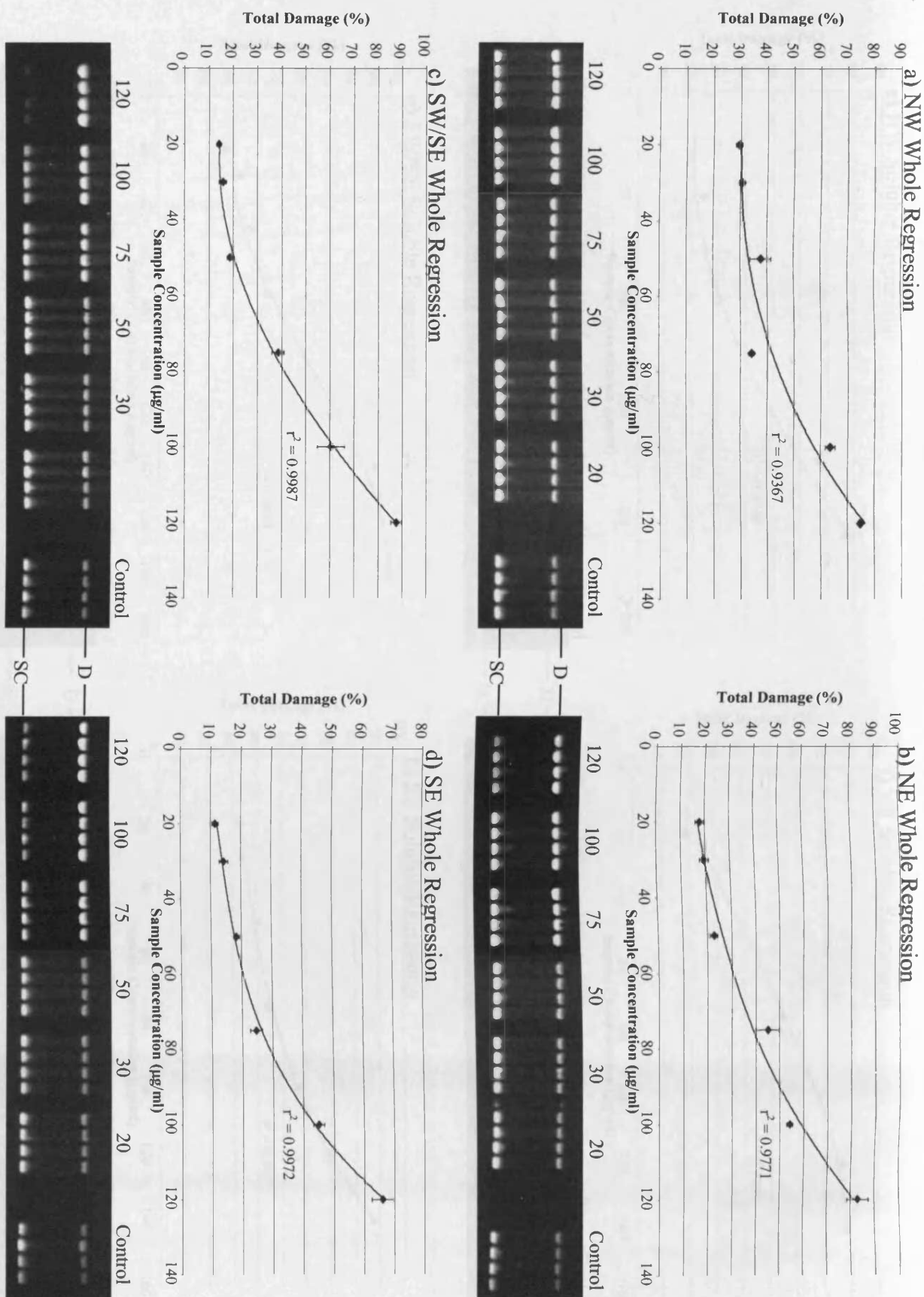


Figure 2.3.1a-c Mathematical modelling of a typical oxidative dose response

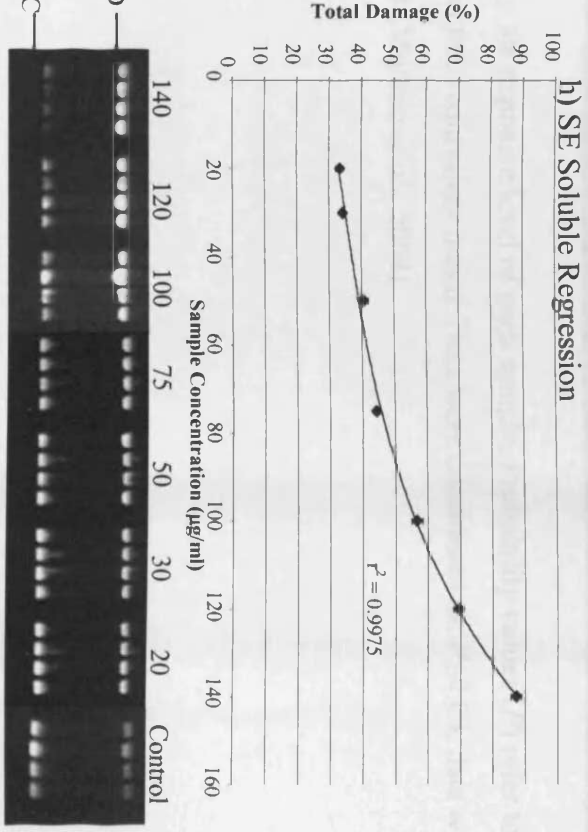
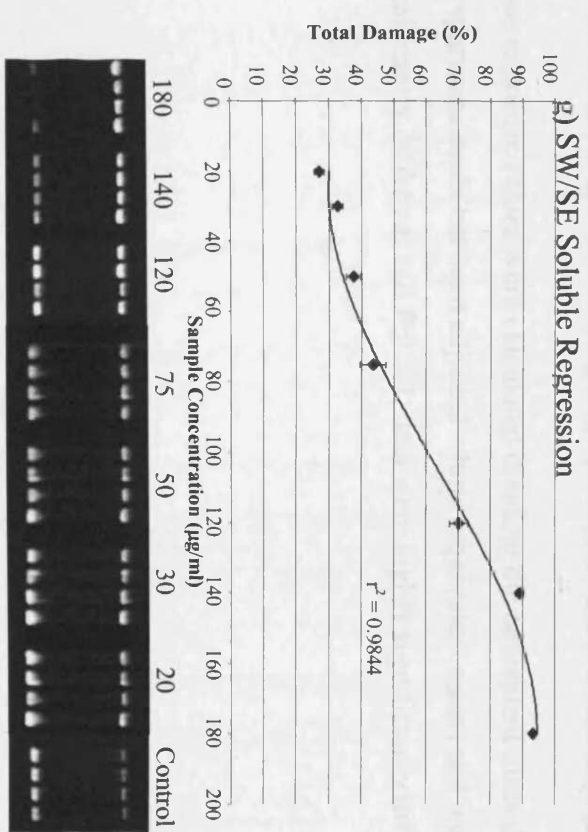
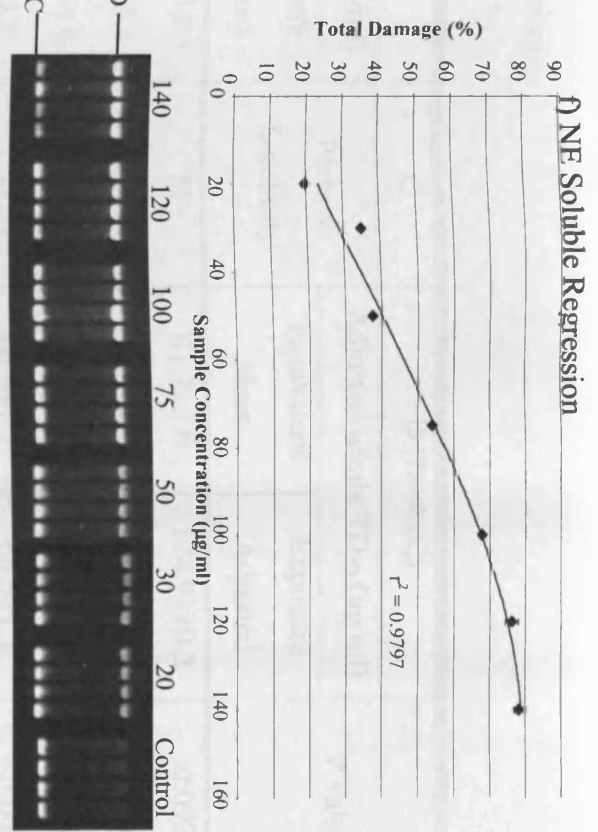
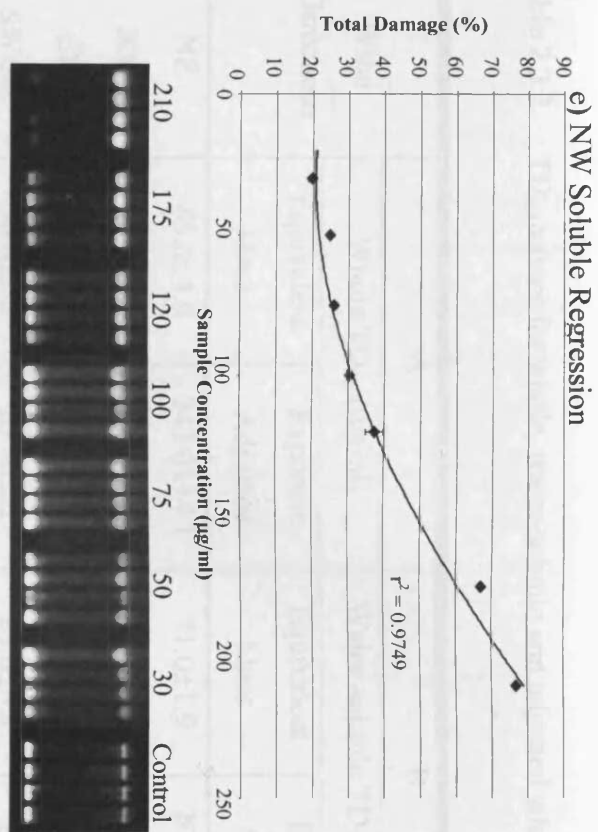
In terms of oxidative capacity, the whole fractions gave similar TD_{50} values with the NE being the most bioreactive and the SE being the least bioreactive when compared on a mass for mass basis (Table 2.3.2). Analysis of the soluble fraction revealed that again the NE sample was the most bioreactive and the NW sample having the lowest bioreactivity. The NE and SE show greater reactivity in the water-soluble fraction than in the whole fraction. However the water-soluble fraction from the NW had a high TD_{50} value which meant a large proportion of the reactivity found in the whole fraction was due to the insoluble components.

The samples had varying degrees of solubility, therefore the data needed to be compared proportionally so the whole samples were corrected to factor in the relative proportion of water solubility. This 'adjusted' value for the whole samples was achieved by multiplying the TD_{50} values for the whole samples by their corresponding percentage solubility (Table 2.3.2). The oxidative capacities of the adjusted whole samples were greater than the corresponding values from their respective soluble fractions. There was a statistically significant difference when comparing TD_{50} values from the soluble fraction with the adjusted whole fraction in every instance, with the exception of the samples from the NE. The fact that there was no significant difference between the NE adjusted whole and its corresponding soluble fraction indicated that all of the oxidative components of the sample were present in the water-soluble fraction (Figure 2.3.2i).

Another factor that was considered in terms of the health implications of inhaling ambient PM, was the rate of exposure from each wind direction. The mean rate varied between each sample, ranging from 0.35 mg/h in the NE, 0.75 mg/h in NW and SE and 1 mg/h in SW/SE. Therefore residents would be exposed to a far greater mass of PM from the SW/SE. The data was subsequently re-adjusted to factor in these differences, termed 'Exposure Adjusted' in Table 2.3.2. This altered the data in such a way as to show that the collections from the SW/SE posed the greatest threat to health as the high bioreactivity combined with the high collection mass lead to a low exposure adjusted TD_{50} and thus the greatest exposure risk. The NW posed the second greatest threat, then the SE. The NE posed the least threat even though the direct, mass for mass comparison found this sample to have the greatest bioreactivity.



Figures 2.3.2a-d Examples of typical dose-response regression analyses of whole fraction PM₁₀ from Port Talbot with associated gel images (SC = supercoiled, D = damaged). All concentrations in µg/ml. n=4 replicates per test, n=4 tests per sample.



Figures 2.3.2e-h Examples of typical dose-response regression analyses of water-soluble fraction PM₁₀ from Port Talbot with associated gel images (SC = supercoiled, D = damaged). All concentrations in µg/ml. n=4 replicates per test, n=4 tests per sample. 53

Table 2.3.2 TD₅₀ values for whole, water-soluble and adjusted whole samples

Wind Directions	A		B		C	D (D=AxC)		P value
	Whole TD ₅₀ (µg/ml)		Water-soluble TD ₅₀ (µg/ml)			Adjusted whole TD ₅₀ (µg/ml)		
	Equivalent Mass	Exposure Adjusted	Equivalent Mass	Exposure Adjusted	Percent Solubility	Equivalent Mass	Exposure Adjusted	
NE	85.0±4.9	243.0±14.1	71.0±1.9	202.9±10.7	72	61.2±3.6	174.9±10.2	0.092
NW	99.0±5.7	133.0±7.6	152.5±8.0	203.3±5.4	58	57.7±3.3	76.9±4.4	0.002
SE	106.0±1.3	142.0±1.8	87.5±3.4	116.7±4.6	62	65.9±0.8	87.9±1.1	0.009
SW/SE	86.0±2.2	87.0±2.2	89.0±0.8	89.0±0.8	77	66.6±1.7	66.6±1.7	<0.001

Mass exposure values were calculated dividing the equivalent mass data by the exposure level of each sample. Probability values (*P*) refer to comparisons made between adjusted whole (equivalent mass) and water-soluble (equivalent mass). Data were considered as: $P \leq 0.05$, data were significantly different, and $P \leq 0.01$, data were highly significantly different (Moreno *et al.*, 2004)

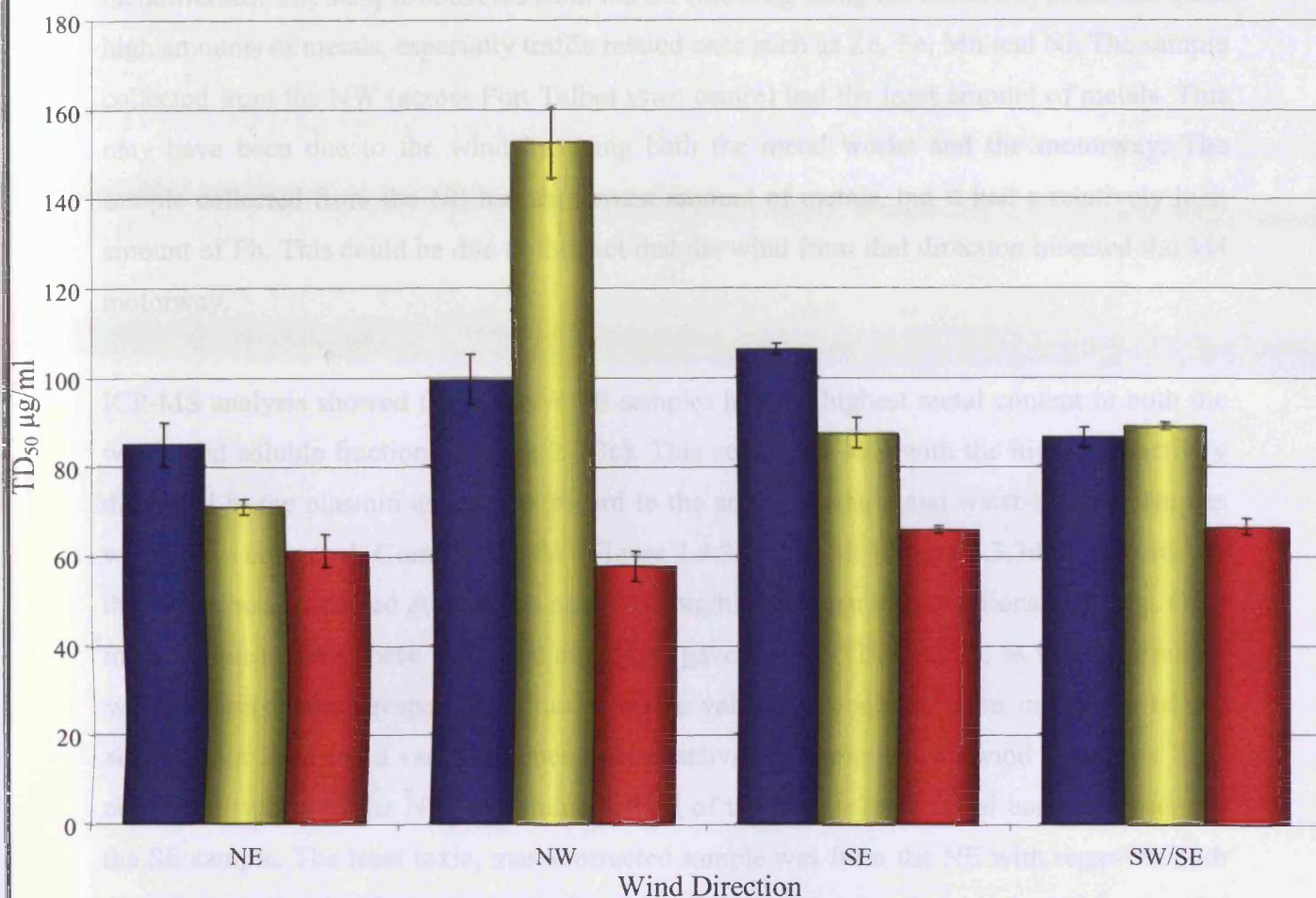


Figure 2.3.2i Comparison of TD₅₀ values for whole, soluble and adjusted whole fractions for each wind direction ■ = whole ■ = soluble ■ =adjusted whole (Moreno *et al.*, 2004)

2.3.3 Port Talbot - ICP-MS

The data from the plasmid assay were correlated with results obtained from ICP-MS analysis of the samples to identify any link between oxidative capacity and metal content. ICP-MS analysis was used as a method of qualitatively and quantitatively characterising the metal content of PM within the samples. The collection mass concentrations were adjusted to take account of the variation in collection rate (mg/h) during the four collection periods. The metal concentrations were normalised to those of the SW/SE sample as this was shown to have the highest collection rate. Fe and Zn were the most abundant metals in both fractions from all samples (Figure 2.3.3a-d). Fe, along with Ni, Ti, and Mo were scarce in the soluble fraction in comparison with their abundance in the whole fraction. The metals that were commonly found in the soluble form were Zn, As and Cu. The amount of metal varied between each sample, with the wind blowing from the SW (over the steel works) being the most

metalliferous. The sample collected from the SE (blowing along the motorway) also had quite high amounts of metals, especially traffic related ones such as Zn, Fe, Mn and Ni. The sample collected from the NW (across Port Talbot town centre) had the least amount of metals. This may have been due to the wind incurring both the metal works and the motorway. The sample collected from the NE had the lowest amount of metals, but it had a relatively high amount of Pb. This could be due to the fact that the wind from that direction bisected the M4 motorway.

ICP-MS analysis showed that the SW/SE samples had the highest metal content in both the whole and soluble fractions (Figure 2.3.3c). This correlated well with the high bioreactivity displayed in the plasmid assay with regard to the adjusted whole and water-soluble samples when mass corrected. Comparing NW (Figure 2.3.3a) with SE (Figure 2.3.3d) was useful as they were both collected at the same rate (0.68 mg/h) and when the conditions were dry. On a mass-for-mass basis these two wind directions gave similar TD_{50} values, as was determined when assessing their respective adjusted whole values. In contrast, upon inspection of the soluble data there was a vast difference in bioreactivity between the two wind directions. This correlated well with the NW containing a third of the total soluble metal content present in the SE sample. The least toxic, mass-corrected sample was from the NE with regard to both the adjusted whole and water-soluble fractions. This correlated well with the NE having the lowest total metal concentration (Figure 2.3.3b).

Further analysis was carried out to gain insight into whether a correlation between individual metal concentration and oxidative damage existed and to see whether oxidative capacity equates well with metal bioavailability. A trend line of oxidative capacity between each wind direction was generated for both adjusted whole and water-soluble mass corrected values. Trend lines for each metal concentration (ppm) were also generated to see whether any of the trends for the individual metals were of similar shape to that of the trend in oxidative capacity (Moreno *et al.*, 2004).

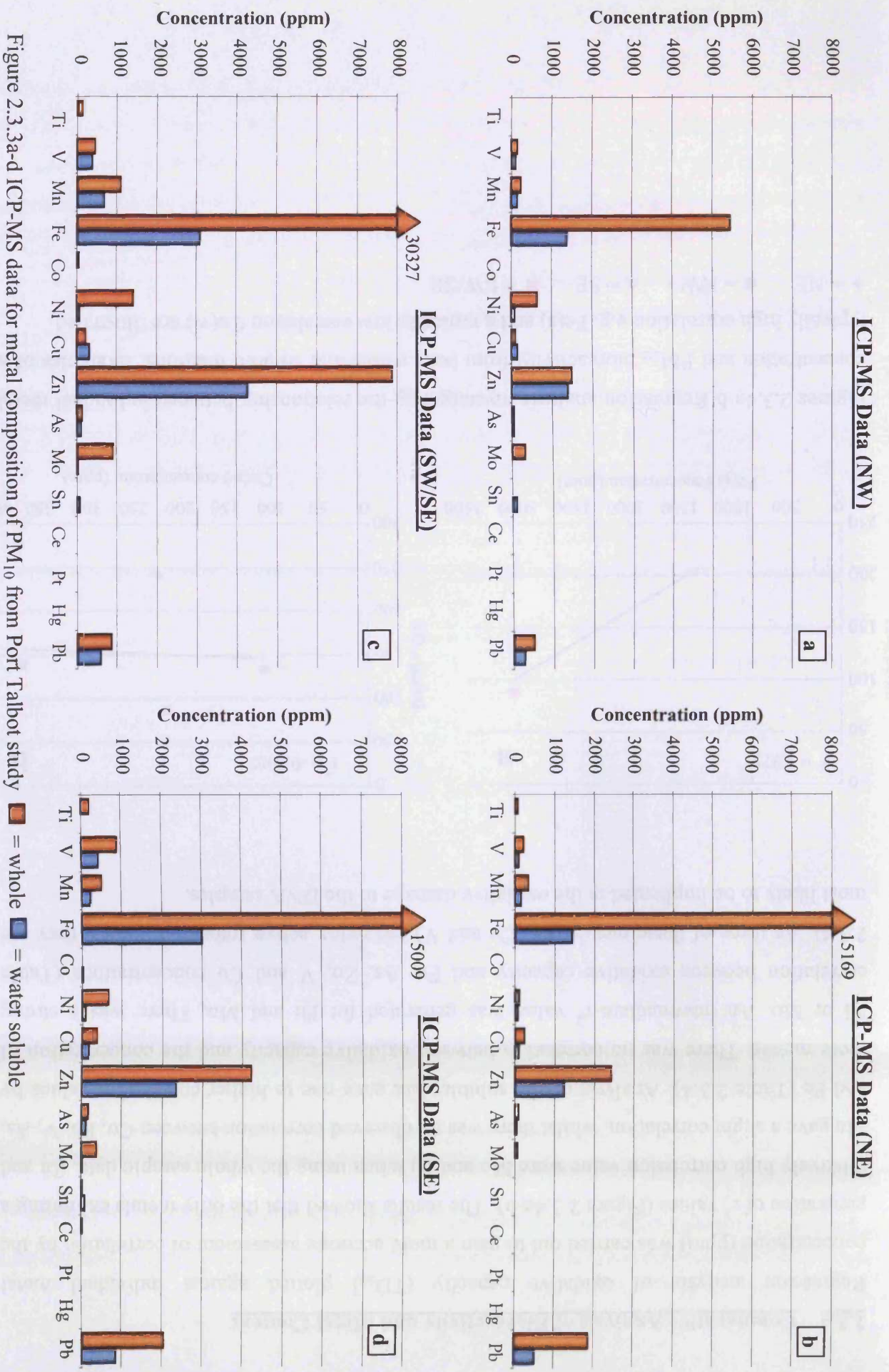
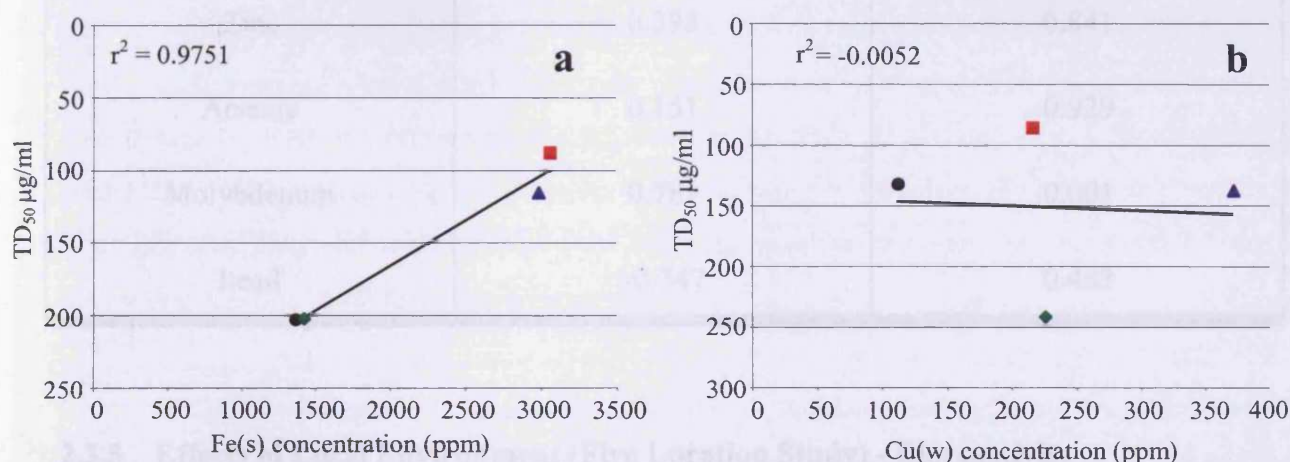


Figure 2.3.3a-d ICP-MS data for metal composition of PM₁₀ from Port Talbot study

■ = whole ■ = water soluble

2.3.4 Comparative Analysis of Bioreactivity and Metal Content

Regression analysis of oxidative capacity (TD_{50}) plotted against individual metal concentration (ppm) was carried out to gain a more accurate assessment of correlation by the generation of r^2 values (Figure 2.3.4a-b). The results showed that the only metals exhibiting a relatively high correlation value were Mo and Ni when using the whole sample data. Zn and Mn gave a slight correlation, whilst there was no observed correlation between Cu, Pb, V, As, and Fe (Table 2.3.4). Analysis of the soluble data gave rise to higher correlation values by more metals. There was no correlation between oxidative capacity and the concentration of Ni or Mo. An intermediate r^2 value was generated for Pb and Mn. There was a strong correlation between oxidative capacity and Fe, As, Zn, V and Cu concentrations (Table 2.3.4). As three of these metals (Fe, Cu and V) are redox active transition metals, they are most likely to be implicated in the oxidative damage to the DNA samples.



Figures 2.3.4a-b Regression analysis investigating the relationship between individual metal concentration and PM_{10} bioreactivity from both whole and soluble fractions. Examples of a typically high correlation e.g. Fe(s) and a typically low correlation Cu(w) are illustrated.

◆ = NE ● = NW ▲ = SE ■ = SW/SE

Table 2.3.4 Regression analysis values investigating relationship between individual metal concentration and bioreactivity of PM₁₀

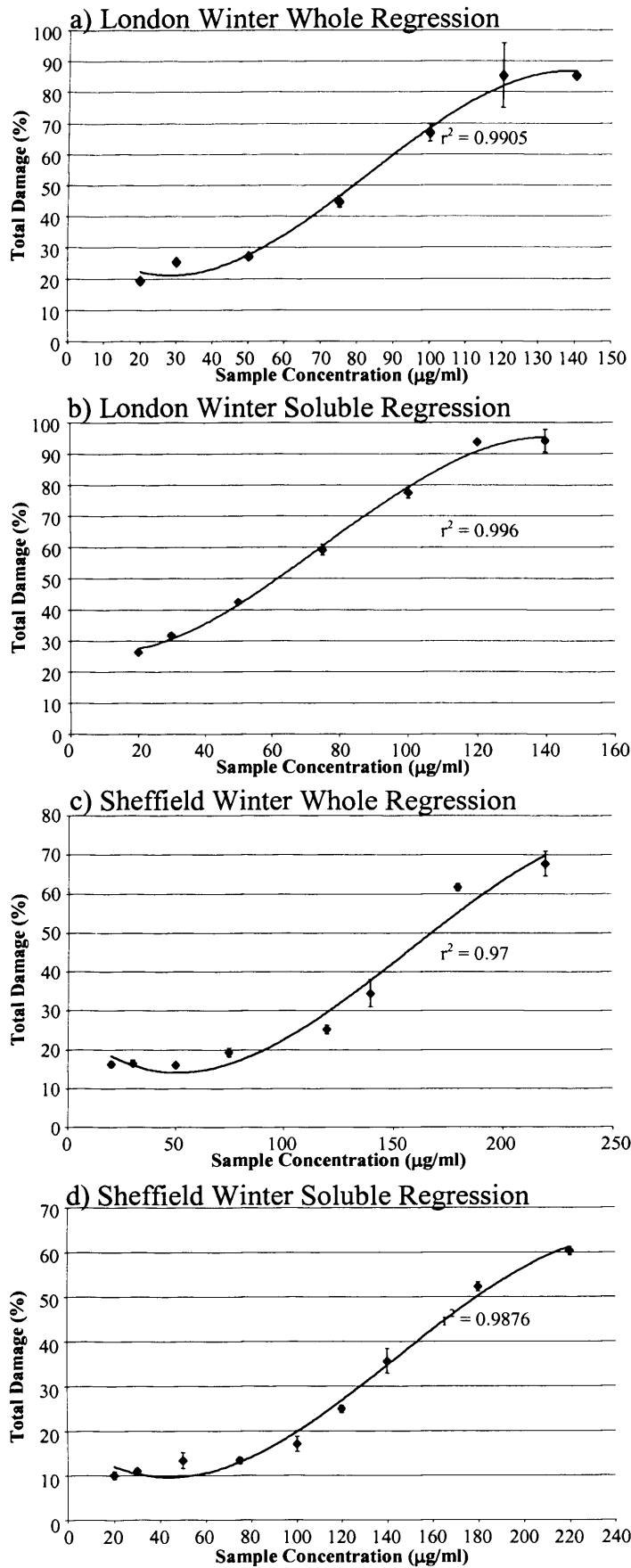
Metal	Regression Coefficient (r ²)	
	Whole	Soluble
Vanadium	0.097	0.895
Manganese	0.406	0.639
Iron	0.153	0.975
Nickel	0.871	0.023
Copper	-0.005	0.746
Zinc	0.398	0.841
Arsenic	0.151	0.929
Molybdenum	0.781	0.001
Lead	-0.347	0.443

2.3.5 Effects of Local Environment (Five Location Study) - Bioreactivity

The collection of airborne PM in five different locations revealed clear differences in the rate that each sample was collected (mg/day). The highest mass per day was collected in Sheffield in the winter (win) (22.67 mg) followed in turn by Cornwall in the summer (sum) (14.34 mg), London (win) (14.02 mg), Birmingham (win) (13.65 mg), Sheffield (sum) (13.01 mg), Port Talbot (win) (12.14 mg), London (sum) (11.52 mg), Cornwall (win) (10.62 mg) and Birmingham (sum) (4.70 mg). The particularly low level collected in Birmingham was due to the fan belt on the motor pumping system progressively failing during the summer collection. The local particle sources as well as meteorological conditions may have influenced the amounts of sample collected. Very wet periods, such as those present during the collection of the London summer sample and the Cornwall winter sample, suppressed the amounts collected.

The bioreactivity of each PM sample from the five locations was studied using the plasmid scission assay. Dose response plots were generated to assess the difference in reactivity between each of the samples. An example of this difference can be seen in (Figures 2.3.5a-d). The TD₅₀ values for each city were calculated using regression analysis for both their whole and soluble fractions. For each of the whole samples, the TD₅₀ values were adjusted to take into account their different percentage solubilities (Table 2.3.5). In terms of oxidative capacity, the whole fractions gave varying TD₅₀ values with London winter being the most bioreactive followed in turn by Cornwall (sum), London (sum), Cornwall (win), Birmingham (sum), Birmingham (win), Sheffield (win) and Port Talbot (win) being the least bioreactive when compared on a mass-for-mass basis. Analysis of the soluble fraction revealed a different hierarchy. As before, the London (win) sample was the most reactive. However Birmingham (win) was the least reactive and both the Cornwall samples were consistently lower in the order of bioreactivities. The adjusted whole data (referring to adjusted solubility) still revealed that the London (win) sample was the most bioreactive followed by Cornwall (sum), with Port Talbot and Sheffield (win) being the least reactive. When the soluble data was compared with the corresponding adjusted whole data, it showed that a considerable proportion of the bioreactivity found in the Cornwall sample was from the insoluble fraction. The data was also corrected to take into consideration the exposure as measured by the different collection mass from the different locations.

From an exposure perspective, the London summer air had the highest bioreactivity owing to the very high collection rate of 28 mg/day. Collections from different seasons in the same sites can result in very similar TD₅₀ values when examining the adjusted whole data, but very different TD₅₀ values for the soluble fractions, as exemplified by Birmingham and Cornwall samples. This may be due to differing local activities occurring throughout the year, be they industrial or urban. This may also be an artefact of meteorological conditions. Due to the extremely similar TD₅₀ values for the whole and soluble fractions of the London summer sample, it gave strong evidence that all of the bioreactivity came from the soluble fraction. This may also be true to a lesser extent for the London winter sample and the Sheffield summer sample.



Figures 2.3.5a-d Dose response regression analysis of whole and soluble fraction PM₁₀ from London (win) and Sheffield (win) (n=4 replicates per test, n=4 tests per sample).

Table 2.3.5 TD₅₀ values for whole, water-soluble and adjusted whole samples from the five locations

Location and Season	A		B		C	D (D=AxC)	
	Whole TD ₅₀ (µg/ml)		Water-soluble TD ₅₀ (µg/ml)			Percent solubility	Adjusted whole
	Equivalent Mass	Mass Exposure	Equivalent Mass	Mass Exposure	Equivalent Mass		Mass Exposure
Birmingham winter	122	209	78	133.7	65	45.39	406.8
Birmingham summer	112	381.8	210	716	63	70.56	240.6
Cornwall summer	76	187.3	204	502.7	81	61.56	151.7
Cornwall winter	87	337.9	137	532	87	75.69	293.9
London summer	79	79	61	61	79	62.41	62.4
London winter	51	120	58	136.5	89	45.39	406.8
Port Talbot winter	180	523.9	205	596.7	65	117	340.5
Sheffield winter	167.5	597.6	179	638.6	83	139.03	496.0
Sheffield summer	124	295.3	100	238.2	68	84.32	200.8

2.3.6 Effects of Local Environment (Five Location Study) – ICP-MS

As in the previous study, comparative analysis of the ICP-MS data along with the oxidative capacities were conducted to see whether there was any correlation between metal concentrations and bioreactivity of PM. ICP-MS data was gathered to assess the metal concentrations of each of the whole and soluble samples as in the previous Port Talbot study (Table 2.3.6). The amount of metal ($\mu\text{g/g}$ or ppm) present in each of the samples varied between the five locations. The highest total amount was found in the Port Talbot sample followed in turn by Sheffield (sum), Birmingham (sum), London (sum), Sheffield (win), Birmingham (win), London (win), Cornwall (sum) and Cornwall (win). The highest values were obtained from highly industrialised areas, which included steel works and high levels of traffic. The lowest values were from a more rural location that had much less traffic and no industrial sites located near the point of collection. Analysis of the ICP-MS data from the whole fraction showed that metal content in the summer for each location was higher than the corresponding values in the winter months.

The total metal concentration found in the water-soluble fraction was also measured from each site. A break down of the metal content and their relative amounts (ppm) for both whole and soluble fractions can be seen in Table 2.3.6. Some metals including Cu and Zn showed anomalous ICP-MS results in two locations, with higher values in the soluble fractions than in the whole sample. This may be due to problems in analysing highly soluble metals or heterogenous samples containing metal rich “nuggets” distorting average values. Birmingham (sum) had the highest total amount of metal in the soluble fractions from the different sites, followed in turn by London (sum), Port Talbot, Sheffield (win), Birmingham (win), Cornwall (sum), London (win), Cornwall (win) and Sheffield (sum). Similar to the data from the whole fraction, the trend of metal concentration in the soluble fraction was that the summer collections contained more than the winter ones, with the exception of Sheffield. The reason for this anomalous result is unclear.

Table 2.3.6 ICP-MS analysis of PM₁₀ samples from the five locations for both the whole and soluble fractions (highest and lowest values in red and blue respectively).

Metal	Whole (ppm)								
	Lon (sum)	Lon (win)	Birm (win)	Birm (sum)	PT (win)	Cn (sum)	Cn (win)	Sheff (win)	Sheff (sum)
Ti	571	131	192	485	2003	372	47	813	1000
V	1441	262	413	78	2150	1000	158	196	381
Mn	1619	424	781	1679	7231	394	195	2010	2705
Fe	94225	52085	31169	39026	567484	26380	7446	49015	78802
Co	0	0	90	1062	0	0	0	0	122
Ni	0	0	0	104364	0	0	0	0	340346
Cu	4789	1982	3352	0	3412	39	203	2498	2148
Zn	6840	1764	21645	6340	22014	1521	1195	9980	91667
As	337	89	169	36	1534	99	58	363	135
Mo	0	0	0	4262	0	0	0	0	41161
Sn	0	0	0	1485	0	0	0	0	0
Ce	66	11	17	19	104	5	3	24	156
Pt	1	3	0	20	1	1	0	0	24
Hg	1	0	0	0	2	1	0	0	115
Pb	6071	1312	2254	377	13228	445	793	13043	1048
Total	115961	58063	60083	159231	619162	30255	10097	77944	559810

Metal	Soluble (ppm)								
	Lon (sum)	Lon (win)	Birm (win)	Birm (sum)	PT (win)	Cn (sum)	Cn (win)	Sheff (win)	Sheff (sum)
Ti	14	3	4	31	7	9	0	0	8
V	571	99	116	62	144	560	103	8	290
Mn	976	247	280	1020	1048	300	47	32	1286
Fe	11078	1514	1681	3327	4787	4428	1238	3	3421
Co	23	4	7	15	11	19	1	1	18
Ni	253	26	31	112	1132	340	10	0	109
Cu	2585	816	636	1032	490	118	120	70	647
Zn	5083	3130	5927	21774	12686	2764	322	1074	2574
As	95	23	26	54	51	23	30	1	94
Mo	41	8	14	105	15	10	8	1	49
Sn	29	1	4	41	11	12	22	0	34
Ce	5	2	1	1	4	2	1	0	2
Pt	0	0	0	0	0	0	0	0	0
Hg	0	0	0	0	0	0	0	0	2
Pb	1778	344	466	173	609	225	353	155	1026
Total	22499	6217	9195	27749	20996	8810	2254	1344	9560

Lon = London

Birm = Birmingham

PT = Port Talbot

Cn = Cornwall

Sheff = Sheffield

Data from the five locations showed that there were differences in metal composition from each site and also differences between samples collected at the same site i.e. summer and winter variation (differences were not measured for significance). The range of metals being analysed were the same as in the previous study (Table 2.3.6). The most abundant metals in all samples were Fe, Zn and Pb (Ni not included as element could not be measured accurately) when looking at both whole and soluble data. A high amount of molybdenum was found in the Sheffield (sum) whole fraction but in very low amounts elsewhere. The two Sheffield samples were rich in Fe, with Sheffield (sum) being rich in Mn. In contrast Zn and Pb dominated Sheffield (win) for both whole and soluble fractions. This was similar to the airborne samples from Port Talbot, which had the highest levels of Fe and Pb of all samples analysed. Fe, Ni, Mn, Mo and Pb were related to industrial sites. This was expected as Fe is normally produced in steel works and Pb tends to be concentrated near smelters and other industries.

Both London samples had high levels of Fe, Zn, Cu and Pb, with these metals being especially concentrated in the London summer sample. Many of these metals are commonly associated with the fingerprint of traffic emissions. The difference in composition within the two London samples was apparent when looking at the solubility of Fe. A greater proportion of soluble Fe was found in the London summer sample. The difference within cities becomes more apparent when looking at the two Birmingham samples. Although total Fe concentrations were similar in both samples, Zn, Cu and Pb were more prevalent in the Birmingham (win) sample whereas Ni, Mo, Mn, Sn and Co were at a higher concentration in Birmingham (sum). Zinc was common both in urban and industrial locations.

The most bioreactive sample was from London in the winter for the whole, adjusted whole and the soluble fractions. This correlates with the sample having the highest total concentration of soluble metals. In contrast Port Talbot had the largest metal concentration from all adjusted whole samples and the third largest metal concentration in the soluble fraction, but a very low bioreactivity. This gives conflicting evidence of the role of soluble metals in bioreactivity. However, when considering all the samples together the trend dictates that if metals are responsible for the bioreactivity of the sample, then it is the soluble metals that are implicated. There was also evidence that it is not simply metals that are involved in the cause of bioreactivity. Analysis of the data generated from the Cornwall

samples revealed a low concentration in metals from ICP-MS but a high oxidative capacity in the plasmid assay. This may have been due to organic compounds or high chloride content.

2.3.7 ROFA

Due to the high solubility of ROFA (approx. 95%), a separate soluble fraction was not isolated and thus the whole fraction was used for the present study. The ROFA sample proved highly bioreactive in comparison to the PM samples tested. The plasmid assay illustrated that there was a clear dose response for ROFA judged from the damage it caused to the plasmid (Figure 2.3.7a). The TD₅₀ value for ROFA was calculated using regression analysis as previously carried out with the PM samples (Figure 2.3.7b)



Figure 2.3.7a Gel image of plasmid scission with varying concentrations of ROFA

(SC = supercoiled, D = damaged. All concentrations in µg/ml).

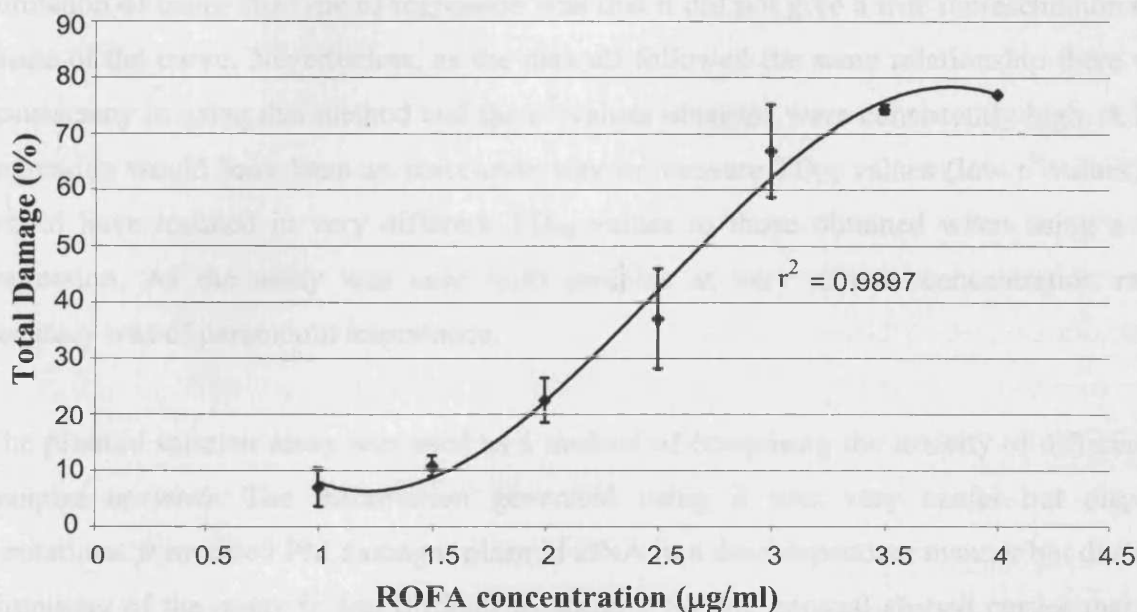


Figure 2.3.7b Dose response regression analysis of a ROFA sample

Regression analysis illustrated that there was an accurate TD₅₀ value attained and the value of 2.7 µg/ml emphasised the great bioreactivity of ROFA compared to that of the most

bioreactive PM sample (48 µg/ml). Contrary to the observed results generated by the PM samples, it would not be expected that the bioreactivity of a water-soluble fraction of ROFA would differ significantly from the whole fraction, due to the high water-solubility of ROFA.

2.4 Discussion

The bioreactivity of PM samples from a variety of urban, rural and industrial locations has previously been ascertained using the plasmid scission assay. Quantification and subsequent generation of arbitrary TD₅₀ values were previously optimised (Greenwell *et al.*, 2003; Whittaker, 2003). There was found to be a linear relationship between concentration of sample and % damage to supercoiled plasmid DNA. The PM₁₀ data from this study was originally analysed using a linear regression model. However, on closer scrutiny using a range of 8-10 different concentrations it was postulated that a more complex relationship was occurring and that the linear regression model was not an appropriate method for generating TD₅₀ values in this case. This relationship was evident for every whole and soluble fraction used in the study.

A cubic regression was then chosen as a possible way of obtaining TD₅₀ values. The limitation of using this type of regression was that it did not give a true representation of the shape of the curve. Nevertheless, as the data all followed the same relationship there was a consistency in using this method and the r^2 values obtained were consistently high. A linear regression would have been an inaccurate way to measure TD₅₀ values (low r^2 values), and would have resulted in very different TD₅₀ values to those obtained when using a cubic regression. As the assay was used with samples at very narrow concentration ranges, accuracy was of paramount importance.

The plasmid scission assay was used as a method of comparing the toxicity of different PM samples *in vitro*. The information generated using it was very useful but displayed limitations. It revealed PM damages plasmid DNA in a dose dependent manner but due to the simplicity of the assay it was difficult to account for the unusual shaped curves that were being generated. One possible explanation for this type of relationship involves looking at the structure of the different forms of plasmid DNA. The conversion of supercoiled DNA to relaxed coiled involves the breaking of a small number of relatively weak hydrogen bonds. The conversion of relaxed coil to linear is more involved as it requires the breaking of both DNA

strands at a complementary site. Therefore DNA in the relaxed coil form may have been damaged by ROS in numerous locations but the relaxed coil structure is maintained until both strands are broken at a complementary site. Supercoiled DNA is a compact structure with a lower surface area than that of the relaxed form. This causes it to have fewer exposed areas prone to attack by ROS.

At a low concentration of PM a large rate of reaction would be observed as the supercoiled DNA is easily converted to the relaxed form. Once a supercoiled molecule has been damaged enough to open out into the relaxed form, the proportion of ROS damaging supercoiled DNA in the reaction would decrease. This is because there would be an increasing total number of sites exposed in the mixture due to the increasing number of supercoiled molecules being converted to the relaxed coil form. As the concentration of PM increases, it reaches a point where there is enough ROS to damage supercoiled DNA as well as the relaxed coil form and thus the percentage damage increases in a sigmoidal type fashion until 100% of the supercoiled substrate (DNA) has been damaged.

The purpose of generating TD₅₀ values was to have a comparison of reactivity between different samples and to gain an insight into how this correlated with bioavailable metal concentrations as well as meteorological effects and surrounding local activity. The primary conclusion from the Port Talbot wind direction study was that samples collected in the same area but sourced from different wind directions had highly variant metal compositions and very different oxidative capacities. This lends support to the theory that external influences such as local industry and vehicle exhaust play a large role in determining the composition of PM and contributes to the high metal content found in some PM samples. The increase in metal content is not positively correlated with increasing bioreactivity when considering the whole fraction. However there is a correlation with the soluble fraction. The correlation that was found between increased bioreactivity and concentration of individual metals highlights further investigation is required. Rather than focussing on metal concentration as a whole it was necessary to look at trends with individual metals, as one sample could have a large amount of a certain metal, which has very low bioreactivity. For example the soluble fraction of the motorway derived SE sample was significantly more bioreactive than that of the metal-depleted town sample from the NW.

The NE sample had a surprisingly high amount of metal, which was unusual in composition given the rural area from which the sample was obtained. There were unexpectedly high

amounts of lead as well as a high salt content. The NE wind blew from an area where there was no industrial influence and a low concentration of vehicles. One theory explaining the presence of these elements can be linked to the local geography. The presence of a steep hill to the NE could be trapping particulates originally carried upon prevailing winds from the steel works and the sea (high salt content). Thus, significant resuspended particles are reentrained during an episode of prevailing wind from the NE and subsequently collected.

The findings pointed to the soluble metal content of PM playing a large role in being part of the cause of the oxidative capacity of PM. It was more likely that a certain number of metals were implicated rather than the total metal concentration. The Port Talbot study showed that there was no correlation between different metal concentration and bioreactivity of the whole fraction. By examining the soluble data, it provides more support for the soluble fraction causing the majority of the damage, and in particular metals such as Fe, Cu, and V that are known to be redox active transition metals. Zn and As were also implicated. However these metals are not redox active, but Zn is known to be able to catalyse hydrolysis of phosphodiester bonds.

The data obtained from the five location study was less conclusive than the Port Talbot wind direction study. There was no significant correlation between total metal content and bioreactivity in either the whole or soluble fractions. There was also no correlation between individual metal concentration and bioreactivity for the whole and soluble fraction. There were certain trends that suggested that metals influence bioreactivity. An example of this was the fact that London (win) was the most bioreactive for the whole and soluble fractions. The London (win) sample also had the highest amount of Fe, Cu, As, V and Pb. Port Talbot had the highest total metal values in the adjusted whole component but had a low bioreactivity. This fact gives further evidence that it is soluble metals implicated in determining bioreactivity.

Analysis of the data showed that dry summer months are more likely to produce a more bioreactive sample. The two most bioreactive samples, with regard to the soluble fraction, were London and Sheffield summer samples, which were collected during dry periods. Samples from industrial sites such as Sheffield and Port Talbot contained the highest amounts of metals but this did not necessarily mean that the samples had a high bioreactivity.

Cornwall samples had the lowest total metal content, but the samples were not the least bioreactive.

Analysis of the data obtained from the ROFA sample supports the theory that soluble metals within ambient particulate samples may contribute to their bioreactivity. Research has shown ROFA to be 95% soluble with high transition metal content (103.77 $\mu\text{g}/\text{mg}$ of ROFA) (Costa and Dreher, 1997). If the hypothesis regarding metal content of PM being the cause of its bioreactivity is true then it would have been expected that ROFA would be more bioreactive than all of the PM samples tested, as borne out by the data.

Due to the restrictions of the plasmid scission assay, it was only known that each PM sample damaged the plasmid at certain concentration ranges and less was known about which components in the PM_{10} were causing its bioreactivity. It had been shown from previous work that PM has an oxidative effect in the assay because it was shown that the reactivity of PM was ameliorated when in the presence of various antioxidants (Greenwell *et al.*, 2002). The sources of ROS had not been determined. Due to the heterogeneity of PM, ROS production could come from various sources such as transition metals, polyaromatic hydrocarbons or redox active quinones (Greife and Warshawsky, 1993). These can also work in tandem and produce ROS as metals potentiating the redox cycling capacity of PAHs, thereby increasing production of ROS. Also oxidation may not be the only process causing the damage. Other mechanisms such as direct hydrolysis via metal ions present in PM such as Zn^{2+} and Fe^{2+} could be associated with damage to the plasmid. These metals can catalyse hydrolysis of phosphodiester bonds. The backbone of DNA comprises phosphodiester linkages and thus can be prone to this type of attack. Due to the structure and shape of DNA, it has many protruding negatively charged molecules. This feature makes it a prime site of attack from various cations by direct co-ordination of the metal.

If metals do play a role in the oxidative capacity of PM as hypothesised, then removal of metals present in PM_{10} samples should cause PM_{10} reactivity to be ameliorated. The removal of metals from PM_{10} samples could be achieved using a resin which binds and removes metal cations from solution (Molinelli *et al.*, 2002). Data using ICP-MS analysis and the plasmid scission assay could be generated to see which metals had been removed and whether the removal had affected the bioreactivity of the sample.

ICP-MS was a useful tool in identifying which metals were present in each sample and at what concentrations. If the bioreactivity of a PM sample was not only affected by the type of metal present and its concentration but also the oxidation state in which the metal existed at the time, then a method by which these states can be identified needs to be utilised. This hypothesis may explain why there was not a clear trend related to metal concentration observed in the five location study.

Research is limited in assessing how different metals interact. Due to the large number of metals present within PM and the complex nature of the pulmonary environment, various interactions could take place which may affect bioreactivity. Synergistic interactions between metals may be enhancing bioreactivity dependant upon oxidation species and concentration. If this was the case, the metals may not need to be at a high concentration to exert a large effect. In contrast the interaction of certain metals may negate the bioreactivity of other metals. Alternatively, metals may cause the production or quenching of different oxidative species through interaction with pulmonary constituents, thus also affecting bioreactivity.

The overall conclusions from this work are that individual metal content within samples can be linked to oxidative capacity (Port Talbot study) but more research is required to explain why this trend is not true for all studies between metals and bioreactivity such as in the five locations study. This present study has reinforced the theory that bioreactivity is mainly found in the soluble fraction and that individual metal content may be the cause of the bioreactivity. This is reinforced by the highly soluble ROFA, which has a large metal content and is very bioreactive when compared to PM samples. The assay revealed particulate samples containing enhanced amounts of the soluble forms of Fe, Zn, As and V as being more bioreactive than average but other factors, such as exact location of collection site, variations in rainfall and non-metal components within PM may also have influence on particulate bioreactivity. Whilst more 'global' factors may affect the epidemiological impact of different PM samples (e.g. prevailing wind, local environment, geographic features), this study has highlighted that when these factors are accounted for, soluble metals may provide a key to understanding the chemical nature of PM bioreactivity.

CHAPTER 3

***IN VITRO* INTERACTIONS OF WATER-SOLUBLE METALS**

3.1 Introduction

Previous studies have shown that the predominant, bioavailable metals found in PM are Cu, Zn, V, As, Pb, Fe and Mn (Whittaker, 2003). Some of these metals are implicated in ROS production via interaction in Fenton-type reactions and many have been shown to exert an oxidative stress both *in vivo* (both in the lung and systemically (Magari *et al.*, 2002)) and *in vitro*. *In vivo* lung injury has been found to correspond to PM metal concentration (Pritchard *et al.*, 1996) and to ROS production (Kadiiska *et al.*, 1997). *In vitro* studies have also correlated toxicity with metal concentration (Costa and Dreher, 1997). Specific metals have been found to exert differing toxicological effects (Stohs and Bagchi, 1995). Fe (most commonly implicated in the induction of health effects due to its bioreactivity and availability) has been found to initiate a range of toxic mechanisms (Halliwell and Gutteridge, 1988) and can lead to acute and chronic conditions (Quinlan *et al.*, 2002). Cu and V are also commonly implicated in oxidative bioreactivity (Wilson *et al.*, 2002) and zinc has been found to have toxic effects (Richards *et al.*, 1989). Studies investigating the toxicity of mixtures of metals have yielded conflicting results. Riley and colleagues (2003) observed that Zn^{2+} appeared to reduce the negative effects caused by V(IV) and Cu^{2+} alone *in vitro* by reducing the inhibition of cell culture metabolism and cell death and thus having a protective effect. However, Pagan and colleagues (2003) found that cell injury was increased when exposed to a mixture of Cu^{2+} and Zn^{2+} when compared with the expected additive effects of damage caused by the metals individually. Therefore work related to metal interactions and possible synergistic effects are subsequently of great interest.

It is not only the interactions between metals present within PM that could be of consequence to bioreactivity, but also the interaction between PM components and the numerous, diverse constituents of the lung. Present within the lung is the epithelial lining fluid which is the first point of contact for any inhaled, deposited xenobiotics. This fluid is highly heterogeneous with a range of properties, including being rich in antioxidants and metal chelators. These function to protect the lung from oxidative damage caused by inhalation of metallic and ROS-producing xenobiotics. Investigation into the protective

role of this fluid is necessary in understanding the potential damage caused by inhaled water-soluble metals endogenous to PM.

The primary aim of this study was to use the plasmid scission assay to compare the observed oxidative bioreactivities of a previously characterised PM sample (London 1958) with a surrogate mixture of the metallic, water-soluble component. The mixture comprised the most prominent water-soluble metals endogenous to the sample as previously identified by inductively-coupled plasma mass spectrometry (ICP-MS) analysis. The subsequent aims were to elucidate the oxidative potential of individual metals endogenous to the water-soluble fraction of PM, to investigate the role of oxidation state in determining bioreactivity and then to evaluate the effects of ambient secondary components (e.g. chloride, sulfate and nitrate groups) on any observed reactivity. Finally, the combined effects of simple mixtures of metals were studied in order to identify possible additive or synergistic effects on oxidative capacity in order to test the hypothesis that the oxidation state determines the bioreactivity of metals.

The secondary aim was to test the hypothesis that pulmonary antioxidants found in broncho-alveolar lavage fluid (BALF) would ameliorate the observed bioreactivity of metals. Previous research had shown that low molecular weight fractions of lavage fluid alone caused damage to plasmid DNA (Greenwell *et al.*, 2002, 2003). Therefore fractions which were known to ameliorate the effects of PM within the assay were used to determine whether they had the same effect with the surrogate. The final aim was to assess whether the low molecular weight antioxidant glutathione, which is endogenous to the lung lining fluid, would exert a protective effect in the assay.

3.2 Materials and Methods

3.2.1 Equipment and Materials

Agarose	Bioline, London, UK
Ascorbate	Sigma, Dorset, UK
Bromophenol Blue	Sigma, Dorset, UK
Cupric Chloride	Fisher, Leicestershire, UK
Cupric Nitrate	Sigma, Dorset, UK
Cupric Sulfate	Fisher, Leicestershire, UK
Densitometer	Syngene, Cambridgeshire, UK
Electrophoresis Maxi Tank	Helena Biosciences, Tyne and Wear, UK
Eppendorfs (0.2ml)	Anachem, Bedfordshire, UK
Ethanol	Fisher, Leicestershire, UK
Ethidium Bromide	Sigma, Dorset, UK
Ferric Chloride Hexahydrate	BDH, Dorset, UK
Ferrous Sulfate	BDH, Dorset, UK
Glycerol	Sigma, Dorset, UK
HPLC-Grade Water	Fisher, Leicestershire, UK
Lead (II) Nitrate	Fisher, Leicestershire, UK
Manganese Sulfate	Sigma, Dorset, UK
Mannitol	BDH, Leicestershire, UK
φX174-RF plasmid	Promega, Hampshire, UK
Reduced Glutathione	Sigma, Dorset, UK
Sodium Arsenite	Fisher, Leicestershire, UK
Sodium Metavanadate	Fisher, Leicestershire, UK
Tris-Acetate-EDTA	Sigma, Dorset, UK
Tris-Borate-EDTA	Sigma, Dorset, UK
Vanadyl Sulfate	Fisher, Leicestershire, UK
Zinc Sulfate	Sigma, Dorset, UK

3.2.2 Preparation of Metal Mixtures

The metal surrogate mixture and solutions of individual metals were prepared using sterile HPLC grade water and weighed out to an absolute metal mass rather than a compound mass. Absolute metal mass was used so accurate comparisons of TD₅₀ values for each metal could be made on a direct, mass-for-mass basis, rather than comparing by relative metal percentage of compound weight. The water-soluble metal salts used were FeSO₄, FeCl₃, VOSO₄, NaVO₃, CuCl₂, Cu(NO₃)₂, CuSO₄, ZnSO₄, MnCl₂, Pb(NO₃)₂ and NaAsO₂. Chloride, sulfate and nitrate compounds were selected as these secondary groups are common to UK PM. Solubilisation was ensured by vigorous vortexing and fresh samples were made before each analysis.

Analysis of a PM sample collected in London in 1958 was performed in order to elucidate which types of metals were present in the water-soluble fraction of the PM and at what concentrations (Whittaker, 2003). The sample was selected due to it having a metal rich water-soluble component. Also the bioreactivity of the sample was well characterised as it had previously been studied using the plasmid assay. A surrogate sample of the bioavailable metals present was generated from the data shown in Table 3.2.2 using the ICP-MS analysis previously described in Chapter 2. In order to simplify the analysis and to broaden the possibility of elucidating a mechanism of damage, the most abundant metals found in PM were selected for analysis, meaning that some of the metals found at minimal concentrations were omitted from the surrogate mixture (e.g. Co, Ti, Sn, Hg). The surrogate mixture of the London PM sample was generated using proportional concentrations of the metals identified in the ICP-MS analysis, in order that the relative proportion of each metal in the surrogate was exactly representative of the original.

As Fe was the most abundant metal after Zn²⁺ and considering that it naturally occurs in more than one oxidation state, two surrogate samples were made. The composition of each was the same with the exception of the substitution of Fe³⁺ with Fe²⁺. Plasmid scission assay analyses were carried out according to the protocol detailed in Chapter 2.

Table 3.2.2 Element concentration in water-soluble London 1958 sample from ICP-MS analysis (ppm is equivalent to µg of metal in 1g of PM sample).

Element	Concentration (ppm)
Ti	-
V	282
Mn	168
Fe	999
Co	-
Ni	-
Cu	59
Zn	1291
As	21
Mo	-
Sn	-
Ce	-
Pt	-
Hg	-
Pb	553

3.2.3 Generation of Concentrated BALF Solution

Generation of broncho-alveolar lavage fluid (BALF) was achieved by sequential washing of the rat lung and pooling the resultant fluid (see below). The fluid obtained can be used to assess inflammatory and biochemical changes in or on the lung tissue. It is a dilute composition of lung lining fluids from all regions of the lung (from alveolar to tracheal) and is thus abundant in antioxidants.

Healthy male rats (150-200 g) were used in accordance with home office guidelines. They were anaesthetised, then euthanised by intra-peritoneal injection of Euthatal. The dissection followed the protocol outlined in Chapter 4. Rat lungs were lavaged in a

volume of 8 ml sterile 0.15 M saline solution. After the first wash, the lavage fluid was reused for three subsequent washes to obtain a concentrated fluid. Lavage samples were centrifuged at 300 g for 20 minutes to remove all free cells. Then the supernatant was poured off and the cell pellet discarded.

3.2.4 BALF Fractionation (Microcon)

Rat BALF was separated into 7 size fractions using the Microcon filter unit system (Millipore, UK). The filter unit with the largest size cut-off (50 kDa) was filled with 0.5 ml of fresh lavage and centrifuged following the guidelines stipulated in the Millipore Microcon User Guide (ref: 99394:9). The concentrate was washed from the surface of the filter, retained and the eluate was then sequentially filtered through 50, 30, 10, then 3 kDa filter units respectively. The concentrates from each filter were retained and diluted with 0.15 M NaCl to the original volume of 0.5 ml to reconstitute each size fraction to the original concentration of the original sample. It should be noted that although this resultant fluid yield is significantly diluted from the physiological concentrations of epithelial lining fluid (approximately 40x more dilute), it would be expected to display similar properties but of lower magnitude. The filtration resulted in five different size fractions - >50, 50-30, 30-10, 10-3, <3 kDa, as well as whole BALF and saline only (0.15 M NaCl) samples. These fractions were stored at -80°C until use.

3.2.5 Preparation of Glutathione

The antioxidant GSH solution was prepared by dissolving a known weight in sterilised HPLC grade water to yield a concentration of 400 µM. This concentration was chosen as it is representative of the concentration of glutathione within the alveolar region of the lung (Cantin *et al.*, 1989). Fresh samples were prepared for each use.

3.2.6 Statistical Analysis

Regression analysis was employed in order to calculate the toxic dose of metal necessary to cause 50% (TD₅₀) of the DNA to become damaged. Data were tested for normality using an Anderson-Darling test. Statistical significance was tested using the two-tailed t-test or the non-parametric Mann-Whitney test (Minitab 13, Microsoft, USA).

3.3 Results

3.3.1 Assessment of PM Surrogate Mixtures

The surrogate metal mixture was analysed to determine whether the metals present in the PM sample alone would exert a comparative oxidative effect in the plasmid scission assay to that of the original sample. Preliminary results indicated a dose response was occurring between the surrogate containing Fe^{3+} and the amount of damage caused to the plasmid DNA. From these preliminary responses, a concentration range between 0.5 $\mu\text{g}/\text{ml}$ to 3.0 $\mu\text{g}/\text{ml}$ was deemed suitable to attain an accurate dose response (Figure 3.3.1a). Using densitometric analysis (Chapter 2), a regression graph was generated and a TD_{50} obtained (Figure 3.3.1b).

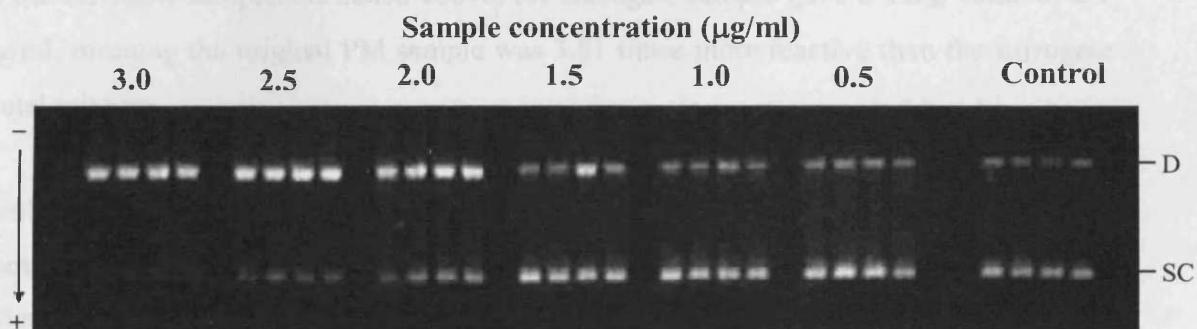


Figure 3.3.1a Bioreactivity of surrogate containing Fe^{3+} (SC = supercoiled D = damaged)

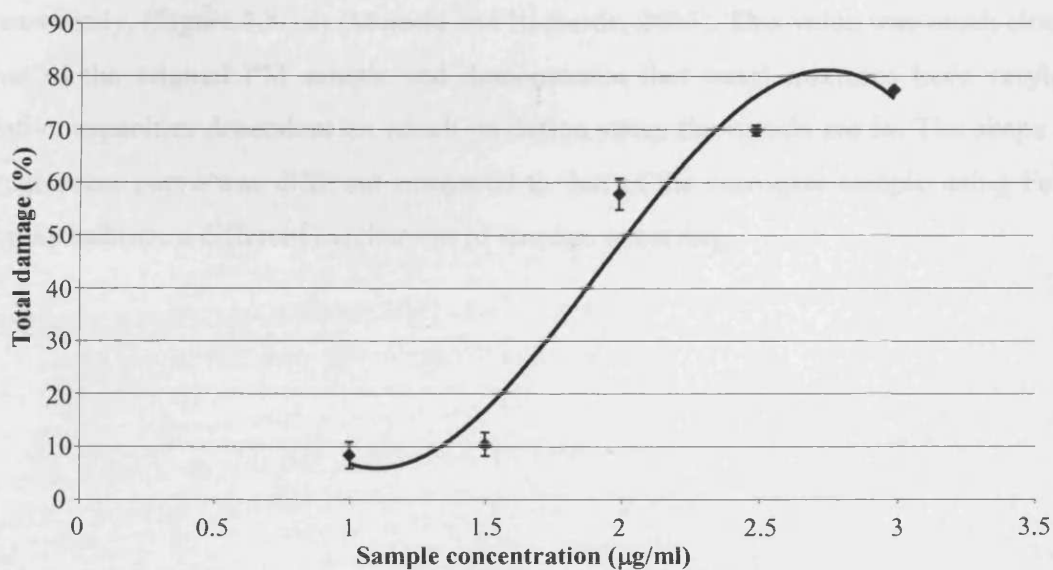


Figure 3.3.1b Dose response of surrogate containing Fe^{3+}

The observed dose response ranged from 5% damage to the plasmid DNA with low surrogate concentrations to total damage of the plasmid (0% remaining in supercoiled form). From regression analysis the surrogate yielded a TD₅₀ value of 2.1 µg/ml. The actual soluble London 1958 sample gave a TD₅₀ value of 162.5 µg/ml (as calculated in Whittaker 2003). In order to establish the relevance of the TD₅₀ of the surrogate compared to that of the PM, the TD₅₀ of the PM sample was recalculated according to the amount of water-soluble metal present. From ICP-MS analysis, the total amount of the metals of interest was 3380 µg/g of PM, therefore the amount of these metals in 162 µg of PM was 0.55 µg ((3380/1,000,000)x162). Hence, the TD₅₀ of the PM sample relates to a metal concentration of 0.55 µg/ml, which can then be directly compared with the results of the surrogate sample. As stated above, the surrogate sample gave a TD₅₀ value of 2.1 µg/ml, meaning the original PM sample was 3.81 times more reactive than the surrogate metal mixture.

Preliminary results indicated a dose response was occurring between the surrogate containing Fe²⁺ and the amount of damage caused to the plasmid DNA (Figure 3.3.1c) (Merolla *et al.*, 2005). The metal surrogate concentrations used in order to generate an accurate TD₅₀ value ranged from 0.01 µg/ml to 2.1 µg/ml. The TD₅₀ value for the second surrogate was 0.44 µg/ml. This value was calculated in exactly the same way as carried out previously. (Figure 3.3.1d) (Merolla and Richards, 2005). This value was much closer to that of the original PM sample and demonstrates that metal mixtures have varying oxidative capacities dependent on which oxidation states the metals are in. The shape of the regression curve was different compared to that of the surrogate sample using Fe³⁺. This may indicate a different mechanism of damage occurring.

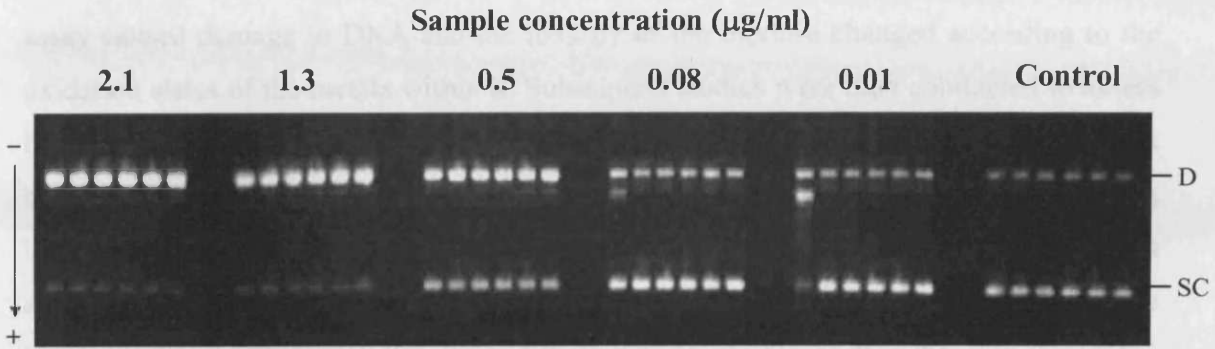


Figure 3.3.1c Bioreactivity of surrogate containing Fe^{2+} (SC = supercoiled D = damaged)

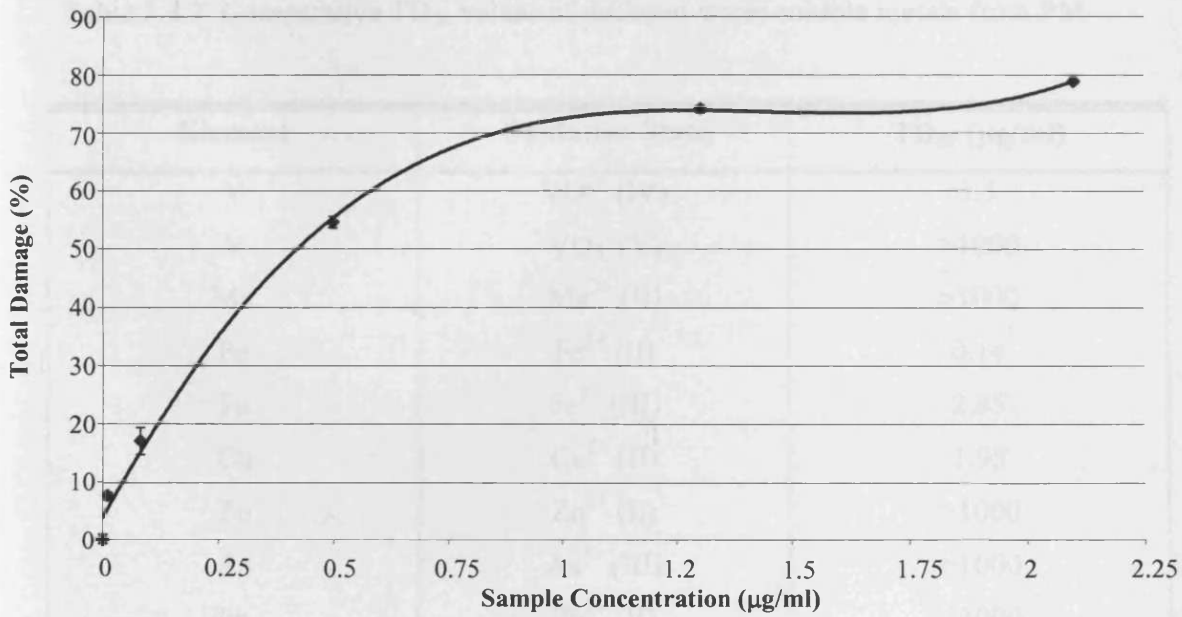


Figure 3.3.1d Dose response of surrogate containing Fe^{2+}

3.3.2 Analysis of Metals and Oxidation States

Results using the surrogate sample highlighted the fact that metals used in the plasmid assay caused damage to DNA and the toxicity of the mixture changed according to the oxidation states of the metals within it. Subsequent studies were then conducted to assess bioreactivities of individual metals with varying oxidation states. It was observed that certain metals were bioreactive whereas others caused minimal damage to the plasmid at high concentrations. Examples of this variation were observed between different metals and also between metals in different oxidation states (Figures 3.3.2a-d). The difference in bioreactivity was large with Fe^{2+} being fifteen times more bioreactive than Fe^{3+} and VO_3^- (V^{V}) showing very little bioreactivity when compared with VO^{2+} (V^{IV}). These differences are illustrated in Figures 3.3.2a-d and the bioreactivities of each metal tested are shown in Table 3.3.2.

Table 3.3.2 Comparative TD_{50} values of different water-soluble metals from PM

Element	Oxidation State	TD_{50} ($\mu\text{g/ml}$)
V	VO^{2+} (IV)	3.5
V	VO_3^- (V)	>1000
Mn	Mn^{2+} (II)	>1000
Fe	Fe^{2+} (II)	0.14
Fe	Fe^{3+} (III)	2.45
Cu	Cu^{2+} (II)	1.95
Zn	Zn^{2+} (II)	>1000
As	As^{3+} (III)	>1000
Pb	Pb^{2+} (II)	>1000

The most bioreactive metals were Fe^{2+} , Cu^{2+} , Fe^{3+} and VO^{2+} (V^{IV}), whereas Zn^{2+} , Pb^{2+} , As^{3+} , VO_3^- (V^{V}) and Mn^{2+} had very low bioreactivity when compared with the previous four metals and with the bioreactivity of PM samples previously analysed.

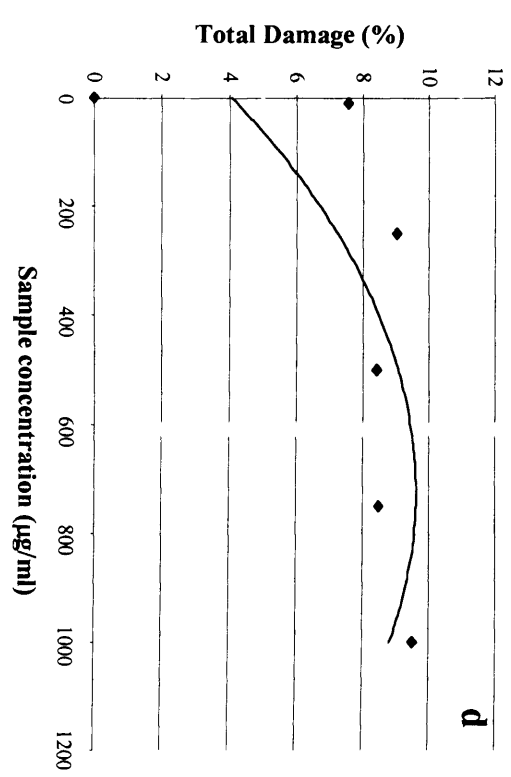
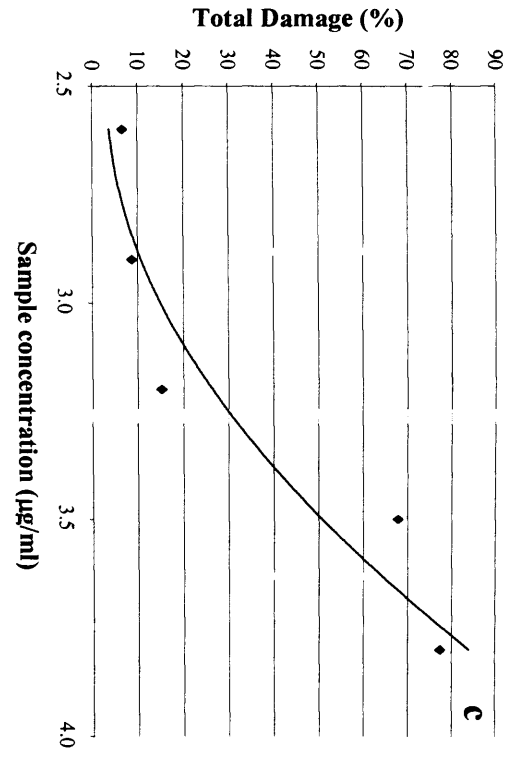
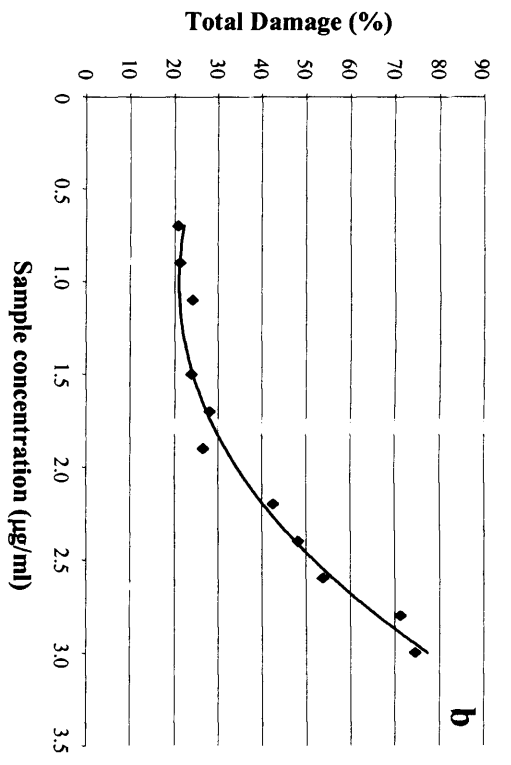
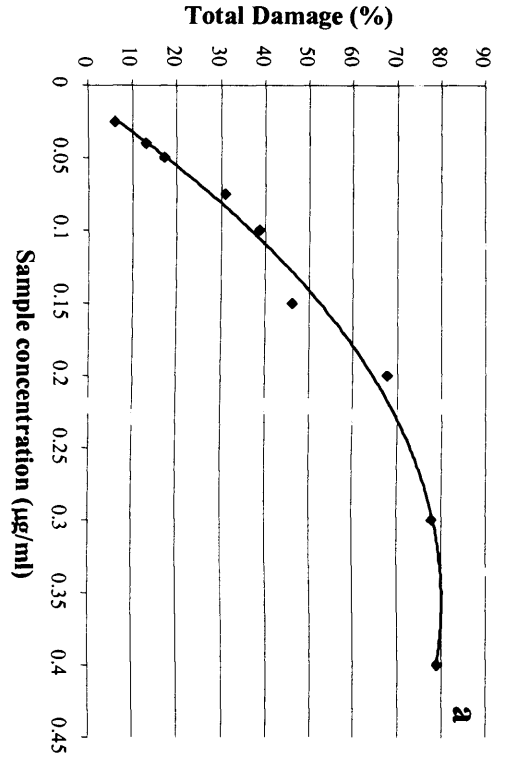


Figure 3.3.2a-d Bioreactivities of different metals and effects of oxidation states a) Fe²⁺ b) Fe³⁺ c) VO²⁺ d) VO₃⁻

3.3.3 Effects of Secondary Components

As oxidation state was found to be important in determining metal bioreactivity, it was hypothesised that the secondary component might also play a role. Key water-soluble secondary components often found in PM are chlorides, nitrates and sulfates. In order to investigate their effects, three different water-soluble copper compounds (CuSO_4 , CuCl_2 and CuNO_3) were incubated with the plasmid. The oxidation state of Cu within these three compounds was the same (+2). There was found to be little difference in the bioreactivity between the samples as the TD_{50} values generated were very similar ($\text{CuCl}_2 = 1.95 \mu\text{g/ml}$, $\text{CuNO}_3 = 1.85 \mu\text{g/ml}$ and $\text{CuSO}_4 = 1.70 \mu\text{g/ml}$). Closer analysis of the data revealed even more faithful homology between the samples as there was little difference in bioreactivity when evaluating any of the individual test concentrations (Figure 3.3.3) (Merolla and Richards, 2005)

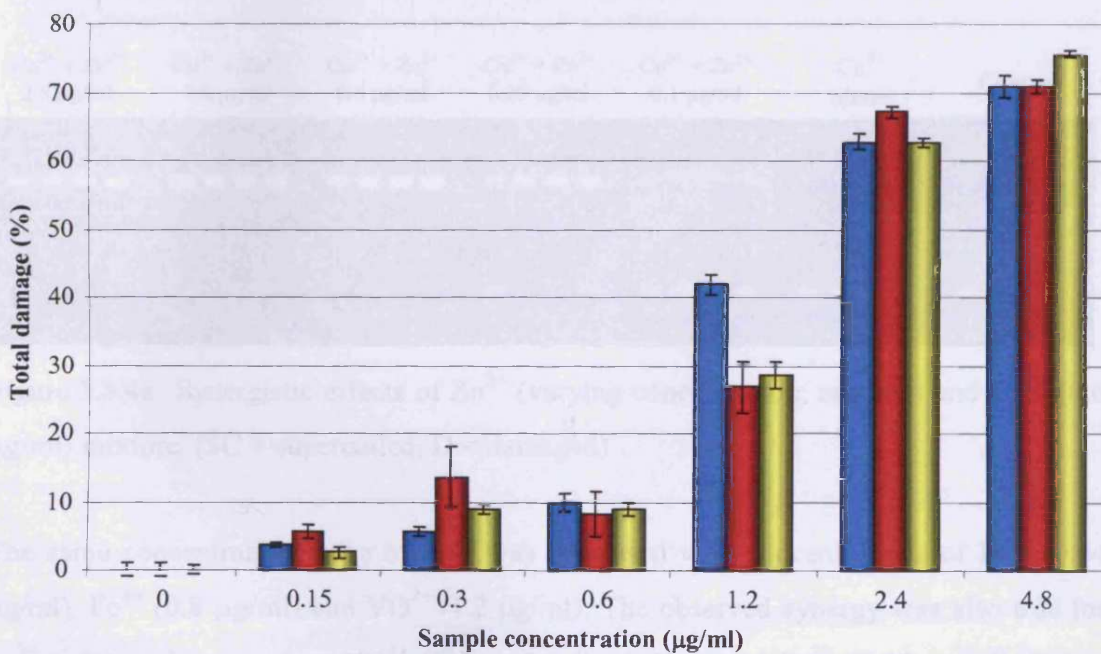


Figure 3.3.3 Comparative bioreactivity of CuSO_4 , CuCl_2 and CuNO_3

(■ = copper sulphate, ■ = copper nitrate, ■ = copper chloride)

3.3.4 Analysis of Metal Combinations

The oxidative impact of combinations of metals were then evaluated, focusing on the redox inactive metal Zn^{2+} and four of the more bio-reactive metals, Cu^{2+} , Fe^{3+} , Fe^{2+} and VO^{2+} (V^{IV}). A preliminary study was carried out using a mixture of Cu^{2+} at a concentration of $0.6 \mu\text{g/ml}$ and varying Zn^{2+} concentrations from $5 \mu\text{g/ml}$ to $80 \mu\text{g/ml}$. The copper was at a concentration that would cause minimal damage (approximately 10 %) to the plasmid as was the case for the varying concentrations of Zn^{2+} . The result was that the plasmid was fully damaged irrespective of dose. Concentrations of Zn^{2+} (0.1 - $2.5 \mu\text{g/ml}$) were then used with Cu^{2+} at $0.6 \mu\text{g/ml}$ and a sub-maximal dose response was observed as illustrated in Figure 3.3.4a. The mixture of Zn^{2+} and Cu^{2+} was shown to be more damaging to the DNA than the total additive effects of Zn^{2+} alone and Cu^{2+} alone, hence revealing a synergistic effect. This effect of Zn^{2+} at concentrations of greater than $0.25 \mu\text{g/ml}$ was as high as 10 times the expected additive effect.

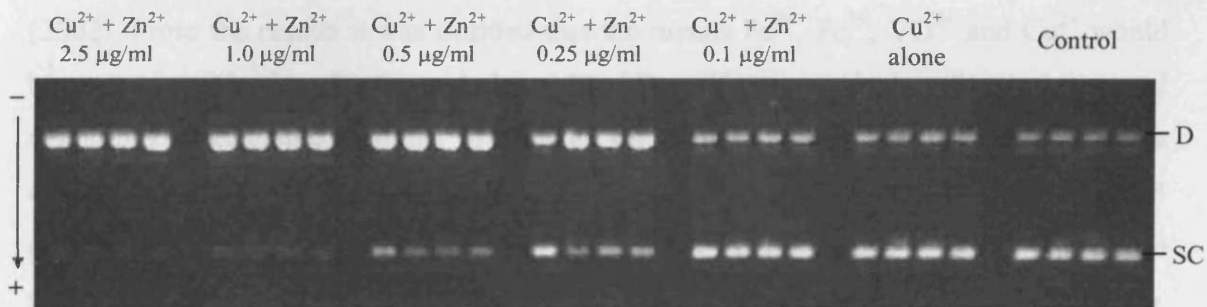


Figure 3.3.4a Synergistic effects of Zn^{2+} (varying concentration, see key) and Cu^{2+} ($0.6 \mu\text{g/ml}$) mixture. (SC = supercoiled, D = damaged)

The same concentration range of Zn^{2+} was then used with concentrations of Fe^{2+} ($0.04 \mu\text{g/ml}$), Fe^{3+} ($0.8 \mu\text{g/ml}$) and VO^{2+} ($1.2 \mu\text{g/ml}$). The observed synergy was also true for Fe^{3+} and to a lesser extent VO^{2+} (Figure 3.3.4b-e). However Fe^{2+} ($0.04 \mu\text{g/ml}$) gave a result that was similar to the expected additive effect of Zn^{2+} alone and Fe^{2+} alone and thus no synergistic effect was observed. The doses of Zn^{2+} were then increased (0.25 - $80 \mu\text{g/ml}$), but there was still no observed synergistic effect.

It is postulated that Zn^{2+} has antioxidant effects (Powell, 2000). Therefore a further proof of principle experiment was conducted to see whether at very high concentrations Zn^{2+} would ameliorate the effects of Fe^{2+} . Fe^{2+} was used at a concentration that would cause 50% damage to the plasmid and Zn^{2+} was used at 1000 $\mu\text{g/ml}$. The observed result was that Zn^{2+} did not cause the damage exerted by Fe^{2+} to be reduced, simply demonstrating the expected additive effect (data not shown).

3.3.5 Effects of BALF on Metal Bioreactivity

Previous research had revealed that different fractions of lavage fluid can itself cause damage to plasmid DNA in this assay (Greenwell *et al.*, 2002). In this study, the fractionated lavage samples were tested both in isolation and concurrently with metals. In isolation, the whole fraction caused 100% damage to the DNA with signs of fragmentation occurring. As the size fractions of the fluid decreased, the damage to the plasmid was reduced (results not shown). This supported the findings from Greenwell (2002). From the results it was decided that the metals Fe^{2+} , Fe^{3+} , VO^{2+} and Cu^{2+} would be mixed with the fractions below 30 kDa. These particular fractions caused negligible/undetectable amounts of damage on their own. The metals were used at a concentration that was known to damage approximately 50% of the plasmid Fe^{2+} (0.14 $\mu\text{g/ml}$), Fe^{3+} (2.45 $\mu\text{g/ml}$), VO^{2+} (3.5 $\mu\text{g/ml}$), and Cu^{2+} (1.95 $\mu\text{g/ml}$) in order to maximise the chance to visualise any amelioration or exacerbation of the metal-induced toxicity. The results revealed that only the 10-3 kDa and <3 kDa fractions exerted protective effects for all four metals. The visible effect of the protection is illustrated in Figure 3.3.5a, which demonstrates the typical response seen with all four metals (using Cu as an example). There is a clear difference between the damage exerted by Cu alone and the damage caused with the presence of the lavage fractions. There was a 22% reduction in damage when co-incubating with the <3 kDa fraction and a reduction of 16% using the 10-3 kDa fraction after the relevant controls were subtracted. Both these differences were significant with *P* values of 0.012 and 0.025 respectively. Similar results were seen for Fe^{3+} , Fe^{2+} and VO^{2+} (data not shown).

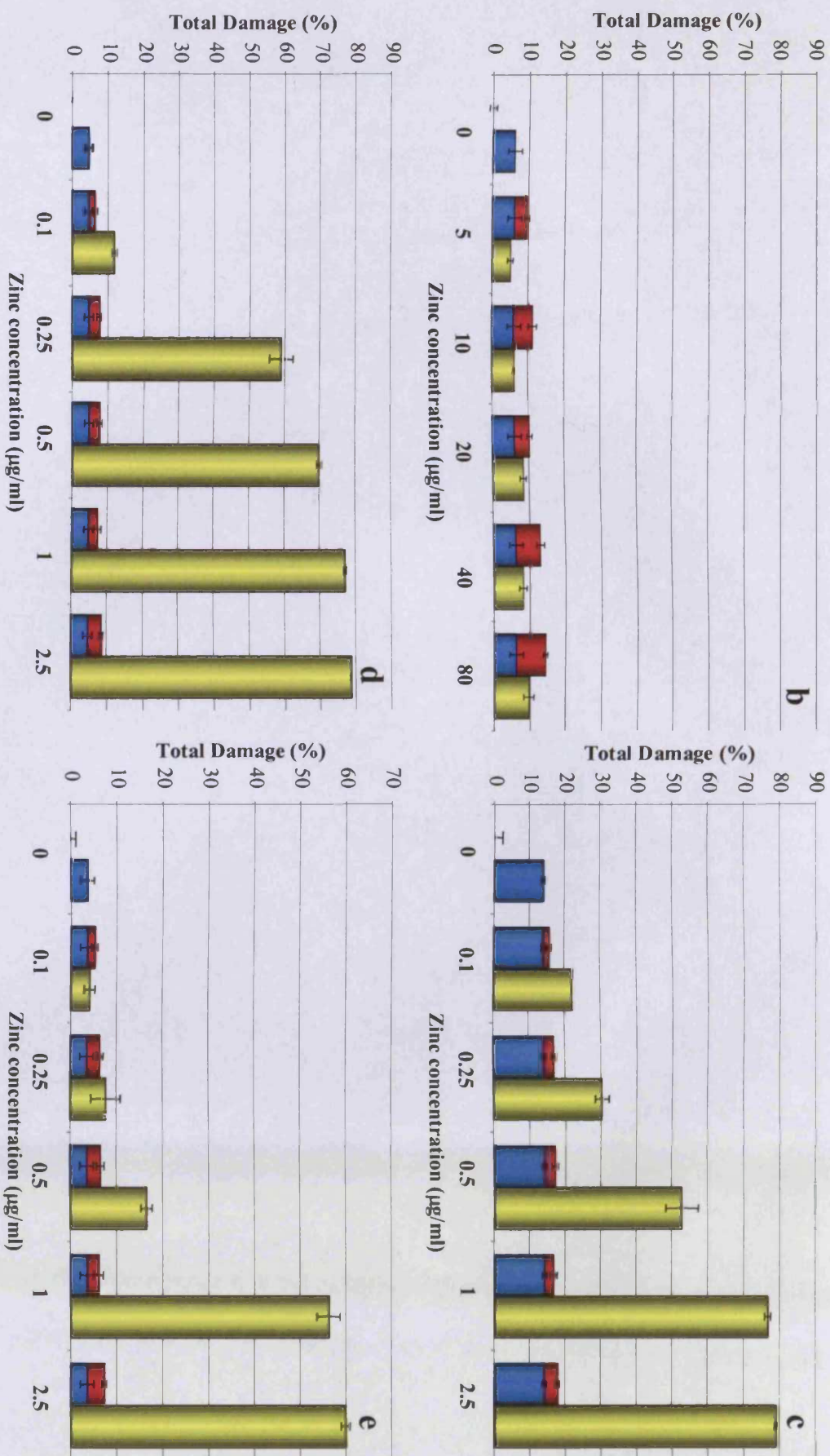


Figure 3.3.4b-e Synergistic effects of Zn²⁺ with transition metals. b) Fe²⁺ (0.04 µg/ml) c) Fe³⁺ (0.8 µg/ml) d) Cu²⁺ (0.6 µg/ml) e) VO²⁺ (1.2 µg/ml)
 ■ = transition metal effect ■ = zinc effect ■ = additive effect ■ = synergistic effect (Merolla and Richards, 2005)

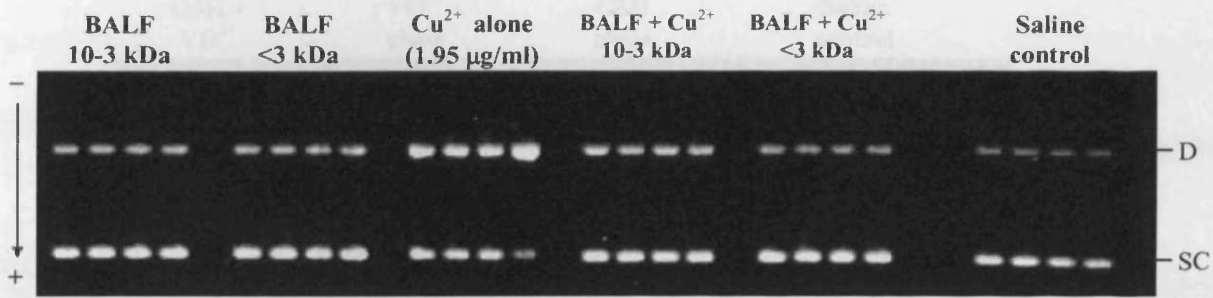


Figure 3.3.5a Effect of low molecular weight BALF fractions on Cu^{2+} bioreactivity (SC = supercoiled, D = damaged)

One of the major, low molecular weight, antioxidant components present in BALF is GSH. Within the plasmid scission assay GSH (at the concentration found in the lower airways) did not ameliorate the effects of the damage caused by Fe^{2+} (Figure 3.3.5 b) and hence there was no significant difference in DNA damage between Fe^{2+} solution and solution of Fe^{2+} and GSH. There were, however, significant differences when comparing the toxicity of other metals both individually and in the presence of glutathione. The damage observed was significantly higher ($P=0.014$) than the expected additive damage with glutathione seemingly exacerbating the bioreactivity of Cu^{2+} , VO^{2+} and Fe^{3+} . An example of this enhanced bioreactivity (VO^{2+} and GSH) effect can be seen in Figure 3.3.5c.



Figure 3.3.5b Effects of GSH on bioreactivity of Fe^{2+} (SC = supercoiled, D = damaged)

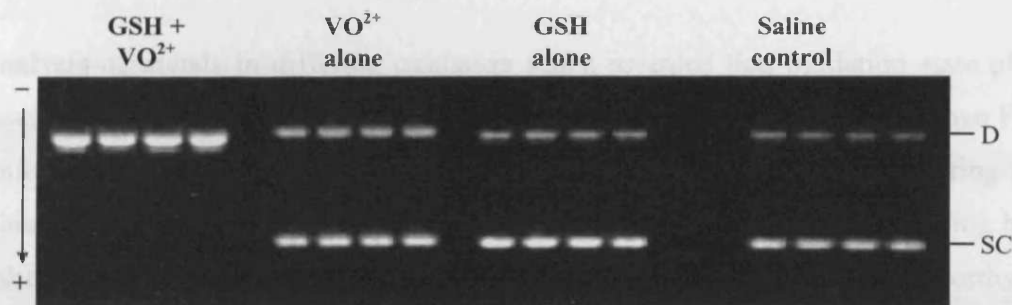


Figure 3.3.5c Effects of GSH on bioreactivity of VO^{2+} (SC = supercoiled, D = damaged)

3.4 Discussion

ICP-MS analysis revealed that the predominant water-soluble metals present in PM consisted of transition metals such as Cu and Fe, as well as metals which exist in one oxidation state but are known to be toxic in the lung such as Zn and Pb. The transition metals were of interest as they pose an oxidative threat due to their ability to exist in more than one oxidation state and thus are able to initiate the generation of free radicals. Their ability to generate ROS can lead to a large number of modifications in DNA, including modifications to sugar and base moieties as well as strand breakage (Box *et al.*, 2001).

A surrogate mixture of water-soluble metals based on analysis of a London 1958 PM sample was created. Analysis of the oxidative capacity of this sample, through a simple *in vitro* assay, revealed that the bioavailable metals present in the water-soluble fraction of PM were highly bioreactive and could perhaps account for the observed oxidative capacity of the original sample. Such an observation is supported by research which has examined metal removal and how this correlates with lower bioreactivity (Molinelli *et al.*, 2002). ICP-MS analysis can only provide information on the metal concentrations but does not provide insight into oxidation states. Thus, the surrogate sample may not have been an absolute representation of the metal composition of the original PM sample. Nevertheless, the surrogate sample did give an indication of the oxidative potential of a mixture of metals at low concentrations. It also emphasised the fact that using mixtures containing metals of different oxidation states caused different severity of damage. The magnitude of the difference highlighted the potency of Fe within the assay.

Analysis of metals in differing oxidation states revealed that oxidation state played an essential role in oxidative capacity. Fe^{2+} was over 15 times more damaging than Fe^{3+} . The ability of Fe^{2+} to exert the greatest oxidative threat is consistent with existing research which has shown that Fe^{2+} has a significant ability to generate ROS (including hydroxyl radicals via Fenton-type reactions (Urbanski and Beresewicz, 2000)). It is worthy of note that although Fenton-type reactions usually implicate the use of H_2O_2 , they can occur using molecular oxygen, Therefore the absence of H_2O_2 in this system does not preclude the initiation of Fenton-type chemistry. These ROS present an oxidative stress both *in vitro* and *in vivo*. In addition, VO^{2+} was highly bioreactive in comparison with VO_3^- (Merolla and Richards, 2005). Thus, further work is required to elucidate the oxidation states of metals when analysing samples of PM. A form of ICP-MS that would take into account mass-to-charge ratio of PM metals would be a useful analytical tool.

PM has been found to be rich in soluble components such as chlorides, nitrates and sulfates. These groups, in certain combinations with metals, allow water-soluble compounds to be formed. The ability of a secondary component to have an effect on the oxidative capacity of the constituent metals was subsequently investigated. It was revealed that chlorides, nitrates and sulfates had no significant impact on the overall oxidative capacity of copper compounds, which supports earlier evidence that the metal constituent exerts the primary oxidative threat.

Zn^{2+} was chosen because there was conflicting literature regarding its toxicity as previously discussed (Chapter 3) (Pagan *et al.*, 2003; Riley *et al.*, 2003). Zn^{2+} has been found to have antioxidant properties by competing for binding sites on DNA with other metal cations such as Cu^{2+} and Fe^{2+} *in vitro* (Prasad and Kucuk, 2002). Zn^{2+} has also been found to exhibit synergistic effects, causing unexpected increases in the severity of toxic endpoints, when in combination with other metals. The simplicity of the plasmid scission assay, permitted the relationships and interactions between metals to be determined without interference or confounding factors. Evidence was found which suggested Cu^{2+} poses a redox threat to DNA (Stohs and Bagchi, 1995). Zn^{2+} presents no redox threat

toward DNA due to existence in only one oxidation state (due to a stable d sub-shell configuration). However Zn^{2+} is able to hydrolyse ester bonds, which may explain the observed synergistic effect between it and other metals. It is possible that the Zn^{2+} either 'weakened' the plasmid molecule or increased the availability of ROS-susceptible sites for attack. This action could have been insufficient to cause any measurable degree of damage but enough so as to leave the plasmid more vulnerable to the redox threat posed by Cu^{2+} , Fe^{3+} and to a lesser extent VO^{2+} . Another possibility is that the presence of Zn^{2+} stabilises the electronic configuration of the phosphate groups (similar to its action with carboxypeptidase A), thus potentiating change from one anionic state to another and possibly damage within the DNA molecule. These hypotheses seem unlikely due to the observed findings when Fe^{2+} was used – if the Zn^{2+} was having a direct effect on the DNA potentiation would be seen with all bioreactive metals but this was not the case with Fe^{2+} . The oxidation state of the metal used with Zn^{2+} seems to be an important factor and a more probable theory is that the Zn^{2+} was having an effect on the metal ion itself as opposed to the plasmid. The present data supports previous *in vitro* findings with cellular systems which have shown that exposure to a Zn^{2+} and Cu^{2+} mixture resulted in significantly greater epithelial toxicity responses than did exposure to Zn^{2+} or Cu^{2+} alone (Pagan *et al.*, 2003). In contrast, other investigators reported that Zn^{2+} appears to diminish the negative impact of V^{2+} and Cu^{2+} but has no effect on Fe^{2+} toxicity (Riley *et al.*, 2003). Zn^{2+} has also been found to counteract iron-induced oxidation by competitive inhibition.(Zago and Otieza, 2001).

The results obtained using the lavage fractions revealed that not all the constituents have a protective effect against bioreactive metals. Considering the complex heterogeneity of pulmonary lavage fluid, it is realistic to hypothesise that substances such as DNAses may be present in the larger molecular weight fractions, which are exerting the observed detrimental effects on the DNA. The lower fractions are known to contain antioxidants such as urate, ascorbate and glutathione (Greenwell 2003). These (along with other small molecular weight molecules) could be reducing the potency of the metals by exerting antioxidant properties. Although this study suggests that oxidation may be one of the key processes by which metals damage DNA, it does not offer definitive proof of this theory

– other mechanisms may be involved. Considering the dilute nature of the BALF obtained within this study when compared to ELF *in situ*, one can only surmise that the protective nature of ELF is approximately 40x more effective *in vivo*.

When considering the antioxidant nature of glutathione, it may be expected to exert a protective effect *in vitro*. However this was not the case. When these results were compared alongside those of the effect of oxidation state on metal bioreactivity, a hypothesis becomes clear. GSH may be exacerbating the damaging effects of the majority of the metals due to its reducing properties. From the previous experiments it has been shown that Fe^{2+} is more bioreactive than Fe^{3+} , therefore glutathione could be reducing Fe^{3+} to Fe^{2+} . Due to the subsequent Fe^{2+} being at a relatively high concentration it caused damage to the plasmid. This hypothesis would be the same for Cu^{2+} and VO^{2+} . Glutathione is unable to reduce Fe^{2+} to a more reactive form and thus there is no observed difference between the damage caused by Fe^{2+} and the damage caused by the mixture of Fe^{2+} and glutathione.

In summary, supporting evidence has been found for the role of water-soluble, redox-active, transition metals in the oxidative bioreactivity of PM (Molinelli *et al.*, 2002), especially the most abundant metals found in a typical historical London PM sample and their known ability to induce toxicological effects. Oxidation state has been shown to be key in determining oxidative capacity and secondary group (chloride, nitrate, sulfate) was found to be insignificant. Also observed was the ability of certain metal mixtures to cause more damage than would have been anticipated. Further work in this area may shed more light on the type of interactions that occur in ambient PM. Investigation into synergistic relationships between metals is necessary to fully explain PM-induced oxidation. BALF components have been shown in this study to exert both pro- and anti-oxidative effects. These results highlight that the simplistic nature of this assay is insufficient to model comprehensively the interactions between PM constituents in the lung. Whilst the assay has been useful in the evaluation of various metal interactions and their effects when mixed with lung components, a more complex system is required to gain a more realistic understanding of the effects exerted by these mixtures for a more rational outcome.

CHAPTER 4

***IN VIVO* TOXICOLOGY OF PM SURROGATES**

4.1 Introduction

It has been established that the inhalation of many types of metal rich particulates affects the respiratory tract, bronchioles and alveoli in both humans and animals i.e. rodents. There have been many *in vivo* studies carried out whereby animals have been exposed to a variety of ambient PM fractions (both whole and water-soluble) (e.g. EHC-93 Adamson, 1999) as well as PM surrogates such as diesel exhaust particles (Reynolds and Richards, 1999) and ROFA (Dreher, 1997; Mollinelli *et al.*, 2002). All of the above studies involved administering particulates in a carrier solution in order to assess their potential toxicity in the lung. Moreover, intratracheal instillation was used as the exposure technique to administer the mixtures as opposed to inhalation, which gives the most authentic exposure compared to real life and is the natural route of entry into the human and rodent hosts. There are many advantages in using both intratracheal instillation or inhalation methods and the choice of technique depends on the requirements of the experimental parameters (e.g. Table 4.1; adapted from Driscoll, (2002))

Table 4.1 Respective advantages of inhalation and instillation.

Inhalation	Instillation
Representative route of exposure	Exact dose can be delivered to lung
Non-invasive delivery of substance but dose can be variable	Large range of doses can be delivered in short period of time – rapid turnover
Exposure of complete respiratory tract (oro-nasal to alveoli)	Used as a screening tool to determine approximate dose range
Vehicle is not needed, so no alteration to the physicochemical properties of the test material occurs	Technical procedure is simpler than inhalation procedure
No toxicology from exposure process, only effects of test material	Specific lobe exposure can be carried out in larger animals (non-dosed lobe from same lung used as control)
Representative distribution of test material	Comparatively inexpensive
No confounding effect of anaesthesia (May affect test material retention and clearance)	Detection of immediate responses possible. More initial aggressive response

Intratracheal instillation was chosen as the optimal method of exposure as this study was being conducted to elucidate possible mechanisms of toxicity. Hence, the administration of exact doses was important as well as being able to assess toxicity at acute time points.

The primary hypothesis of this study was that the composition of different metal mixtures determines the degree of pulmonary toxicological damage induced in both a concentration and oxidation state dependent manner. In order to investigate this, metals that were deemed bioreactive from the *in vitro* studies (Fe^{2+} , Fe^{3+} , Cu^{2+} , and VO^{2+} ; Chapter 3) as well as Zn^{2+} , selected for its observed synergistic effects were used in differing combinations. The concentrations of the soluble metals used were based upon their proportions found in a London 1958 sample, as used in previous *in vivo* studies (Whittaker, 2003). The first study (herein referred to as study 1) involved using the four metals at exactly the same concentrations as present in the 1958 sample and comparing the observed toxicology with that induced by three times these concentrations (see Section 4.2.2). A second study (herein referred to as study 2) was then carried out to assess the effects of replacing Fe^{2+} with Fe^{3+} in the surrogate mixture and comparing this to a mixture without Zn^{2+} (see Table 4.2.3). These were also compared to Zn^{2+} alone in order to gauge whether any synergistic effects could be observed *in vivo*.

The bioreactivity of the mixtures was assessed by conventional toxicological methods such as analysing lung parenchymal weight:body mass ratio in order to assess the health status of the lung. An increase in lung:body mass ratio is usually associated with oedema or an inflammatory response in the lung. Analysis of lavage free cells (LFC) was also conducted to gain an insight into possible inflammatory effects. Calculating the neutrophil concentration as a proportion of total LFC assessed the severity of this type of response. Lung surface protein concentrations were also measured as a means to evaluating the development of oedema.

The second hypothesis tested in this study was that instillation of soluble metal ions would affect metal equilibrium within the lung and systemic organs. Of specific interest were the heart, liver, and kidneys and how the equilibrium of metals varied over three different time points. It has been well documented that the water-soluble

fraction of PM has been linked to adverse effects in organs other than the lung, particularly the cardiovascular system (Dockery 2001; Watkinson *et al.*, 1998; Seaton *et al.*, 1999; Dreher, 2004). Dreher (2002), in his work using ROFA, has shown that the translocation of bioavailable metals such as vanadium into the circulation was rapid (as quickly as 15 minutes). Therefore, early time points were selected for this study. Other organs, such as the liver and kidney, were also analysed as they are responsible for the biotransformation and clearance of xenobiotics, respectively. The appropriate procedure necessary in obtaining metal concentration was considered to be inductively coupled plasma mass spectrometry (ICP-MS). This was because the method was fully quantitative and sensitive enough to measure minute fluctuations in metal concentrations (Dr Iain McDonald, personal communication, 2005).

4.2 Materials and Methods

4.2.1 Equipment and Materials

96 Well Plate-Reader	Jencons, Bedfordshire, UK
Bovine Serum Albumin	Sigma, Dorset, UK
Copper Sulfate	Fisher, Leicestershire, UK
Coomassie Blue	Sigma, Dorset, UK
Cytospin	Centurion, West Sussex, UK
DPX fixative	BDH, Leicestershire, UK
Ethanol	Sigma, Dorset, UK
Euthatal	Rhone Merieux, Essex, UK
Halothane	Rhone Merieux, Essex, UK
HPLC-Grade Water	Fisher, Leicestershire, UK
Image Analyser	Leica Imaging Systems, Cambridgeshire, UK
Iron (II) Sulfate	BDH, Dorset, UK
Iron (III) Chloride	BDH, Dorset, UK
Male Wistar Rats (specific pathogen-free, 150-180 g)	Charles River Ltd., Kent, UK
Microtitre Plates	Sigma, Dorset, UK
Primar Nitric Acid	Fisher, Leicestershire, UK
Quick Stain	Raymond Lamb, E. Sussex, UK

Sodium Chloride	Fisher, Leicestershire, UK
Sterile Luer Cannulae (200/300/050)	Portex, Kent, UK
Vanadyl Sulfate	Fisher, Leicestershire, UK
X-Series ICP-MS	Thermo-Elemental, Cambridgeshire, UK

4.2.2 Dose Justification

The surrogate dose (SD) of metals used was in the exact proportions and concentrations found in the London 1958 sample. Adamson *et al.* (2000) used zinc at 10x the concentration that it was found within a particulate sample (EHC-93) in studies using mice, eliciting rapid effects. Another parameter that was considered when choosing the 3x surrogate dose (3SD) was the physiological relevance it had when compared with comparative inhalation exposure in human lungs. An approximate calculation of the human dose of PM inhaled over a 2 week exposure period was calculated from 1958 data in order to compare the dosimetry between human exposure and the surrogate dose used in this study. Previous data (Whittaker, 2003) regarding airborne PM concentration (5.21 mg/m^3), solubility (10 %) and metal concentration (7.2 % of total soluble PM) were used alongside standard values (100 l/min human inhalation rate, 20 % particle deposition, 650 g mean human lung weight (Vincent, 1995)) to calculate the dose per unit of lung as 0.023 mg/g over a 2 week exposure period. This was compared to the instilled rat dose calculated using total deposition mass and mean rat lung mass data (0.0716 mg and 0.894 g respectively) from the study. The resulting value of 0.8 mg/g lung for the rat exposure was found to be only around 3 times greater than the expected human dose over the same total exposure period without taking into account translocation, clearance etc. A 3SD was therefore selected as a high dose in order to elicit a rapid effect as it was not known what type of effect would be seen with the SD.

4.2.3 Sample Preparation

The metal mixtures were prepared as discussed in Chapter 3, Section 3.2.3. Metal mixtures containing iron (II) sulfate, iron (III) chloride, zinc sulfate, copper sulfate, and vanadyl sulfate were prepared using sterile HPLC grade water containing 0.15 M sodium chloride. There were five different test mixtures generated, as well as a saline only control. The first test mixture was a surrogate for the 1958 London PM sample. A second surrogate mixture was also generated using the same ratio of metals but at a



three-fold greater concentration. Three further mixtures were generated in order to assess the effects of individual components on toxicity. These included a surrogate mixture in which the Fe^{2+} used in the original was replaced with Fe^{3+} , a surrogate mixture not containing zinc and a solution of zinc alone. Each mixture was assigned a code as follows:

- saline control = SC
- surrogate dose = SD
- 3x surrogate dose = 3SD
- 3x surrogate dose including Fe^{3+} = 3SD(Fe^{3+})
- 3x surrogate dose without zinc = 3SD(- Zn^{2+})
- 3x zinc only = 3 Zn^{2+}

The metal compounds were weighed out to an absolute metal weight rather than a compound weight. The contents of the different mixtures can be seen in Table 4.2.3.

Table 4.2.3 Relative metal concentrations in the surrogate test mixtures.

Metal	Metal concentration $\mu\text{g}/0.5$ ml				
	SD	3SD	3SD(- Zn^{2+})	3SD(Fe^{3+})	3 Zn^{2+}
Cu^{2+}	1.9	5.7	5.7	5.7	-
Zn^{2+}	43	129	-	129	129
Fe^{2+}	22.7	68.1	68.1	-	-
Fe^{3+}	-	-	-	68.1	-
VO^{2+}	4	12	12	12	-
Total Metal	71.6	214.8	85.8	214.8	129

4.2.4 Instillation

Rats were anaesthetised with Halothane and their body weight recorded. The different mixtures of metals (0.5 ml per animal) were then administered by non-invasive intra-tracheal instillation where n=5 animals per group. Exposure periods for study 1 were 4 h, 24 h, 72 h (3 days), 168 h (7 days) and 336 h (14 days). For study 2 the exposure periods were 4 h, 24 h and 168 h (7 days). The exposure period for the second study lasted only seven days because results from the first study revealed

sufficient recovery by this time-point. Control animals were dosed with 0.5 ml 0.15 M NaCl solution.

4.2.5 Body Mass Monitoring

The animals were monitored everyday to check for ill health. Signs of distress to be noted included whether they had ruffled fur, irregular breathing, a hunched posture and blood shot eyes. These observations were carefully recorded. The animals were weighed so as to assess that they were not losing more than 20% of their body mass compared to control animals in accordance with Home Office Guidelines (2005). If any animal had lost over 20% body mass, when compared with saline treated animals, they were culled.

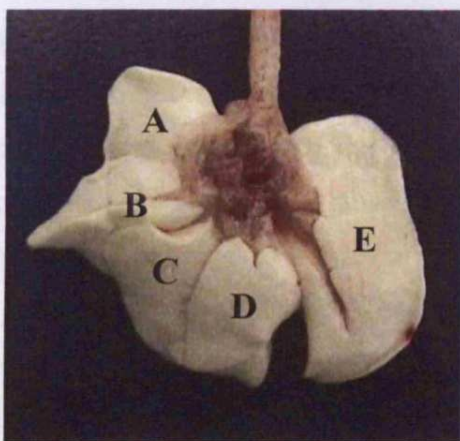
Analysis of the change in body mass gave an indication of the effects the metal mixtures exerted when instilled into the lungs. The body mass difference for each animal was calculated at each time point as a difference from its original starting mass. The results obtained within each of the test groups (n=5) were combined and averaged with the standard error calculated.

4.2.6 Sacrifice and Dissection

The animals were anaesthetised with Halothane and then a lethal dose of Euthatal (1-2 ml dependant upon animal size) was administered intraperitoneally. Each animal was weighed and cardiorespiratory death was confirmed by noting whether breathing had stopped and by assessing loss of sensitivity of the feet before starting the dissection. The dissection procedure was as follows:

- The ventral fur of each animal was washed in 70% ethanol and the surface skin removed. The peritoneal cavity was opened by a midline incision and the major dorsal blood vessels cut.
- Having exposed the throat, a tracheotomy was performed and a Luer cannula attached to a 20 ml syringe was tied into position in the open trachea.
- The diaphragm was then opened and a large portion of the rib cage and thymus removed.

- An incision in the right ventricle allowed a Luer cannula attached to a gravity feed of sterile saline (0.15 M) to be fed into the pulmonary artery and the right atrium was then cut to allow fluid to exit.
- The lungs were perfused with 0.15 M NaCl using artificial ventilation with 8-10 ml of air via the syringe attached to the Luer cannula tied into the trachea. Approximately 7 or 8 ventilations were necessary to clear all blood from the pulmonary circulation, resulting in white parenchymal lung tissue.
- The heart was then removed along with a part of the liver and two kidneys. The lungs and trachea were detached from the rest of the carcass. The oesophagus and any fatty tissues were cleared from the lungs and trachea. The lymph nodes were excised from the carcass and pooled by experimental group.
- Mucoidal tissue from the outer tracheal surface was removed with absorbent tissue and the excised lungs were then weighed and the lung parenchymal mass plus tracheal weight recorded. The groups of lungs for pathology (from additional animals in control and 3SD groups) were fixed and stored in 10% formalin solution at 4°C until further analysis, as discussed in Chapter 5, Section 5.2.3.
- The lungs were then lavaged (detailed in Chapter 4, Section 4.2.10). The trachea was excised from the parenchymal tissue and weighed. This tracheal weight was then subtracted from the lung weight previously recorded to provide an accurate measurement of the mass of the lung parenchymal tissue. The parenchymal tissue was then separated into the five lobes and stored at -80°C. The right apical lobe was used for genomic analysis. The left diaphragmatic and apical lobe was used for ICP-MS analysis (Figure 4.2.6).



- A = Right Apical
- B = Right Intercostal
- C = Right Diaphragmatic
- D = Right Cardiac
- E = Left Diaphragmatic and Apical

Figure 4.2.6 Differentiation of rat lung lobes

4.2.7 Pulmonary Lavage

After the lung mass was measured, the lungs were lavaged by a gravity-feed of 6-8 ml of 0.15 M NaCl. This occurred 5 times and the washes were pooled. The volume noted and kept on ice. The lavage collections then underwent 300 x g centrifugation for 20 minutes to remove the free cells. The resulting supernatant was poured off, separated into 1 ml aliquots and stored at -80 °C until analysis.

4.2.8 Free Cell Counts

The cell pellet was resuspended in 3 ml 0.15 M NaCl and a standard haemocytometer was used to calculate the number of large free cells alveolar macrophages (AM) and polymorphonuclear leukocytes (PMN) in each lavage pool. Any residual red blood cells were not included in the cell count. The residual free cells were re-suspended to a concentration of 200000 cells per ml in saline.

4.2.9 Cytospins

Standard light microscopy slides and filters were sealed into cytospin chambers and 0.5 ml of the diluted lavage free cells (LFC) suspension was transferred into the chamber. Duplicate pools of each cellular suspension underwent cytospin centrifugation at 13000 rpm for 6 minutes. The resulting slides with the LFC adhered to the surface were stored at 0-4 °C until further analysis.

4.2.9.1 Staining

The cytospin slides, comprising the LFC harvested from the pulmonary lavage, were stained using the Quick Stain system. This system consisted of a fixative, an acidic dye and a basic dye. Each slide was placed in the fixative for 5 seconds to stop metabolic processes, then into the first dye which had an affinity for basic cell components and finally into the second dye which had an affinity for acidic cell components. The slides were rinsed in a beaker of sterile double distilled water (dd-H₂O) and then allowed to air dry at room temperature. Once the slides were dry the cells were rinsed in xylene (5 seconds) to clear the specimens of water in order to prepare them for coverslipping. The mounting media DPX was used to ensure permanent sealing of the cells following placement of the coverslip.

4.2.9.2 Differential Cell Counts

The stained cells were visualised using a light microscope attached to an image analysis (IA) software system. The relative proportion of AM to PMN was calculated and recorded for each of two random areas of each slide. The mean data for each slide was then used for comparison. More acute inflammatory responses could be characterised by a greater increase in neutrophil concentration. Macrophages could be identified on the basis of cellular size (i.e. large) and by the shape of their nuclei (neutrophils have a more lobal shaped nucleus).

4.2.10 Total Lavage Protein

The total concentration of protein in the acellular lavage fluid was quantified using a standard Bradford technique (Bradford, 1976). Standards of differing concentrations of bovine serum albumin (0.5-8 µg/ml) were created in 0.15 M NaCl and duplicate 200 µl aliquots were pipetted into a 96 well microtitre plate. Triplicate 200 µl aliquots of the lavage samples (diluted 10-400 times) from each animal were also pipetted into the microtitre plates and 50 µl of Coomassie Blue protein reagent dye was added to each well. Separate metal mixture with exactly the same compositions as the test samples but which had not been instilled was used in the study to assess whether the metal ions would react with the Coomassie Blue and cause a colour change. The colour was left to develop for 2 minutes and then the optical density of each well was read on a plate reader using a 595 nm light filter. The total protein concentration of each test well was then calculated using a linear regression of the standards. Each duplicate pair of tests was averaged and the mean used to extrapolate back to the total protein value for each whole lung according to dilution factors and the comparative total volumes of each lavage sample. These data were then used for comparative and statistical analyses.

4.2.11 Inductively-Coupled Plasma Mass Spectrometry

ICP-MS was employed in this study to analyse the chemical elements present in each of the organs at the time of sacrifice. This highly sensitive technique can detect ions at concentrations as low as 0.1 part per trillion (ppt). The elements assayed for in this investigation were Fe, Zn, Cu and V.

4.2.11.1 Operational Process of ICP-MS

The principles of operation of ICP-MS are illustrated in Figure 4.2.11.1. An aliquot (approx. 1.5 ml) of liquid sample is drawn from an automated sampler and injected into the nebulizer. Here it is converted into a fine aerosol using argon gas as a carrier. The sample continues into the spray chamber in which large droplets are removed (approx. 98-99% of sample). The remaining 1-2% is then injected into the plasma torch. The plasma torch produces a stream of positively charged ions by passing a stream of gas into a strong magnetic field through a concentric quartz tube. This ionises the gas, which produces a high-voltage spark (and subsequent high temperature plasma discharge) when seeded with a source of electrons. When in the plasma the ions are then directed through the interface region. This is maintained at 1-2 torr (133.33-266.66 Pascals) vacuum by a mechanical roughing pump consisting of two nickel cones each with a 0.6-1.2 mm orifice through which the ions are directed to the ion optics. This region is maintained at approximately 10^{-2} torr (1.33 Pascals) by a turbo-molecular pump and its purpose is to focus the ions into the mass separation device and to remove any photons, particles and neutral species from reaching the detector. The mass separation device (in this instance a quadrupole mass spectrometer) is commonly maintained at 10^{-6} torr (1.33×10^{-4} Pascal) by a second turbo-molecular pump. This consists of 4 rods of equivalent size and diameter. Two opposing rods are charged using a direct current (dc) and the other two charged using a radio frequency (rf) electric current. By altering the electric current supplied to the rods, ions of specific mass can be allowed to pass through the spectrometer on to the deflector and then into the ion detector. Ions of any other mass are ejected from the quadrupole through the spaces between the rods. As the mass:charge ratio is different for each ion, the current is then altered for the next ionic mass and the scan is repeated. This occurs for each element under investigation. The data for the total concentration of each element in each sample is then transferred to a PC-based analysis package.

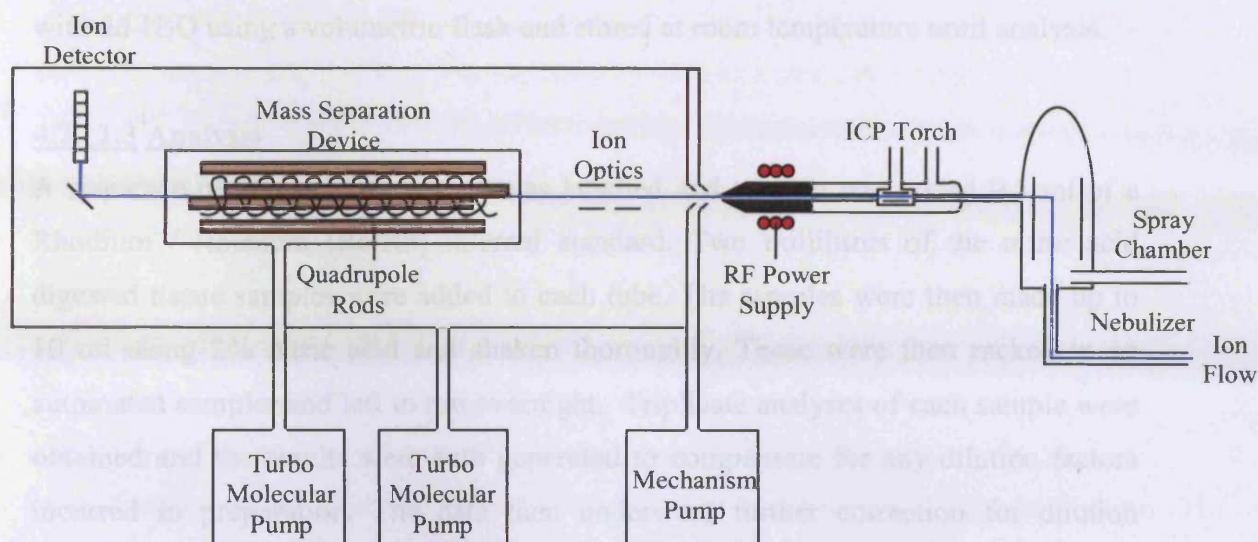


Figure 4.2.11.1 Operational Process of the ICP-MS

4.2.11.2 Sample Preparation – (Microwave Digestion of Tissues)

Pieces of organs (lung, heart, liver and kidney) ranging in mass (300-600 mg) from animals dosed with 3SD, where n=4 for each time point (4, 24, 72 h), were weighed and placed into labelled vials and 5 ml, 70% Primar nitric acid was added to each of the tubes. After fitting lids and cuffs to the vials, rupture membranes were inserted into the pressure caps, which were in turn attached to the tops of the lids (Figure 4.2.11.2). The vials were inserted into the 'plate' of the microwave and the eluant outlets attached to the pressure caps. The pressure sensor outlet was rinsed using dd-H₂O and having ensured no air bubbles remained in the tubing, this was attached to the vial containing the sample of the greatest mass. A pre-set program entailing the microwave digestion of the tissues at 180°C and 552 kPa pressure for 60 minutes, continued digestion for 30 minutes. Then sample cooling for a minimum of 30 minutes was activated. At the end of this process, the eluant outlets and pressure sensors were detached from the vials and the vials returned to the fume hood. Pressure caps, lids and cuffs were removed and the samples were poured out of the heating vials into labelled 30 ml collection beakers. Any residue was rinsed out of the heating vials using dd-H₂O. These samples were left open on a heating block overnight to volatilise and evaporate the nitric acid. The next day, the samples were resuspended in 2 ml of 10% nitric acid, capped and left on a warm heating block for

2 h to ensure full resuspension. After this time, samples were reconstituted to 20 ml with dd-H₂O using a volumetric flask and stored at room temperature until analysis.

4.2.11.3 Analysis

A sequence of 15 ml Falcon tubes was labelled and to each was added 0.5 ml of a Rhodium / Rhenium (Ro/Rh) internal standard. Two millilitres of the nitric acid digested tissue samples were added to each tube. The samples were then made up to 10 ml using 2% nitric acid and shaken thoroughly. These were then racked in an automated sampler and left to run overnight. Triplicate analyses of each sample were obtained and the results were auto generated to compensate for any dilution factors incurred in preparation. The data then underwent further correction for dilution incurred in the digestion process, as well as a mass correction due to each tissue being of a different mass. The final results were expressed in terms of parts per million (ppm) or parts per billion (ppb) (i.e. µg or ng of metal per gram of tissue).

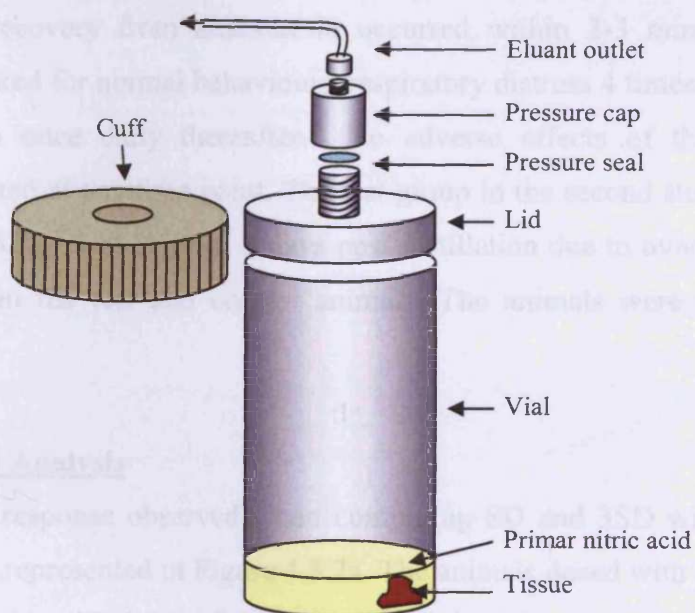


Figure 4.2.11.2 Diagram of apparatus used in tissue digestion for ICP-MS

4.2.12 Statistical Analysis

All data handling and graphical representation of results were performed in Microsoft Excel '97. Statistical analyses included Andersson-Darling normality tests, 2-sample

t-test and non-parametric Mann-Whitney tests. A two-sample t test was chosen as an appropriate test due to the data being derived from two independent random samples. This test was used if the data was normal and the variances were equal within each group. If this was not the case, a non-parametric Mann-Whitney test was used. All analyses were performed in Microsoft Minitab 13. Significance was assumed at $p \leq 0.05$. High significance was assumed at $p \leq 0.01$.

4.3 Results

The primary aim of this investigation consisted of two studies – investigation of the effects of a surrogate London PM sample (herein referred to as study 1), and investigation into the effects of individual components of the surrogate sample (herein referred to as study 2). Both studies were conducted in the same manner, but results will be discussed separately.

4.3.1 Instillation

In both studies, recovery from anaesthesia occurred within 2-3 minutes and the animals were checked for normal behaviour / respiratory distress 4 times a day for the first 2 days, then once daily thereafter. No adverse effects of the instillation procedure were noted at any time point. The test group in the second study involving the instillation of 3Zn^{2+} was stopped 3 days post instillation due to over 20% loss of body mass between the test and control animals. The animals were subsequently culled.

4.3.2 Body Mass Analysis

There was a dose response observed when comparing SD and 3SD with the saline control animals, as represented in Figure 4.3.2a. The animals dosed with SD lost mass between the time of instillation and 4 h. At each of the subsequent time points they gained mass, but more slowly than the controls until day 7. Between 7 (168 h) and 14 days (336 h) they gained mass at similar rates. The animals lost body mass over the first 24 h when instilled with 3SD. They neither lost nor gained mass between 24 h and 3 days (72 h). From this time point they started gaining mass and finally reached the same mass as the controls by day 14.

The second study revealed that animals dosed with 3Zn^{2+} and $3\text{SD}(\text{Fe}^{3+})$ lost mass until 24 h post-instillation as represented in Figure 4.3.2b. This effect was transient for $3\text{SD}(\text{Fe}^{3+})$ and at day 7 significant recovery was observed. The animals dosed with $3\text{SD}(-\text{Zn}^{2+})$ showed similar results to that of SD, with initial loss of mass between 0-4 h and then a slower gain of mass to that of the saline control until 24 h. Between 24 h and 7 days the rate of gain in mass seemed similar to that of the control. The effects of 3Zn^{2+} alone could not be analysed beyond 24 h post instillation, as this study had to be stopped as discussed in Section 4.2.4.

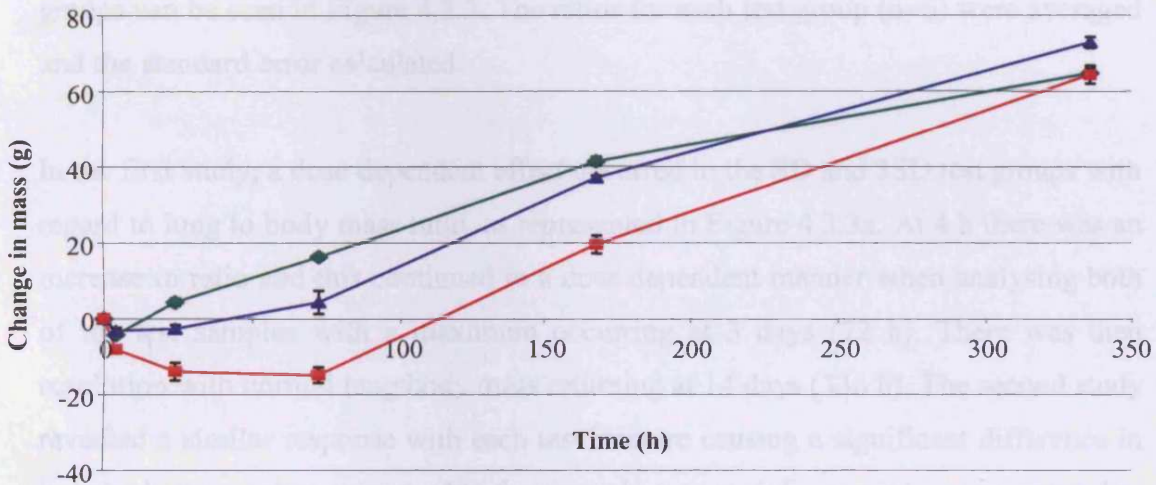


Figure 4.3.2a Mean body mass change, study 1 (mean ± std. err.)

◆ = SC ▲ = SD ■ = 3SD

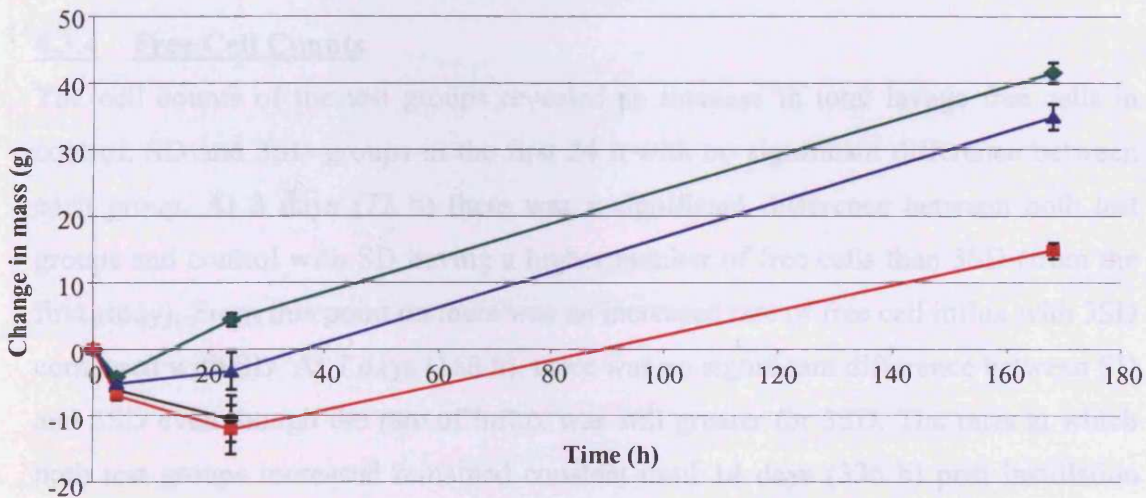


Figure 4.3.2b Mean body mass change, study 2 (mean ± std. err.)

◆ = SC ● = 3Zn^{2+} ▲ = $3\text{SD}(-\text{Zn}^{2+})$ ■ = $3\text{SD}(\text{Fe}^{3+})$

4.3.3 Lung:Body Mass Ratio

A primary indication of possible lung damage was obtained when lung:body mass ratios were analysed. In control animals, this ratio usually remained between 0.004 and 0.005 and was a good guide to 'healthy' lungs. However, an increase in this ratio is usually a sign of lung damage due to oedema/inflammation. The cause of the increase in weight of the lung is usually due to an increase in water accumulation and an influx of plasma components (including free cells and proteins). This is caused by damage to the pulmonary epithelium. Results from each animal from the different test groups can be seen in Figure 4.3.3. The ratios for each test group (n=5) were averaged and the standard error calculated.

In the first study, a dose dependant effect occurred in the SD and 3SD test groups with regard to lung to body mass ratio, as represented in Figure 4.3.3a. At 4 h there was an increase in ratio and this continued in a dose dependent manner when analysing both of the test samples with a maximum occurring at 3 days (72 h). There was then resolution with normal lung:body mass returning at 14 days (336 h). The second study revealed a similar response with each test mixture causing a significant difference in lung:body mass when compared to the controls over each time point, as represented in Figure 4.3.3b. The 3SD(Fe³⁺) mixture resulted in the highest lung:body mass at 4 h and the highest average ratio was observed at 24 h with 3Zn²⁺.

4.3.4 Free Cell Counts

The cell counts of the test groups revealed an increase in total lavage free cells in control, SD and 3SD groups in the first 24 h with no significant difference between each group. At 3 days (72 h) there was a significant difference between both test groups and control with SD having a higher number of free cells than 3SD (from the first study). From this point on there was an increased rate of free cell influx with 3SD compared with SD. At 7 days (168 h), there was no significant difference between SD and 3SD even though the rate of influx was still greater for 3SD. The rates at which both test groups increased remained constant until 14 days (336 h) post instillation (Figure 4.3.4a). Analysis of the free cells conducted in the second study revealed similar results with no difference in free cell numbers between controls and

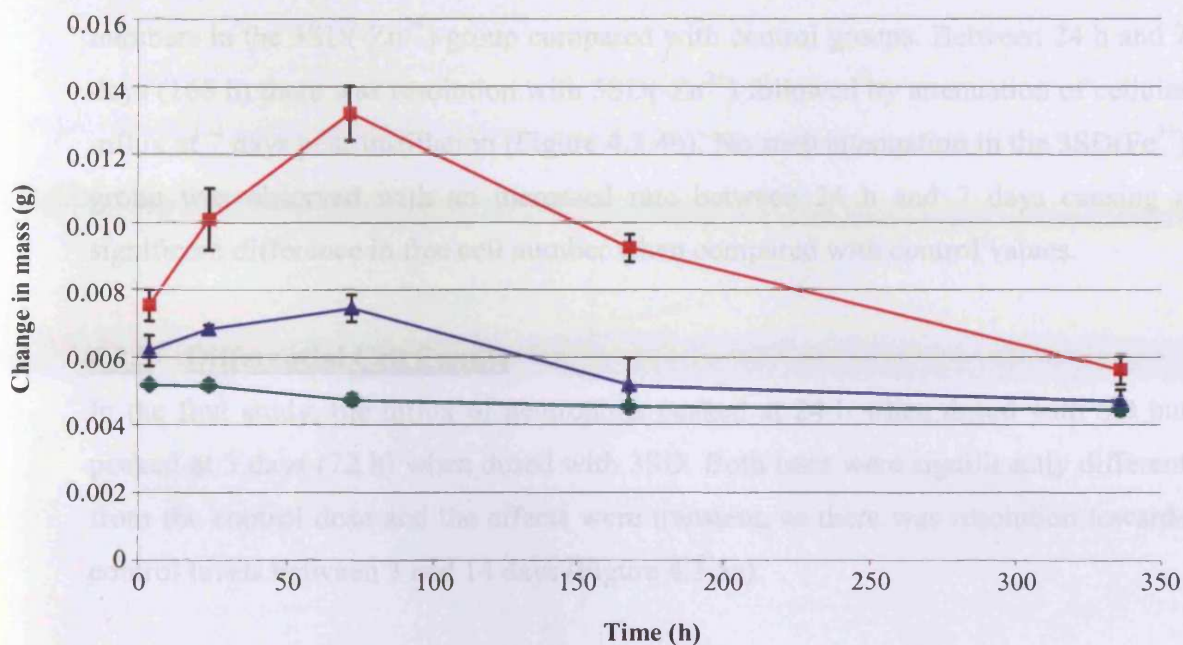


Figure 4.3.3a Lung:body weight ratio, study 1 (mean \pm std. err.)

◆ = SC ▲ = SD ■ = 3SD

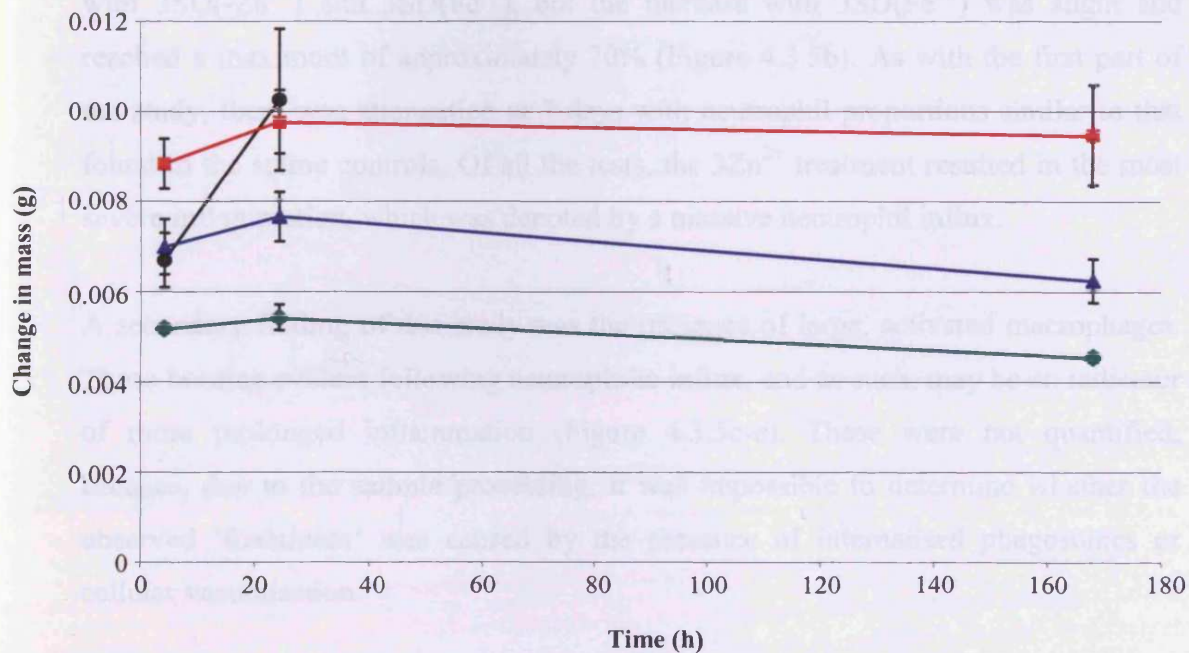


Figure 4.3.3b Lung:body weight ratio, study 2 (mean \pm std. err.)

◆ = SC ● = 3Zn²⁺ ▲ = 3SD(-Zn²⁺) ■ = 3SD(Fe³⁺)

each of the test groups. However at 24 h there was a significant increase with LFC numbers in the 3SD(-Zn²⁺) group compared with control groups. Between 24 h and 7 days (168 h) there was resolution with 3SD(-Zn²⁺) followed by attenuation of cellular influx at 7 days post-instillation (Figure 4.3.4b). No such attenuation in the 3SD(Fe³⁺) group was observed with an increased rate between 24 h and 7 days causing a significant difference in free cell number when compared with control values.

4.3.5 Differential Cell Counts

In the first study, the influx of neutrophils peaked at 24 h when dosed with SD but peaked at 3 days (72 h) when dosed with 3SD. Both tests were significantly different from the control dose and the effects were transient, as there was resolution towards control levels between 3 and 14 days (Figure 4.3.5a).

The second study revealed a large proportion of neutrophils being present with the 3SD(Fe³⁺) and 3SD(-Zn²⁺) samples as early as 4 h post-instillation. However, Zn alone produced a very low proportion of neutrophils. At 24 h there was a substantial increase in the proportion ($\approx 70\%$) of neutrophils. Further increases were also seen with 3SD(-Zn²⁺) and 3SD(Fe³⁺), but the increase with 3SD(Fe³⁺) was slight and reached a maximum of approximately 70% (Figure 4.3.5b). As with the first part of the study, there was attenuation at 7 days with neutrophil proportions similar to that found in the saline controls. Of all the tests, the 3Zn²⁺ treatment resulted in the most severe inflammation, which was denoted by a massive neutrophil influx.

A secondary finding of this study was the presence of large, activated macrophages. These became evident following neutrophilic influx, and as such, may be an indicator of more prolonged inflammation (Figure 4.3.5c-e). These were not quantified, because, due to the sample processing, it was impossible to determine whether the observed 'foaminess' was caused by the presence of internalised phagosomes or cellular vacuolisation.

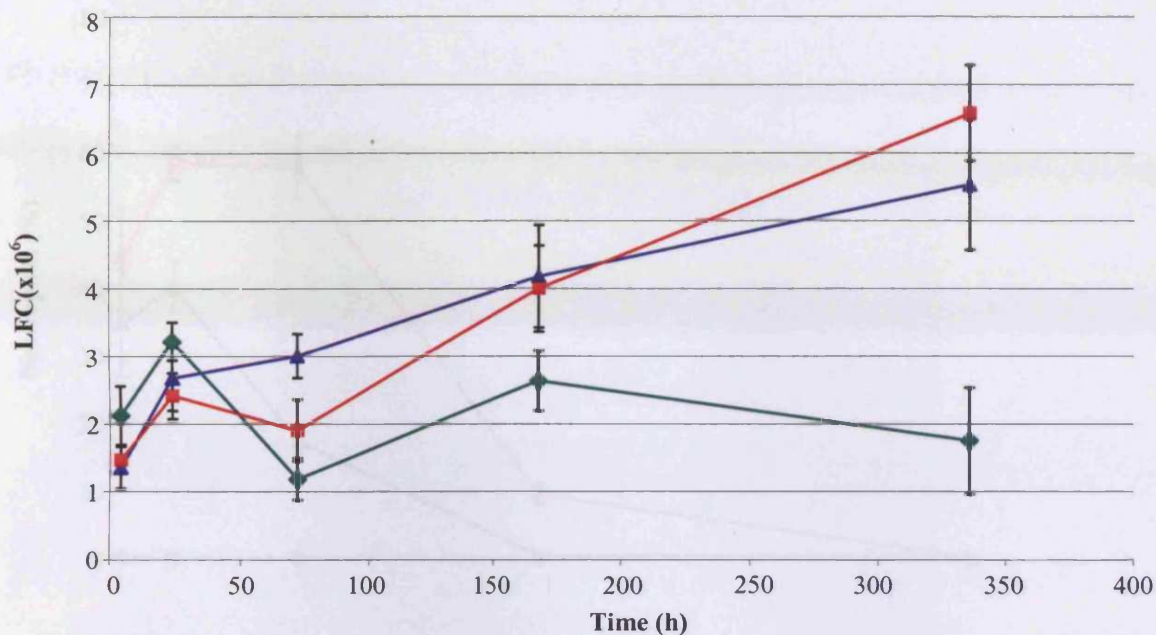


Figure 4.3.4a Lavage free cell count, study 1 (mean \pm std. err.)

◆ = SC ▲ = SD ■ = 3SD

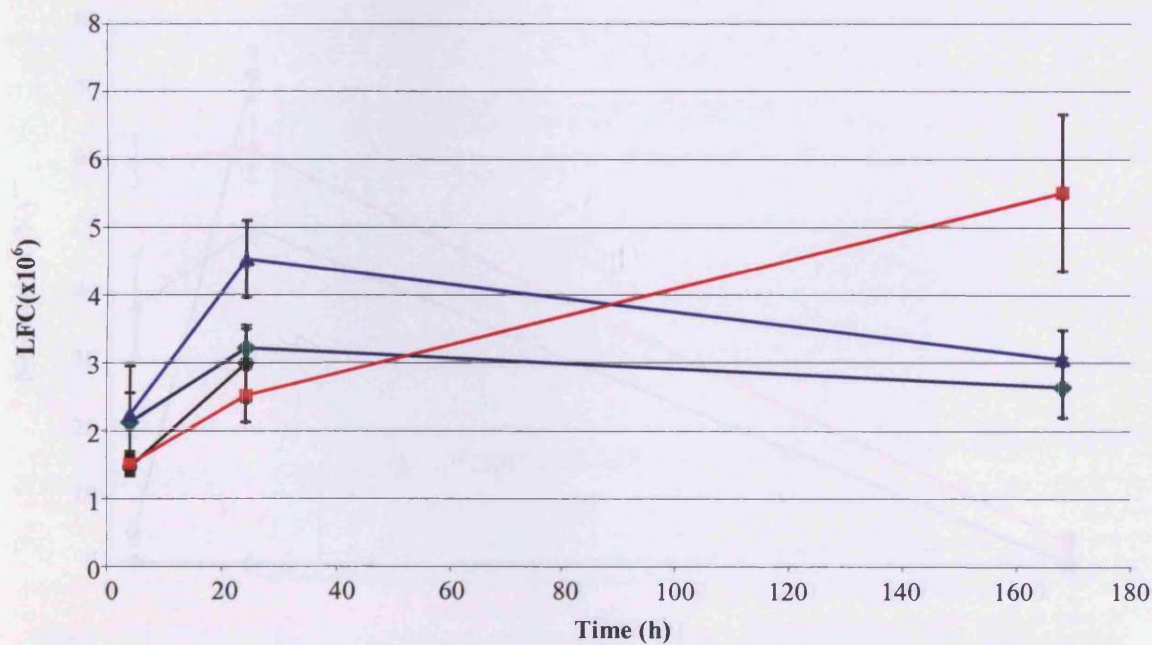


Figure 4.3.4b Lavage free cell count, study 2 (mean \pm std. err.)

◆ = SC ● = 3Zn²⁺ ▲ = 3SD(-Zn²⁺) ■ = 3SD(Fe³⁺)

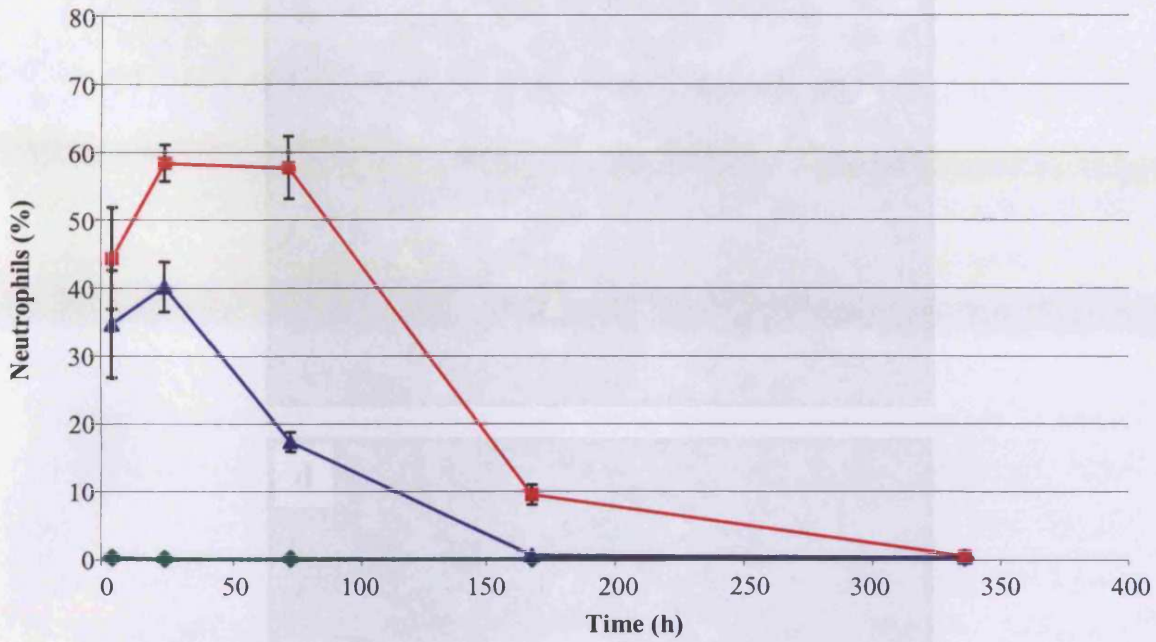


Figure 4.3.5a Differential cell count, study 1 (mean ± std. err.)

◆ = SC ▲ = SD ■ = 3SD

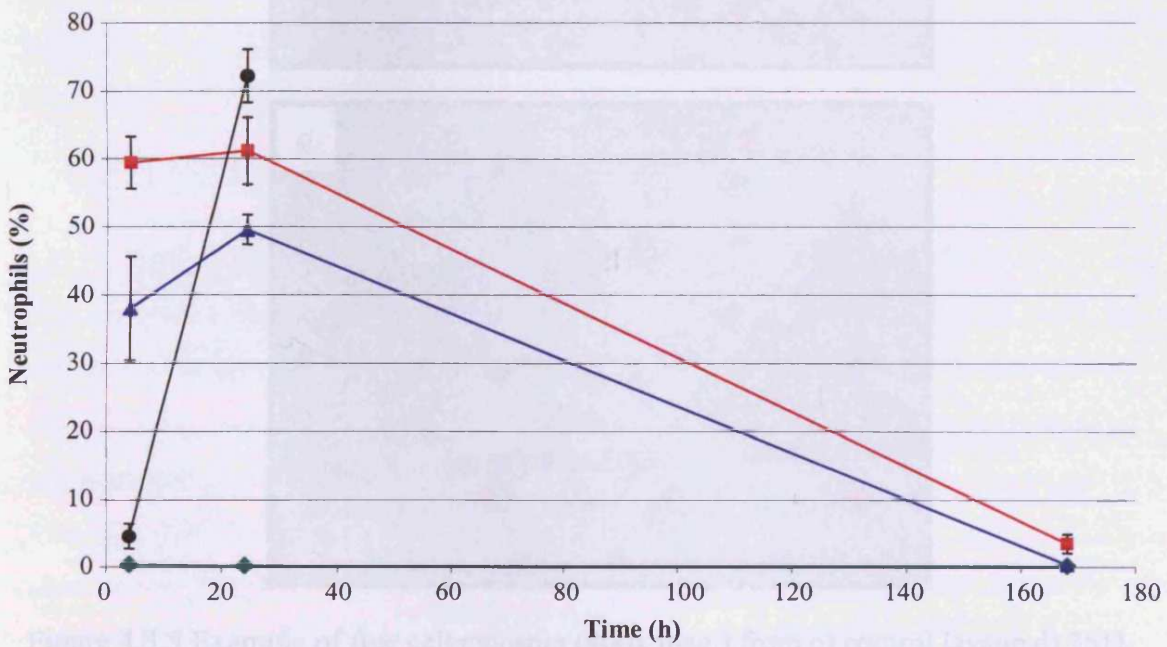


Figure 4.3.5b Differential cell count, study 2 (mean ± std. err.)

◆ = SC ● = 3Zn²⁺ ▲ = 3SD(-Zn²⁺) ■ = 3SD(Fe³⁺)

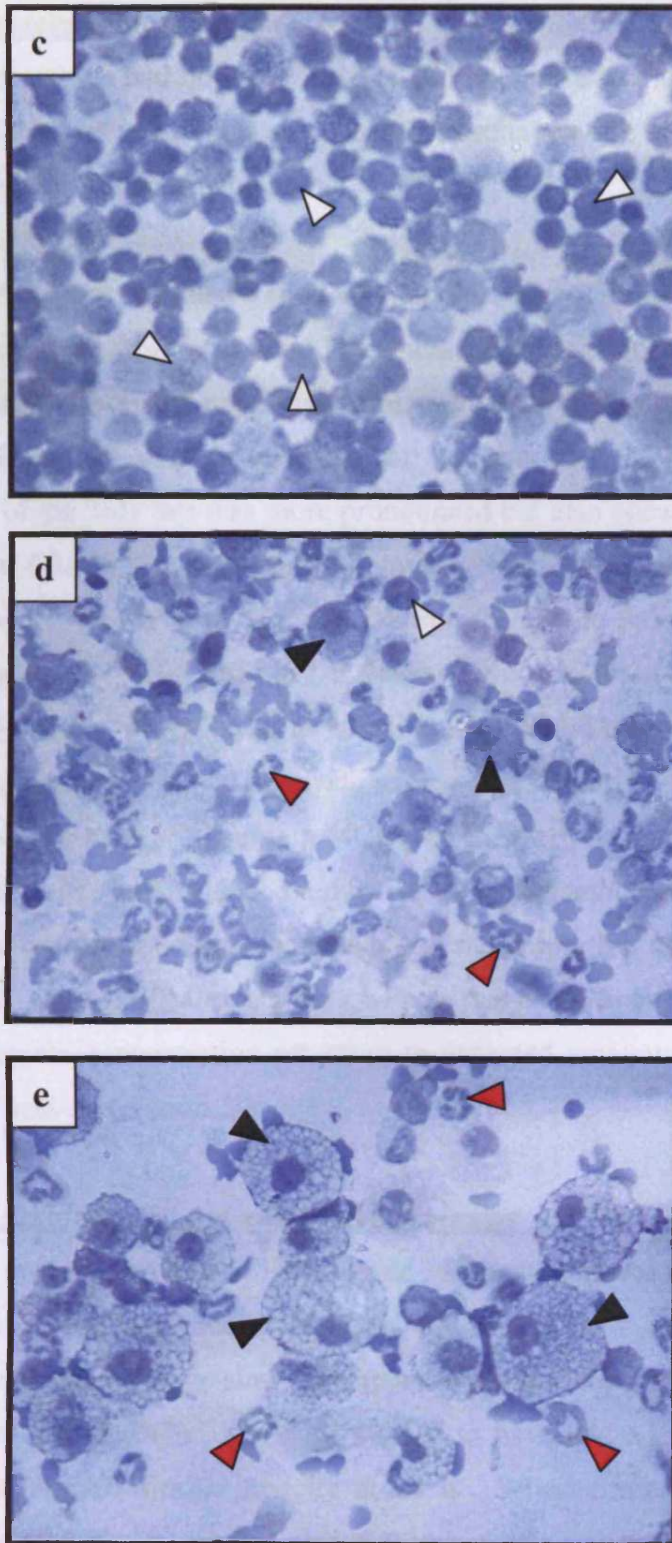


Figure 4.3.5 Example of free cell cytospin (400x mag.) from c) control lavage d) 3SD, 24 h exposure e) 3SD, 7 days exposure. White arrowheads = 'normal' macrophages, red arrowheads = neutrophils, black arrowheads = foamy macrophages.

4.3.6 Lavage Protein Concentration

The metal solutions which had not been instilled did not cause a colour change when mixed with Bradford reagent and thus any observed results relating to BALF were due to differences in protein concentration alone.

The results of both studies revealed a moderate amount of protein being found in the lavage of the entire test samples at 4 h. There was an evident dose response when comparing SD with 3SD, as previously observed with all other toxicological indicators. The SD dosed animals gave a peak concentration of protein at 24 h, whereas the peak of the 3SD test was more pronounced but also occurred at 24 h post instillation (Figure 4.3.6a). The tests using the mixtures 3SD(Fe³⁺), 3Zn²⁺ and 3SD(-Zn²⁺) showed a peak concentration of protein within the lavage fluid at 24 h (Figure 4.3.6b) which was similar to the 3SD test. As there were only three time points used in the second study, it was uncertain as to whether these would have been the highest concentration of protein at 3 days. Analysis showed that 3SD(Fe³⁺) and 3SD gave similar maximal concentrations of protein (40 mg/rat). However, on closer scrutiny it can be seen that 3SD(Fe³⁺) test induced a more severe oedematous effect earlier than the 3SD. A similar trend was found when analysing the proportion of neutrophils. As with the previous toxicological tests, the effects were transient and there was resolution with protein concentration returning to expected amounts between seven and fourteen days post-instillation.

4.3.7 Effects of Oxidation States and Metal Synergies

The difference in content between 3SD(Fe³⁺) and 3SD test mixtures resided solely in the oxidation state of the iron present (3SD(Fe³⁺) = Fe³⁺, 3SD = Fe²⁺). The overall toxicological tests showed a large similarity between the two mixtures, apart from at the 4 h time point. The 3SD(Fe³⁺) mixture seemed to have had a more rapid effect than the 3SD but showed similar toxicity at 24 h. When comparing the effects statistically (Figure 4.3.7), it was revealed that the neutrophil content and protein concentration were significantly different at the 4 h time point due to severe inflammation and epithelial cell damage.

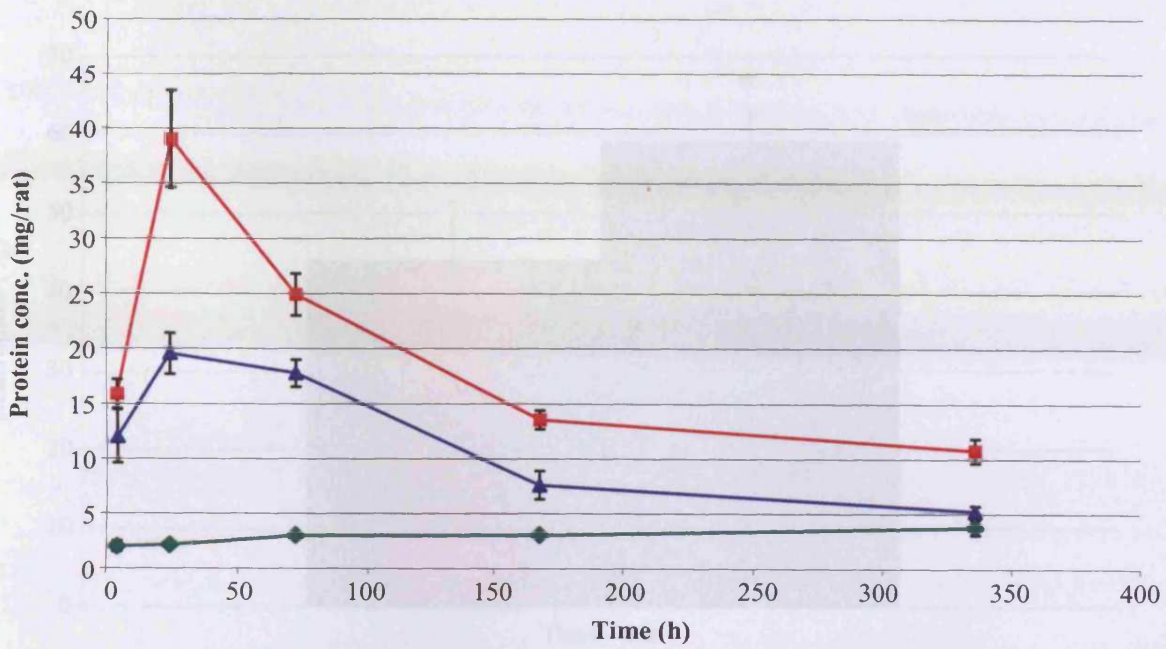


Figure 4.3.6a Protein concentrations present in BALF, study 1 (mean \pm std. err)

◆ = SC ▲ = SD ■ = 3SD

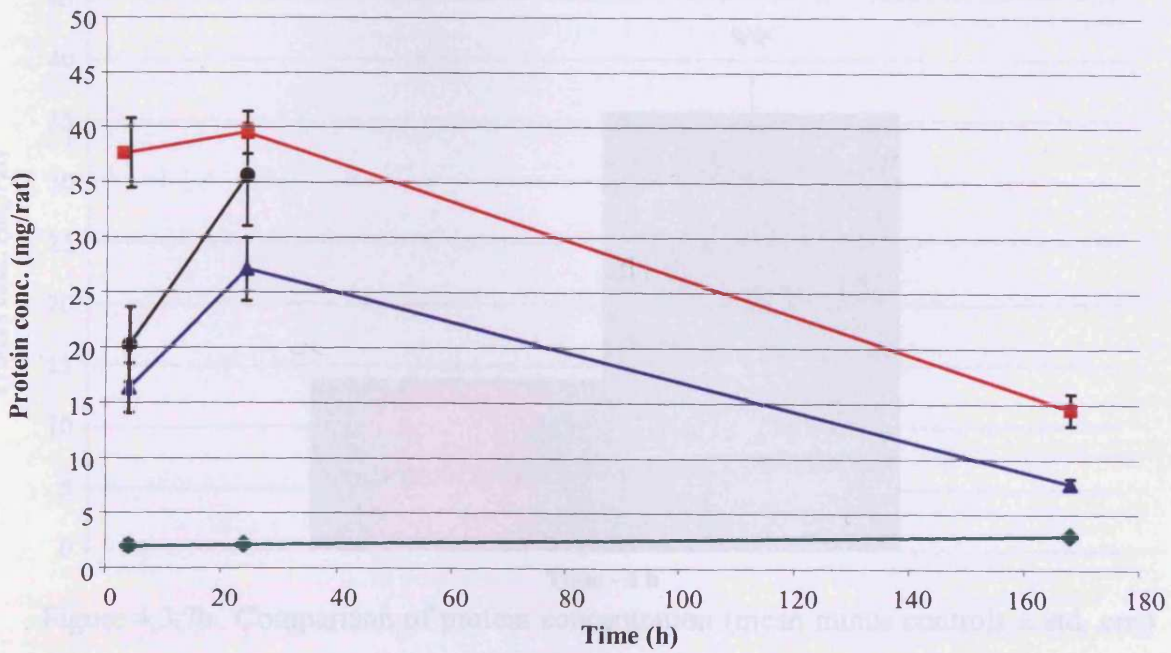


Figure 4.3.6b Protein concentrations present in BALF, study 2 (mean \pm std. err)

◆ = SC ● = 3Zn²⁺ ▲ = 3SD(-Zn²⁺) ■ = 3SD(Fe³⁺)

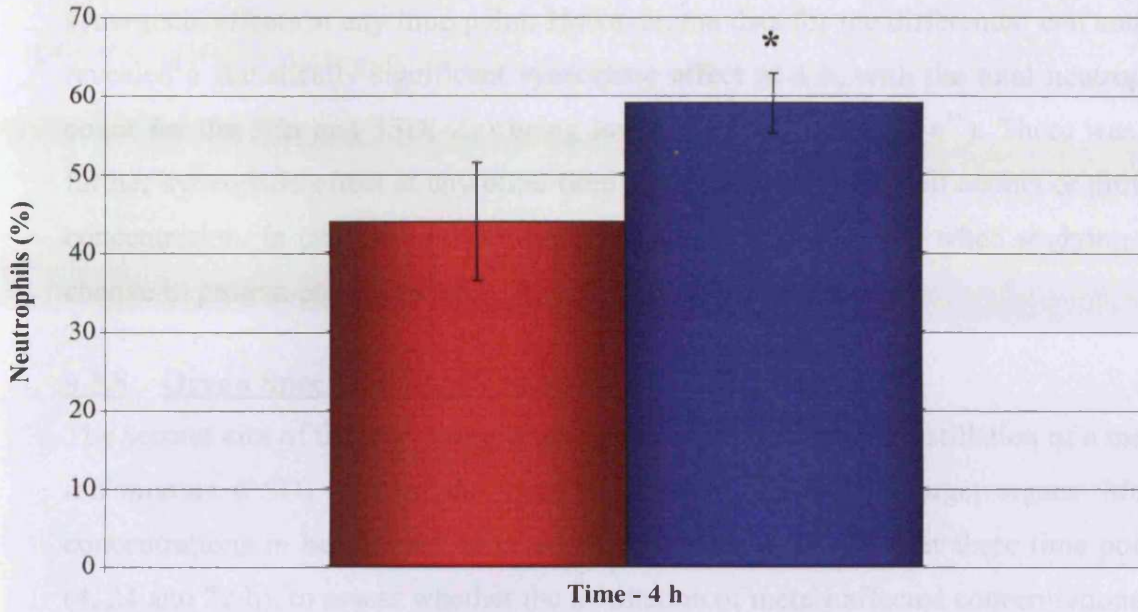


Figure 4.3.7a Comparison of % neutrophils (mean minus controls \pm std. err.)

(* = $p \leq 0.05$, ** = $p \leq 0.01$) ■ = 3SD ■ = 3SD(Fe³⁺)

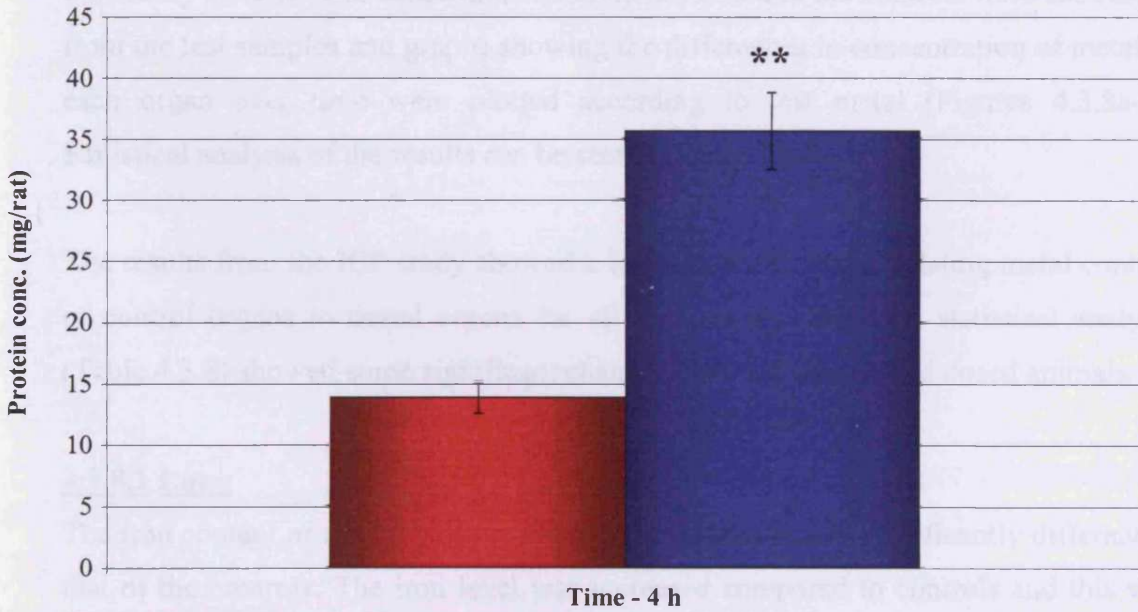


Figure 4.3.7b Comparison of protein concentration (mean minus controls \pm std. err.)

(* = $p \leq 0.05$, ** = $p \leq 0.01$) ■ = 3SD ■ = 3SD(Fe³⁺)

The metal content of 3SD(Fe^{3+}) is the same as the content of the 3Zn plus 3SD(-Zn) tests. When the bulk toxicology was analysed there was no evidence of additive or synergistic effects at any time point. However, the data for the differential cell counts revealed a statistically significant synergistic effect at 4 h, with the total neutrophil count for the 3Zn and 3SD(-Zn) being lower than that of 3SD(Fe^{3+}). There was no further synergistic effect at any other time point for differential cell counts or protein concentration. In contrast, an additive effect was observed at 4 h when studying the change in protein concentration.

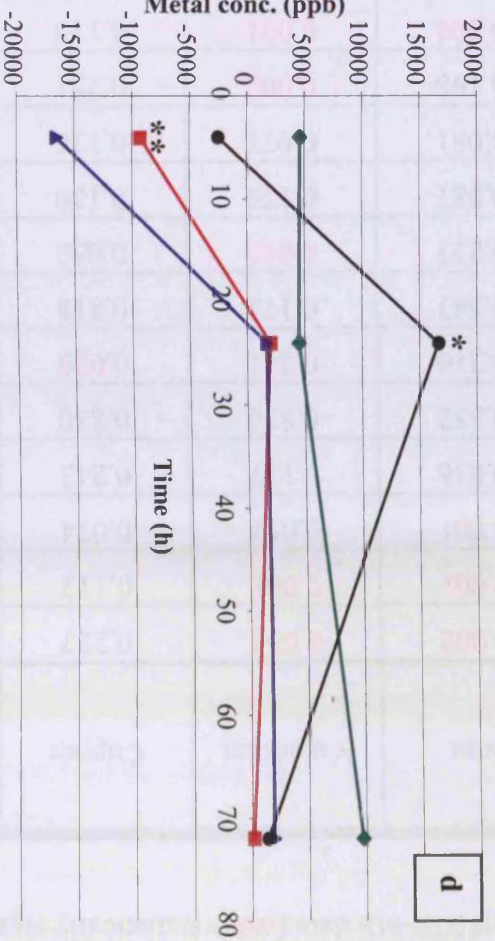
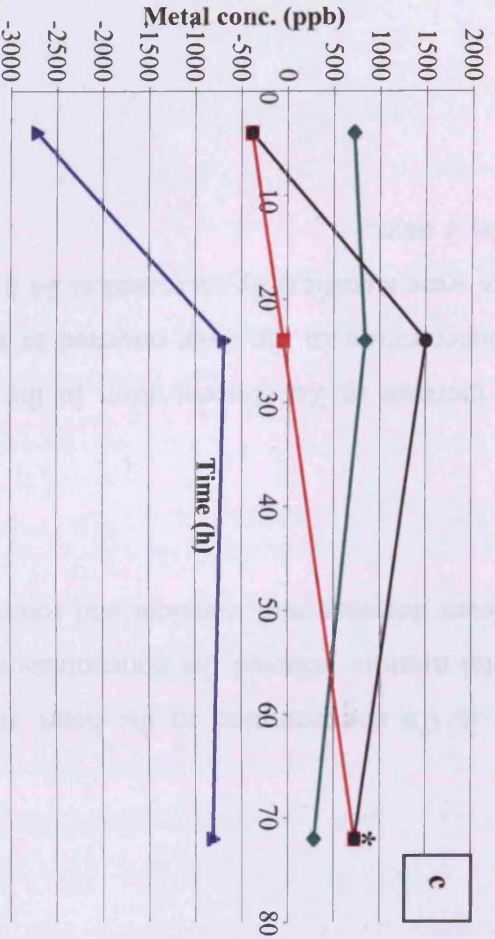
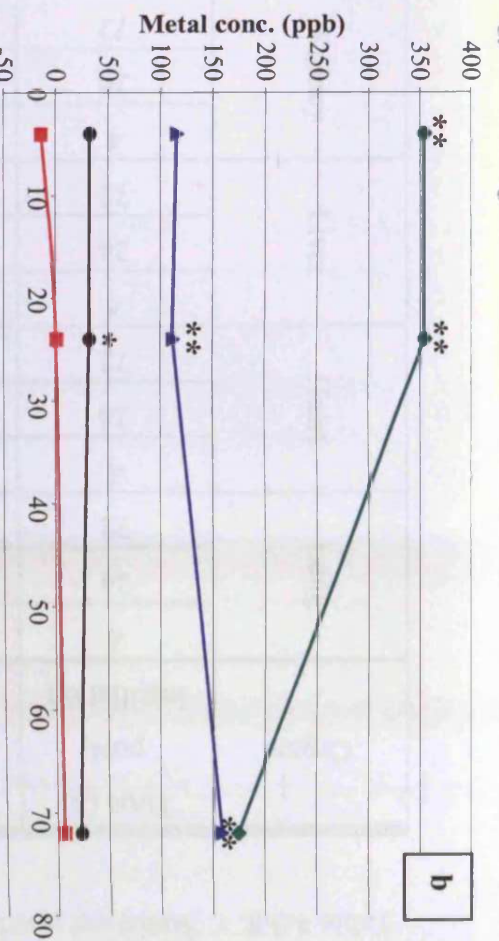
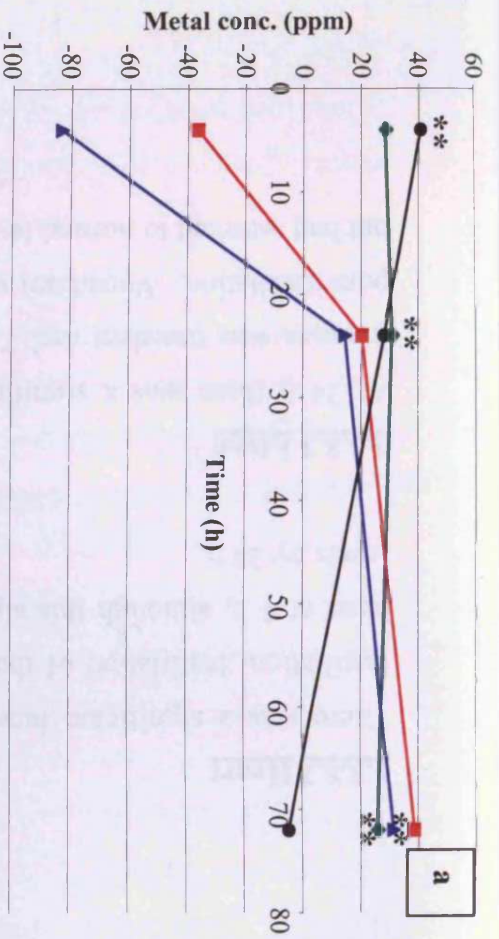
4.3.8 Organ Specific ICP-MS Analysis

The second aim of the study was to gain an insight into whether instillation of a metal ion mixture (3SD) affected the metal equilibrium within four target organs. Metal concentrations in heart, lung, liver and kidney were analysed over three time points (4, 24 and 72 h), to assess whether the instillation of metals affected concentrations of metals found in each organ compared with the controls. The theory was that the translocation of the instilled ions would cause an increase in metal concentration in the lung and heart during the first few hours and possibly in excretory organs such as the kidney at 72 h. The concentrations of metals found in the controls were subtracted from the test samples and graphs showing the differences in concentration of metal in each organ over time were plotted according to test metal (Figures 4.3.8a-d). Statistical analysis of the results can be seen in Table 4.3.8.

The results from the ICP study showed a low correlation when relating metal content of control organs to dosed organs for all four metals. However statistical analysis (Table 4.3.8) showed some significant changes between control and dosed animals.

4.3.8.1 Lung

The iron content of the lung of the dosed animals was highly significantly different to that of the controls. The iron level was increased compared to controls and this was maintained over three days. Flux in V concentrations was the most prevalent out of all four metals, being significant at both 4 h and 24 h in the lung.



Figures 4.3.8a-d ICP-MS analysis of metal concentration in different organs. Data is mean test minus control value. Error bars omitted for clarity. (* = $p \leq 0.05$, ** = $p \leq 0.01$) a) iron b) vanadium c) copper d) zinc

◆ = Lung ■ = Heart ● = Liver ▲ = Kidney

Table 4.3.8 Statistical p values of ICP-MS data (red = statistically significant)

Organ	Time (h) post instillation	Iron	Vanadium	Copper	Zinc
Lung	4	0.002	0.004	0.227	0.166
	24	0.001	0.001	0.112	0.121
	72	0.001	0.052	0.074	0.085
Heart	4	0.036	0.117	0.243	0.008
	24	0.352	0.830	0.830	0.120
	72	0.216	0.241	0.039	0.377
Liver	4	0.547	0.175	0.818	0.812
	24	0.253	0.010	0.052	0.049
	72	0.887	0.179	0.139	0.667
Kidney	4	0.081	0.071	0.136	0.081
	24	0.198	0.002	0.251	0.377
	72	0.004	0.001	0.110	0.086

4.3.8.2 Heart

There was a significant increase in Cu concentration in the heart at 3 days post-instillation. Instillation of the metal mixture affected the concentration of Zn in the heart at 4 h, although this significant decrease was transient and returned to normal levels by 24 h.

4.3.8.3 Liver

At 24 h there was a significant increase in Zn concentration in the liver but this increase was transient and Zn concentration in the liver returned to normal 3 days post-instillation. Vanadium values were significantly increased at 24 h post exposure but had returned to normal levels by 3 days.

4.3.8.4 Kidney

Analysis of the kidney revealed Fe levels to be significantly increased in the kidney at 3 days. A change in V concentration occurred at both 24 h and 72 h post-instillation in the kidney.

4.4 Discussion

Transition metals have a unifying characteristic such as their ability to exist in more than one oxidation state, which subsequently enables them to participate in the production of ROS via Fenton type reactions. Although these similarities exist, it has been shown that each of the metals differs substantially in their ability to induce pulmonary inflammation, as well as cytotoxicity when administered in equimolar doses (Rice *et al.*, 2001). For the purpose of this study, metal concentrations were used based on the proportion of each metal present in an ambient particulate sample and not on an equimolar basis.

In the study using the surrogate mixtures of PM, both bulk toxicological indicators such as change in lung body mass and lung:body mass ratio showed that peak changes occurred between 24 h and 72 h with every mixture, with attenuation occurring thereafter. The effects were transient and at 14 days there was no significant difference between the tests and the saline treated controls. The results from the differential cell counts and the levels of protein found in BALF showed a similar pattern to the bulk toxicology over this time period. There was an acute phase response occurring and elevated levels being seen until 3 days (72 h) post-instillation with attenuation at 7 and 14 days. The results indicated that the surrogate PM metal mixtures were having an effect at very early time points. This may have been due to their bioavailability, which could potentiate their translocation in the lung cells.

The study involving SD and 3SD mixtures revealed that the toxicological damage to the rats caused by these mixtures was dose-dependent. The only unexpected result that occurred involved the calculation of the free cell counts. The free cell counts were conducted to ascertain whether the different metal mixtures caused an inflammatory response. More specifically, an increase in macrophages in comparison with the control groups would indicate a mild inflammation whereas in the case of a more severe inflammation, the presence of foamy, activated macrophages in addition to a

neutrophil influx would be observed. When assessing the other conventional toxicological end points a difference between test and control had usually occurred by 24 h post-instillation. This was not the case when looking at the free cell population, which saw no change at this time point. The other unexpected result was found at 72 h where SD gave a significantly higher concentration of lavage free cells than 3SD. An explanation for this may be due to the damage caused by each mixture being so severe that elimination of macrophages outweighed influx from monocytes at the beginning of the time course. This is supported by the amount of neutrophils present at the early stages and the fact that when analysing the different slides there was a noticeable decrease in macrophage numbers as well as a large presence of neutrophils. Thus, at 3 days post instillation the instillate may have lost some of its bioreactivity or the rate of monocyte translocation could have increased. This would mean that the influx of the macrophages would be larger than the amount eliminated. As the bioreactivity would be lower for SD, the amount of macrophages present would therefore be greater than for 3SD. Even at 14 days the concentration of macrophages was still increasing for both mixtures but the rates of production had increased more rapidly for 3SD than that for SD, thus supporting the above hypothesis. The time course would have needed to proceed for a longer period of time to see if an expected attenuation would have occurred.

Previous studies have found a high correlation between the numbers of neutrophils observed after either instillation of an emission source air pollution particle or a surrogate mixture of its soluble components (Dreher, 1997). However, instillation of the insoluble components produced increases in neither inflammatory cells nor cellular injury. No such correlation was found between the surrogate samples used in this study and the original instillation of London 1958 PM, which showed very limited toxicological effects. This may be due to other components of the PM acting as sacrificial substrates for the reactive species or retarding their effects, hence protecting the lung from damage. The observed disparity between the ROFA and London PM samples may be explained by the far higher degree of solubility of the ROFA.

Measurements of lung protein concentration within BALF were carried out as an indicator of possible oedema via the loss of integrity of the pulmonary epithelium.

This type of damage could occur by different mechanisms, such as oxidation of pulmonary epithelium e.g. lipid peroxidation (see Chapter 1, Section 1.4.1). Another possible mechanism of damage resulting in protein leakage could be due to calcium channels being disrupted by zinc influx. The competition between calcium and zinc could result in disruption of the epithelial membrane. Zinc has been known to affect calcium channel function, especially permeability characteristics, which can lead to adverse effects to cells. This is possibly due to their similar electron orbital configurations (Atchison, 2003)

The instillation of Zn^{2+} alone caused greater loss of overall well being of the animal than with any other mixture in the whole study. This was assessed when looking at the decrease in body mass and the subsequent termination of the study at 3 days, as the loss in body mass fell below Home Office guidelines. Previous studies have shown Zn^{2+} to cause damage in the lung (Richards *et al.*, 1989 and Adamson *et al.*, 2000) had postulated that zinc was the predominant metal found in the water-soluble fraction of PM_{10} causing pulmonary damage.

Instillations of soluble metal compounds such as $VOSO_4$ and Fe_2SO_4 have been linked to free radical production *in vivo* using the method of electron spin resonance (Kadiiska *et al.*, 1997). Copper has also been linked to the production of ROS. However zinc, which is not redox active, is unlikely to be involved in ROS production. This lends weight to different types of mechanisms of damage occurring. Evidence of this was seen when looking at neutrophilic influx at 4 h. Zinc alone at 4 h had the lowest number of neutrophils and did not attenuate in the same manner as the neutrophilic influx stimulated by the $3SD(-Zn^{2+})$ or $3SD(Fe^{3+})$ mixtures. This slow influx of neutrophils was surprising due to the amount of actual metal present in $3Zn^{2+}$, being approximately 40 μg higher than that of $3SD(-Zn^{2+})$. This suggests that the response induced by $3Zn^{2+}$ was not an early onset oxidative response, and hence, took longer to manifest. The result also suggests that the effect exerted by transition metals was oxidative. That is, as oxidation is an immediate-acting mechanism, it was not surprising that $3SD(Fe^{3+})$ induced a large influx of neutrophils at an early time point. This may have been due the interaction between Fe^{3+} and Zn^{2+} causing the mixture to be more toxic than would have otherwise have been expected. This type of

interaction could explain why Fe^{3+} and Zn^{2+} were initially more potent than a mixture of Fe^{2+} and Zn^{2+} . Other reasons for this may be due to the fact that Fe^{3+} is initially more bioreactive than Fe^{2+} , or that interaction of Fe^{3+} with other oxidative metal ions is initially more potent than those with Fe^{2+} . These different hypotheses may also explain the observed elevated levels of protein present in BALF with 3SD(Fe^{3+}) compared with 3SD at 4 h.

When comparing predicted additive effects of 3Zn^{2+} with $3\text{SD}(-\text{Zn}^{2+})$ to the observed effects with $3\text{SD}(\text{Fe}^{3+})$, there was a high degree of correlation (therefore little synergy); the only observed synergistic effect was seen with neutrophilic influx at 4 h. At later time points, the predicted additive effect far outweighed the bioreactivity of the $3\text{SD}(\text{Fe}^{3+})$, suggesting that $3\text{SD}(\text{Fe}^{3+})$ had reached a toxicological plateau and was no longer inducing dose-dependant responses. Previous studies have shown metal mixtures may lead to antagonistic interactions in the form of lung pathology (Kodavanti, 1997; Dreher, 1997).

In vitro studies conducted in the previous chapter revealed that synergistic effects occurred between Zn^{2+} and Fe^{3+} but not with Fe^{2+} when using the plasmid scission assay. A possible synergistic effect could be the reason for a higher neutrophilic concentration found at 4 h when comparing $3\text{SD}(\text{Fe}^{3+})$ with 3SD. The damage could therefore have occurred by the same mechanism but at a faster rate or by a different mechanism related to the properties of the interaction between Zn^{2+} and Fe^{3+} . The observed effects *in vitro* do not always apply *in vivo*, as the *in vivo* system is far more complex. For example, there could be substances present within the pulmonary milieu that also increase the bioreactivity of certain metals, and different metals could be prone to different rates of clearance within the lung. Inflammatory injury *in vivo* can also occur as a result of oxidative stress either by the free radicals generated within the instilled mixture or from endogenous oxidants and proteases generated by the recruited inflammatory cells (Simeonova *et al.*, 1995). *In vitro* studies have revealed that the high molecular weight fractions of BALF can damage plasmid DNA at a concentration 40 x weaker than that found in the lung. The damage could be via an oxidative mechanism. Certain antioxidants present in the alveolar region (such as ascorbate) have a protective effect against ROS mediated oxidation. Ascorbate can also have a pro-oxidant effect, as it is also a reducing agent that, as seen *in vitro*, can

reduce metals such as iron from Fe^{3+} to a more bioreactive Fe^{2+} , which is a key component of Fenton chemistry and the subsequent production of ROS. Part of the *in vitro* investigations carried out in chapter 3 involved assessing whether the secondary component of the metal compound such as chlorides, nitrates or sulfates affected the bioreactivity of the metal with which it was associated. The findings revealed that there was no significant difference found in regard to secondary component, whereas the work conducted by Adamson *et al.* (2000) revealed that zinc sulfate gave a more severe toxic response than zinc chloride *in vivo*.

The results suggest different mechanisms were occurring depending on the type of metal instilled. This was supported when comparing the difference between Fe^{2+} and Fe^{3+} and the roles that Zn^{2+} played on its own. To assess whether synergistic effects were occurring *in vivo*, it perhaps would have been useful to have used zinc at a variety of lower concentrations to assess whether its effect was greater than the combined effects of Zn^{2+} and Fe^{3+} or VO^{2+} or Cu^{2+} , as was carried out in the previous chapter.

The study involving ICP-MS analysis of metal concentrations present in different organs was not particularly conclusive. There were some significant differences observed. The data did reveal that the instillation of certain metals caused an increase in metal concentration within certain organs and that some metals could have a longer retention time in the lung than others. This would explain the lack of significant increase in copper and zinc concentrations at 4 h as opposed to vanadium and iron when compared with the control lungs. The effect of metal flux was not confined just to the primary organ of entry but instances of change were also seen in the liver, kidney and heart. Changes in copper concentration when compared to that of zinc were time-dependant in relation to the heart, with changes in zinc occurring at 4 h and changes in copper occurring at 72 h. The movement of metals as far as the liver and kidney could be time-dependent, with no change occurring at the first two time points with any metal other than vanadium and only vanadium and iron concentrations changing at 3 days in the kidney. This could be due to damage caused in the lung hindering the translocation of certain metals. Moreover, the actual metals instilled could be contributing to the increase in concentration and it might take this period of time for the metal to reach the kidney. One drawback of this experiment

became obvious, which was that there was no way to identify the precise distribution profiles of each metal. Some metals may accumulate in an organ-specific manner, others may ‘bypass’ specific organs. Also, the transportation time of each metal may differ. This issue could be better addressed by the instillation of tagged metals either using fluorescent or radioactive labelling, and subsequent analysis (e.g. whole body autoradiography). This would give a greater insight into the precise movements of the metals from the lung, how quickly each is distributed and what the target organs are (including the blood and lymphatic systems). If using fluorescent labels, each metal could be tagged differently in order to investigate translocation within a mixture as the route that the metals take may differ if administered in a mixture.

The original premise of this work was to use metals at the proportions found in an UK PM sample. The findings from this study indicated that the metal mixture used as a surrogate of the 1958 PM sample caused a much larger amount of damage than the original sample and was not very representative. However, it did highlight the fact that the water-soluble metal content could still be responsible for the bioreactive effects seen *in vivo* of other PM samples. The synergy data that was observed in the work conducted in Chapter 3 was far less apparent *in vivo*. This may have been due to the very high concentration of zinc present in the mixtures. The bioreactivity of a high concentration of zinc may mask the potential synergistic effects that could be occurring *in vivo*.

CHAPTER 5

HISTOPATHOLOGY OF METAL- INDUCED PULMONARY EFFECTS

5.1 Introduction

Conventional toxicological end-points provide a quantitative assessment of the inflammatory and oedematous effects produced by instilled mixtures in the lung (Chapter 4). A number of cellular effects could be detected utilising lavage techniques whereby marked increases were noted in macrophages and neutrophils accumulating on the lung surface.

The above studies provide little information of cellular changes in the lung parenchymal tissue, specifically of the effects of metal mixtures on epithelial lining cells, the endothelium or on connective tissue cells such as fibroblasts. Such information can be obtained utilising specific cell markers but preliminary information can also be obtained by employing histopathological techniques.

Histopathology can provide a subjective but visual assessment of oedema and the inflammatory process. It is also useful in assessing when recovery from initial damage may occur. Thus, data may be obtained on the progression of injury, epithelial repair and the subsequent involvement of connective tissue with fibroblast replication and collagen deposition.

The hypothesis tested in this study was that a surrogate PM metal mixture would cause an acute pathological change in the lung including damage to and repair of the pulmonary microarchitecture. This was conducted using histopathology to complement the observed changes induced by instilled metal mixtures, as described in Chapter 4, and to look for any further changes in lung microarchitecture. The effects of the metal mixtures on mediastinal lymph nodes were also investigated, as these are the sites of clearance of the inflammatory products following lung damage. When the lung is injured, products of any damage induced as well as cells involved in clearance accumulate in these lymph nodes, leading to an enlargement in their size. Such changes can be detected by dissecting out the nodes and observing their features.

Finally, consideration was given to re-evaluation of the quantity of lavage fluid recovered from animals instilled with metal mixtures (Chapter 4), conducted as a

means to compare and contrast the findings from conventional toxicology techniques with histopathological observations.

5.2 Materials and Methods

5.2.1 Equipment and Materials

Acetic Acid	Fisher, Leicestershire, UK
Cannulae	Portex, Hampshire, UK
Celestine Blue	Raymond A Lamb, E Sussex, UK
Coverslips	Fisher, Leicestershire, UK
DPX	Fisher, Leicestershire, UK
Eosin (Gribble)	Raymond A Lamb, E Sussex, UK
Ethanol	Fisher, Leicestershire, UK
Formalin	Sigma Aldrich, Dorset, UK
Gills Haematoxylin (No. 3)	Raymond A Lamb, E Sussex, UK
Hydrochloric Acid	Sigma Aldrich, Dorset, UK
Leica EG1140 Embedding Centre	Leica, Cambridgeshire, UK
Leica RM2135 Microtome	Leica, Cambridgeshire, UK
Neutral Buffered Formalin	Sigma Aldrich, Dorset, UK
Paraffin	Raymond A Lamb, E Sussex, UK
Phosphomolybdic Acid	Fisher, Leicestershire, UK
Ponceau/Acid Fuchsin	Raymond A Lamb, E Sussex, UK
Slides	Raymond A Lamb, E Sussex, UK
Vacuum Tissue Processor (Leica TP1050)	Leica, Cambridgeshire, UK
Xylene	Fisher, Leicestershire, UK

5.2.2 Gross Morphology of Lungs and Lymph Nodes

Lungs excised from rats following the instillation/sacrifice (Chapter 4) were photographed for each metal mixture (SD, 3SD, 3SD(Fe³⁺), 3Zn²⁺ and 3SD(-Zn²⁺)) as well as saline-treated controls, to assess the difference in gross pathology. The lymph nodes were also recovered from the sacrificed animals and were pooled according to each experimental group. They were placed in petri dishes of a known size (35 mm) and a digitised image of each dish was taken. Comparative size analyses of control and test lymph nodes were conducted using quantitative image analysis (IA) based on

the projected area (equivalent spherical diameter (ESD)) of the nodes in the digitised photograph. The lymph node size was calibrated from the diameter of the petri dish. The mean and standard error was calculated for each group and time point. Comparative size analysis of lungs was considered inaccurate due to slight differences in animal size, weight age etc., therefore not included in this study.

5.2.3 Lung Tissue Fixation

The animals were exposed by instillation to a 3x surrogate dose (3SD) of a surrogate metal mixture based on a 1958 London PM sample as in the previous chapter. They were sacrificed (n=2) as outlined previously, along with saline-treated rats (n=2) at four different time points (4 h, 24 h, 3 days, 7 days). The lungs were dissected intact (without saline perfusion) following sacrifice and immediately fixed in 10% v/v neutral buffered formalin (pH 7.0). This was achieved via gravity feed into a tracheal cannula. Once fully inflated the right apical lobe from each lung was tied off and dissected from the other lung lobes. This lobe was then stored in a universal tube containing enough formalin for the tissue to be submerged. Each of the lobes were then stored at 4°C for 7 days.

5.2.4 Processing Tissue for Light Microscopy

Tissue processing, sectioning and staining for light microscopy (LM) were carried out by a histotechnologist, Mr Derek Scarborough, at the School of Biosciences, Cardiff University. A brief overview of these procedures has been outlined below in Sections 5.2.4.1 to 5.2.4.5.

5.2.4.1 Tissue Processing

Once the tissue was fixed it had to be processed into a form in which it could be made into thin microscope sections. This was achieved by embedding tissues in paraffin, which is similar in density to tissue and can be sectioned from 3 to 10 µm thickness. The main steps in preparing the tissue for microscopic evaluation were 'dehydration', 'clearing' and 'paraffin infiltration'. Prior to tissue processing, the fixed tissues were placed into processing cassettes that were used to carry the tissues through the various stages of dehydration, clearing and paraffin infiltration. The cassettes were then loaded into a basket, which was placed inside a fully enclosed Vacuum Tissue

Processor. Automation consisted of the movement of the tissues through the various agents on a preset time scale. Wet-fixed tissues, such as the lung samples from this study, could not be directly infiltrated with paraffin. The water from the tissues was first removed by 'dehydration' via a series of alcohols (e.g. 70% to 95% to 100%). Following dehydration, the next step was "clearing" and consisted of replacement of the dehydrant, i.e. alcohol, with a substance that would be miscible with the paraffin. The common clearing agent was xylene and the tissues were processed through several changes of xylene. The final step in processing was to infiltrate the tissue with molten paraffin wax at 60°C, several changes of wax being used. Tissues were placed in plastic processing cassettes prior to loading on the automatic processing machine.

5.2.4.2 Paraffin Embedding

It was important for the tissue to be fully supported by paraffin wax to prevent the tissue shredding during sectioning. This was achieved by placing the "cleared" tissue into a vacuum to remove all air pockets. The lung tissue was then placed into a plastic "embedding mould" and a Leica EG1140 Embedding Centre was used to embed the tissue in warm paraffin wax. After allowing the wax to set (30 minutes on a cold plate), the tissue was removed from the embedding mould and the sample was ready for sectioning.

5.2.4.3 Sectioning

Following tissue processing and paraffin embedding, the lung tissue had to be cut into sections that could be placed on a glass slide for the purpose of LM. Sectioning was achieved using a Leica RM2135 microtome (i.e. a knife with a mechanism for advancing a paraffin block standard distances across it). The embedded lung tissue samples were placed on ice to ensure uniform sections were obtained. The ice hardens the wax and softens the tissue so the entire sample is of the same consistency for sectioning. The tissue was then cut into 5 µm sections via the microtome (4 sections per lung, 1 section per slide).

Once the sections were cut, they were floated on a warm water bath (40-50°C) that facilitated the removal of wrinkles and air bubbles produced during sectioning. The paraffin embedded sections of lung tissue were then collected on a glass microscope

slide. The slides used were coated in poly-L-lysine to improve adhesion of sections. The samples were then left to bind to the slides on a hot plate for 15-30 minutes, and afterwards in an oven at 37-45°C for a minimum of 24 h.

To evaluate the lung architecture by light microscopy (LM) the tissue sections were stained with Haematoxylin & Eosin (H&E) and Masson's Trichrome (MT). H&E was used as it is a general purpose stain universally used for routine histopathological examination. It gives clear differentiation of the cellular structures, therefore highlighting differences between cell types and cellular changes. Haematoxylin is a basic dye that stains nuclear heterochromatin and cytoplasm rich in ribonucleoprotein blue. Eosin is an acid dye that stains cytoplasm, muscle and connective tissue various shades of pink. MT is commonly used to assess the deposition of collagen as well as mucin and cartilage. Cell nuclei stain blue-black, connective tissues stain blue-green and muscle and fibrin stain red.

5.2.4.4 Haematoxylin and Eosin Staining

The embedding process must be reversed in order to get the paraffin wax out of the tissue and allow water-soluble dyes to penetrate the sections. Therefore, before any staining could be done, the slides were 'deparaffinised' by running them through xylene followed by series of graded alcohol (100% to 70%). The dewaxed tissue sections were stained with Mayer's haematoxylin for 1.5 minutes. Sections were washed in running tap water for five minutes, and then stained with 1% aqueous eosin for 10 minutes. Following a 20 second wash in running tap water, sections were dehydrated once again (increasing strengths of alcohol and subsequently replaced by xylene).

5.2.4.5 Masson's Trichrome Staining

The dewaxed tissue sections were immersed in two changes of xylene for 4 minutes each and then two changes of absolute ethanol for a further 4 minutes each. They were then dipped into 95% ethanol followed by 70% ethanol (2 minutes each), then washed in running tap water until clear. The samples were stained in Celestine Blue B (5 minutes), rinsed in water and stained with Mayer's haematoxylin (5 minutes each) followed by washing in running tap water for 5 minutes. Ponceau/Acid Fuchsin stain

was used to stain the slides (5 minutes), followed by washing briefly in running tap water for 30 seconds. The cells were differentiated in 1% Phosphomolybdic Acid for 4 minutes and then transferred directly to Light Green stain for 3 minutes. This was followed by washing in running tap water until clear and then immersion in 1% acetic acid for 2 minutes. The acetic acid was rinsed off in water for 15 seconds. The slides were then dipped in 95% ethanol followed by 100% ethanol for a minute at a time. Finally they were immersed in two changes of xylene and then mounted with glass coverslips using DPX.

5.2.4.6 Slide Production

The stained section on a slide must be covered with a glass coverslip to protect the tissue from being scratched, to provide better optical quality for viewing under LM, and to preserve the tissue section for archival purposes. The stained slides were taken through the reverse process that it went through from paraffin section to water, (i.e. series of graded alcohol to xylene). Finally, the permanent mountant DPX was placed over the section and the coverslip on top of the mountant. The stained sections were then ready to view by LM.

5.2.5 Light Microscopy

The lung sections were then analysed under a light microscope using up to four different magnifications (40x, 160x, 250x and 400x). Images were captured as a digital image using the Leica IA system and a histopathological comparison was carried out to assess morphological changes to the lung microarchitecture arising as a result of the instillation of the metal mixture. Pathology was conducted under the guidance of Dr Philip Carthew. No quantitative analysis was carried out due to the low n number per group (n=2). However examples of damage shown in the results section were found on both slides for each group.

5.2.6 Statistical Analysis

All data handling and graphical representation of results was performed in Microsoft Excel '97. Statistical analyses included Andersson-Darling normality tests two-sample t-test and non-parametric Mann-Whitney tests. A two-sample t test was chosen as an appropriate test due to the data being derived from two independent random samples. This test was used if the data was normal and the variances were

equal within each group. If this was not the case, a non-parametric Mann-Whitney test was used. All statistical analyses were performed in Microsoft Minitab 13. Statistical significance was assumed at $p \leq 0.05$ and a high significance was assumed at $p \leq 0.01$.

5.3 Results

5.3.1 Recovery of Lavage Fluid

As described in Chapter 4, Section 4.2.6 (biochemical/cellular evaluation study) lungs of each animal were instilled with approximately 25 ml of saline. The return of lavage fluid was approximately 80-90% with control animals at each time point. At 4 h the total volume of lavage fluid obtained was noticeably lower to that of the control animals for all test groups and this decrease continued for 72 h. It is worthy to note that the intake capacity of the lungs for lavage in test animals was also reduced, but disproportionately to the volume of fluid returned. At 3 days the total lavage fluid in the SD group had dropped to 50% of that observed in saline-treated animals. The recovery of fluid was dose dependent as there was only a 25% return when looking at the 3SD treated group (compared to control animals). The effects were transient for all test groups and resolution of the effect occurred between 7-14 days (Table 5.3.1).

Table 5.3.1 Dose and time effect on lavage volumes

Time (h)	Lavage fluid volume (ml)					
	SC	SD	3SD	3SD (-Zn ²⁺)	3SD(Fe ³⁺)	3Zn ²⁺
4	23.5	14.9	13.6	16.4	15.9	19.5
24	25.3	13.4	12.7	21.2	15	16.7
72	21.3	12.8	6.9	-	-	-
168	23.6	21.4	22	25.8	20.6	-
336	22.5	21.6	20.8	-	-	-

5.3.2 Gross Morphology

The control lungs showed no signs of morphological change such as swelling or focal deposition. Each of the parenchymal lobes was perfectly white (Figures 5.3.2a-e) and



Figure 5.3.2a-o Gross pathology of lungs at 4, 24, 72, 168, 336 h post exposure. Saline treated lungs (a-e), surrogate dose (SD) (f-j), 3x surrogate dose (3SD) (k-o). Pictures also include thymus tissue (top left) at 4 h and 24 h sacrifice points (not assessed)



Figure 5.3.2p-z Gross pathology of lungs at 4, 24, 168 h post exposure. Saline treated lungs (SC) (p-r), 3x zinc only (3Zn²⁺) (s-t), 3x surrogate dose including Fe³⁺ (3SD(Fe³⁺)) (u-w), 3x surrogate dose without zinc (3SD(-Zn²⁺)) (x-z).

deflated well during the lavage process at each time point during the 14 day study. Analysis of the surface of post-instilled lungs following treatment with the differing metal mixtures revealed focal points of damage at the various time points. The lobes were not white and did not deflate well which was evident during the lavage process. Each test group displayed a visible difference in gross morphology from the control lungs. Larger, random areas of damage became more noticeable as the dose was increased (Figures 5.3.2f-j). Lungs administered with the 3SD solution appeared (subjectively) swollen compared to controls (Figures 5.3.2k-o), as did those instilled with 3Zn^{2+} (Figures 5.3.2p-r vs s-t). In all tests, including $3\text{SD}(\text{Fe}^{3+})$ and $3\text{SD}(-\text{Zn}^{2+})$ (Figures 5.3.2u-w, x-z), as early as 4 h post instillation, haemorrhaging was noticeable and attributed to the deposition of the metal mixture in focal areas. There was both a dose and time dependant response when comparing SD and 3SD that resulted in an increase in visible inflammatory areas over the course of the study. At 14 days there was resolution in inflammation and observed swelling but still signs of focal scarring.

5.3.3 Morphology of Lymph Nodes

Animals instilled with SD and 3SD showed differences in morphology of the lymph nodes at 7 and 14 days. There was a red/brown colour found in all test groups which may have resulted from lung haemorrhage and blood being present in the lymphatic fluid (Figure 5.3.3a).

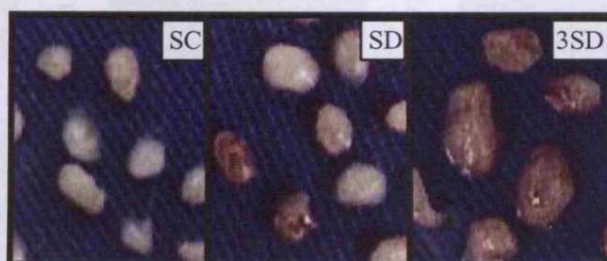


Figure 5.3.3a Examples of discoloration and enlargement of lymph nodes with increasing dose

The nodes from the control group were small and showed no signs of discoloration or swelling at any of the time points during the study (Figures 5.3.3b-f) compared to tests (Figures 5.3.3g-p). The sizes of the lymph nodes revealed a dose and time dependant response related to SD and 3SD (Figure 5.3.3q). At 4 h there was no significant difference between controls and SD, but there was a significant difference



Figures 5.3.3b-f Lymph node morphology at 4, 24, 72, 168, 336 h post exposure. Saline treated lungs (b-f) (scale bar = 10 mm).
 b) 4 h c) 24 h d) 72 h (3 days) e) 168 h (7 days) f) 336 h (14 days)



Figures 5.3.3g-k Lymph node morphology at 4, 24, 72, 168, 336 h post exposure. Surrogate dose (SD) (g-k) (scale bar = 10 mm).
 g) 4 h h) 24 h i) 72 h (3 days) j) 168 h (7 days) k) 336 h (14 days)



Figures 5.3.3l-p Lymph node morphology at 4, 24, 72, 168, 336 h post exposure. 3x surrogate dose (3SD) (l-p) (scale bar = 10 mm).
 l) 4 h m) 24 h n) 72 h (3 days) o) 168 h (7 days) p) 336 h (14 days)

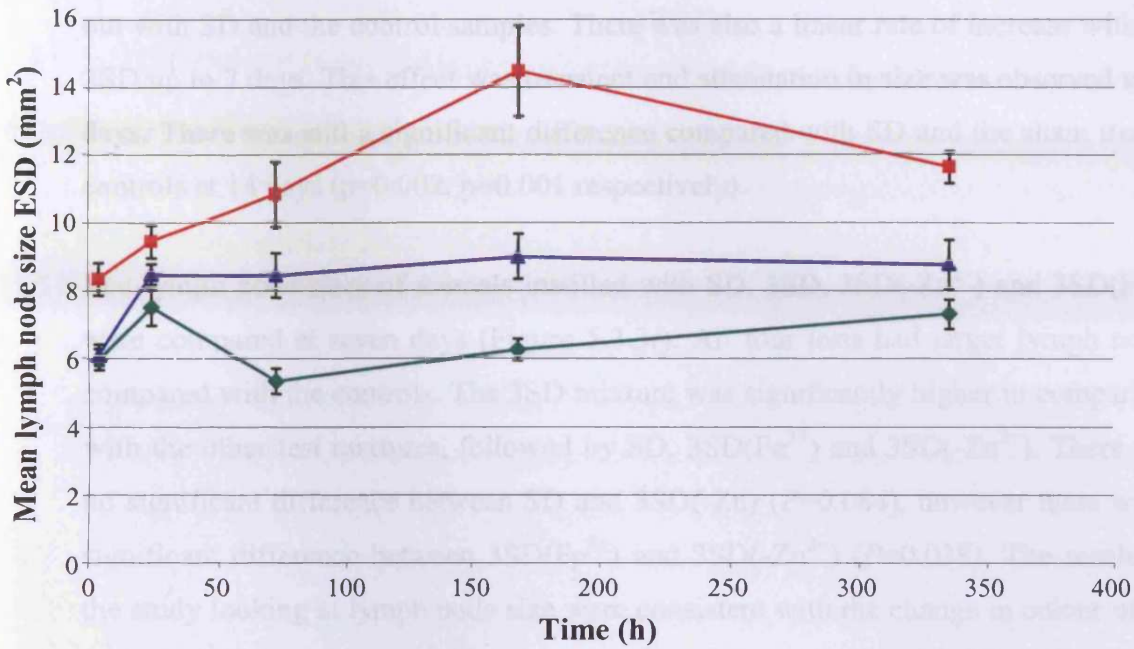


Figure 5.3.3q Change in mean lymph node size (ESD) (mean ± std. err.)

◆ = SC ▲ = SD ■ = 3SD

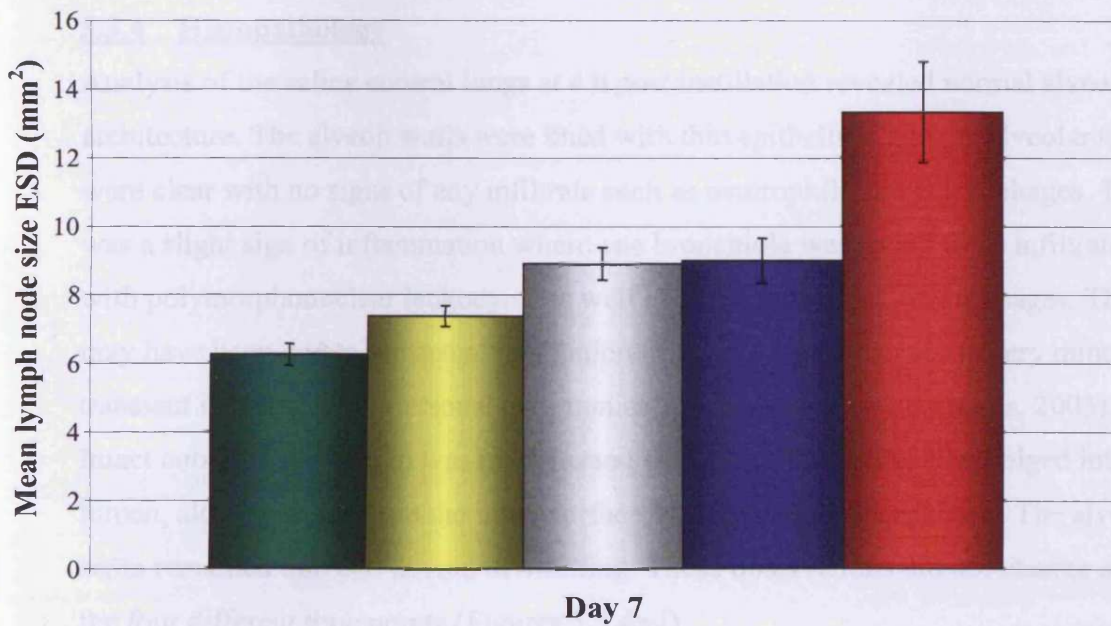


Figure 5.3.3r Comparison of mean lymph node (ESD) between test mixtures and control at 7 days post instillation (mean ± std. err.)

■ = SC ■ = 3SD(-Zn) □ = 3SD(Fe³⁺) ■ = SD ■ = 3SD

in size between controls and 3SD at this early time point ($p=0.021$). There was an increase in size in all three groups at 24 h compared to 4 h. This effect then levelled out with SD and the control samples. There was also a linear rate of increase with the 3SD up to 7 days. This effect was transient and attenuation in size was observed at 14 days. There was still a significant difference compared with SD and the sham treated controls at 14 days ($p=0.002$, $p=0.001$ respectively).

The lymph node sizes of animals instilled with SD, 3SD, 3SD(-Zn²⁺) and 3SD(Fe³⁺) were compared at seven days (Figure 5.3.3r). All four tests had larger lymph nodes compared with the controls. The 3SD mixture was significantly higher in comparison with the other test mixtures, followed by SD, 3SD(Fe³⁺) and 3SD(-Zn²⁺). There was no significant difference between SD and 3SD(-Zn) ($P=0.084$), however there was a significant difference between 3SD(Fe³⁺) and 3SD(-Zn²⁺) ($P=0.038$). The results of the study looking at lymph node size were consistent with the change in colour of the nodes at 7 days. The most marked change in colour occurred with 3SD followed by SD. A few of the nodes that related to 3SD(Fe³⁺) and 3SD(-Zn²⁺) were also a red colour.

5.3.4 Histopathology

Analysis of the saline control lungs at 4 h post instillation revealed normal alveolar architecture. The alveoli walls were lined with thin epithelium and the alveolar spaces were clear with no signs of any infiltrate such as neutrophils and macrophages. There was a slight sign of inflammation where one bronchiole was found to be infiltrated with polymorphonuclear leukocytes as well as small number of macrophages. This may have been due to the actual instillation of saline, which can cause very minor, transient inflammation (personal communication Professor Roy Richards, 2003). Intact cuboidal epithelium was interspersed with taller Clara cells that bulged into the lumen, along with cilia, on the inner surface of the terminal bronchioles. The alveolar septa remained thin and devoid of swelling. These observations did not change over the four different time points (Figures 5.3.4a-i).

5.3.4.1 Four Hours Post Instillation with 3SD

Analysis of the test lungs at 4 h revealed extensive inflammation as suggested by the presence of PMNs and macrophages (Figures 5.3.4j-l). There was also evidence of

margination occurring at 4 h (Figures 5.3.4l), which is the adhesion of monocytes to the endothelium and the subsequent migration of these monocytes from the lumen of the vasculature into the surrounding tissue. Evidence of their movements could be observed as they were seen clustered around debris found within the airspaces (Figure 5.3.4l). Present within the alveolar spaces were inflammatory cells comprising foci of lung free cells (likely to be PMNs and alveolar macrophages). Macrophages would most likely be phagocytosing debris, which was either administered material or cell debris released through cytotoxicity. There was also evidence of the loss of terminal bronchiolar epithelium and the basement membrane in certain areas. The lung sections revealed focal oedematous changes with aggregates of lung free cells (possibly PMN, macrophages, monocytes) and general debris, possibly including desquamated (detached) bronchial epithelial cells which together formed 'plugs' within the bronchioles (Figure 5.3.4k). These plugs would obstruct and block the airways, which may hinder the passage of air and removal of waste material.

5.3.4.2 Twenty Four Hours Post Instillation

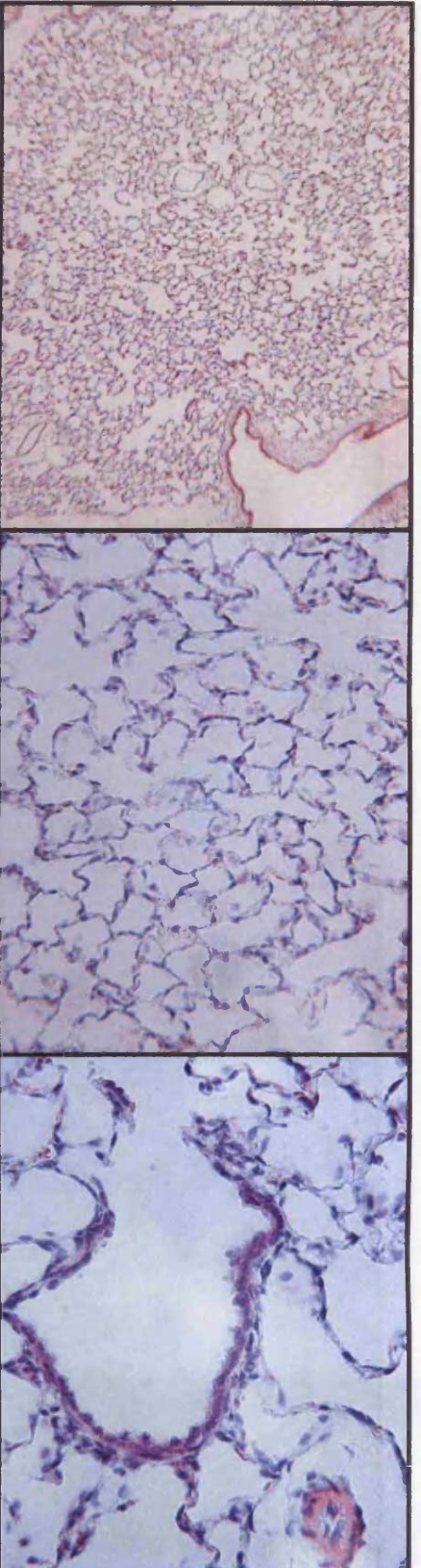
Low power LM analysis showed that damage did not occur everywhere in the lung (Figure 5.3.4m). The peripheral part of the lobules or acini of the lung showed normal alveolar architecture (Figure 5.3.4m (ii)) whereas in the centrilobular region greater damage seemed to have occurred (Figure 5.3.4m (i)). This may suggest that the test material was preferentially deposited closer to the conducting airways. Low power analysis of the test lungs at twenty-four hours revealed reactive hypertrophy i.e. increased size of the bronchiolar epithelium (Figure 5.3.4n). Multiple focal inflammatory infiltrates were also present (Figure 5.3.4o). These comprised alveolar macrophages and PMN and were again found around the terminal bronchioles. There was also desquamation of the bronchiolar epithelium, with adjacent plugs of inflammatory cells and debris in the bronchioles. At 24 h, the infiltration of PMN and macrophages was more diffuse in the alveolar air spaces than at four hours, with more evidence of activated macrophages (Figure 5.3.4o), the result of which caused the macrophages to increase in size. At this time point there was no sign of epithelial or connective tissue cell proliferation as evidenced by the lack of alveolar and fibroblastic hyperplasia.

5.3.4.3 Three Days Post Instillation

At 3 days post instillation the damaged areas had extended to the periphery of the lungs. This had not been evident at the previous two time points (Figure 5.3.4p). The first signs of epithelial and connective tissue repair were evident in the alveolar epithelium adjacent to the terminal bronchioles. Focal regions of tissue were observed to undergo bronchiolisation (Figure 5.3.4q), i.e. the replacement of the normal alveolar epithelium with cuboidal epithelial cells that have similar characteristics to bronchial epithelium. There was also evidence of extensive thickening of the alveolar septa around the terminal bronchioles (Figure 5.3.4r) due to proliferation of fibroblasts and alveolar type II pneumocytes.

5.3.4.4 Seven Days Post Instillation

At 7 days post instillation there was less focal damage observed at the periphery (Figure 5.3.4s) when compared to 3 days and the tissue began to show signs of recovery. Perivascular and peribronchial alveolar macrophages and PMN infiltrates could be seen (Figure 5.3.4t). There was evidence of cilia rich columnar epithelial regeneration (Figure 5.3.4u) and of cellular hyperplasia (Figure 5.3.4v) (possibly a repair mechanism for damaged tissue), which was denoted by the proliferation of the bronchial epithelium, as opposed to an increase in size of cells (hypertrophy). Elongated fibroblast nuclei were also observed as well as the evidence of fibroblast cell proliferation. Increased collagen deposition, as well as hypertrophied bronchial epithelium due to an increased mucin secretion, were evident (Figure 5.3.4v). The collagen present appeared loose and could therefore be degraded at a later time point. There were also more prevalent areas of alveolar septal thickening (Figure 5.3.4w), which may be due to the translocation and clearance of xenobiotics and free cells from the alveolar surface.

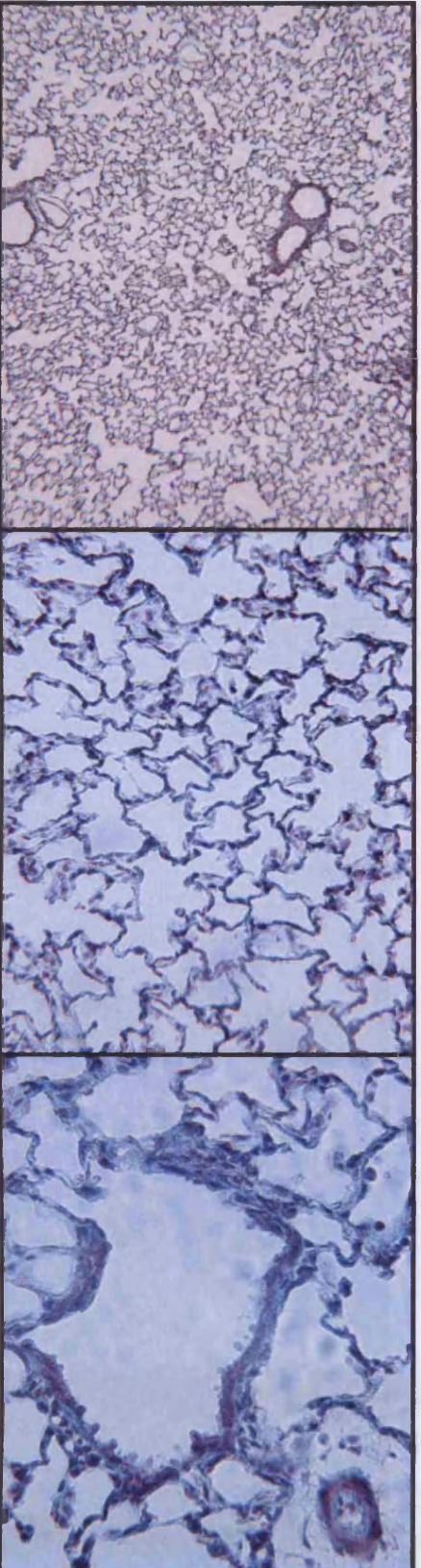


Figures 5.3.4a-c Examples of control lungs at 4 h at three different magnifications using H&E Stain

a) 40x mag

b) 160x mag

c) 250x mag

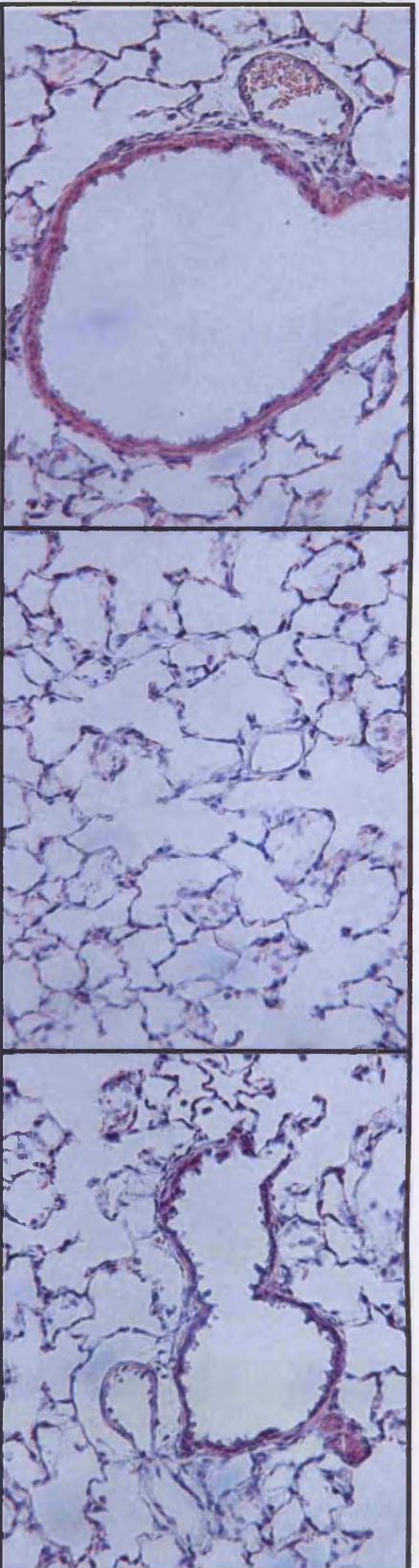


Figures 5.3.4d-f Examples of control lungs at 4 h at three different magnifications using Masson's Trichrome Stain

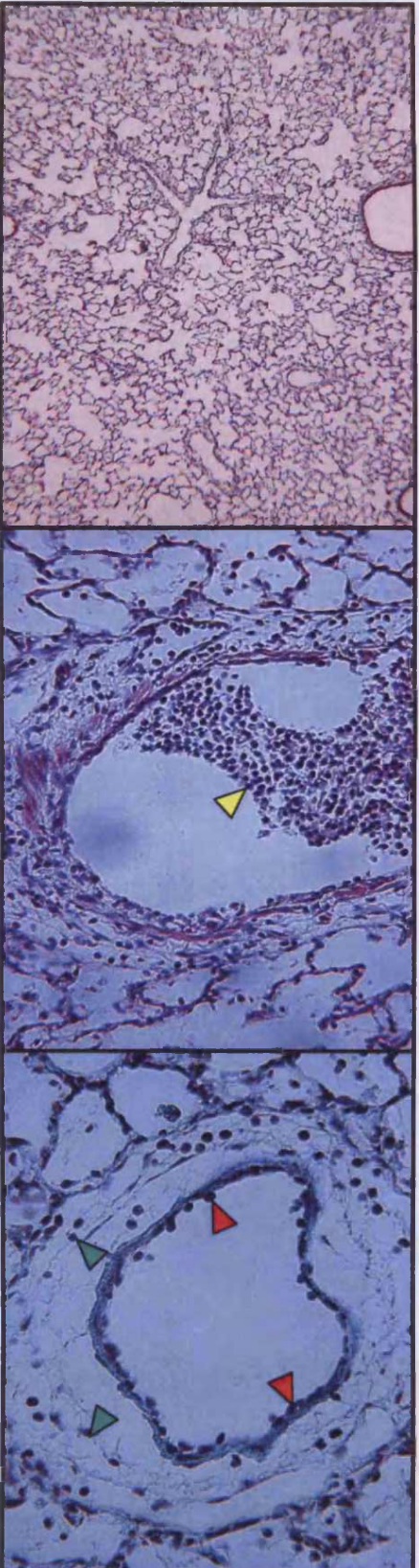
d) 40x mag

e) 160x mag

f) 250x mag



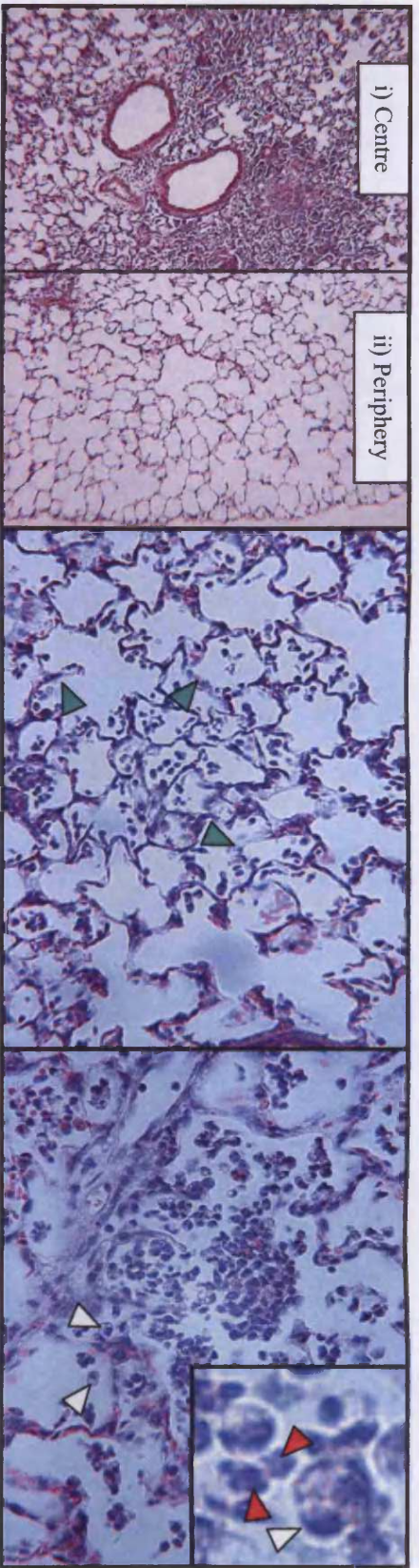
Figures 5.3.4g-i Examples of control lungs at three further time points, H&E Staining
g) 160x mag (24 h) h) 160x mag (3 days) i) 160x mag (7 days)



Figures 5.3.4j-1 3x surrogate dose, 4 h
j) 40x mag (H&E) General lung morphology

k) 160x mag (H&E) ▶ = bronchiolar plug (mostly damaged and detached epithelium)

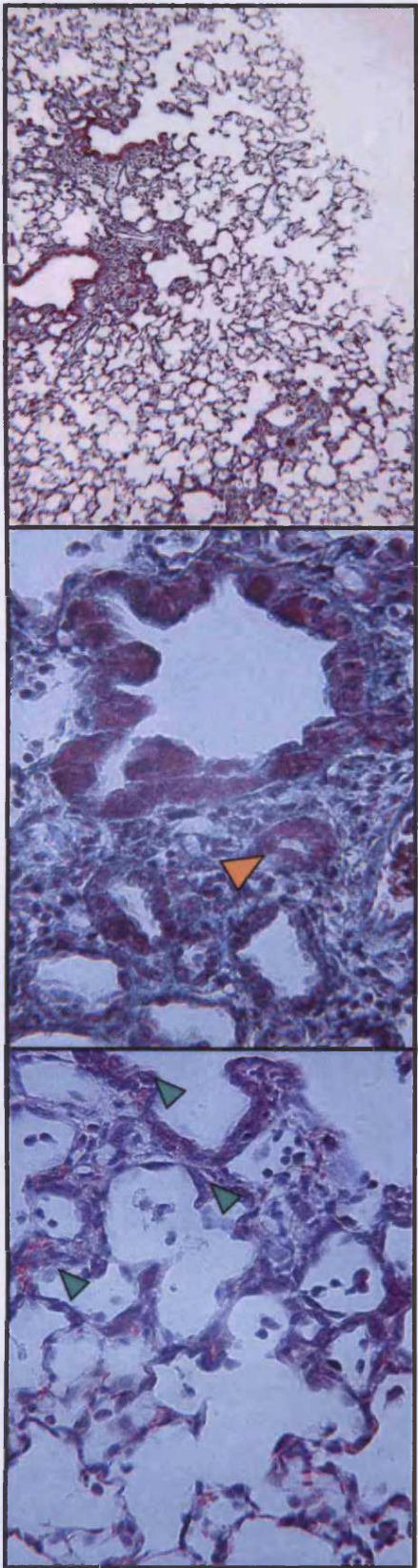
l) 250x mag (Masson's) ▶ = monocyte migration ▶ = monocyte margination



Figures 5.3.4m-o 3x surrogate dose, 24 h
m) 40x mag (H&E)

n) 160x mag (H&E) ▼ = hypertrophy

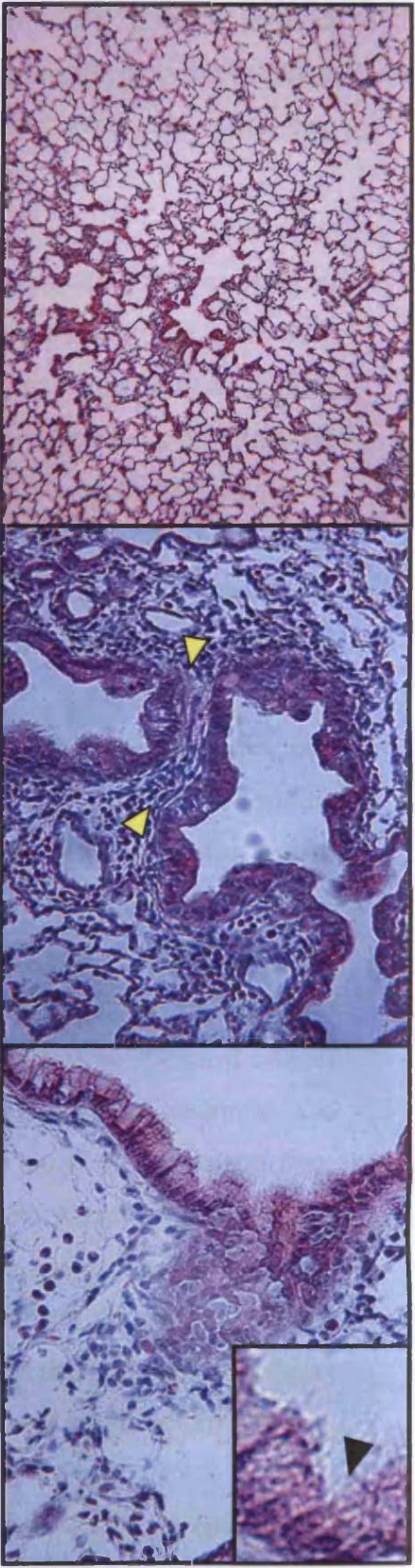
o) 250x mag (H&E) ▽ = activated AMs
inset: 1125x mag ▽ = activated AMs ▲ = PMN



Figures 5.3.4p-r 3x surrogate dose, 3 days
p) 40x mag (H&E) peripheral damage

q) 250x mag (Masson's) ▲ = bronchiolisation

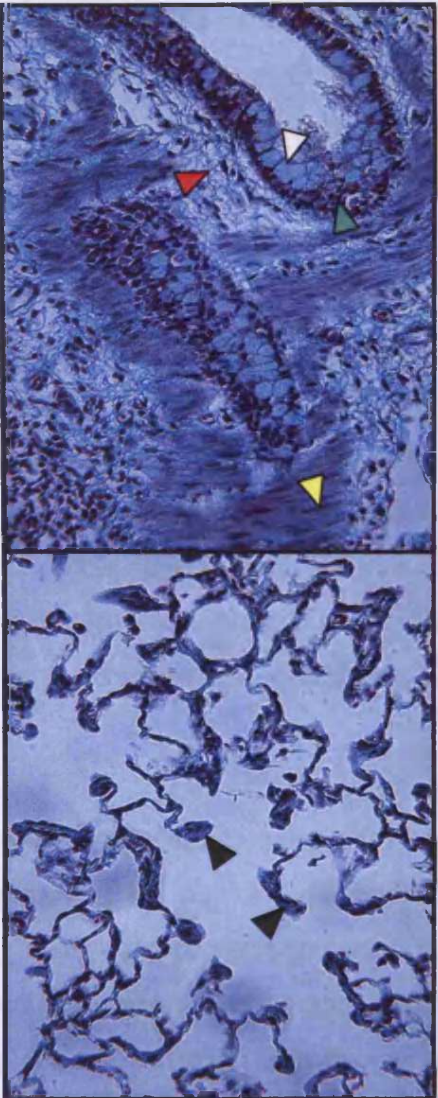
r) 250x mag (H&E) ▼ = Alveolar septal thickening



Figures 5.3.4s-u 3x surrogate dose, 7 days
s) 40x mag (H&E) peripheral recovery

t) 160x mag (H&E) ▽ = peribronchiolar
and perivascular free cell infiltrate

u) 250x mag (H&E) bronchiolar regeneration
inset: 625x mag ◀ = cilia



Figures 5.3.4v-w 3x surrogate dose, 7 days

v) 160x mag (Masson's) ▽ = Elongated nuclei
◀ = Increased collagen

◀ = Mucin
◀ = Hyperplasia

w) 160x mag (Masson's) ◀ = alveolar septal thickening

5.4 Discussion

The objectives of this part of the study were to examine the gross pathology and histopathology of the lung and lymph tissues following the instillation of a 3SD metal mixture and to assess whether the data supported previous toxicological findings (Chapter 4).

The instillation of the metal mixtures also had an effect on saline retention during the lavage process. An explanation for this may be due to the elasticity of the lung being impaired or lost by the disruption of elastins and maybe smooth muscle. This would make it more difficult to instil saline into the lungs and also, due to the surface tension of the water, render it more difficult to collect. Another reason for the difficulty in lung inflation with saline could be due to the oedematous fluid and cellular infiltrate occupying alveolar regions, which would normally be filled by the saline during the lavage process. Saline that was successfully instilled would be residing in a large number of alveoli and due to the impairment of structure caused by the loss in elasticity the lung would be difficult to deflate. These effects were most severe at 3 days post instillation, with repair being observed between 7-14 days. The mechanism of this repair was unclear but it was quite rapid as the lungs started to take in an amount of saline comparable to the controls. Furthermore, the retention of the saline had been reduced markedly between 7 and 14 days.

Analysis of the gross pathology of the lung and lymph nodes revealed that the metal mixtures, at each concentration used, caused visible signs of haemorrhaging. The haemorrhaging was seen at focal points around the lung. This would suggest that both the epithelium and microvascular endothelium had been disrupted. The observed disruption had possibly occurred exactly where the metal was first in contact with the cellular environment. The increase in visual swelling found upon gross analysis of the lung could be linked to oedema and the influx of fluid and proteins as observed with increase in lung:body mass ratio from the previous experiments conducted in Chapter 4.

Analysis of the change in size (ESD) of the lymph nodes provided an indication of the extent of clearance that was occurring in the lymphatic system. The combination of an increase in macrophage number and foreign bodies, due to an inflammatory response,

caused a thickening of the lymph fluid and thus a swelling of the nodes. The lymph nodes changed size at 4 h post instillation with 3SD which suggested that an immune response was initiated at a very early stage. The peak increase in lymph node size was at 7 days post instillation. This correlated well with visible increases in lavage free cell numbers that continued to increase at 14 days post instillation. However, this is not the only exit route for macrophages. They can also be cleared via the muco-ciliary escalator. A comparison of size of lymph nodes at 7 days post instillation between 3SD and 3SD(Fe^{3+}) showed a highly significant difference (3SD being the larger). This effect did not correlate with changes in lavage free cell numbers between the two groups at the same time point. The lavage free cell production at that time point was not significantly different and therefore, the mechanisms of free cell generation could be similar. However, the two mixtures could be invoking different clearance mechanisms. The difference could be related to the oxidation states of the iron, as this is the only variable in the contents of the two mixtures. Therefore it can be suggested that Fe^{2+} is more prone to clearance by the lymphatic system than Fe^{3+} .

Studies into the effects of metals and metal mixtures and the pathological changes they have caused to the lung (Adamson *et al.*, 1999, 2000; Dreher, 1997 and Kodavanti *et al.*, 1998) have shown certain similarities to that observed in this study, such as inflammatory responses and a change in morphology of bronchial and alveolar architecture.

The H&E and MT stains gave an insight into the changes to the general cellular structure in the lung. The combination of both stains yielded a more precise insight into cellular effects, for example areas of collagen deposition could be accurately identified.

The toxic effect observed at 4 h post instillation would have induced an inflammatory response via signalling pathways that resulted in the translocation and presence of monocytes and PMN within the alveolar space. The epithelial plugs that were formed would hinder gas exchange and possibly removal of waste material.

At 24 h post instillation there were focal points of damage observed under low power magnification, with little evidence of damage at the periphery. This changed when

looking at lungs at 3 days post instillation. This could indicate a time response reaction to the metals with the damage being more ubiquitous at 3 days. There was no evidence of this increase in peripheral damaged areas at 7 days post instillation. This correlated well with the low lavage volume being instilled and collected at 3 days due to the greater volume of lung being affected. The area of damage was less at 7 days which agreed with a greater recovery of lavage fluid.

Activated macrophages were present at 24 h post instillation. This is supported by the presence of activated macrophages found in the free cell counts obtained from lavage fluid (chapter 4). Alveolar macrophages form a key alveolar defence against inhaled substances and are important regulators of inflammation and fibrosis.

At 3 days, alveolar damage was evident. Damage to type II cells would affect the regeneration of type I cells, as they are the precursors of the latter. Type II cells are also the primary secretors of surfactant. Therefore a reduction in surfactant secretion would affect the surface tension of the lining fluid and could result in alveolar collapse. Type II cells are also one of the main sites of biotransformation of xenobiotics in the alveoli. Thus, damage to Type II cells could render the lung more susceptible and would slow down the recovery process, as regeneration of alveolar epithelium would be impaired.

The process of bronchiolisation of the alveolar epithelium is a less usual event and does not often accompany the lung repair process. This type of repair has been seen in studies involving the instillation of bleomycin (Witschi and Nettesheim, 1982). There is uncertainty into the mechanisms of this type of cell generation. It could result from the downward growth of bronchial epithelial cells which would explain why bronchiolisation occurs near bronchioles. Further investigations involving kinetic studies have raised the possibility that type II pneumocytes are the progenitor cells (Witschi and Nettesheim, 1982). As this type of repair is unusual, it was interesting to find that this type of change was seen in rats after inhalation studies oxidant gases (Gross and White, 1986). Therefore, an oxidant response could be occurring with regard the metal mixture via the initiation of reactive oxygen species. The inflammatory responses that often accompany these types of injury may exacerbate oxidant stress. In addition to extracellular oxidative stress occurring, intracellular

sources of free radical formation occur via mitochondria and normal cytosolic processes (Freeman and Crapo, 1981). The ROS formed could interact chemically with constituents of cells causing lipid peroxidation or oxidation of various functional groups such as sulfhydryls and amines. This could alter membrane permeability and thus cause cell death.

The histological lung sections at day 3 and especially day 7 post instillation illustrated the commencement of cellular regeneration as denoted by the proliferation of fibroblasts, reduction of alveolitis, hyperplasia and hypertrophy. The presence of elongated nuclei was evidence of a repair mechanism in which fibroblasts alter their morphology in order to replace damaged alveolar structure. The alveolar septal thickening appeared to be due to an increase in collagen deposition. Collagen can be generated from fibroblasts and is needed for additional connective support for the cells present in the septal structure. Thickened alveolar septa can interfere with pulmonary gas exchange, as this is a larger barrier for the air to travel through and there is a decrease in alveolar space, which means less air is respirable.

The presence of bronchiolar hyperplasia could be due to the regenerative capabilities of both ciliated and nonciliated bronchiolar (Clara) cells as the hyperplasia was near a bronchiole and the hyperplastic region stained similarly to that of the ciliated columnar epithelial cells. Hyperplasia can persist for a long period of time. For example the work conducted using the instillation of bleomycin, by Snider *et al.*, 1978 showed the commencement of hypertrophy at 4 days which persisted as long as 180 days post instillation. There was also evidence of hypertrophied bronchial epithelium due to increased mucin secretion. Globules of mucin could have possibly been seen as part of the clearance mechanism. An increase in mucin production leads to increased mucin exuded from the cell, which then traps more xenobiotics. The trapped xenobiotics are then removed via the mucociliary escalator.

Even though Masson's does stain for mucin it stains both cartilage and collagen green as well. Therefore it was difficult to assess the amount of collagen and the amount of mucin as separate entities.

The overall conclusions from the histopathological study showed an acute phase response to the instillation of the metal mixture. The target site for lung injury primarily involved the terminal bronchioles and adjacent alveolar epithelium. There was an expected inflammatory response followed by a change in the relative proportions of alveolar macrophages and PMN, commonly seen with time after injury. The repair process followed the time scale normally associated with a toxic injury to the lung (personal communication Prof. Roy Richards, 2003), with the less usual feature of bronchiolisation of the alveolar epithelium that does not always accompany the lung repair process.

CHAPTER 6

SYSTEMIC TOXICOGENOMICS

6.1 Introduction

Research has shown that the water soluble-fraction of PM can cause toxicological and histopathological changes within the lung as well as systemically and the postulated causes of these effects can be correlated to the metals present within that fraction. There is far less understanding on the mechanistics of damage caused at the molecular level. In order to investigate biological responses to perceived bioreactive metals and their toxicological mechanisms the application of genomic technology allows examination of the global effects on gene expression. This technique can also be used for identifying candidate, metal-specific, genetic markers of exposure and response.

Various methods have been used to assess changes in gene expression, such as quantitative polymerase chain reaction (qPCR), *in situ* hybridisation and Northern blotting. There are, however, problems in selecting which genes to investigate as important links may be missed between different gene activities. Emerging 'hybridisation array technologies' have addressed this problem as they can be used to analyse global gene expression.

Array technology is based on hybridisation by base pairing of the target (reverse complemented DNA representing messenger RNA from study samples) to the probe (DNA that is fixed, as spots on planar surfaces like glass slides or nylon filters). The arrays are scanned and hybridisation signals of the spots are quantified by suitable image analysis software. To gain further biologically relevant information, complex hybridisations from parallel experiments with different target samples, as well as experimental repetitions, are carried out. This technology is not without its drawbacks - arrays only measure relative, not absolute, levels of mRNA expression and changes in RNA does not necessarily correlate to a change in protein expression. It may also be difficult to differentiate between members of a gene family that have high homology.

The two most common hybridisation array formats are macroarrays and microarrays. Both these types of arrays differ in that the platforms to which the probes are attached are made of different materials (e.g. nylon and glass respectively). The type of label used in the target also varies as well as the number and type of probes per platform. In addition to these differences, each array system comes with advantages and

disadvantages. The main advantages of the microarray are that the labelling is usually done with fluorescent dyes whereas macroarrays tend to use radiolabelled molecules. As there can be high variability using array technology, microarrays limit variability by using competitive hybridisation of separate fluorescent labelled targets to the same array. Also, higher numbers and density of probes allow more involved analyses to take place. The advantages of using macroarray technology is that it is a lot less expensive than using microarrays as it does not require access to specialist equipment. It also generates more focussed data enabling specific investigation of target responses. For these reasons and the fact that the array system selected has a manageable number of relevant genes (and was commercially available) a Clontech rat cDNA expression stress array was considered to be optimal for the purpose of this study. It had proved successful in previous experiments (Reynolds and Richards, 2001; Whittaker, 2003). The arrays were composed of 207 cDNAs double spotted onto a positively charged nylon membrane, including plasmid and bacteriophage DNA as negative controls (confirmation of hybridisation specificity) as well as housekeeping genes as positive controls.

The hypothesis tested was that instillation of metal mixtures would alter gene expression profiles related to redox activity in both the lung and heart directly post-instillation. The metal mixture chosen was a 3x surrogate dose (3SD) previously reported in Chapters 4 and 5 of this thesis. The optimal time point was considered to be four hours post-instillation. This time-point was selected because previous research had shown that highly soluble metals found in ROFA had translocated from the lung into the circulation as early as 15 minutes post-instillation thereby indicating that the heart was a potential primary target (Roberts *et al.*, 2003). Other studies also had shown changes in gene expression for inflammation in the heart at periods between 1-6 h post lung instillation of ROFA decreasing thereafter and returning to control levels by 24 h (Roberts *et al.*, 2004).

6.2 Materials and Methods

6.2.1 Equipment and Materials

β -Mercaptoethanol	BDH Biochemical Laboratory Supplies, Dorset, UK
[α - ³² P] dATP (9.25 MBq)	Amersham, Buckinghamshire, UK
Agarose	Bioline, London, UK
Atlas Navigator™ 2.0	Clontech, Oxfordshire, UK
Atlas™ Nylon Rat Stress Array System (containing all required solutions and preparations)	Clontech, Oxfordshire, UK
AtlasImage™ 2.01	Clontech, Oxfordshire,UK
Bromophenol Blue	Sigma-Aldrich, Dorset, UK
CDS Primer	Clontech, Oxfordshire, UK
Chloroform (>99%, containing no iso-amyl alcohol or additives)	Sigma-Aldrich, Dorset, UK
Densitometer	Syngene, Cambridgeshire, UK
Dismembrator	Sartorius, Surrey, UK
EDTA	Sigma-Aldrich, Dorset, UK
Ethidium Bromide	Sigma-Aldrich, Dorset,UK
GeneQuant	Amersham, Cardiff, UK
Isopropanol (>99%)	Sigma-Aldrich, Dorset, UK
Kodak Phospho-imager Screen	Biorad, Hertfordshire, UK
Loading Dye	Sigma-Aldrich, Dorset, UK
Molecular Grade Ethanol (95% v/v)	Fisher Life Sciences, Leicestershire, UK
Moloney Murine Leukaemia Virus	Clontech, Oxfordshire, UK
NaOH	Sigma-Aldrich, Dorset, UK
Phosphorimaging screen	Amersham, Cardiff, UK
Reverse Transcriptase (MMLV RT)	Clontech, Oxfordshire,UK
RNase-Free DNase Set	Qiagen, West Sussex, UK
RNeasy Mini kit	Qiagen, West Sussex, UK
Salmon Testes DNA	Sigma-Aldrich, Dorset, UK
SDS Solution (ultra pure) (20%)	National Diagnostics, Yorkshire, UK

SSC Solution (ultra pure) (20x)	National Diagnostics, Yorkshire, UK
TBE (10x)	Sigma-Aldrich, Dorset, UK
Tri-reagent™ Solution	Sigma-Aldrich, Dorset, UK
Ultra-pure Water (HPLC-grade)	Fisher Life Sciences, Leicestershire, UK

6.2.2 Sample Preparation

In order to conduct toxicogenomic studies of the effects of metal mixtures on the lungs and heart, excised tissues from saline instilled rats (n=3) and 3SD mixture instilled rats (n=3) were used. Previous experiments have revealed that extraction of RNA from heart tissue using the RNeasy membrane extraction kit (Qiagen) was difficult and resulted in low RNA yield (personal communication Whittaker, 2003). This was thought to be due to the abundance of contractile proteins, connective tissue and collagen present in the heart samples. A more robust method combining the use of Tri-reagent as well as the RNeasy membrane extraction kit was thought to be optimal giving a high yield of RNA with low residual contaminants. To ensure comparability within the tissue samples, this method of isolation was also used on lung tissue.

6.2.2.1 RNA Isolation

The lung tissue used was always taken from the right apical lobe (Chapter 4; Section 4.2.5) from each lung, as well as half the tissue of each heart. The tissue was snap frozen in liquid nitrogen and then homogenized using a dismembrator. The frozen tissue was placed in a dismembrator vessel that had been pre-cooled in liquid nitrogen. The vessel was then locked into the disembrator and freeze-milled for 1 minute at 2000 rpm. The vessel was then removed, taken apart and 1 ml of Tri-reagent added to both the top and bottom halves. The lysate was passed through a 20-gauge needle fitted to an RNase-free syringe at least five times and decanted into a liquid nitrogen-cooled 1.5 ml eppendorf. A volume of 0.2 ml of molecular biology grade tri-chloromethane was added to the mixture and this was incubated at room temperature for 15 minutes. The tube was then microcentrifuged at 13000 rpm for 15 minutes. The upper phase was carefully transferred into a new, sterile eppendorf containing an equal volume of molecular biology grade ethanol (70% v/v) (to create conditions that promoted selective binding of RNA to the RNeasy silica gel membrane) and mixed by inversion. The mixture was then transferred to a RNeasy mini column placed in a 2 ml

collection tube and microcentrifuged for 15 seconds at 13000 rpm. The RNA was adsorbed on to the membrane and the flow through discarded. The column was rinsed with 350 µl of RW1 wash buffer and again microcentrifuged at 13000 rpm for 15 seconds.

An additional clean up step to remove any residual DNA was also carried out. DNase 1 stock solution (10 µl) was added to 70 µl of buffer RDD and mixed by gentle inversion. The DNase 1 incubation mix (80 µl) was pipetted directly onto the RNeasy silica-gel membrane and left at room temp for 15 minutes. The column was then washed with 350 µl of buffer RW1 and microcentrifuged at 13000 rpm for 15 seconds. The flow-through again discarded. The column was washed with the ethanol-containing buffer RPE (500 µl), centrifuged at 10000 rpm for 15 seconds and the flow through discarded. This step was repeated one further time in order to remove all contaminants. The column was then microcentrifuged at 13000 rpm for 2 minutes to remove any residual ethanol which would damage the purified RNA. The spin column was transferred to a 1.5 ml sterile eppendorf and the RNA was eluted using RNase/DNase-free water (30 µl).

6.2.2.2 RNA Quantitation

The various washing steps in the previous section were carried out to ensure that the RNA was of sufficient quality to be used with the Atlas macroarrays. This was important in obtaining reproducible results as poor quality RNA could result in a high background on the membrane, and/or an inaccurate hybridisation pattern.

The purity and yield of each RNA sample was established by measuring 260:280 nm absorption ratio using the GeneQuantTM. Measuring the ratio of the ribosomal RNA subunits 28s and 18s assessed the purity and a ratio between 1.75-2.1 was considered acceptable for subsequent gene analysis (the higher the ratio, the purer the sample). Lower ratios could indicate contamination in the sample. The yield of the sample was deduced from the absorbency of the sample at a wavelength of 260 nm.

6.2.2.3 RNA Quality Assessment

In order to support evidence from the GeneQuant™ of the condition of the RNA an electrophoretic gel was run to assess integrity of the two RNA bands (28s and 18s) as well as identifying the presence of any genomic DNA. A sample of the RNA was run on a 1% agarose gel (0.5 g in 50 ml 1x TBE with 3 µl of 10 mg/ml ethidium bromide). Each well was loaded with 10 µl of a solution containing 1-2 µg RNA and 2 µl loading dye in high purity RNase/DNase free water. The gel was electrophorised (approximately 40 minutes, 90 volts) and viewed under UV using the Syngene™ Gel Doc System.

6.2.3 Macroarray Procedure

6.2.3.1 Prehybridisation of Array Membranes

The membranes were washed with deionised water, rolled (gene side inwards) and placed in hybrid bottles. Salmon sperm DNA (75 µl of a 9.5 mg/ml solution per membrane) was incubated at 100°C for 5 minutes and then placed on ice immediately. The salmon sperm was then added to 5 ml of prewarmed hybridisation solution in each bottle. The bottles were then rotated at 68°C for at least 30 minutes.

6.2.3.2 Preparation of Targets

A master mix comprising 20 µl reaction buffer, 10 µl 10x dNTP mix, 5 µl DTT and 25 µl [α -³²P] dATP was made up in a 1.5 ml eppendorf and incubated at 70°C for 2 minutes. Another mixture comprising 3 µg of test sample target RNA in a 2 µl volume and 2 µl CDS primer was also made up and incubated at 70°C for 2 minutes. The tubes were then removed and placed at 40°C for 1 minute. Enzyme MMLVRT (5 µl) was added to the master mix and the mixture was incubated at 40°C for a further 2 minutes. The master mix (14 µl) was added to the RNA mixture and incubated at 48°C for 25 minutes. The reaction was then stopped by the addition of 1 µl of termination mix to each reaction. The target was then stored on ice.

6.2.3.3 Column Chromatography (Purification of Target)

The target was diluted with 190 µl of NT2 buffer and mixed well. The mixture was placed into nucleospin extraction (NE) spin columns and centrifuged at 14000 rpm for

1 minute. The flow through and collection tubes were discarded. The columns were transferred to new collection tubes and 400 µl of NT3 solution was added to each. The columns were centrifuged as before and this step was repeated a further three times. The NE columns were transferred to clean, labelled 1.5 ml eppendorfs. NE buffer (100 µl) was added to each column, after which they were left to soak for 2 minutes at room temperature. The columns were then centrifuged for 1 minute at 14000 rpm. The eluted target was mixed with 11 µl of 10x denaturing solution (1 M NaOH, 10 mM EDTA) and incubated at 68°C for 20 minutes. After incubation, 5 µl of CoT-1 DNA and 115 µl of 2x neutralisation solution (1 M NaH₂PO₄ (pH 7.0)) were added and incubated for 10 minutes. CoT-1 DNA is a non-specific nucleic acid competitor and was added in order to reduce cross-hybridisation to highly repetitive sequences. It was critical for limiting sequence detection to specific RNA sequences. Each target was then added to the solution in the hybrid bottles containing the membranes so as to avoid spotting of concentrated target directly on the membrane. The bottles were sealed and placed in a bag and rotated at 68°C overnight.

After incubation the membranes were subsequently washed until the radioactive counts dropped to 10-20 counts per minute (cpm). Wash solution 2 (0.1x SSC, 0.5% v/v SDS) was used for a very stringent wash or wash solution 1 (2x SSC, 1% v/v SDS) for a less stringent wash. Wash solution 1 was used initially to determine the level of washing required. Then wash solution 1 or 2 was used as necessary. The membrane was removed, wrapped well to prevent drying and placed under a phosphorimager screen within a cassette and left (room temperature) for two to seven days depending on the final radioactivity on the membrane.

6.2.3.4 Processing the Phosphorimager Screen

The exposed phosphorimager screen was scanned (50 µm resolution) and the resultant image analysed using the AtlasImage 2.0 computer software. A report was generated and saved as a Microsoft Excel file for further analysis.

6.2.3.5 Stripping the Membranes

The cDNA target was stripped from the membrane prior to storage at -20°C. The membranes were boiled vigorously in 0.5% SDS solution (5-10 minutes) and rinsed in

wash solution 1. The membrane was checked for radioactivity (cpm<5) before sealing in a bag for storage at -20°C. The phosphorimager screen was cleaned by exposure to bright light (15 minutes) and stored at room temperature until required.

6.2.4 Quality Control

Due to the potential variation associated with using array technology some quality control steps were implemented to ensure the most accurate protocol was being followed, and therefore the most accurate results could be achieved.

- Animals (Chapter 4) were from the same source, same strain, same sex and approximately same age and weight and housed in identical conditions to reduce biovariability.
- Controls instilled with saline were included to avoid procedure-induced anomalies.
- Quality of RNA was assessed (see Section 6.2.2.3) and samples discarded if falling below required purity.
- Fresh reagents that accompanied the rat stress arrays were used. Fresh solutions generated in the lab were made each time. On receipt of the rat stress array system, hybridisation solution was aliquoted into required volumes to avoid reheating.
- Radionucleotide was only used if at a total activity level of 9.25 MBq or more.
- Biological replicates of RNA were used as opposed to technical replicates (i.e. RNA from single tissue source) in order to ensure biological accuracy.
- The procedure was carried out by one person to reduce operator-induced discrepancies.
- The array system selected used a nylon membrane containing double spots instead of single to reduce hybridisation errors.
- Consistent concentrations of RNA were used for each array.
- Arrays were processed for a similar amount of time in order to avoid over exposure.

6.2.5 Data Handling, Filtering and Analysis

The data obtained from control and test samples for both lung and heart were generated using the AtlasImage 2.0 software. The data comprised the intensity of the spot, the background intensity of the membrane and an adjusted intensity that was taken to be a quantitative measure of gene expression (i.e. spot intensity minus background intensity). In order to compare hybridisation signal intensities across the membranes a normalised signal intensity for each spot was obtained. Normalisation can be defined as the process of removing certain systematic biases from macroarray data, including corrections for differences in overall array intensity i.e. background noise.

The first part of the normalisation process involved transforming expression data to a log scale (in this instance \log_{10}). This was done to produce a normal distribution throughout the data set so as to reduce skewness and random error in the raw expression data and to allow normal statistical assumptions to be made. Preliminary statistical analysis using an Anderson Darling test for normality ($p > 0.05$) confirmed the raw array data after \log_{10} transformation was normally distributed. Following this step global normalisation between membranes was carried out which involved dividing the \log_{10} transformed spot intensity of each gene by the median \log_{10} transformed spot intensity of the whole array to correct for variations between arrays. As the mean value can be distorted by the effects of a few extreme outliers, the median value was considered the most accurate basis for normalisation, thus reducing the possibility of data variance due to anomalous data points (Balharry *et al.*, 2005). Further Anderson Darling tests were conducted between arrays to ensure normality of resultant comparable data. Once normalisation was complete, a legitimate comparison of gene expression could be made. The globally normalised data was the data used for the subsequent analysis.

6.2.5.1 Fold Change

An elementary method for identifying differentially expressed genes is to analyse fold change. This was carried out to evaluate the ratio between saline control and test for each gene and consideration was given to all genes that differed by more than a specific cut-off value. Calculating the fold change between control and test samples for each gene involved using the higher of the two numbers as the numerator and the

lower number as the denominator. If the results for the control were higher than those of the test for any specified gene then a negative sign was placed in front of the resultant number and the gene was deemed to be down-regulated. Only genes with a fold change of $\geq \pm 1.5$ were selected for further analysis. It has been shown that 75% of genes with a ratio change of $\geq \pm 1.5$ are likely to be detected by conventional quantitative polymerase chain reaction (qPCR) studies (Treadwell and Singh, 2004; Balharry *et al.*, 2005).

6.2.5.2 Coefficient of Variation

The coefficient of variation (CV) was calculated from the replicates of control and test data. This was not a statistical analysis, but was useful in determining whether enough replicates for each gene had been used. The CV was calculated using the mean and standard deviation (CV= standard deviation/mean). If the reproducibility for each data set was perfect then a value of zero was obtained. If it is poor the value tended towards 1. If a CV value of 0.6 was obtained it would mean that almost 60% of the measurement was erroneous (Wierling *et al.*, 2003). The use of the CV value performs similar function to the use of r^2 values in that judging whether a r^2 value is acceptable or unacceptable is subjective. Published studies have shown CV values of between 0-0.25 as acceptable levels of accuracy (Herwig *et al.*, 2001; Salin *et al.*, 2002). For this particular study a cut off of 30% was deemed appropriate (i.e. using CV values of 0-0.3).

6.2.5.3 Statistical Analysis

The two tests described previously were not statistical tests and thus did not indicate a level of confidence in the data sets. Therefore, the significance of differentially expressed genes could only result when statistical analyses were applied. The appropriate statistical analysis in this instance was a two-tailed student's t-test. All analysis was conducted on \log_{10} normalised data.

The two-tailed student's t-test is a test used to examine a difference between mean values of two groups of data. A null hypothesis of no expression-level difference in individual genes between saline control and test animals was adopted. The resultant statistical value could then be used to determine which genes were significantly differentially expressed. A p value of ≤ 0.05 was deemed significant.

6.2.5.4 Functional Grouping

Each of the genes present on the array could be categorised under functional group headings. These groups are listed in Table 6.2.5.4. The purpose of looking at the functional groups was to assess whether genes contributing to the same type of response were being altered to gain more evidence as to the type of damage that was occurring and whether specific families of genes were being affected by the 3SD dose.

Table 6.2.5.4 Broad functional classifications of genes present on the rat stress array

AtlasTM rat stress array (7735-1)
Apoptosis Associated Proteins
Cell Cycles
Cell Receptors
Cytoskeleton Motility Proteins
DNA Binding and Chromatin Proteins
DNA Synthesis, Recombination and Repair
Functionally Unclassified
Intracellular Transducers Effectors & Modulators
Protein Turnover
Stress Response Proteins
Trafficking Targeting Proteins
Transcription
Translation

6.2.6 Methodological Summary

For clarity, each step from RNA isolation to final statistical analysis is summarised in Figure 6.2.6. It is broken down into three main stages: i) Experimental ii) Data Preparation iii) Data Analysis.

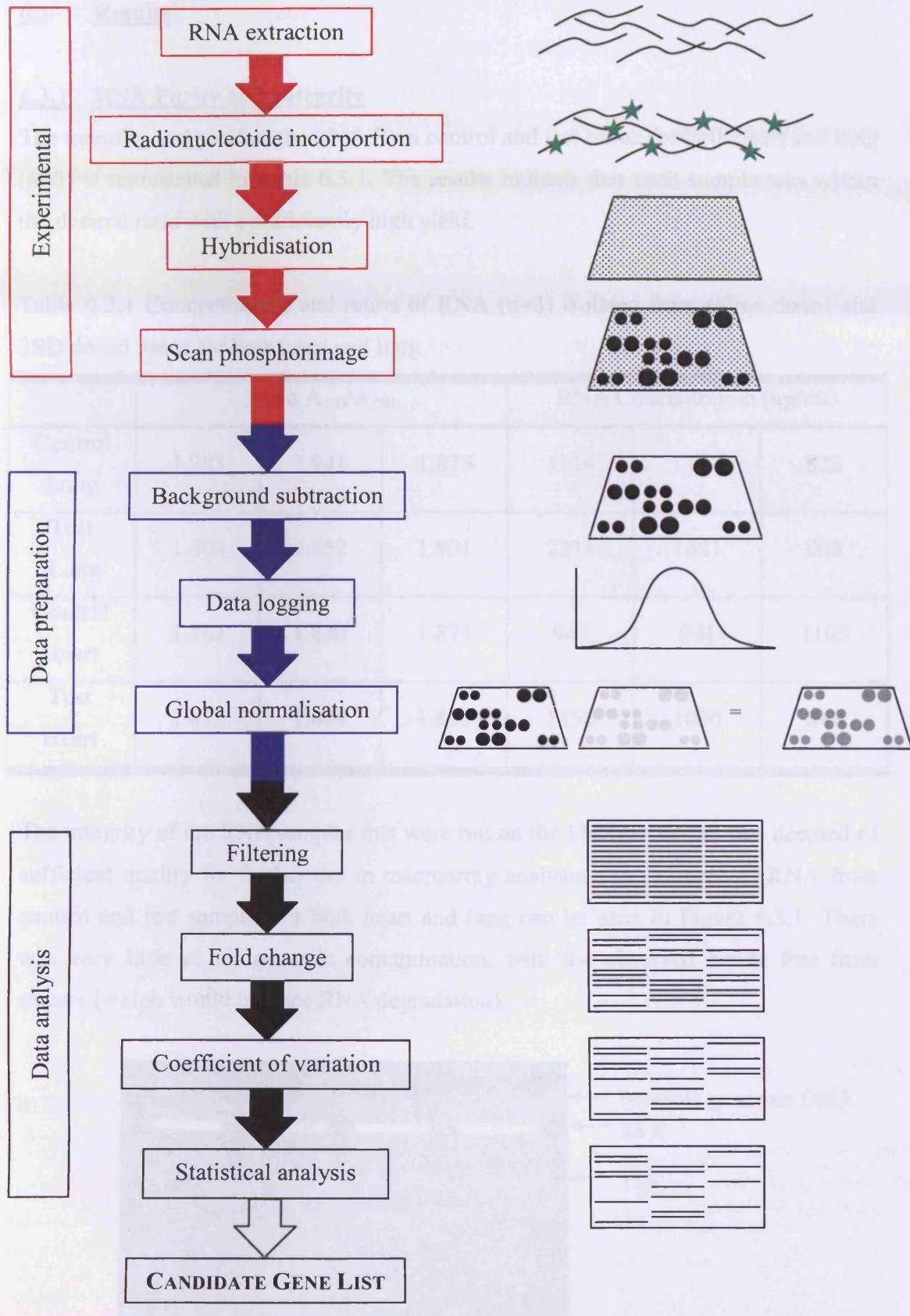


Figure 6.2.6 Flow chart summarising macroarray analysis process

6.3 Results

6.3.1 RNA Purity and Integrity

The integrity and yield of the RNA from control and test tissue for both heart and lung (n=3) is represented in Table 6.3.1. The results indicate that each sample was within the desired ratio with a sufficiently high yield.

Table 6.3.1 Concentrations and ratios of RNA (n=3) isolated from saline dosed and 3SD dosed tissue for both heart and lung

	Ratio A ₂₆₀ /A ₂₈₀			RNA Concentration (ug/ml)		
Control Lung	1.983	1.941	1.875	1114	1197	822
Test Lung	1.804	1.852	1.901	2211	1481	803
Control Heart	1.762	1.830	1.874	947	841	1105
Test Heart	1.835	1.809	1.870	1456	1030	848

The integrity of the RNA samples that were run on the 1% agarose gel was deemed of sufficient quality for further use in macroarray analysis. An example of RNA from control and test samples for both heart and lung can be seen in Figure 6.3.1. There was very little or no genomic contamination, with the observed bands free from smears (which would indicate RNA degradation).

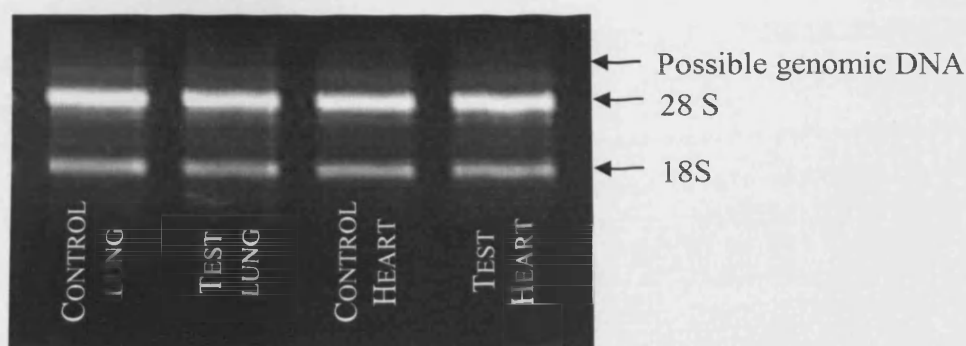


Figure 6.3.1 Typical agarose gel depicting RNA integrity

6.3.2 Macroarray Analysis

Array analysis was used to detect possible genetic changes at 4 h post-instillation. A positive degree of hybridisation had occurred with a low level of background noise and each pair of arrays was thus distinguishable from the next. The different arrays showed varying degrees of intensity but any variation was corrected using the global normalisation process.

6.3.2.1 Lung

Having processed the arrays and obtained suitable phosphorimages (e.g. Figure 6.3.2.1a-b), quantitative comparative analyses were carried out and a report was generated which was exported to Excel. Initial results gave rise to 35 genes having fold changes greater than ± 1.5 (15 up-regulated and 20 down-regulated genes between control and test for the lung). The CV was then assessed to examine whether enough replicates had been used for both test and control for each gene. Of the 35 genes selected 19 were omitted due to CV values falling outside the limit of 0-0.3 stated earlier. The 19 omitted consisted of 13 up-regulated genes and 6 down-regulated genes. The candidate genes that had been filtered (16) were then subjected to statistical analysis to assess whether there was a significant difference between the mean control value and the value obtained from the test animal for each of the 16 genes. A t-test was used to gauge whether the difference between control and test genes was significant. The results obtained from the t-test indicated that 13 genes of the 16 previously identified were significantly altered and 3 not significantly altered. Ten of the genes were significantly down-regulated and 3 genes were significantly up-regulated. The statistically altered genes are presented in Table 6.3.2.1. The name of the genes along with fold changes, CV values and statistical p values are also shown.

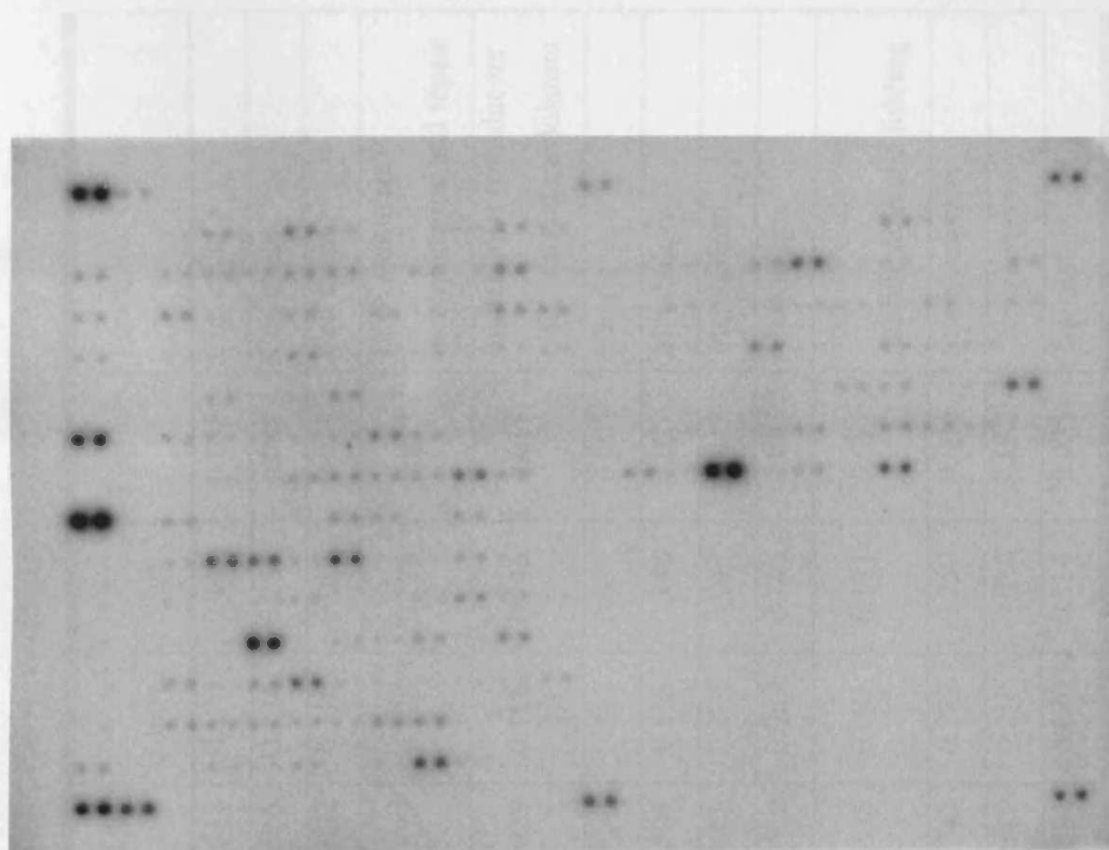


Figure 6.3.2.1a Lung control macroarray image

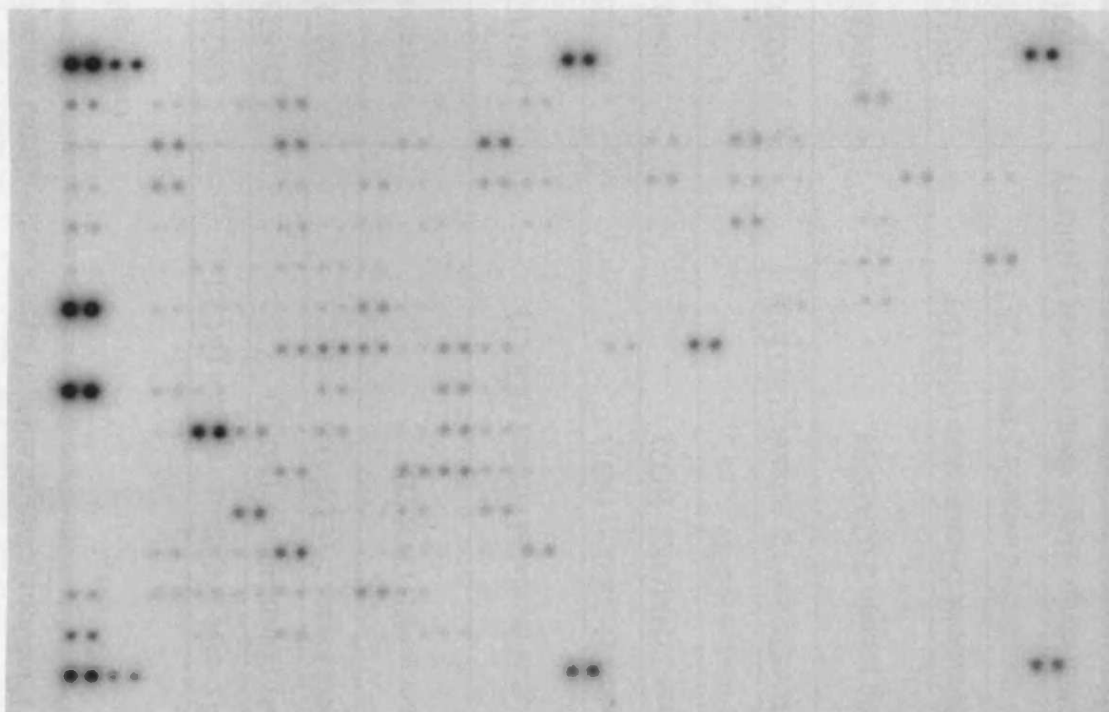


Figure 6.3.2.1b Lung 3SD test macroarray image

Table 6.3.2.1 Functional classification of significantly altered genes from lung tissue (up-regulated genes in red)

Name	Genebank ID	Ratio	CV		P-value	Functional Group
			Control	Test		
Growth-related c-myc-responsive protein (RCL)	U82591	-1.518	0.170	0.122	0.035	Cell cycle
M-phase inducer phosphatase 2 (MPI2)	D16237	-1.568	0.134	0.255	0.041	Cell cycle
Cyclin-dependent kinase 5 (CDK5)	L02121	-1.932	0.116	0.012	0.024	Cell cycle
DNA topoisomerase IIB (TOP2B)	D14046	-1.579	0.126	0.128	0.013	DNA synthesis recombination and repair
Extracellular signal regulated kinase1 (ERK1)	M61177	-1.538	0.116	0.145	0.015	Intracellular transducers effectors and modulators
Heme oxygenase 1 (HMOX1; HO1)	J027222	1.952	0.245	0.079	0.005	Metabolism
Heme oxygenase 2 (HMOX2; HO2)	J05405	-1.504	0.138	0.148	0.027	Metabolism
Glutathione reductase (GSR)	U73174	1.812	0.293	0.077	0.012	Metabolism
Glutathione S-transferase Yb subunit (GSTM2)	J02592	-1.559	0.069	0.248	0.023	Metabolism
Calcium binding protein 2 (CABP2)	M86870	-1.516	0.085	0.171	0.014	Post translational modification and folding
Microsomal glutathione S-transferase (GSTI2)	J03752	-1.743	0.217	0.250	0.046	Stress response
Glutathione S-transferase subunit 5 theta (GST5-5)	X67654	1.643	0.217	0.080	0.012	Stress response
Eukaryotic peptide chain release factor subunit 1 (ERF1)	M75715	-1.591	0.170	0.114	0.025	Translation

6.3.2.2 Heart

Having processed the arrays and obtained suitable phosphorimages (e.g. Figure 6.3.2.2a, b), quantitative comparative analyses took place and a report was generated and exported to Excel. Results obtained from the heart revealed a lower number of genes with fold changes greater than ± 1.5 compared to those from the lung. Twenty-eight genes were identified (14 down-regulated, 14 up-regulated) with a fold change greater than ± 1.5 . Further analysis calculating the CV for each of the selected genes revealed that 19 genes (12 down-regulated 7 up-regulated) had a CV higher than 0.3 either for control or test or both and thus were not used for further statistical analysis.

Of the 9 candidate genes that remained the vast majority were up-regulated (7). Results obtained from the t-test revealed that the two down-regulated genes were significantly different from that observed in control heart tissue. Analysis of the up-regulated genes revealed that all but one of the seven genes were significantly altered.

Once the significantly altered genes had been identified they were classified according to their corresponding functional group. The statistically altered genes are represented in Table 6.3.2.2. The name of the genes along with fold changes, CV values and statistical p values are also presented.

6.3.2.3 Comparative Functional Classification

The total number of classified groups within the rat stress array was 13 as outlined in Table 6.2.5.4. Seven of those groups contained significantly altered genes for both lung and heart samples. Each group significantly altered in the lung was also significantly altered in the heart apart from one. A gene involved in translation was altered in the lung but not the heart and a gene classified within the group DNA binding and chromatin proteins was altered in the heart but not the lung. The 3 groups showing the greatest response in the lung were metabolism, cell cycle and stress response that together accounted for 68% of all genes altered (Figure 6.3.2.3a). Of these groups, metabolism and stress response were also the two major groups altered in the heart (Figure 6.3.2.3b), together accounting for nearly 50% of all genes altered. Metabolism and stress response were the only groups that showed any up-regulation in the lung. Genes represented within these groups were all up-regulated in the heart.

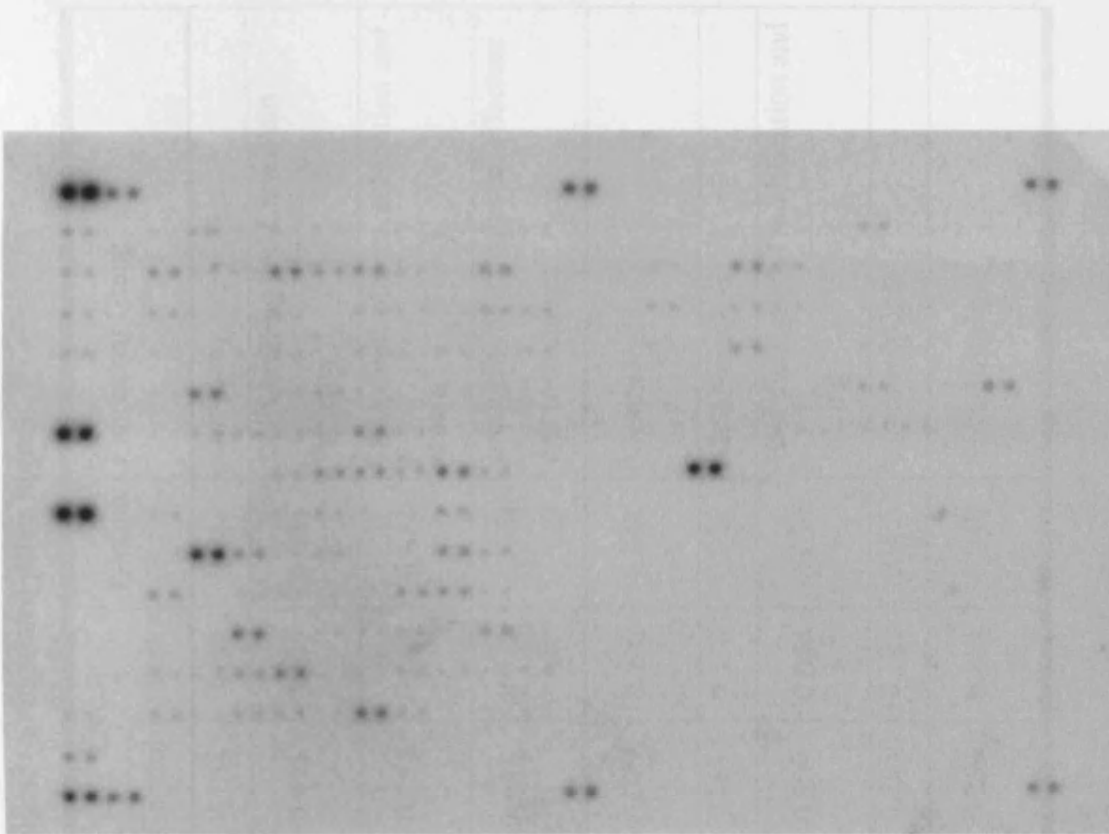


Figure 6.3.2.2a Heart control macroarray image

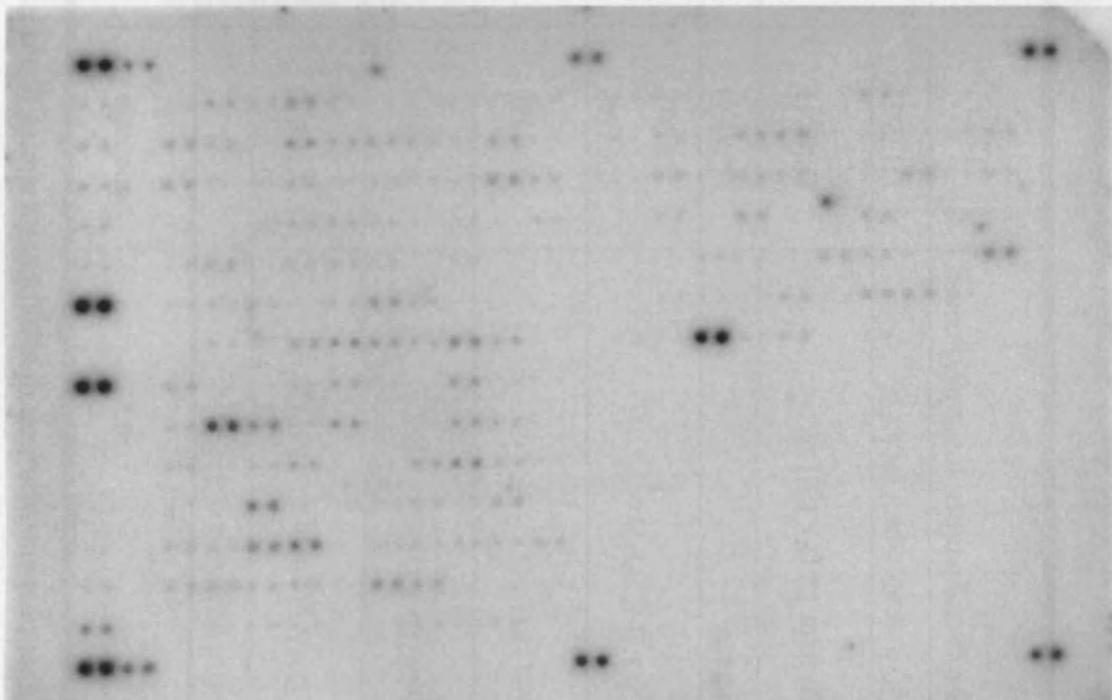


Figure 6.3.2.2 b Heart 3SD test macroarray image

Table 6.3.2.2 Functional classification of significantly altered genes from heart tissue (up-regulated genes in red)

Name	Genebank ID	Ratio	CV		P-value	Functional Group
			Control	Test		
Cell division control protein 2 (CDC2)	X60767	1.537	0.162	0.154	0.032	Cell cycle
N-methylpurine DNA glycosylase (MPG)	X56420	-1.530	0.055	0.129	0.003	DNA binding and Chromatin Proteins
DNA repair protein (RAD51)	D13804	1.800	0.354	0.066	0.021	DNA synthesis recombination and repair
Adrenal ferredoxin (FDX1)	D50436	1.679	0.218	0.166	0.029	Intracellular transducers effectors and modulators
Cytochrome P450 VIII (CYP7)	J05460; J05509	1.515	0.079	0.300	0.048	Metabolism
Glutathione reductase	U73174	1.512	0.161	0.136	0.027	Metabolism
FK506-binding protein 12 (FKBP12)	D86641	-1.595	0.209	0.046	0.039	Post translational modification and folding
Arylamine N-acetyltransferase 2 (NAT2)	U17261	1.681	0.205	0.109	0.025	Stress response
N-oxide-forming dimethylamine monooxygenase 4 (FMO4)	Z11737	1.648	0.259	0.164	0.040	Stress response

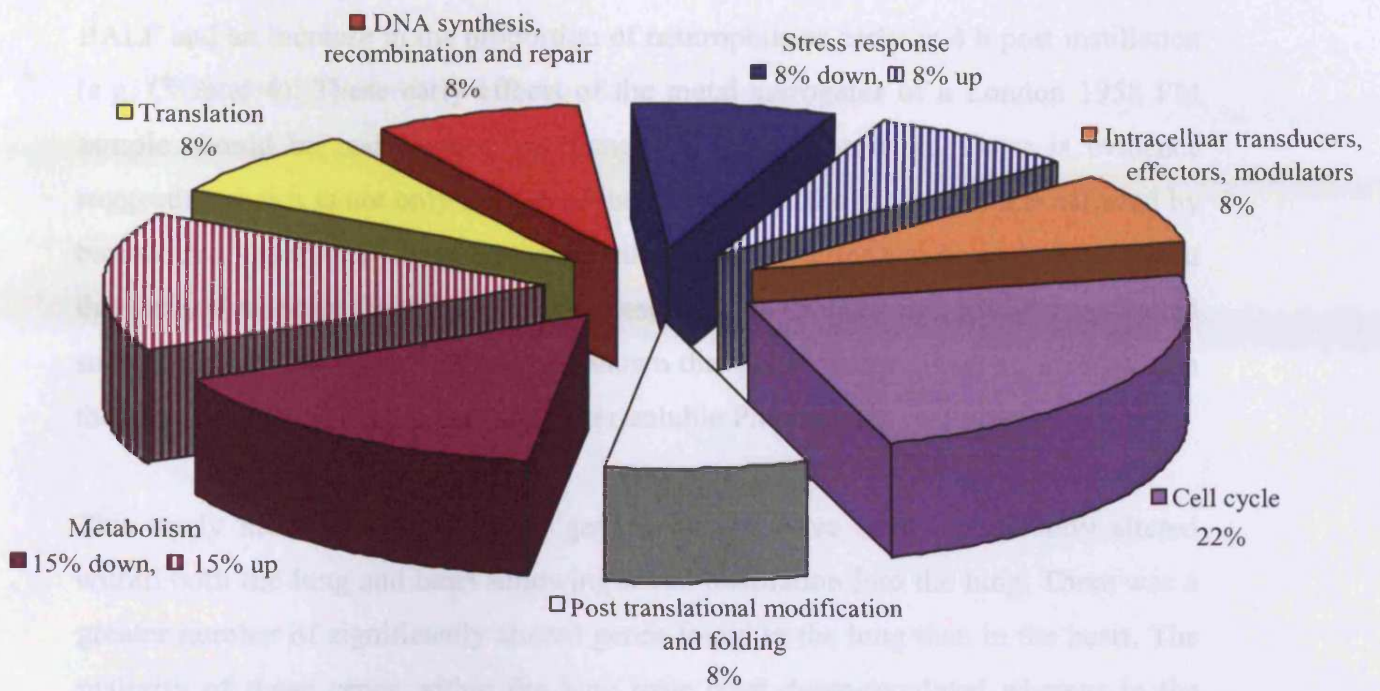


Figure 6.3.2.3a Functional classification of the significant genes from lung tissue (solid colour indicates down-regulation, stripes indicate up-regulation)

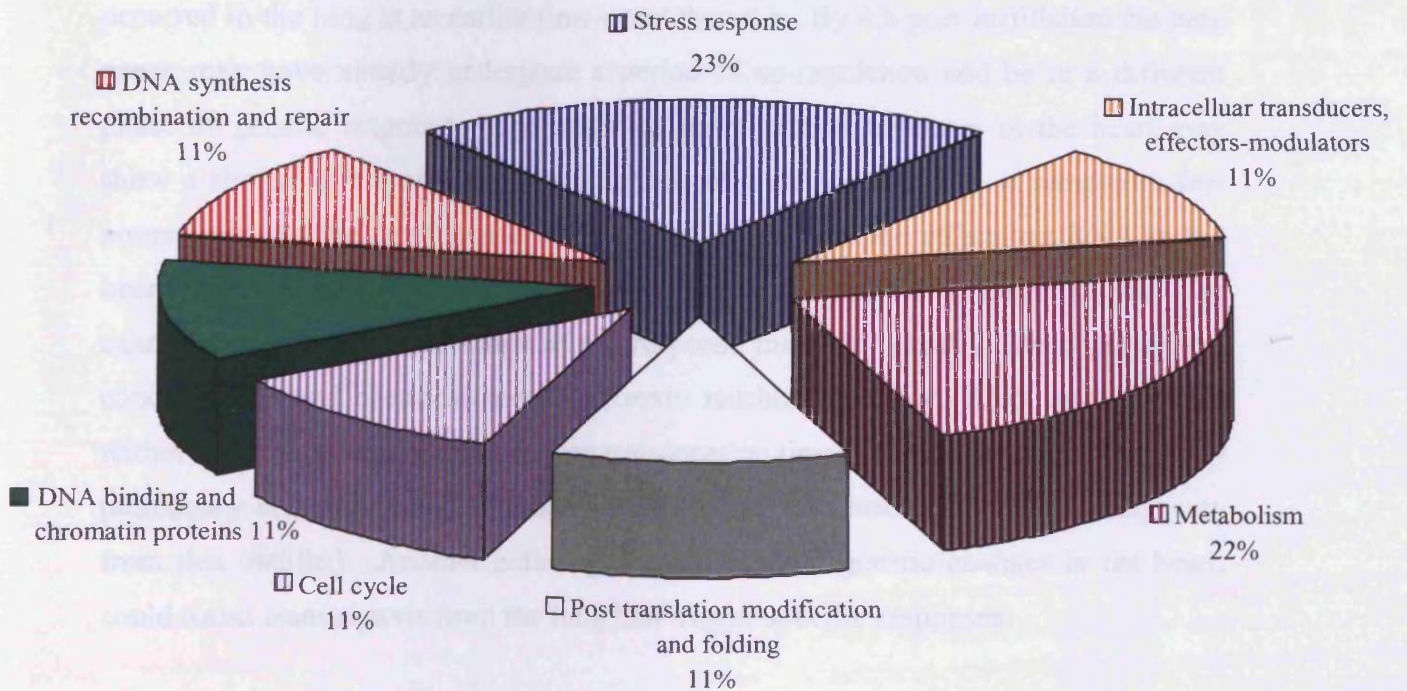


Figure 6.3.2.3b Functional classification of the significant genes from heart tissue (solid colour indicates down-regulation, stripes indicate up-regulation)

6.4 Discussion

Analysis of toxicological data has revealed an increase in protein concentration within BALF and an increase in the proportion of neutrophils as early as 4 h post instillation (e.g. Chapter 4). These early effects of the metal surrogates of a London 1958 PM sample should be underpinned by changes in gene expression. There is evidence suggesting that it is not only the site of instillation (i.e. the lung) which is affected by bioactive xenobiotics, but also the effects of such mixtures can occur in the heart at this early time-point (Whittaker, 2003). Research has revealed that ROFA has exerted such effects and Whittaker (2003) has shown that gene changes have occurred within the heart at 4 h post-instillation of a water-soluble PM sample.

This study has shown that certain gene pathways have been significantly altered within both the lung and heart following metal instillation into the lung. There was a greater number of significantly altered genes found in the lung than in the heart. The majority of these genes within the lung have been down-regulated whereas in the heart the majority of significantly altered genes have been up-regulated. Due to the high solubility of the mixture instilled an overall up-regulation of genes may have occurred in the lung at an earlier time-point than 4 h. By 4 h post-instillation the lung genes may have already undergone a period of up-regulation and be in a different phase of genetic response. The observed up-regulation of genes in the heart may show a similar effect of down-regulation, as was seen in the lung, if sampled a few hours later. As the heart was not the site of instillation, the effects on RNA in the heart from the metal mixture may be different from that of the target organ. For example, the severity and scope of the response may vary greatly dependant on the concentration and chemical species of toxin reaching the heart. Also, as the metals within the mixture may have different translocation times or be differently affected by pulmonary constituents, the species within the mixture reaching the heart may vary from that instilled. Another pathway that may induce genetic changes in the heart, could result from signals from the lung that trigger specific responses.

6.4.1 Functional Groups

The thirteen genes in the lung and the nine in the heart deemed significantly altered following exposure to the metal mixture were classified within their functional

groups. The following scenarios have been postulated based upon current information obtained for the genes from universal databases (www.genecards.org)

6.4.1.1 Metabolism

Haem oxygenase 1 and 2 (HO1, HO2) are part of the haem oxygenase family which cleave the haem ring of haemoglobin to form biliverdin (subsequently converted to bilirubin). Haem oxygenase 1 is an inducible gene widely regarded as a protective agent against ROS injury from chemical agents and up-regulation may be induced by heavy metals (Bach, 2002) and involve reduced intracellular GSH (Ryter and Choi, 2005). The observed up-regulation in the present study may suggest metal-induced oxidative injury and GSH depletion in the lung. Whilst concurrent down-regulation of HO2 seems counter-intuitive, HO2 is constitutively expressed and not implicated in redox mechanisms to the same degree as HO1 (Bach, 2002).

Glutathione S-transferase Yb subunit (GSTM2) forms part of the GST molecule responsible for conjugating GSH to hydrophobic electrophiles. The down-regulation of this molecule will serve to maximise free intracellular GSH levels to enhance protective capacity against oxidant stress. Glutathione reductase (GSR) is involved in cycling glutathione from the oxidised form and therefore involved in maintaining high levels of cytosolic GSH (Rahman *et al.*, 1999). GSR was found to be up-regulated in both the lung and heart. As the primary function of GSH is antioxidative scavenging of various ROS, it seems logical to infer that the metals instilled exerted an oxidative effect within the lung and subsequently the heart, necessitating increased redox cycling of cellular antioxidants.

Cytochrome P450 7 (CYP7) belongs to the cytochrome P450 family involved in the biotransformation of xenobiotics. The observed up-regulation in the heart may be indicative of increased cellular activity in metabolising xenobiotics that could damage the cell.

6.4.1.2 Cell Cycle

All of the identified genes that were involved in the cell cycle were down-regulated in the lung such as growth-related c-myc-responsive protein (RCL) (involved in cell proliferation pathway), M-phase inducer phosphatase 2 (MPI2) (functions as a

dosage-dependent inducer in mitotic control, required for progression of the cell cycle) and cyclin-dependent kinase 5 (CDK5) (involved in the control of the cell cycle and histone phosphorylation). These results may suggest that genes required for cell growth and survival may be compromised by damage caused by the metal mixture. An alternative hypothesis to this could be that cells were utilising energy for other processes in response to the damage caused by the metal mixture and subsequently the genes used in other cellular functions, e.g. the cell cycle, were temporarily down-regulated.

Only one gene identified in the heart was involved in the cell cycle and that was cell division control protein 2 (CDC2). This plays a key role in the control of the eukaryotic cell cycle. It is required in higher cells for entry into S-phase and mitosis. Up-regulation of this gene could suggest that there might be an acceleration of the cell cycle as a consequence of tissue damage. Whether this damage is triggered by cellular signals from the lung or direct interaction of the metals with heart tissue is unclear.

6.4.1.3 Stress Response

Another member of the family of proteins responsible for the regulation of GSH levels, microsomal glutathione S-transferase (MGST1), was found to be down-regulated in the lung. Functionally similar to GSTM1 (above) and GST5-5 but commonly located in microsomes, down-regulation of the MGST1 gene again might suggest maximisation of free intracellular GSH levels. However, concurrent up-regulation of glutathione S-transferase subunit 5 theta (GST5-5) in the lung seems counter-intuitive. It may be that one GST gene is more closely associated with responses in the lung than the others, but this is unknown.

The responsive genes identified in the heart again differed completely from those identified in the lung. The up-regulation of n-oxide-forming demethylaniline monooxygenase 4 (FMO4) (involved in the oxidative metabolism of a variety of xenobiotics) again reinforces the idea that the heart tissue is responding to redox activity as a result of the instillation of the metals into the lung. The concurrent up-regulation of arylamine N-acetyl transferase 2 (NAT2) (participates in the detoxification of a plethora of hydrazine and arylamine compounds) also indicates a strong biotransformation response in the heart tissue. However, as the protein

encoded by FMO4 is oxidative, it seems unlikely that it is responding to the metals in the manner that they were instilled (as they too are likely to be oxidative). It is therefore possible that FMO4 is up-regulated in response to redox-active products of metal-induced damage that may include formation or release of NAT2-specific compounds. Alternatively, these genes may form part of a generic stress response.

6.4.1.4 Intracellular Transducers, Effectors, Modulators

In the lung, extracellular signal-regulated kinase 1 (ERK1) (involved in the phosphorylation of extra-cellular signalling molecules) was found to be down-regulated, whereas in the heart adrenal ferredoxin (FDX1) was up-regulated. FDX1 is involved with the P450 enzymes in that it transfers electrons from adrenodoxin reductase to the cholesterol side chain cleavage cytochrome P450. These results may suggest that an increase in FDX1 may cause an increase in xenobiotic metabolism by P450 enzymes. This would concur with the up-regulation of members of the cytochrome P450 family such as CYP7.

6.4.1.5 DNA Synthesis, Recombination and Repair

The only gene identified in the lung in this functional group was DNA topoisomerase IIB (TOP2B) which is involved in the control of topological states of DNA by transient breakage and subsequent rejoining of DNA strands. Alteration of the DNA conformation is implicated in translation. Therefore the observed down-regulation of this gene may indicate that the process of translation is being compromised.

The only gene identified in the heart in this functional group was DNA repair protein (RAD51). The protein encoded by this gene may participate in a common DNA damage response pathway associated with the activation of homologous recombination and double-strand break repair. The up-regulation of this gene indicates that the metal mixture may have a bioreactive effect on DNA either through the production of ROS or direct hydrolysis as shown *in vitro* (Merolla and Richards, 2005, see Chapter 3). As a result DNA strand-break repair was required.

6.4.1.6 Post Translational Modification Protein Folding

In the lung, the gene encoding calcium binding protein 2 (CABP2) was down-regulated. This gene product is involved in calcium ion binding and signal

transduction. Therefore the observed down-regulation suggests a possible effect on fluid balance or cellular signalling within the tissues and the requirement for more free calcium ions.

In the heart a similar response was seen in that FK506-binding protein 12 (FKBP12) was also down-regulated. FKBP12 is thought to play a role in modulation of ryanodine receptor isoform-1 (RYR-1), a component of the calcium release channel in the endoplasmic reticulum. This again indicates that calcium balance is being affected. Research has shown that zinc can affect calcium channel function (Atchison, 2003) and supports previous findings regarding protein leakage into BALF (see Chapter 4).

6.4.1.7 Translation

Translation specific genes were not significantly altered in the heart but eukaryotic peptide chain release factor subunit 1 (ERF1) was down-regulated in the lung. This gene product directs the termination of nascent peptide synthesis in response to termination codons and its suppression could indicate a reduction in protein synthesis.

6.4.1.8 DNA Binding and Chromatin Proteins

DNA binding genes were unaltered in the lung but in the heart there was down-regulation of N-methyl purine DNA glycosylase (MPG). This gene is involved in the hydrolysis of the deoxyribose N-glycosidic bond to excise 3-methyladenine and 7-methylguanine from damaged DNA and its down-regulation again seems incongruous, as it would be expected that metals might directly oxidise DNA. Nevertheless it might be concluded that direct DNA damage was not occurring in the heart and therefore genetic alterations were the result of cellular signals and triggers.

6.4.2 Technical Critique

The method used to isolate sufficiently pure RNA was successful. The combination of the two techniques to increase both yield and purity was necessary, especially with regard to the heart. The techniques used to establish a candidate gene list were carried out as accurately as possible and the analysis procedures were deemed the most appropriate given the circumstances. Even though the rat stress array chosen was double spotted and thus allowed an average of each gene to be taken, no technical

replicates were used. This would have added to the accuracy of the experiment by showing reproducibility of the procedure using RNA from the same animal. Variability would have also occurred with different membranes. This is one disadvantage of using macroarray technology, as outlined in the introduction. Nevertheless, biological replicates were used to ensure that results were not affected by any individual animal being predisposed to up-or down-regulation of candidate genes.

The results (as expected) gave rise to array membranes with different overall intensities and thus global normalisation was necessary to standardise across replicates. Even though the same lobe of each lung was used to try to standardise the procedure the deposition and exposure from each instillation procedure can never be entirely uniform, and hence, variability in severity of damage effect can occur. Another confounder was that as damage may have been localised within different areas of the lobe, the effects of up or down-regulation may have been diluted with RNA from unaffected areas. Use of a laser capture microdissection procedure could have combated this type of variation as it uses lung material from one lung for both control and test samples. This would reduce variability as the control and test comparison would be from the same animal (Roberts *et al.*, 2004).

Even though a coefficient of variation was used as part of the filtering process, the threshold value is subjective and a greater number of replicates would provide greater accuracy of data. The combination of more replicates used in conjunction with a quantitative method such as qPCR to support findings from the macroarray analysis would add support to subsequent findings. Using a similar macroarray system Balharry (2005) has reported excellent agreement between qPCR and array data and as a consequence qPCR was not undertaken in the present study.

6.4.3 General Summary

The results obtained from the present study support evidence that transition metals which can be found in PM contribute to oxidative stress within the lung as well as systemically. The evidence suggests that control of antioxidants such as glutathione is involved in a pivotal role in combating this type of damage (BeruBe *et al.*, 2006).

Overall, the results of the toxicogenomic analysis support the data found in previous chapters, which indicated that the water-soluble metals that comprised the test mixture have a redox effect on the lung. This effect was also seen in the heart. In both organs the primary responses revolved around up-regulating redox-specific stress mechanisms and metabolism pathways in order to neutralise the xenobiotics. No genetic support for inflammatory processes was observed, although the presence of inflammatory effects was clear (see Chapters 4 and 5). Again, the lack of any inflammation-related genes may be due to the time point used, i.e. 4 h post instillation and any changes in responsive genes were missed.

CHAPTER 7

GENERAL DISCUSSION

7.0 General Discussion

This investigation started by investigating the bioreactivity of PM samples derived from urban, suburban and rural conurbations around the UK. Assessment of variations in meteorological conditions, geographical collection (e.g. industrial versus non-industrial) and seasonal variation was carried out to gain insight into whether these factors affected the bioreactivity of collected PM samples. Further to this, numerous links have been made between PM and adverse health effects and although many viable hypotheses exist, as yet there is little definitive explanation of the underlying causes. More light therefore needed to be shed on the mechanisms by which PM was causing health effects. Water-soluble metals and more specifically transition metals have frequently been implicated in adverse health effects. Consequently it was considered important to elucidate whether any observed differences in PM bioreactivity correlated to the water-soluble metal content of a given sample. If it were the case that such were deemed contributory to PM bioreactivity then research into the mechanistics of damage would be of vital importance. Therefore it was necessary to assay the bioreactivity of each metal found in the water-soluble fraction of PM individually and from this assess whether bioreactivity was valence dependent within the assay. Consequently, a subsequent aim was to use the more bioreactive metals found *in vitro* and carry out *in vivo* studies to gain an insight into the types of damage caused from a toxicological perspective. Use of conventional toxicological techniques, including histopathology, could then be carried out to detail any damage to the lung microarchitecture as well as providing information on the progression of injury and repair mechanisms. Finally, toxicogenomic studies were implemented to explain the observed effects at the molecular level. This providing a more 'holistic' evaluation of the role/effects of soluble metal components in the bioreactivity of UK PM.

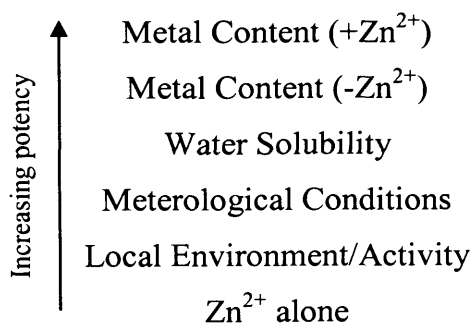
The initial experimental work revealed that a number of factors did affect PM bioreactivity. From a human health perspective the following parameters affected the physicochemical composition and hence bioreactivity of PM: geographical location, contribution of natural versus anthropogenic aerosols and variations in wind direction. For example industrial collection sites produced PM rich in Fe, Mn and Ni whereas locations near motorways were dominated by Pb, V and As. Recent studies have confirmed that individuals living close to highly traffic-polluted areas show a

significant increase in expected mortality (Brunekreef and Holgate, 2002), possibly due to their inhalation of PM, rich in metals present in the SE related PM sample of this study. The toxicity of PM samples could be affected by changes in meteorological conditions other than wind direction. Rain may influence a change in oxidation state and hence bioreactivities of certain metals. Due to the heterogeneity of PM it is clear that concentrating on one criterion alone would not reveal the true complexity of influencing factors. The Port Talbot wind direction study implicates metals (particularly soluble metals such as Fe and Zn) as being most likely linked to negative health effects involving damage to DNA. This is in agreement with previous investigations into pulmonary cell reactivity (Adamson *et al.*, 2000). Such a high correlation was not observed in the five location study. Nevertheless, there was still evidence that implicated the causative role of metals, for example the most bioreactive PM sample in the water-soluble fraction was collected in London (win) which had the highest concentrations of Fe, V, Cu and Pb. The fact that ROFA, which had a higher water-soluble metal component than all the PM samples, had the greatest bioreactivity again supports this hypothesis. These results led to the conclusion that future ambient pollution limits should consider individual PM constituents (such as metals) in the same way as specific gases are currently monitored (e.g. SO_x and NO_x). The reduction or removal of toxic components within ambient PM may have greater effect in reducing epidemiological outcomes than reducing PM levels as a whole. From these conclusions investigations were carried out to assess the bioreactivity of individual water-soluble metals in order to gain further insight into which metal might be implicated in the cause of bioreactivity within PM₁₀.

The prevalent metals within the PM samples on a proportional mass basis were found to be Fe and Zn. Within the study correlations were made between the presence of high levels of Fe and Zn with bioreactivity in the water-soluble fraction. This was supported in ensuing studies (Chapter 3) in which a surrogate London 1958 PM sample comprising the prevalent metals at exactly the same concentration and ratios was made and a comparison was drawn between the bioreactivities of that sample with the original. This gave rise to similar TD₅₀ values being obtained. In order to ensure that the similarity in TD₅₀ values was not a coincidence peculiar to this sample, further plasmid scission assay work involving surrogates of other PM samples would be useful. This would either refute or validate any correlation in bioreactivity

between the metal content of the PM sample and that of the surrogate. To this end it was determined that different metals had varying bioreactivities and more importantly that metals in different oxidation states also had very distinct bioreactivities. This was observed with experiments involving Fe^{2+} and Fe^{3+} as well as VO^{2+} and VO_3^- . Further investigations need to be conducted before direct correlations can be drawn between increased metal content and increased bioreactivity. This may explain why the direct correlation between metal content and bioreactivity was not seen in the five location study.

The most interesting observation that did arise from using the plasmid scission assay was that a metal found to have very low bioreactivity within the assay such as Zn^{2+} could exert synergistic effects with other metals such as Fe^{3+} and Cu^{2+} . The magnitude of the observed synergistic effects far exceeded the expected additive effect. This has significant implications when analysing the toxicity of PM. Zn^{2+} was required only in minute quantities to cause a large synergistic effect and thus would not need to be present at high concentrations to cause the bioreactivities of other metals to increase. The synergistic effect was selective in that mixed with Fe^{3+} there was a synergistic effect but when mixed with Fe^{2+} there was not. In all, a brief hierarchy of factors influencing PM-induced health effects can be generated from the data obtained.



Due to the heterogeneity of PM and the fact that even within the metal components there is such variation, more detailed characterisation of PM needs to be conducted. The synergistic behaviour of the metals raises questions about other synergies between components of PM. You could state that at present, techniques are not readily available to deduce valence characteristics of metals *in vitro/in vivo* that would assist in the elucidation of bioreactive mechanisms.

The findings from *in vitro* studies cannot necessarily be correlated directly to *in vivo* studies. This was demonstrated when examining the results with Zn^{2+} . *In vitro*, Zn^{2+} was not bioreactive at high concentrations but *in vivo* Zn^{2+} was found to be extremely bioreactive in comparison with the other metal mixtures. The reason for this may be due to different mechanisms of damage occurring. For example, the results from *in vitro* and *in vivo* studies using a test mixture without Zn^{2+} revealed similar bioreactivities. This bioreactivity was significantly lower than that of Zn^{2+} alone *in vivo*. These data suggest that Zn^{2+} is a potent toxin in the lung at a high concentration and in certain assays it was more bioreactive on its own than in a mixture. This highlights the mechanistic differences between the *in vitro* and *in vivo* studies as zinc alone did not cause significant damage to DNA when on its own at very high concentrations *in vitro*, but far greater toxicity *in vivo*.

The histopathological analysis of the lung tissue following exposure to the metal mixtures highlighted the rapid nature of the damage induced. Due to their water-solubility the metal mixtures were very fast acting, hence rapid recovery was observed. This is not necessarily a true reflection of the effects of typical, ambient PM exposure in humans, as a single bolus dose is not representative of continuous, low level exposure. Therefore, repeat-dose studies at lower concentrations may yield different pathological responses in terms of adaptive change of the pulmonary epithelium (e.g. fibrosis). The rapid nature of the response to the metals is suggestive of an oxidation-based toxicology, as was the observed 'bronchiolisation', which is rare in most pulmonary responses but a characteristic observed in response following exposure to ozone.

Toxicogenomic studies provided a more detailed account of the possible causes to the toxicological responses seen *in vivo*. The findings were indicative of oxidative processes since genes related to the antioxidant glutathione were being altered. The results also suggested that this response was not confined to the lung but also occurred in the heart in which genes related to the metabolism of xenobiotics were also altered. These data infer that bioavailable metals can exert effects not only at the site of instillation but also systemically. This agrees with current hypotheses that the water-soluble fraction of PM is related to adverse health effects systemically (particularly cardiovascular effects). The implications for these observations could be that PM

exposure might be a causative factor in many more diverse health effects than is currently linked.

The work carried out in this research programme supports the premise that there are possible links with PM bioreactivity and metal concentration and re-enforces the point that due to the heterogeneity of PM there could be a variety of mechanisms causing the bioreactivity. However, the evidence does highlight soluble Zn as being a potential key to elucidating the precise mechanisms of PM-induced bioreactivity. From ICP-MS analysis soluble Zn was found at extremely high concentrations when compared with other metals. *In vitro* it caused no damage on its own but it did have remarkable synergistic properties with other metals. *In vivo* Zn²⁺ alone seemed to exert greater general morbidity on the animals than when in a mixture with other metal ions. Herein lies a problem from an environmental perspective. It seems apparent that by reducing the levels of Zn, this could improve air quality by limiting the bioreactivity of PM. However the observed synergies that Zn²⁺ has with other metals dismisses that environmental action. Moreover from the *in vitro* studies even tiny amounts of Zn²⁺ can significantly enhance the bioreactivity of other metals, which may also occur *in vivo*. Synergistic effects were not conclusive from the *in vivo* study, as Zn²⁺ was present at such a high concentration. Better understanding of the complex interactions between Zn²⁺, other metals and endogenous pulmonary constituents is vital in elucidating the activity/loss of these synergies *in vivo*.

Zinc is often referred to as the ubiquitous trace element but it would appear that its roles extend further than its well characterised biological uses. To briefly recap, Zn is essential to many biosystems such as its involvement in gene expression, including playing a role in the activity of transcription factors and DNA repair (Falchuk, 1998). Metallothionein responses to inflammatory mediators have been found to be conditional upon the presence of Zn and when complexed within metallothioneins, Zn contributes to protection against cytokine-mediated oxidative stress. Zn is also essential for maintaining the stability of insulin storage systems (Dodson and Steiner, 1998). Zn deficiency has been linked to the depressed responses of primary and secondary antibodies (Dardenne, 2002) as well as being a major intracellular regulator of lymphocyte apoptosis. With regard to enzymes, Zn has three types of role: catalytic (e.g. carbonic anhydrase), co-catalytic (e.g. Fe/Zn dependant alcohol dehydrogenase)

and structural (e.g. aspartate transcarbamylase). Over 300 enzymes are known to be dependent on Zn. Although Zn has so many uses it needs to be tightly regulated as it can also cause various types of toxicity on which much research has been carried out (as previously discussed). Research has been conflicting in judging the potency of Zn - for an element which exists in only one oxidation state its activity is far more complex than is intuitive. This investigation has highlighted the potentiation of activity by Zn in redox reactions, even though it is not redox active itself. Thus adding another novel aspect to the toxicological profile of Zn reinforces the scientific need for full investigations of xenobiotics, both in isolation and combination, in order to achieve a comprehensive mechanistic understanding.

REFERENCES

References

Aardema MJ, MacGregor JT. (2002) "Toxicology and genetic toxicology in the new era of "toxicogenomics": impact of "-omics" technologies" *Mutation Research* **499(1):13-25**

ACGIH (American Conference of Governmental Industrial Hygienists) (1986) "Copper" In: *Documentation of the Threshold Limit Values and Biological Exposure Indices*" 5th ed. ACGIH, Cincinnati, Ohio, USA.

Ackermann-Liebrich U, Rapp R. (1999). "Epidemiological effects of oxides of nitrogen, especially NO₂". In: *Air Pollution and Health* Holgate S, Samet J, Koren H, Maynard R. (Editors). New York, Academic Press, 561–584

Adamson IYR, Preiditis H, Hedgecock C, Vincent R. (2000) "Zinc is the toxic factor in the lung response to an atmospheric particulate sample" *Toxicology and Applied Pharmacology* **166:111-119**

Adamson IYR, Preiditis H, Vincent R (1999) "Pulmonary toxicity of an atmospheric particulate sample is due to the soluble fraction" *Toxicology and Applied Pharmacology* **157:43-50**

Afshari CA. (2002) "Perspective: microarray technology, seeing more than spots" *Endocrinology* **143(6):1983-1989**

Ali, M. (2004) Available: [www.doctorslisted.com/ images/lungs.jpg](http://www.doctorslisted.com/images/lungs.jpg)

Alizadeh AA, Eisen MB, Davis RE, Ma C, Lossos IS, Rosenwald A, Boldrick JC, Sabet H, Tran T, Yu X, Powell JI, Yang L, Marti GE, Moore T, Hudson J, Lu L, Lewis DB, Tibshirani R, Sherlock G, Chan WC, Greiner TC, Weisenburger DD, Armitage JO, Warnke R, Levy R, Wilson W, Grever MR, Byrd JC, Botstein D, Brown PO, Staudt LM. (2000) "Distinct types of diffuse large B-cell lymphoma identified by geneexpression profiling" *Nature* **403:503-11**

Amdur MO, McCarthy JF, Gill MW. (1982) "Respiratory response of guinea pigs to zinc oxide fume" *American Industrial Hygiene Association Journal* **43(12)**:887-889

Anbar M, Neta P. (1967) "A compilation of specific bimolecular rate constants for the reactions of hydrated electrons, hydrogen atoms and hydroxyl radicals with inorganic and organic compounds in aqueous solution" *International Journal of Applied Radiation and Isotopes* **18**:493-523

Anderson HR, Limb ES, Bland JM, Ponce de Leon A, Strachan DP, Bower JS. (2001) "Health effects of an air pollution episode in London, December 1991" *Thorax* **50**:1188-1193

Antonini JM, Taylor MD, Zimmer AT, Roberts JR. (2004) "Pulmonary responses to welding fumes: role of metal constituents" *Journal of Toxicology and Environmental Health* **67(3)**:233-49

Atchison WD. (2003) "Effects of toxic environmental contaminants on voltage-gated calcium channel function: from past to present" *Journal of Bioenergetics and Biomembranes*. **35(6)**:507-532

Aust AE, Eveleigh JF. (1999) "Mechanisms of DNA oxidation" *Proceedings of the Society for Experimental Biology and Medicine* **222(3)**:246-252

Babior BM. (1978a) "Oxygen-dependent microbial killing by phagocytes (first of two parts)" *New England Journal of Medicine* **298(12)**:659-668

Babior BM. (1978b) "Oxygen-dependent microbial killing by phagocytes (second of two parts)" *New England Journal of Medicine* **298(13)**:721-725

Bal W, Kasprzak KS. (2002) "Induction of oxidative DNA damage by carcinogenic metals" *Toxicology Letters* **127(1-3)**:55-62

Balharry DC, Oreffo, VIC, Richards RJ. (2005) "Use of toxicogenomics for identifying genetic markers of pulmonary oedema. *Toxicology and Applied Pharmacology* **204**:101-108

Barbouti A, Doulias P-T, Zhu B-Z, Frei B, Galaris D. (2001) "Intracellular iron, but not copper, plays a critical role in hydrogen peroxide-induced DNA damage" *Free Radical Biology and Medicine* **31(4)**:490-498

Barceloux DG. (1999a) "Copper" *J Toxicol Clin Toxicol.* **37(2)**:217-230

Barceloux DG. (1999b) "Vanadium" *J Toxicol Clin Toxicol.* **37(2)**:265-278
(Erratum in: *J Toxicol Clin Toxicol* (2000) **38(7)**:813)

Barceloux DG. (1999c) "Zinc" *J Toxicol Clin Toxicol.* **37(2)**:279-292

Becker BF. (1993) "Towards the physiological function of uric acid" *Free Radical Biology and Medicine* **14**:615-631

Becker S, Soukup JM, Gilmour MI, Devlin RB. (1996) "Stimulation of human and rat alveolar macrophages by urban air particulates: effects on oxidant radical generation and cytokine production" *Toxicol Appl Pharmacol.* **141(2)**:637-648

Beeson WL, Abbey DE, Knutsen SF (1998) "Long-term concentrations of ambient air pollutants and incident lung cancer in California adults: results from the AHSMOG study (Adventist Health Study on Smog)" *Environmental Health Perspectives* **106(12)**:813-823

Bell ML, Davis DL, Fletcher T. (2004) "A retrospective assessment of mortality from the London smog episode of 1952: The role of influenza and pollution" *Environmental Health Perspectives* **112(11)**:6-8

Berg I, Schluter T, Gercken G. (1993) "Increase of bovine alveolar macrophage superoxide anion and hydrogen peroxide release by dusts of different origin" *J Toxicology and Environmental Health* **39(3)**:341-354

Berger M, Keller H. (1983). "Why I cough, sneeze, shiver, hiccup, & yawn" New York, Crowell.

Berube KA, Jones TP, Moreno T, Sexton K, Balharry D, Hicks M, Merolla L, Mossman BT. (2006) "Characterisation of airborne particulate matter and related mechanisms of toxicity." In: *Air Pollution Reviews*, Vol. 3. Ayres J, Maynard R, Richards R (Editors). Imperial College Press, London, *in press*.

Berube KA, Jones T P and Williamson B J - Physicochemical characterisation of urban airborne particulate matter, Proceedings of the Royal Microscopy Society 33 (1998) A101, ISSN 0035 9017

Berube KA, Murphy SA, Richards RJ. (1998) "Effects of carbon black physicochemistry on primary isolates of lung epithelial cells" *European Respiratory Journal* **12**:A335

Bielski BH. (1985) "Fast kinetic studies of dioxygen-derived species and their metal complexes" *Philosophical Transactions of the Royal Society of London Series B: Biological Sciences* **311(1152)**:473-482

Bittner S, Gorohovsky S, Lozinsky E, Shames AI. (2000) "EPR study of anion radicals of various N-quinonyl amino acids" *Amino Acids*. **19(2)**:439-449

Bodner C, Godden D, Brown K, Little J, Ross S, Seaton A (1999) "Antioxidant intake and adult-onset wheeze: a case-control study" *European Respiratory Journal* **13**:22-30

Box HC, Dawidzik JB, Budzinski EE. (2001) "Free radical-induced double lesions in DNA" *Free Radical Biology and Medicine* **31(7)**:856-868

Bradford MM. (1976) "A rapid and sensitive method for the quantitation of microgram quantities of protein utilising the principle of protein-dye binding" *Analytical Biochemistry* **72**:248-254

Braga AL, Zanobetti A, Schwartz J. (2000) "Do respiratory epidemics confound the association between air pollution and daily deaths?" *European Respiratory Journal* **16(4)**:723-728

Braga AL, Zanobetti A, Schwartz J. (2001) "The lag structure between particulate air pollution and respiratory and cardiovascular deaths in 10 US cities" *Journal of Occupational and Environmental Medicine* **43(11)**:927-933

Brain JD, Valberg PA. (1979) "Deposition of aerosol in the respiratory tract" *American Review of Respiratory Disease* **120(6)**:1325-73

Bremner SA, Anderson HR, Atkinson RW, McMichael AJ, Strachan DP, Bland JM, Bower JS (1999) "Short term associations between outdoor air pollution and mortality in London 1992-1994" *Occupational and Environmental Medicine* **56**:237-244

Brimblecombe P. (1977) "London Air Pollution, 1500-1900" *Atmospheric Environment* **11**:1159-162

Brimblecombe P. (1978) "Interest in air pollution among early Fellows of the Royal Society" *Notes Recorded from the Royal Society of London*. **32(2)**:123-129

Brunekreef B, Forsberg B. (2005) "Epidemiological evidence of effects of coarse airborne particles on health" *European Respiratory Journal* **26(2)**:309-18

Brunekreef B, Holgate ST. (2002) "Air pollution and health" *The Lancet* **360(9341)**:1233-1242

Bryson C (1998) "The Donora Fluoride Fog: A Secret History of America's Worst Air Pollution Disaster" *Earth Island Journal*. Spring 36-37

Budavari, S (Editor). (1989) "Merck Index—An Encyclopedia of Chemicals, Drugs and Biologicals" Merck & Co. Inc. Rahway, NJ, USA. 266

Cai, F. S., and Yu, C. P. (1988). Inertial and interceptional deposition of spherical particles and fibers in bifurcating airways. *J. Aerosol Sci.* 19, 679–688

Campbell MJ, Tobias A. (2000) “Causality and temporality in the study of short-term health effects of air pollution on health” *International Journal of Epidemiology* **29**:271-273

Cantin AM, North SL, Hubbard RC, Crystal RG. (1987) “Normal alveolar epithelial lining fluid contains high levels of glutathione” *Journal of Applied Physiology* **63(1)**:152-157

Cantin AM, Hubbard RC, Crystal RG. (1989) “Glutathione deficiency in the epithelial lining fluid of the lower respiratory tract in idiopathic pulmonary fibrosis” *American Review of Respiratory Disease* **139(2)**:370-2

Chan PC, Peller OG, Kesner L. (1982) “Copper(II)-catalyzed lipid peroxidation in liposomes and erythrocyte membranes” *Lipids* **17(5)**:331-337

Chance B, Sies H, Boveris A. (1979) “Hydroperoxide metabolism in mammalian organs” *Physiology Review* **59**:527-605

Chen YK, Yu CP. (1993) “Particle deposition from duct flows by combined mechanism” *Aerosol Science and Technology* **19**: 389–395

Cho AK, Sioutas C, Miguel AH, Kumagai Y, Schmitz DA, Singh M, Eiguen-Fernandez A, Froines JR. (2005) “Redox activity of airborne particulate matter at different sites in the Los Angeles Basin” *Environmental Research.* **99(1)**:40-7

Cohen AJ, Ross Anderson H, Ostro B, Pandey KD, Krzyzanowski M, Kunzli N, Gutschmidt K, Pope A, Romieu I, Samet JM, Smith K. (2005) “The global burden of disease due to outdoor air pollution” *Journal of Toxicology and Environmental Health* **68(13-14)**:1301-7

Comhair SA, Erzurum SC. (2002) "Antioxidant responses to oxidant-mediated lung diseases" *American Journal of Physiology: Lung Cell and Molecular Physiology* **283(2)**:L246-255

Cooper WC, Wong O, Kheifets L. (1985) "Mortality among employees of lead battery plants and lead-producing plants, 1947 – 1980" *Scandinavian Journal of Work and Environmental Health* **11**:331-345.

Cortizo AM, Bruzzone L, Molinuevo S, Etcheverry SB. (2000) "A possible role of oxidative stress in the vanadium-induced cytotoxicity in the MC3T3E1 osteoblast and UMR106 osteosarcoma cell lines" *Toxicology* **147(2)**:89-99

Costa DL, Dreher KL. (1997) "Bioavailable transition metals in particulate matter mediate cardiopulmonary injury in healthy and compromised animal models" *Environmental Health Perspectives* **105(5)**:1053-1060

Cross CE, van der Vliet A, O'Neill CA, Louie S, Halliwell B. (1994) "Oxidants, antioxidants and respiratory tract lining fluids" *Environmental Health Perspectives* **102(S11)**:185-191

Cummings MC, Winterford CM, Walker NI. (1997) "Apoptosis" *American Journal of Surgical Pathology* **21**:88-101

Dardenne M. (2002) "Zinc and immune function" *European Journal of Clinical Nutrition* **56 Suppl 3**:S20-3

Davies KJA. (1987) "Protein damage and degradation by oxygen radicals I. General aspect" *Journal of Biological Chemistry* **262**:9895–9901

Davies MJ (2005) "The oxidative environment and protein damage" *Biochimica et Biophysica Acta - Proteins & Proteomics* **1703(2)**:93-109

Davies NF, Oreffo VIC, Richards RJ. (1988) "The toxic effects of metal ions on rat alveolar epithelial type II cells in primary culture" *Chimicaoggi* **5**:11-16

Denke SM. (2000) "Thiol-based antioxidants" *Current Topics in Cellular Regulation* **36**:151–180

Diaz-Sanchez D. (1997) "The role of diesel exhaust particles and their associated polyaromatic hydrocarbons in the induction of allergic airway disease" *Allergy* **52(S38)**:52-56

Dizdaroglu M, Jaruga P, Birincioglu M, Rodriguez H. (2002) "Free radical-induced damage to DNA: mechanisms and measurement" *Free Radical Biology and Medicine* **32(11)**:1102-1115

Dobbs LG, Wright JR, Hawgood S, Gonzalez R, Venstrom K, Nellenbogen J. (1987) "Pulmonary surfactant and its components inhibit secretion of phosphatidylcholine from cultured rat alveolar type II cells" *Proceedings of the National Academy of Science U.S.A.* **84(4)**:1010-1014

Dockery DW. (2001). "Epidemiologic evidence of cardiovascular effects of particulate air pollution" *Environmental Health Perspectives* **109(4)**:483-486

Dockery DW, Pope CA. (1994) "Acute respiratory effects of particulate air pollution" *Annual Review of Public Health* **15**:107-132

Dodson GG, Steiner D. (1998) "The role of assembly in insulin's biosynthesis" *Current Opinion in Structural Biology* **8**:189-194

Dominici F, McDermott A, Daniels M, Zeger SL, Samet JM. (2005) "Revised analyses of the National Morbidity, Mortality, and Air Pollution Study: mortality among residents of 90 cities" *Journal of Toxicology and Environmental Health* **68(13-14)**:1071-92

Donaldson K. (2003) "The biological effects of coarse and fine particulate matter" *Occupational and Environmental Medicine* **60**:313-314

Donaldson K, Brown DM, Mitchell C, Dineva M, Beswick PH, Gilmour P, MacNee W. (1997) "Free radical activity of PM₁₀: iron mediated generation of hydroxyl radicals" *Environmental Health Perspectives* **105(5)**:1285-1289

Donaldson K, Gilmour IM, MacNee W. (2000) "Asthma and PM₁₀" *Respiratory Research* **1**:12-15

Donaldson K, Stone V, Seaton A, MacNee W. (2001) "Ambient particle inhalation and the cardiovascular system: potential mechanisms" *Environmental Health Perspectives* **109(4)**:523-527

Dreher K, Jaskot R, Kodavanti U, Lehmann J, Winsett D, Costa D. (1996) "Soluble transition metals mediate the acute pulmonary injury and airway hyperreactivity induced by residual oil fly ash particles" *Chest* **109**:33-34

Dreher KL, Jaskot RH, Lehmann JR, Richards JH, McGee JK, Ghio AJ, Costa DL. (1997) "Soluble transition metals mediate residual oil fly ash induced acute lung injury" *Journal of Toxicology and Environmental Health* **50**:285-305

Driscoll KE, Costa DL, Hatch G, Henderson R, Oberdorster G. (2000) "Intratracheal instillation as an exposure technique for the evaluation of respiratory tract toxicity: uses and limitations" *Toxicological Sciences* **55**:24-35

Dye JA, Lehmann JR, McGee JK, Winsett DW, Ledbetter AD, Everitt JI, Ghio AJ, Costa DL (2001) "Acute pulmonary toxicity of particulate matter filter extracts in rats: coherence with epidemiologic studies in Utah valley residents" *Environmental Health Perspectives* **109(3)**:395-403

Evans P, Halliwell B. (2001) "Micronutrients: oxidant/antioxidant status" *British Journal of Nutrition* **85 Suppl 2**:S67-74

Falchuk KH. (1998) "The molecular basis for the role of zinc in developmental biology" *Molecular and Cellular Biochemistry* **188**:41-48

Ferguson-Miller S, Babcock GT. (1996) "Heme/Copper Terminal Oxidases" *Chemical Review* **96(7)**:2889-2908.

Fialkow L, Chan CK, Rotin D, Grinstein S, Downey GP. (1994) "Activation of the mitogen-activated protein kinase signaling pathway in neutrophils. Role of oxidants" *Journal of Biological Chemistry* **269(49)**:31234-31242

Finkel T. (1998) "Oxygen radicals and signalling" *Current Opinions in Cell Biology* **10(2)**:248-53

Finkel T. (1999). "Signal transduction by reactive oxygen species in non-phagocytic cells" *Leukocyte Biology* **65(3)**:337-40

Finkel T. (2000) "Redox-dependent signal transduction" *FEBS Letters* **476(1-2)**:52-4

Fiorentino DF, Zlotnik A, Mosmann TR, Howard M, O'Garra A. (1991) "IL-10 inhibits cytokine production by activated macrophages" *Journal of Immunology* **147(11)**:3815-3822

Firket J. (1936) "Fog along the Meuse valley" *Transactions of the Faraday Society* **32**:1192-1197

Floyd RA, Watson JJ, Wong PK, Altmiller DH, Rickard RC. (1986) "Hydroxyl free radical adduct of deoxyguanosine: sensitive detection and mechanisms of formation" *Free Radical Research Communications* **1(3)**:163-172

Frampton MW, Ghio AJ, Samet JM, Carson JL, Carter JD, Devlin RB. (1999) "Effects of aqueous extracts of PM₁₀ filters from the Utah Valley on human airway epithelial cells" *Lung Cellular and Molecular Physiology* **21**:L960-L967

Freeman BA, Crapo JD. (1981) "Hyperoxia increases oxygen radical production in rat lungs and lung mitochondria" *Journal of Biological Chemistry* **256(21)**:10986-10992

Gadek JE. (1992) "Adverse effects of neutrophils on the lung" *American Journal of Medicine* **92(6A):27S-31S**.

Gerhardsson L, Brune D, Nordberg GF, Wester PO. (1988) "Multielemental assay of tissues of deceased smelter workers and controls" *Science of the Total Environment* **74:97-110**

Ghio AJ, Stonehuerner J, Dailey LA, Carter JD. (1999) "Metals associated with both the water-soluble and insoluble fractions of an ambient air pollution particle catalyze an oxidative stress" *Inhalation Toxicology* **11(1):37-49**

Ghio AJ, Devlin RB. (2001) "Inflammatory lung injury after bronchial instillation of air pollution particles" *American Journal of Respiratory Critical Care Medicine* **164(4):704-708**

Ghio AJ, Silbajoris R, Carson JL, Samet JM. (2002) "Biologic effects of oil fly ash" *Environmental Health Perspectives* **110(1):89-94**

Ghio AJ, Kim C, Devlin RB (2000) "Concentrated ambient air particles induce mild pulmonary inflammation in healthy human volunteers." *American Journal of Respiratory Critical Care Medicine* **162(3):981-988**

Ghio AJ. (2004) "Biological effects of Utah Valley ambient air particles in humans: a review" *Journal of Aerosol Medicine* **17(2):157-64**

Gibbs A. (1996) "Occupational Lung Disease" In: *Spencer's Pathology of the Lung* Hasleton P. (Editor) McGraw-Hill, New York, USA.

Giles GI, Tasker KM, Jacob C. (2001) "Hypothesis: the role of reactive sulphur species in oxidative stress" *Free Radical Biology and Medicine* **31(10):1279-1283**

Gilmour PS, Brown DM, Lindsay TG, Beswick PH, MacNee W, Donaldson K. (1996) "Adverse health effects of PM₁₀ particles: involvement of iron in generation of hydroxyl radical" *Occupational and Environmental Medicine* **53:817-822**

Gladstone IM Jr, Levine RL. (1994) "Oxidation of proteins in neonatal lungs" *Pediatrics* **93(5)**:764-768.

Glantz SA. (2002) "Air pollution as a cause of heart disease. Time for action" *Journal of the American College of Cardiology* **39(6)**:943-945

Goldsmith CA, Imrich A, Danaee H, Ning YY, Kobzik L. (1998) "Analysis of air pollution particulate-mediated oxidant stress in alveolar macrophages" *Journal of Toxicology and Environmental Health* **54(7)**:529-545

Gong H, Linn WS, Terrell SL, Anderson KR, Clark KW, Sioutas C, Cascio WE, Alexis N, Devlin RB. (2004) "Exposures of elderly volunteers with and without chronic obstructive pulmonary disease (COPD) to concentrated ambient fine particulate pollution" *Inhalation Toxicology* **16(11-12)**:731-44

Greenwell LL, Moreno MT, Jones TP, Richards RJ. (2002) "Particle-induced oxidative damage is ameliorated by low-molecular weight antioxidants" *Free Radical Biology and Medicine* **32(9)**:898-905

Greenwell LL, Moreno MT, Richards RJ. (2003) "Pulmonary antioxidants exert differential protective effects against urban and industrial particulate matter" *Journal of Biosciences* **28(1)**:101-107

Greife AL, Warshawsky D. (1993) "Influence of the dose levels of cocarcinogen ferric oxide on the metabolism of benzo[a]pyrene by pulmonary alveolar macrophages in suspension culture" *Journal of Toxicology and Environmental Health* **38(4)**:399-417

Grimminger F, Menger M, Becker G, Seeger W. (1988) "Potentiation of leukotriene production following sequestration of neutrophils in isolated lungs: indirect evidence for intercellular leukotriene A4 transfer" *Blood* **72(5)**:1687-1692

Grisham MB, Ware K, Gilleland HE Jr, Gilleland LB, Abell CL, Yamada T. (1992) "Neutrophil-mediated nitrosamine formation: role of nitric oxide in rats" *Gastroenterology* **103(4)**:1260-6.

Grune T, Reinheckel T, Davies KJ. (1997) "Degradation of oxidized proteins in mammalian cells" *FASEB Journal* **11(7)**:526-534

Guidotti TL, Audette RJ, Martin CJ. (1997) "Interpretation of the trace metal analysis profile for patients occupationally exposed to metals" *Occupational Medicine (London)* **47(8)**:497-503

Haldane JS & Priestley JC (1935). "Respiration" *Yale University Press*, New Haven, USA

Haldane J (1931) "Atmospheric pollution and fogs" *British Medical Journal* 366-7

Halliwell B, Gutteridge JMC (1989) "The chemistry of oxygen radicals and other oxygen-derived species". *Free Radicals in Biology and Medicine*. Oxford, Clarendon Press. 30-45

Halliwell B, Gutteridge JM, Cross CE. (1992) "Free radicals, antioxidants, and human disease: where are we now?" *Journal of Laboratory Clinical Medicine* **119(6)**:598-620

Halliwell B (1988) "Albumin - an Important Extracellular Antioxidant?" *Biochemical Pharmacology* **37**:569-571

Harris ME, Carney JM, Cole PS, Hensley K, Howard BJ, Martin L, Bummer P, Wang Y, Pedigo NW Jr, Butterfield DA. (1995) " β -amyloid peptide-derived, oxygen-dependent free radicals inhibit glutamate uptake in cultured astrocytes: implications for Alzheimer's disease" *Neuroreport* **6(14)**:1875-9.

Harrison P and Jones TP (1995) "Chemical composition of airborne particles in the UK atmosphere" *Science of the Total Environment* **168**:231-234

Hauser R, Elreedy S, Hoppin JA, Christiani DC. (1995) "Airway obstruction in boilermakers exposed to fuel oil ash. A prospective investigation" *American Journal of Respiratory and Critical Care Medicine* **152(5 Pt 1):1478-84**

Heffner JE, Repine JE. (1990) "Pulmonary strategies of antioxidant defense" *American Review of Respiratory Disease* **140:431-554**

Heinrich J, Hoelscher B, Wichmann HE. (2000) "Decline of ambient air pollution and respiratory symptoms in children" *American Journal of Respiratory and Critical Care Medicine* **161(6):1930-1936**

Helbock HJ, Beckman KB, Ames BN. (1999) "8-Hydroxydeoxyguanosine and 8-hydroxyguanine as biomarkers of oxidative DNA damage" *Methods in Enzymology* **300:156-166**

Helfand WH, Lazarus J, Theerman P. (2001) "Donora, Pennsylvania: an environmental disaster of the 20th century" *American Journal of Public Health* **91(4):553**

Henry C. (2002) "Genomics and the chemical industry" Presentation to the NRC Committee on Emerging Issues and Data on Environmental Contaminants. Available: <http://dels.nas.edu/emergingissues/docs/Henry.pdf>

Herwig R, Aanstad P, Clark M, Lehrach H. (2001) "Statistical evaluation of differential expression on cDNA nylon arrays with replicated experiments" *Nucleic Acids Research* **29(23):117-125**

Holgate ST, Finnerty JP. (1988) "Recent advances in understanding the pathogenesis of asthma and its clinical implications" *Quarterly Journal of Medicine* **66(249):5-19**

Huang YC, Ghio AJ, Stonehuerner J, McGee J, Carter JD, Grambow SC, Devlin RB. (2003) "The role of soluble components in ambient fine particles-induced changes in human lungs and blood" *Inhalation Toxicology* **15(4):327-342**

Ingham, D. B. (1975). Diffusion of aerosols from a stream flowing through a cylindrical tube. *J. Aerosol Sci.* 6, 125–132.

Jarabek AM, Menache MG, Overton JH Jr, Dourson ML, Miller FJ. (1989) “Inhalation reference dose (RfDi): an application of interspecies dosimetry modeling for risk assessment of insoluble particles” *Health Physics* **57 Suppl 1**:177-183

Jiang N, Dreher KL, Dye JA, Li Y, Richards JH, Martin LD, Adler KB. (2000) “Residual oil fly ash induces cytotoxicity and mucin secretion by guinea pig tracheal epithelial cells via an oxidant-mediated mechanism” *Toxicology and Applied Pharmacology* **163(3)**:221-230

Johansson A, Camner P. (1986) “Adverse effects of metals on the alveolar part of the lung” *Scanning Electron Microscopy* **2**:631-637

Johnson PR, Graham JJ. (2005) “Fine particulate matter national ambient air quality standards: public health impact on populations in the northeastern United States” *Environmental Health Perspectives* **113(9)**:1140-7

Kadiiska MB, Mason RP, Dreher KL, Costa DL, Ghio AJ. (1997) “*In vivo* evidence of free radical exposure formation in the rat lung after exposure to an emission source air pollution particle” *Chemical Research of Toxicology* **10 (10)**:1104-1108

Kanner J, German JB, Kinsella JE. (1987) “Initiation of lipid peroxidation in biological systems” *CRC Critical Reviews in Food Science and Nutrition* **25**:317-364

Kasprzak KS. (2002) “Oxidative DNA and protein damage in metal-induced toxicity and carcinogenesis” *Free Radical Biology and Medicine* **32(10)**:958-967

Keane MP, Strieter RM. (2002) “The importance of balanced pro-inflammatory and anti-inflammatory mechanisms in diffuse lung disease” *Respiratory Research* **3(1)**:5

Kelly FJ, Richards RJ. (1999) "Antioxidant defences in the extracellular compartment of the human lung". *Air Pollution and Health*. Holgate ST, Samet JM, Koren HS and Maynard RL. London, UK, Academic Press. 341-355

Klaunig JE, Xu Y, Isenberg JS, Bachowski S, Kolaja KL, Jiang J, Stevenson DE, Walborg EF Jr. (1998) "The role of oxidative stress in chemical carcinogenesis" *Environmental Health Perspectives* **106 Suppl 1**:289-295

Knaapen AM, Seiler F, Schilderman PA, Nehls P, Bruch J, Schins RP, Borm PJ. (1999) "Neutrophils cause oxidative DNA damage in alveolar epithelial cells" *Free Radical Biology and Medicine* **27(1-2)**:234-40

Knaapen AM, Shi T, Borm PJ, Schins RP. (2002) "Soluble metals as well as the insoluble particle fraction are involved in cellular DNA damage induced by particulate matter" *Molecular and Cellular Biochemistry* **234-235(1-2)**:317-26

Kodavanti UP, Hauser R, Christiani DC, Meng ZH, McGee J, Ledbetter A, Richards J, Costa DL. (1998) "Pulmonary responses to oil fly ash particles in the rat differ by virtue of their specific soluble metals" *Toxicological Sciences* **43(2)**:204-212

Kodavanti UP, Jaskot RH, Costa DL, Dreher KL. (1997b). "Pulmonary proinflammatory gene induction following acute exposure to residual oil fly ash: Roles of particle-associated metals" *Inhalation Toxicology* **9**:679-701

Kodavanti UP, Jaskot RH, Su WY, Costa DL, Ghio AJ, Dreher KL. (1997a) "Genetic variability in combustion particle-induced chronic lung injury" *American Journal of Physiology* **272**:L521-L532

Lagerkvist B, Linderholm H, Nordberg GF. (1986) "Vasospastic tendency and Raynaud's phenomenon in smelter workers exposed to arsenic" *Environmental Research* **39(2)**:465-474

Lam CF, Caterina P, Filion P, van Heerden PV, Ilett KF. (2002) "The ratio of polymorphonuclear leucocytes (PMN) to non-PMN cells: a novel method of assessing acute lung inflammation." *Experimental Toxicology and Pathology* **54(3)**:187-91

Lambert AL, Dong W, Selgrade MJK, Gilmour IM. (2000) "Enhanced allergic sensitization by residual oil fly ash particles in mediated by soluble metal constituents" *Toxicology and Applied Pharmacology* **165**:84-93

Li ASH, Bandy B, Tsang SS, Davison AJ. (2001) "DNA breakage induced by 1,2,4-benzenetriol: relative contributions of oxygen-derived active species and transition metal ions" *Free Radical Biology and Medicine* **30**:943-956

Li N, Sioutas C, Cho A, Schmitz D, Misra C, Sempf J, Wang M, Oberley T, Froines J, Nel A. (2003) Ultrafine particulate pollutants induce oxidative stress and mitochondrial damage. *Environmental Health Perspectives*. **111(4)**:455-60.

Liu Y, Woodin MA, Smith TJ, Herrick RF, Williams PL, Hauser R, Christiani DC. (2005) "Exposure to fuel-oil ash and welding emissions during the overhaul of an oil-fired boiler" *Journal of Occupational and Environmental Hygiene* **2(9)**:435-43

Lobenhofer EK, Bushel PR, Afshari CA, Hamadeh HK. (2001) "Progress in the application of DNA microarrays" *Environmental Health Perspectives* **109(9)**:881-891

Lohmann-Matthes ML, Steinmuller C, Franke-Ulmann G. (1994) "Pulmonary macrophages". *European Respiratory Journal* **7**:1678-1689

Long H, Shi T, Borm PJ, Maatta J, Husgafvel-Pursiainen K, Savolainen K, Krombach F. (2004) "ROS-mediated TNF-alpha and MIP-2 gene expression in alveolar macrophages exposed to pine dust." *Particle and Fibre Toxicology* **1(1)**:3

Lovchik JA, Lipscomb MF. (1993) "Role for C5 and neutrophils in the pulmonary intravascular clearance of circulating *Cryptococcus neoformans*" *American Journal Respiratory Cell Molecular Biology* **9(6)**:617-27.

Lund LG, Aust AE. (1990) "Iron mobilization from asbestos by chelators and ascorbic acid" *Archives of Biochemistry and Biophysics* **278(1)**:61-64

Maccarrone M, Rosato N, Agro AF. (1997) "Lipoxygenase products induce ultraweak light emission from human erythroleukemia cells" *Journal of Bioluminescence and Chemiluminescence* **12(6)**:285-293

Magari SR, Schwartz J, Williams PL, Hauser R, Smith TJ, Christiani DC. (2002) "The association of particulate air metal concentrations with heart rate variability" *Environmental Health Perspectives* **110(9)**:875-880

Mark L, Ingenito E. (1999) "Surfactant function and composition after free radical exposure generated by transition metals" *Lung Cellular and Molecular Physiology* **20**:L491-L500

Marx JJ, van Asbeck BS. (1996) "Use of iron chelators in preventing hydroxyl radical damage: adult respiratory distress syndrome as an experimental model for the pathophysiology and treatment of oxygen-radical-mediated tissue damage" *Acta Haematologica* **95(1)**:49-62.

Mason RJ, Dobbs LG, Greenleaf RD, Williams MC. (1977) "Alveolar type II cells" *Federal Proceedings* **36(13)**:2697-2702

Mazumder DN. (2001) "Clinical aspects of chronic arsenic toxicity" *Journal of the Association of Physicians in India* **49**:650-655

McCay PB. (1985) "Vitamin E: interactions with free radicals and ascorbate" *Annual Review of Nutrition* **5**:323-340

McDonald RJ, Usachenko J. (1999) "Neutrophils injure bronchial epithelium after ozone exposure" *Inflammation* **23(1)**:63-73

McDonnell WF, Nishino-Ishikawa N, Petersen FF, Chen LH, Abbey DE. (2000) "Relationships of mortality with the fine and coarse fractions of long-term ambient

PM₁₀ concentrations in nonsmokers” *Journal of Exposure Analysis and Environmental Epidemiology* **10(5)**:427-436

McKee M. (2002) Available: <http://www.mmi.mcgill.ca/mmimediiasampler2004>

McNeilly JD, Heal MR, Beverland IJ, Howe A, Gibson MD, Hibbs LR, MacNee W, Donaldson K. (2004) “Soluble transition metals cause the pro-inflammatory effects of welding fumes *in vitro*” *Toxicology and Applied Pharmacology* **196(1)**:95-107

Meduri GU, Kohler G, Headley S, Tolley E, Stentz F, Postlethwaite A. (1995) “Inflammatory cytokines in the BAL of patients with ARDS. Persistent elevation over time predicts poor outcome” *Chest* **108(5)**:1303-1314.

Melandri C, Prodi V, Tarroni G, Formignani M, De Zaiacomo T, Bompane CF, Maestri G, Giacomelli-Maltoni G. (1977) “Inhaled Particles IV” In: Walton WH (editor) *Proceedings of an International Symposium organized by BOHS Edinburgh, 22–26 September, 1975*. Pergamon Press, Oxford, UK. 193–200

Merolla L, Richards RJ. (2005) “In vitro effects of water-soluble metals present in UK particulate matter” *Experimental Lung Research* **31(7)**:671-83

Ministry of Health. (1954) “Mortality and morbidity during the London fog of December 1952” *Report on Public Health and Medical Subjects No 95*. Her Majesty’s Stationery Office, London, UK

Minotti G, Aust SD. (1992) “Redox cycling of iron and lipid peroxidation” *Lipids* **27(3)**:219-226

Molinelli AR, Madden MC, McGee JK, Stonehuerner JG, Ghio AJ. (2002) “Effect of metal removal on the toxicity of airborne particulate matter from the Utah Valley” *Inhalation Toxicology* **14(10)**:1069-1086

Monton C, Torres A. (1998) “Lung inflammatory response in pneumonia” *Monaldi Archives for Chest Disease*. **53(1)**:56-63

Moreno T, Jones TP, Richards RJ. (2004) "Characterisation of aerosol particulate matter from urban and industrial environments: examples from Cardiff and Port Talbot, South Wales, UK." *Science of the Total Environment* **334-335**:337-346

Moreno T, Merolla L, Gibbons W, Greenwell L, Jones T, Richards R. (2004) "Variations in the source, metal content and bioreactivity of technogenic aerosols: a case study from Port Talbot, Wales, UK" *Science of the Total Environment* **333(1-3)**:59-73

Morgan W and Seaton A (1975) "Occupational lung diseases" WB Saunders, Philadelphia, USA.

Morton WE, Caron GA. (1989) "Encephalopathy: an uncommon manifestation of workplace arsenic poisoning?" *American Journal of Industrial Medicine* **15**:1-5

Munoz X, Cruz MJ, Orriols R, Torres F, Espuga M, Morell F. (2004) "Validation of specific inhalation challenge for the diagnosis of occupational asthma due to persulphate salts" *Occupational Environmental Medicine* **61(10)**:861-6

Murphy ME, Kehrer JP. (1989) "Oxidative stress and muscular dystrophy" *Chemical and Biological Interactions* **69(2-3)**:101-173

Murphy S, BeruBe K, Pooley F, Richards R. (1998) "The response of lung epithelium to well characterised fine particles." *Life Science* **62(19)**:1789-1799

Nakai M, Watanabe H, Fujiwara C, Kakegawa H, Satoh T, Takada J, Matsushita R, Sakurai H. (1995) "Mechanism on insulin-like action of vanadyl sulfate: studies on interaction between rat adipocytes and vanadium compounds" *Biology and Pharmacy Bulletin* **18(5)**:719-725

Nemery B, Hoet PH, Nemmar A. (2001) "The Meuse Valley fog of 1930: an air pollution disaster" *The Lancet* **357(9257)**:704-708

Nicholson EM, Mo H, Prusiner SB, Cohen FE, Marqusee S. (2002) "Differences between the prion protein and its homolog Doppel: a partially structured stat with implications for scrapie formation" *Journal of Molecular Biology* **316**:807–815

Niki E, Yoshida Y, Saito Y, Noguchi N. (2005) "Lipid peroxidation: Mechanisms, inhibition, and biological effects" *Biochemistry and Biophysics Research Communications* (e-publication ahead of print)

O'Halloran TV and Culotta VC (2000) "Metallochaperones, an intracellular shuttle service for metal ions" *Journal of Biological Chemistry* **275**(3): 25057-25060

Okeson CD, Riley MR, Fernandez A, Wendt JO. (2003) "Impact of the composition of combustion generated fine particles on epithelial cell toxicity: influences of metals on metabolism" *Chemosphere* **51**(10):1121-8

Olden K. (2004) "Genomics in environmental health research--opportunities and challenges" *Toxicology* **198**(1-3):19-24

Olden K, Guthrie J. (2001) "Genomics: implications for toxicology" *Mutation Research* **473**(1):3-10

Pacht ER Davis WB. (1988) "Role of transferrin and ceruloplasmin in antioxidant activity of lung epithelial lining fluid" *Journal of Applied Physiology* **64**(5):2092-2099

Packer L, Slater TF, Willson RL. (1979) "Direct observations of a free radical interaction between vitamin E and vitamin C" *Nature* **278**:737-738

Paige RC, Wong V, Plopper CG. (2000) "Long-term exposure to ozone increases acute pulmonary centriacinar injury by 1-nitronaphthalene: II. Quantitative histopathology" *Journal of Pharmacological Experimental Therapeutics* **295**(3):942-950

Pandey A, Mann M. (2000) "Proteomics to study genes and genomes" *Nature* **405(6788):837-846.**

Park JH, Han KT, Eu KJ, Kim JS, Chung KH, Park B, Yang GS, Lee KH, Cho MH. (2005) "Diffusion flame-derived fine particulate matters doped with iron caused genotoxicity in B6C3F1 mice" *Toxicology and Industrial Health* **21(3-4):57-65**

Peden DB, Swiersz M, Ohkubo K, Hahn B, Emery B, Kaliner MA (1993) "Nasal secretion of the ozone scavenger uric acid" *American Review of Respiratory Disease* **148(2):455-461**

Pennie WD. (2000) "Use of cDNA microarrays to probe and understand the toxicological consequences of altered gene expression" *Toxicology Letters* **112-113:473-477**

Pennie WD, Kimber I. (2002) "Toxicogenomics; transcript profiling and potential application to chemical allergy" *Toxicology In Vitro* **16(3):319-326**

Pennie WD, Tugwood JD, Oliver GJ, Kimber I. (2000) "The principles and practice of toxigenomics: applications and opportunities" *Toxicological Science* **54(2):277-283**

Perou CM, Sorlie T, Eisen MB, van de Rijn M, Jeffrey SS, Rees CA, Pollack JR, Ross DT, Johnsen H, Akslen LA, Fluge O, Pergamenschikov A, Williams C, Zhu SX, Lonning PE, Borresen-Dale AL, Brown PO, Botstein D. (2000) "Molecular portraits of human breast tumours" *Nature* **406(6797):747-752**

Petris MJ, Strausak D, Mercer JFB (2000) "The Menkes copper transporter is required for the activation of tyrosinase" *Human Molecular genetics* **9(19): 2845-2851**

Pich, J. (1972) "Theories of gravitational deposition of particles from laminar flows in channel" *Journal of Aerosol Science* **3:351-361**

Polosa R. (2001) "The interaction between particulate air pollution and allergens in enhancing allergic and airway responses" *Current Allergy and Asthma Reports* **1(2)**:102-107

Pope CA 3rd. (1989) "Respiratory disease associated with community air pollution and a steel mill, Utah Valley" *American Journal of Public Health* **79(5)**:623-628

Pope CA 3rd. (1991) "Respiratory hospital admissions associated with PM₁₀ pollution in Utah, Salt Lake, and Cache Valleys." *Archives of Environmental Health* **46(2)**:90-97

Pope CA 3rd, Schwartz J, Ransom MR. (1992) "Daily mortality and PM₁₀ pollution in Utah Valley" *Archives of Environmental Health* **47(3)**:211-217

Pope CA 3rd, Dockery DW, Schwartz J (1995) "Review of epidemiological evidence of health effects of particulate air pollution" *Inhalation Toxicology* **7**:1-18

Pope CA 3rd, Burnett RT, Thurston GD, Thun MJ, Calle EE, Krewski D, Godleski JJ. (2004) "Cardiovascular mortality and long-term exposure to particulate air pollution: epidemiological evidence of general pathophysiological pathways of disease" *Circulation* **109(1)**:71-7

Powell SR. (2000) "The antioxidant properties of zinc" *Journal of Nutrition* **130(5S Suppl)**:1447S-54S

Prasad AS, Kucuk O (2002) "Zinc in cancer prevention" *Cancer Metastasis Review* **21(3-4)**:291-5

Prescott GJ, Cohen GR, Elton RA, Fowkes FGR, Agius RM. (1998) "Urban air pollution and cardiopulmonary ill health: a 14.5 year time series study" *Occupational and Environmental Medicine* **55**:697-704

Prieditis H, Adamson I. (2002) "Comparative pulmonary toxicity of various soluble metals found in urban particulate dusts" *Experimental Lung Research* **28(7)**:563-576

Pritchard RJ, Ghio AJ, Lehmann JR, Winsett DW, Tepper JS, Park P, Gilmour MI, Dreher KL, Costa DL. (1996) "Oxidant generation and lung injury after particulate air pollutant exposure increase with the concentrations of associated metals" *Inhalation Toxicology* **8**:457-477

Proctor NH, Highes JP, Fischman ML. (1988) "Chemical hazards at the workplace" (2nd ed.) JB Lippincott Co, Philadelphia, USA.

QUARG (Quality of the Urban Air Review Group) (1996) "Diesel vehicle emissions and urban air pollution" *Third report of the Quality of the Urban Air Review Group* Department of the Environment, London

Quinlan G, Evans T, Gutteridge J. (2002) "Iron and the redox status of the lung" *Free Radical Biology and Medicine* **33(10)**:1306-1313

Quinton PM (1979) "Composition and control of secretions from tracheal bronchial submucosal glands" *Nature* **279(5713)**:551-2

Ragosta M, Caggiano R, D'Emilio M, Macchiato M. (2002) "Source origin and parameters influencing levels of heavy metals in TSP, in an industrial background area of southern Italy" *Atmospheric Environment* **36**:3071–3087

Ramstoeck ER, Hoekstra WG, Ganther HE. (1980) "Phenobarbital-induced decomposition of triethyllead in the rat" *Chemical and Biological Interactions* **32(1-2)**:243-247

Requena JR, Groth D, Legname G, Stadtman ER, Prusiner SB, Levine RL. (2001) "Copper-catalyzed oxidation of the recombinant SHa(29-231) prion protein" *Proceedings of the National Academy of Science U.S.A.* **98(13)**:7170-7175

Reynolds LJ, Richards RJ. (2001) "Can toxicogenomics provide information on the bioreactivity of diesel exhaust particles?" *Toxicology* **165(2-3)**:145-152

Rice T, Clarke R, Godleski J, Al-Mutairi E, Jiang N-F, Hauser R, Paulauskis J. (2001) "Differential ability of transition metals to induce pulmonary inflammation" *Toxicology and Applied Pharmacology* **177**:46-53

Richards RJ. (1997) "Small particles, big problems" *Biologist* **44(1)**:249-251

Richards RJ, Atkins J, Marrs TC, Brown RFR, Masek LC. (1989) "The biochemical and pathological changes produced by the intratracheal instillation of certain components of zinc-hexachloroethane smoke" *Toxicology Letters* **54**:79-88

Riley MR, Boesewetter DE, Turner RA, Kim AM, Collier JM, Hamilton A. (2005) "Comparison of the sensitivity of three lung derived cell lines to metals from combustion derived particulate matter" *Toxicology In Vitro* **19(3)**:411-9

Roberts ES, Richards JH, Jaskot R, Dreher KL. (2003) "Oxidative stress mediates air pollution particle-induced acute lung injury and molecular pathology" *Inhalation Toxicology* **15(13)**:1327-46

Roberts E, Charboneau L, Espina V, Liotta L, Petricoin E, Dreher K. (2004) "Application of laser capture microdissection and protein microarray technologies in the molecular analysis of airway injury following pollution particle exposure" *Journal of Toxicology and Environmental Health* **67(11)**:851-61

Roholm K. (1937) "Fluorine intoxication" HK Lewis, London, UK

Ryan TP, Aust SD. (1992) "The role of iron in oxygen-mediated toxicities" *Critical Reviews in Toxicology* **22(2)**:119-141

Ryter SW Choi AM (2005) "Heme oxygenase-1: redox regulation of a stress protein in lung and cell culture models" *Antioxidant Redox Signalling* **7(1-2)**:80-91

Salin H, Vujasinovic T, Mazurie A, Maitrejean S, Menini C, Mallet J, Dumas S. (2002) "A novel sensitive microarray approach for differential screening using probes labelled with two different radioelements" *Nucleic Acids Research* **30(4)**:e17-23

Samet JM. (1994) "Learning about air pollution and asthma" *American Journal of Respiratory Critical Care Medicine* **149(6)**:1398-1399

Samet JM, Dominici F, Curriero FC, Coursac I, Zeger SL. (2000) "Fine Particulate Air Pollution and Mortality in 20 US Cities, 1987-1994." *New England Journal of Medicine* **343(24)**:1742-1749

Sandstrom T, Cassee FR, Salonen R, Dybing E (2005) "Recent outcomes in European multicentre projects on ambient particulate air pollution" *Toxicology and Applied Pharmacology* **207(2 Suppl)**:261-8

Sandstrom PA, Tebbey PW, Van Cleave S, Buttke TM. (1994) "Lipid hydroperoxides induce apoptosis in T cells displaying a HIV-associated glutathione peroxidase deficiency" *Journal of Biological Chemistry* **269(2)**:798-801

Sarangapani R, Wexler AS. (2000) "The role of dispersion in particle deposition in human airways" *Toxicological Sciences* **54**:229-236

Satir P, Sleight MA. (1990) "The physiology of cilia and mucociliary interactions" *Annual Review of Physiology* **52**:137-155

Schonwalder C, Olden K. (2003) "Environmental health moves into the 21st century" *International Journal of Hygiene and Environmental Health*. **206(4-5)**:263-7

Schwartz J. (1994) "What are people dying of on high air pollution days?" *Environmental Research* **64**:26-35

Schwartz J, Neas LM (2000) "Fine particles are more strongly associated than coarse particles with acute respiratory health effects in schoolchildren" *Epidemiology* **11(1)**:6-10

Seaton A, Soutar A, Crawford V, Elton R, McNerlan S, Cherrie J, Watt M, Agius R, Stout R. (1999) "Particulate air pollution and the blood" *Thorax* **54(11)**:1027-1032

Sharan, M. (1996) "A mathematical model for the dispersion of air pollutants in low wind conditions" *Atmospheric Environment* **30**:1209–1220

Shi JP, Knaapen AM, Begerow J, Birmili W, Borm PJA, Schins RPF. (2003) "Temporal variation of hydroxyl radical generation and 8-hydroxy-2'-deoxyguanosine formation by coarse and fine particulate matter" *Occupational and Environmental Medicine* **60(5)**:315-321

Shi X, Dalal NS. (1993) "Vanadate-mediated hydroxyl radical generation from superoxide radical in the presence of NADH: Haber-Weiss vs Fenton mechanism" *Archives of Biochemistry and Biophysics* **307(2)**:336-341

Shi X, Wang P, Jiang H, Mao Y, Ahmed N, Dalal N. (1996) "Vanadium(IV) causes 2'-deoxyguanosine hydroxylation and deoxyribonucleic acid damage via free radical reactions" *Annals of Clinical Laboratory Science* **26(1)**:39-49

Shima M, Nitta Y, Ando M, Adachi M (2002) "Effects of air pollution on the prevalence and incidence of asthma in children" *Archives of Environmental Health* **57(6)**:529-535

Simeonova PP, Luster MI. (1995) "Iron and reactive oxygen species in the asbestos-induced tumor necrosis factor-alpha response from alveolar macrophages" *American Journal of Respiratory Cell and Molecular Biology* **12(6)**:676-83

Sinclair AH, Tolsma D. (2004) "Associations and lags between air pollution and acute respiratory visits in an ambulatory care setting: 25-month results from the aerosol research and inhalation epidemiological study" *Journal of the Air and Waste Management Association* **54(9)**:1212-8

Snider GL, Hayes JA, Korthy AL. (1978) "Chronic interstitial pulmonary fibrosis produced in hamsters by endotracheal bleomycin: pathology and stereology" *American Review of Respiratory Disease* **117(6)**:1099-108

Snyder LP. (1994) "The death-dealing smog over Donora, Pennsylvania: industrial air pollution, public health and federal policy, 1915–1963" University of Pennsylvania, Philadelphia, PA.

Sorensen M, Schins RP, Hertel O, Loft S. 2005 Transition metals in personal samples of PM_{2.5} and oxidative stress in human volunteers. *Cancer Epidemiology Biomarkers Preview* **14(5)**:1340-3

Stadtman ER, Berlett BS. (1991) "Fenton chemistry: amino acid oxidation." *The Journal of Biological Chemistry* **266(26)**:17201-17211

Stadtman ER, Oliver CN. (1991) "Metal-catalysed oxidation of proteins. Physiological consequences" *The Journal of Biological Chemistry* **266(4)**:2005-2008

Staub NC (1993) "The Respiratory System" in *Physiology* (3rd edit) Berne RM, Levy MN (eds) Mosby Year Book, Missouri 545-611

Stemmler AJ, Burrows CJ. (2001) "Guanine versus deoxyribose damage in DNA oxidation mediated by vanadium(IV) and vanadium(V) complexes" *Journal of Biology and Inorganic Chemistry* **6(1)**:100-106.

Sun G, Crissman K, Norwood J, Richards J, Slade R, Hatch GE. (2001) "Oxidative interactions of synthetic lung epithelial lining fluid with metal-containing particulate matter" *American Journal of Physiology of the Lung and Cell and Molecular Physiology* **281**:L807-815

Suzuki K, Nakamura M, Hatanaka Y, Kayanoki Y, Tatsumi H, Taniguchi N. (1997) "Induction of apoptotic cell death in human endothelial cells treated with snake venom: implication of intracellular reactive oxygen species and protective effects of glutathione and superoxide dismutases." *Journal of Biochemistry* **122(6)**:1260-1264

Thomas RS, Rank DR, Penn SG, Zastrow GM, Hayes KR, Hu T, Pande K, Lewis M, Jovanovich SB, Bradfield CA. (2002) "Application of genomics to toxicology research" *Environmental Health Perspectives* **110 Suppl 6**:919-923

Thurston GD, Ito K. (2001) "Epidemiological studies of acute ozone exposures and mortality" *Journal of Exposure Analysis and Environmental Epidemiology* **11(4)**:286-294

Toyokuni S, Sagripanti JL. (1996) "Association between 8-hydroxy-2'-deoxyguanosine formation and DNA strand breaks mediated by copper and iron" *Free Radical Biology and Medicine* **20(6)**:859-864

Treadwell JA, Singh SM, (2004) "Microarray analysis of mouse brain gene expression following acute ethanol treatment" *Neurochemical Research* **29**:257-269

Triebig G, Weltle D, Valentin H. (1984) "Investigations on neurotoxicity of chemical substances at the workplace. V. Determination of the motor and sensory nerve conduction velocity in persons occupationally exposed to lead" *International Archives of Occupational Environmental Health* **53(3)**:189-203

U.S. AF (U.S. Air Force) (1990) "Copper" In: *The Installation Program Toxicology Guide* Vol. 5. Wright-Patterson Air Force Base, Ohio, USA. 77(1-43).

Vajanapoom N, Shy CM, Neas LM, Loomis D. (2002) "Associations of particulate matter and daily mortality in Bangkok, Thailand" *Southeast Asian Journal of Tropical Medicine and Public Health* **33(2)**:389-399

Vallejo M, Ruiz S, Hermosillo AG, Borja-Aburto VH, Cardenas M. (2005) "Ambient fine particles modify heart rate variability in young healthy adults" *Journal of Exposure Analysis and Environmental Epidemiology* (e-publication ahead of print)

van Eeden SF, Tan WC, Suwa T, Mukae H, Terashima T, Fujii T, Qui D, Vincent R, Hogg JC. (2001) "Cytokines involved in the systemic inflammatory response induced by exposure to particulate matter air pollutants PM₁₀" *American Journal of Respiratory Critical Care Medicine* **164(5):826-830**

Vanden Heuvel JP. (1999) "Peroxisome proliferator-activated receptors: a critical link among fatty acids, gene expression and carcinogenesis" *Journal of Nutrition* **129:575-580**

Vincent (1995) "Aerosol science for industrial hygienists" Pergamon Press, UK. 156-158

Vincent R, Bjarnason SG, Adamson IY, Hedgecock C, Kumarathasan P, Guenette J, Potvin M, Goegan P, Bouthillier L. (1997a) "Acute pulmonary toxicity of urban particulate matter and ozone" *American Journal of Pathology* **151(6):1563-1570**

Wang, C. S. (1975). Gravitational deposition of particles from laminar flows in inclined channels. *J. Aerosol Sci.* 6, 191–204.

Wanner A, Salathe M, O'Riordan TG. (1996) "Mucociliary clearance in the airways" *American Journal of Respiratory Critical Care Medicine* **154(6 Pt 1):1868-1902**

Waters M, Boorman G, Bushel P, Cunningham M, Irwin R, Merrick A, Olden K, Paules R, Selkirk J, Stasiewicz S, Weis B, Van Houten B, Walker N, Tennant R. (2003) "Systems toxicology and the chemical effects in biological systems (CEBS) knowledge base" *Environmental Health Perspectives - Toxicogenomics* **111:15–28**

Watkinson WP, Campen MJ, Costa DL. (1998) "Cardiac arrhythmia induction after exposure to residual oil fly ash particles in a rodent model of pulmonary hypertension" *Toxicological Science* **41(2):209-216**

Whittaker A, BeruBe K, Jones T, Maynard R, Richards R. (2004) "Killer smog of London, 50 years on: particle properties and oxidative capacity" *Science of the Total Environment* **334-335:435-445**

Whittaker AG. (2003) "Black smokes: past and present" *Thesis for PhD Candidacy, Cardiff University, Cardiff*

Wierling CK, Steinfath M, Elge T, Schulze-Kremer S, Aanstad P, Clark M, Lehrach H, Herwig R. (2002) "Simulation of DNA array hybridization experiments and evaluation of critical parameters during subsequent image and data analysis" *BMC Bioinformatics* **3**:29

Williams K. (1993) "Ifenprodil discriminates subtypes of the N-methyl-daspartate receptor: selectivity and mechanisms at recombinant heteromeric receptors" *Molecular Pharmacology* **44**:851– 859

Wilson MR, Lightbody JH, Donaldson K, Sales J, Stone V. (2002) "Interactions between ultrafine particles and transition metals" *Toxicology and Applied Pharmacology* **184**:172-179

Winkler BS. (1992) "Unequivocal evidence in support of the nonenzymatic redox coupling between glutathione/glutathione disulfide and ascorbic acid/dehydroascorbic acid" *Biochimica et Biophysica Acta* **1117**(3):287-290

Witschi, H, Nettesheim P (editors). (1982) "*Mechanisms in Respiratory Toxicology*", Vol, I, CRC Press, Boca Raton, Florida, USA

Zago M, Oteiza P. (2001) "The antioxidant properties of zinc: interactions with iron and antioxidants" *Free Radical Biology and Medicine* **31**(2):266-274

Zhang J, Qian Z, Kong L, Zhou L, Yan L, Chapman RS. (1999) "Effects of air pollution on respiratory health of adults in three Chinese cities" *Archives of Environmental Health* **54**(6):373-381

